FTNMR AND ASPECTS OF GERMANIUM CHEMISTRY

A thesis
submitted to the
University of Waikato
for the degree of
Doctor of Philosophy

by

PHILIP JOHN WATKINSON

M.Sc., (Hons., First Class)

University of Waikato

March 1984

To Rosalyn

and

My Parents

ABSTRACT

Experimentally determined baseline parameters were obtained for the NMR observation of 32 isotopes, notably including ^{73}Ge.

Extensive ^{73}Ge studies were performed, despite the technical difficulties from a low NMR receptivity, and a low observation frequency. The majority of germanium compounds studied gave ^{73}Ge resonances. Germanium-73 chemical shifts, linewidths, and germanium proton coupling constants have been obtained, doubling the total number of compounds studied directly by ^{73}Ge NMR. Sample concentrations must be typically at least 0.1 M to avoid using excessive instrument time (> 5 hours).

The larger spectral disperson of ^{73}Ge NMR than ^{1}H or ^{13}C NMR often makes it a better tool for characterization. Trends in ^{73}Ge chemical shifts and coupling constants are surveyed and their use in characterizing hydrides and organogermanes are illustrated. Germanium-73 NMR gave more spectral information on redistributions in the GeY_4:SiX_4, GeX_4:SnY_4, and GeX_4:$HgCl_2$ systems than did ^{29}Si, ^{119}Sn, or ^{199}Hg NMR, revealing a slower redistribution than in MX_4:MY_4 systems (M = Ge or Sn; X, Y = Cl or Br).

Nuclear relaxation studies on ^{73}Ge have been greatly extended, increasing the total number of compounds studied three-fold. Values of T_1 from inversion-recovery experiments ranged from 13 to 1300 ms near RT. The dominance of the quadrupolar relaxation mechanism has been established, and the non-existence of signals from compounds with germanium in an asymmetric environment is attributed to rapid relaxation. Estimates of activation energies for molecular reorientation, and nuclear quadrupole coupling constants (2.3-17 MHz) using ^{13}C correlation times have been obtained.

Proton PT to ^{73}Ge via the sequence INEPT was established and its value demonstrated both for sensitivity enhancement and for help in spectral assignment. Observations imply that all compounds with $^{1}J(Ge,H)$ or $^{2}J(Ge,C,H)$ coupling give proton PT. Large enhancements (2-20 fold) were obtained, although long proton T_1 values reduced instrument time savings to 3-100 fold, with the addition of a relaxant in some cases. The loss of signal during the sequence via nuclear relaxation is smaller for INEPT than for another multinuclear PT sequence, UPT, and this difference is maximized for a nucleus with a large spin, like ^{73}Ge.

Preliminary work on ^{77}Se INEPT and multinuclear studies on transition metal carbonyls are presented.

ACKNOWLEDGEMENTS

I especially wish to thank my chief supervisor, Prof. K.M. MacKay for conceiving this research project, for guidance and support. Dr A.L. Wilkins also provided invaluable supervision and support.

Thanks are also due to Drs D.W. Smith and B.K. Nicholson for their helpful words of advice.

My colleagues J.A. Christie and S.P. Foster gave many helpful hints on vacuum line techniques and germanium chemistry, and together with F.S. Wong, C.C. Ngo, and Y.M. Choo, provided many of the germanium compounds. I also wish to thank R.A. Thomson for technical advice on aspects of the operation of the FTNMR spectrometer.

I acknowledge the financial assistance of the N.Z. University Grants Committee, who provided a post-graduate scholarship throughout the course of this research.

I would also like to express my gratitude to Miss M. France for her most patient and efficient preparation of the typescript.

A well deserved thank you is due to my dear wife Rosalyn for her constant encouragement and support, and also to my two families for their support.

Philip Watkinson

C O N T E N T S

LIST OF TABLES

LIST OF FIGURES

LIST OF SYMBOLS , ABBREVIATIONS , AND PHYSICAL CONSTANTS

Me methyl , $-CH_3$
Et ethyl , $-C_2H_5$
Pr propyl , $-C_3H_7$
Bu butyl , $-C_4H_9$
Pn pentyl , $-C_5H_{11}$
Hx hexyl , $-C_6H_{13}$
Ph phenyl , $-C_6H_5$
acac acetylacetonato , $-C_5H_7O_2$

Et_2O diethyl ether
$n\text{-}Bu_2O$ di-n-butyl ether
EDTA ethylenediaminetetracetic acid
py pyridine
THF tetrahydrofuran
TMS tetramethyl silane

t time
T temperature
RT room temperature

Physical constant	Symbol	Numerical value (SI units)
Velocity of light in a vacuum	c	$2.99792 \times 10^{8}\ m\ s^{-1}$
Permeability of a vacuum	μ_0	$4\pi \times 10^{-7}\ m\ kg\ s^{-2}\ A^{-2}$
Permittivity of a vacuum	ϵ_0	$8.85418 \times 10^{-12}\ m^{-3}\ kg^{-1}\ s^{4}\ A^{2}$
Proton rest mass	M_p	$1.67261 \times 10^{-27}\ kg$
Electron rest mass	m_e	$9.10955 \times 10^{-31}\ kg$
Electronic charge	e	$1.60219 \times 10^{-19}\ s\ A$
Bohr radius	a_0	$5.29177 \times 10^{-11}\ m$
Electron radius	r_e	$2.81792 \times 10^{-15}\ m$
Planck constant ($\hbar = h/2\pi$)	h	$6.6262 \times 10^{-34}\ m^{2}\ kg\ s^{-1}$
Boltzmann constant	k_B	$1.3806 \times 10^{-23}\ m^{2}\ kg\ s^{-2}\ K^{-1}$
Gas constant	R	$8.3143\ m^{2}\ kg\ s^{-2}\ K^{-1}\ mol^{-1}$
Avogadro number	N	$6.02217 \times 10^{23}\ mol^{-1}$
Bohr magneton	β_e	$9.2741 \times 10^{-24}\ A\ m^{2}\ (J\ T^{-1})$
Nuclear magneton	β_N	$5.0505 \times 10^{-27}\ A\ m^{2}\ (J\ T^{-1})$
Proton magnetogyric ratio	γ_N	$2.6752 \times 10^{8}\ kg^{-1}\ s\ A$
Proton Lande factor	g_N	5.585
Electron Lande factor	g_e	2.002

$\pi = 3.14159$ $e = 2.71828$ $\ln(10) = 2.30259$

From: *Physicochemical Quantities and Units, The Grammar and Spelling of Physical Chemi* M.L.McGlashan, 2nd edn. RIC, London, 1971.

LIST OF NMR SYMBOLS AND ABBREVIATIONS , TABLE A

English and greek symbols are followed by abbreviations. A copy of this table is found in the inside back cover pocket .

A line integral
ACQTM FID acquisition time (for JEOL FX90Q spectrometer)
B_0 magnetic induction for spin-system orientation,called magnetic field in text
B_1 magnetic induction for resonance,called magnetic field in text
B_2 magnetic induction for double irradiation,called mag. field in text
B_{eff} effective magnetic field
D dimensionless pulse spacing , $(\Delta J)^{-1}$
Di detectability of isotope i
DELAY delay time between final pulse and acquisition (JEOL FX90Q)
E magnetic energy , or S/N enhancement
Ea activation energy (Arrhenius equation)
Ed proton decoupled S/N enhancement
E% % fraction of theoretical enhancement attained experimentally
ΔE energy difference between two spin levels
f(t) time function (fourier spectroscopy)
$f(\nu)$,$f(\omega)$ frequency function (fourier spectroscopy)
FREQU observed frequency range (JEOL FX90Q)
I observed NMR isotope
I_τ,I_∞ intensities of lines
J coupling constant
K reduced coupling constant
k factor with Ξ yielding JEOL FX90Q resonant frequency
k_i i=1,2,3,4 constants pertaining to PT enhancement
l^i nuclear spin quantum number
L linewidth factor
M_0 macroscopic magnetization
M_i magnetization vector components (i= x,y,z)
m_H,M_H proton spin, and total proton spin, respectively
m^i discrete spin variable
m_i orientational magnetic quantum number for isotope i
n^i number of scalar coupled nuclei (protons) transferring PT or principal quantum number for valence orbital
N natural abundance of an isotope (%)
N_d number of resonating spins in the detector coil
OBFRQ primary frequency parameter for (JEOL FX90Q) (MHz)
OBSET carrier offset (JEOL FX90Q) (kHz)
-(opt) optimum timing giving max. E(- = τ,Δ) or max. E (- = E,Ed)
$\underline{P}$ nuclear angular momentum vector
PD delay between acquisition and next pulse (JEOL FX90Q)
POINT total number of computer memory locations (JEOL FX90Q)
PW1 pulse time (JEOL FX90Q) (μs)
q electric field gradient (subscripts refer to tensor components)
Q nuclear electric quadrupole moment
r ratio of recycle time of INEPT,r_1 to that of single-pulse seq.,r_0
r_{IS} distance between nucleus I and nucleus S (metres)
R_i NMR receptivity of isotope i
R^k_i NMR receptivity of isotope i relative to isotope k

R% % contribution of a relaxation mechanism to total relaxation rate
RES frequency resolution (JEOL FX90Q)
s number of scans to reach a certain S/N
S irradiated NMR isotope
T dimensionless pulse spacing $(\tau J)^{-1}$
T_1 spin-lattice (longitudinal) relaxation time
T_1° value of T_1 at infinitely high temperature
$T_1\rho$ T_1 in the rotating frame
T_1x T_1 from mechanism x,x=csa(chemical shift anisotropy),dd(dipole-dipole),(e)electron-nuclear,(q)quadrupolar,(sc)scalar,(sr)spin-rotation
T_2 spin-spin (transverse) relaxation time
T_2^* apparent spin-spin (transverse) relaxation time
T_{ex}, T_{th} experimental,theoretical pulse time delay, respectively
T% % deviation of experimental pulse sequence timing from theoretical
$t_{1/2}$ time for reactant signal to be reduced two fold
t_p duration of B_1 (s)
$t_{90}^{\wedge}$ pulse width of $\alpha=90°$ for isotope A
u dispersion component of $\underline{M}$
W waiting time between pulse sequences,including ACQTM
$W_{1/2}$ half height line width (Hz)

α tip angle of M,or spin state,or a defined function of timing, τ
α_o optimal flip angle of M
β spin state, or a defined function of timing, Δ
γ magnetogyric ratio
δ chemical shift
Δ the second inter-pulse spacing , or expresses a difference
η NOE enhancement factor
$\bar{\eta}$ macroscopic viscosity of a solution
η_a asymmetry parameter
$\theta i, \phi i$ r.f. pulse applied along i axis (default is x) with $\alpha=\theta°$,or $\phi°$
90i,180i r.f. pulse applied along i axis (default is x) with $\alpha=90°,180°$
$\underline{\mu}$ magnetic moment vector
ν frequency (Hz)
σi screening constant for isotope i
τ the first inter-pulse spacing (defined for a given sequence)
τ_c correlation time for molecular reorientation
v absorption component of $\underline{M}$
χ nuclear quadrupole coupling constant
χ' nuclear quadrupole coupling constant as a function of η_a
ω angular frequency $(rads^{-1})$
Ξ_I resonant frequency of isotope I in a field for which protons of TMS resonate at exactly 100.00 MHz

ADC analogue to digital converter
e.n.c. extreme narrowing condition
FID free induction decay
FIRFT fast inversion recovery FT
FT fourier transform
IRFT inversion recovery FT
LF low frequency
NQCC nuclear quadrupole coupling constant
NMR nuclear magnetic resonance
NOE nuclear Overhauser effect
o.d. outside diameter

PT	polarization transfer
QPD	quadrature phase detection
r.f.	radio frequency
S/N	signal to noise ratio
SRFT	saturation recovery FT

CHAPTER 1 OUTLINE OF FOURIER TRANSFORM NUCLEAR MAGNETIC RESONANCE

1.1 BASIC CONCEPTS

1.1.1 Introduction

The study of chemical structure and dynamics forms an important part of chemistry. Spectroscopic techniques such as nuclear magnetic resonance contribute to this study. Moreover, the uses of NMR can be directly viewed with respect to the Periodic Table, since NMR is based on atomic properties. Two other commonly used forms of spectroscopy, infrared and ultraviolet absorption, cannot be directly linked with the Periodic Table because they are not based on atomic properties, but on molecular properties. At the present time, most research chemists are probably practising NMR spectroscopists.

There are numerous general texts on NMR. Some books emphasize the experimental aspects[1,2] while others are concerned with theory.[3,4,5] The first book[6] to relate NMR to the Periodic Table as a whole contains lists of representative NMR parameters obtained from most NMR isotopes. A more recent book[7] has a comprehensive list of the experimental parameters required to observe most NMR isotopes while another contains lists of NMR parameters for selected nuclei.[8] To gain a state-of-the-art knowledge of the subject, several periodicals[9,10] and review series[11-15] are available. Since there is no lack of general information on NMR, this chapter will provide only an outline of the basic concepts, methods, and NMR parameters, with an emphasis on aspects of relevance to later chapters. Extensive use is made of material from the books[6,7] and several sections from the general texts[1,2,3] are used.

The reader is referred to table A, for lists of symbols and abbreviations pertaining to NMR.

1.1.2 Overview of Nuclear Magnetic Resonance[1,6]

The nuclear magnetic resonance phenomenon depends primarily on the nuclear spin. Each isotope of an element has a ground state nuclear spin quantum number, I which can have values $\frac{x}{2}$ ($x = 0,1,2,...$). For chemically useful NMR isotopes, I can range up to $^9/_2$. The associated angular momentum is:

$$P = \hbar[I(I+1)]^{0.5} \qquad ---(1.1)$$

When $I = 0$, there is no NMR effect. Isotopes with this spin arise when both the mass number and the charge number of the isotope are even, e.g. ^{12}C, ^{16}O, and ^{32}S. For non-zero I, the isotope has a magnetic moment given by:

$$\underline{\mu} = \gamma\underline{P} \qquad ---(1.2)$$

where the constant γ, the magnetogyric ratio, is an intrinsic property of the nucleus in question. When $\underline{\mu}$ is parallel to $\underline{P}$, γ is positive, and vice versa.

If an isotope with a non-zero I is placed in a strong magnetic field, B_o, (1T to 10T) the orientation of the spin axis becomes quantized, each with a different energy. Radiofrequency (r.f.) radiation of an appropriate frequency will cause transitions. The associated absorption of r.f. radiation can be detected. These are the fundamental concepts in NMR spectroscopy.

1.1.3 The NMR Phenomenon[1]

In order to discover the r.f. radiation energy which is needed to induce transitions, a more detailed examination of the nuclear magnetic properties is required.

Although nuclear spin is quantized, it is often useful to describe the motion in terms of classical mechanics. In the presence of B_o, the magnetic moment experiences a torque $\underline{\mu}.\underline{B}_o$. According to Newton's laws of motion, the torque is equal to the rate of change of $\underline{P}$, thus by

equation (1.2) the equation of motion is

$$d\underline{\mu} / dt = \gamma\underline{\mu} \times \underline{B}_0 \qquad ---(1.3)$$

This describes a precession of $\underline{\mu}$ about $\underline{B}_0$ (FIG.(1.1(a)) at the Larmor angular velocity; $\omega_0 = -\gamma B_0$, which corresponds to the frequency

$$\nu_0 = (\gamma/2\pi)B_0 \qquad ---(1.4)$$

Using the alternative quantum mechanical description, in the field $\underline{B}_0$, $2l + 1$ spin levels are separated into different states (FIG.(1.1(b)) of energies $E = -\underline{\mu}.B_0 = -\gamma\underline{P}.\underline{B}_0$. Since the component of $\underline{P}$ takes on values, $m\hbar$, where m has $2l + 1$ values $-l,-(l-1), \ldots l$, the energies are:

$$E = -\gamma\hbar m B_0 \qquad ---(1.5)$$

Using the maximum observable component of μ; $\gamma\hbar l$, the energy difference between two adjacent levels is:

$$\Delta E = E_{(m-1)} - E_{(m)} = \gamma\hbar B_0 = \mu B_0/l \qquad ---(1.6)$$

Since μ is small, ΔE is very small, even in fields of several Tesla. For a proton, $\mu \simeq 1.4 \times 10^{-26} JT^{-1}$, giving an excess fraction of nuclei orientated in the B_0 direction of only 1.6×10^{-5}. Thus the resulting macroscopic magnetization, M_0, (measured by magnetic moment per unit volume) is expected to be small. Eventual signal intensity is determined by M_0. This subject of low-signal intensity is discussed in section 2.1.1.

The actual resonance phenomenon is determined by the interaction between $\underline{\mu}$, which precesses about $\underline{B}_0$ at the Larmor frequency, ν_0, and an additional, small magnetic field, $\underline{B}_1$. Furthermore, $\underline{B}_1$ must be perpendicular to $\underline{B}_0$ and rotating about $\underline{B}_0$ at frequency ν in the same direction as $\underline{\mu}$. In practice $\underline{B}_1$ is a linear r.f. field oscillating in the x or y direction (FIG.(1.1((a))), which is equivalent to a pair of circularly polarized components rotating in the x-y plane with equal angular velocities, but opposite directions. Only the component which rotates

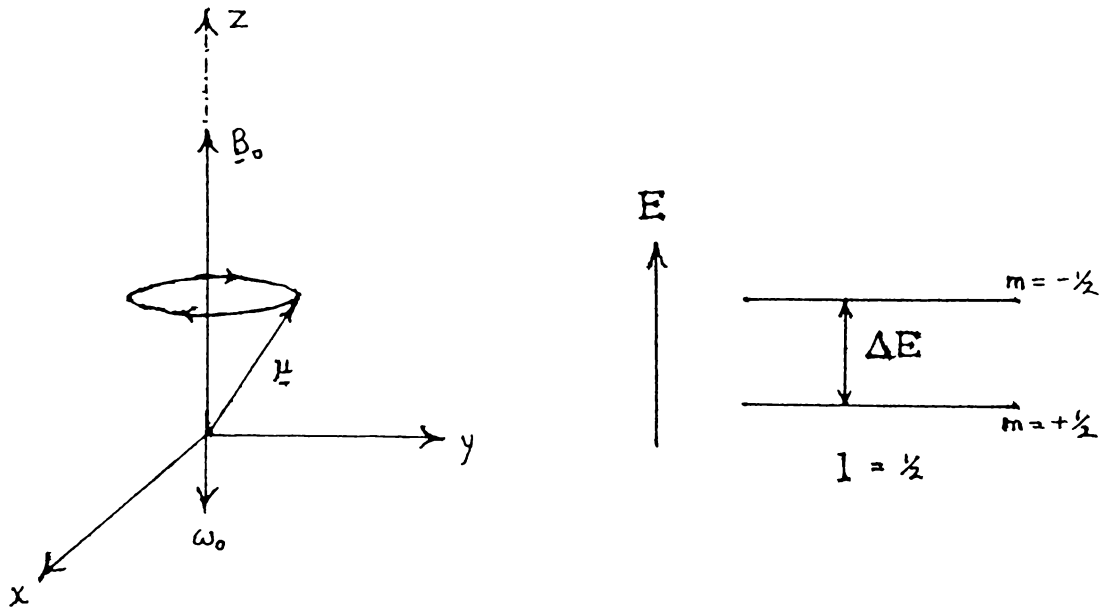

FIG. 1.1 (a)Precession of a nuclear magnetic moment, $\underline{\mu}$ in a magnetic field, $\underline{B}_0$. ($\gamma > 0$) (b)Energy levels of spin 1/2 nuclei in $\underline{B}_0$. m is chosen to be positive when in the direction of the field.

in the same direction as $\underline{\mu}$ is able to influence its motion. Resonance occurs when the frequency of $\underline{B}_1$, ν, exactly equals ν_0:

$$\nu = \nu_0 = (\gamma/2\pi)B_0 \qquad ---(1.7)$$

For example, in a field of 2.11T, the resonance of protons occurs when $\nu = \nu_0 = 90$ MHz.

Note that resonance only occurs when $\nu = \nu_0$ or $\Delta E = h\nu$, and not when $h\nu > \Delta E$ or $\nu > \nu_0$. Thus a single sharp r.f. absorption can be observed.

1.1.4 Overview of NMR Parameters[6]

In the previous section, an idealized situation was used in order to simplify explanation of the concepts. But now a less idealized situation is introduced to produce equations which more closely approximate experimental data.

To a first order approximation, non-viscous fluids in NMR have stationary state energies given by the equation

$$E = -h \sum_A \nu_A m_A + h \sum_{A<B} {}^nJ_{AB} m_A m_B \qquad ---(1.8)$$

The first term is due to ineractions between the spins and B_o, while the second term is due to coupling between spins in pairs. The parameter ${}^nJ_{AB}$ is the scalar spin-spin coupling constant between nuclei A and B which themselves are connected through n bonds. (m_i is the orientational magnetic quantum number for nucleus i.)

Larmor frequencies are now given by:

$$\nu_A = (\gamma_A/2\pi)B_0(1-\sigma_A) \qquad ---(1.9)$$

To account for the electronic environment of nucleus A, the shielding or screening constant σ_A is introduced (σ is a dimensionless number). Normally it is not possible to measure shielding constants directly, but measurements of changes in shielding are possible. These lead to chemical shifts in resonance frequency, which are usually quoted in ppm relative to the resonance of a chosen reference compound. Chemical shifts and coupling constants are the two most often used NMR parameters, and both can be related to chemical structure.

Nuclear relaxation time is the third measurable parameter which is useful in chemistry. It characterizes the rate at which a nucleus recovers its equilibrium properties after being perturbed. In simple cases, there are two distinct relaxation times, namely T_1, the spin-lattice (longitudinal) relaxation time, which relates to magnetization parallel to B_o (Mz), and T_2, the spin-spin (transverse) relaxation time, which pertains to relaxation perpendicular to B_o (M_x or M_y). Relaxation times can yield information on chemical structure and molecular dynamics.

A further nuclear spin parameter, the quadrupole coupling constant, is involved with one type of relaxation mechanism and can also be related to structure and dynamic processes.

1.1.5 Chemical Shifts[6,7]

Chemists are concerned with relating the resonant frequencies of a molecule with some chemical property. Equation (1.9) provides a simple basis for relating frequency with electronic properties.

Differences in resonant frequency arise because different nuclei in a molecule experience different magnetic fields as a result of the secondary magnetic fields arising from the induced circulation of electrons in a molecule under the influence of the applied field. These secondary fields may either oppose B_o or reinforce B_o; that is, the nucleus is either shielded or deshielded by the secondary field. In the former case, the effective magnetic field, $B_o(1-\sigma_A)$, ($\sigma_A > o$) is less than B_o, so the resonant frequency is less than for the original 'zero-shielding' case. When the nucleus is deshielded, the resonance shifts to higher frequency.

The field experienced by a nucleus may be modified by fields set up by induced circulation of electrons localized on that nucleus (local shielding) or by fields set up by induced circulation of electrons within neighbouring groups, or over the entire molecule.(long-range shielding).

Chemical shift, δ_i is a dimensionless parameter expressed in ppm. It is independent of spectrometer frequency ν_o, and is defined as:

$$\delta_i = \frac{(\nu_i - \nu_{ref})10^6}{\nu_{ref}} \qquad ---(1.10)$$

where ν_i denotes the frequency of the line of the observed species, i, and ν_{ref} denotes the frequency of the line of a reference. More information on chemical shift is found in volume 2 of references.[16,17] The IUPAC convention clearly defines chemical shifts scales[18,19] with the following recommendations:

$\delta > o$ for any line detected at a higher frequency than the chosen reference (deshielding, low field);

$\delta < o$ for any line detected at a lower frequency than the chosen reference (shielding, higher field).

Since all FTNMR spectrometers are similarly constructed, experimental results are always presented with increasing frequency from right to left.

For heteronuclei, the referencing resonance is generally concentration and temperature dependent.

Although referencing is discussed in sections 1.2.5, and 1.2.6, the basis of a universal type of referencing needs mentioning. Several groups have recommended[20] that all measured resonance frequencies be related to a field, B_o, in which the protons of TMS resonate at exactly 100.00 MHz. Absolute frequencies on this scale are denoted by Ξ, and are defined as:

$$\Xi_I = \frac{100\gamma_I(1-\sigma_I)}{\gamma_H(1-\sigma_H(TMS))} \qquad ---(1.11)$$

Values of Ξ are given in several general texts on FTNMR.[6,7]

1.1.6 Coupling Constants[6,7]

The scalar spin-spin (or indirect) coupling constant is independent of B_o, and can be positive or negative. A positive sign implies that the coupling interaction stabilizes anti-parallel rather than parallel spin. Absolute signs are difficult to obtain from experiment or theory. However, absolute signs are often based on the assumption that all values of $^1J(^{13}C, ^1H)$ are positive. In the literature, the absolute values of coupling constants are normally quoted, although the modulus sign is omitted.

Coupling constants are proportioned to the product of the relevant two magnetogyric ratios. The proportionality constant depends on the A-B bond electronic structure and is often parameterized by the angular geometry of the A-B bond.

In a comparison of the relative magnitude of $^{n}J_{XA}$ with $^{n}J_{YA}$, a reduced coupling constant, $^{n}K_{MA}$ is introduced (M = X or Y)

$$^{n}J_{MA} = (h/4\pi^2)\gamma_M\gamma_A{}^{n}K_{MA} \qquad ---(1.12)$$

where $^{n}K_{MA}$ is expressed in $NA^{-2}m^{-3}$.

Frequently, the $^{n}J_{AB}$ couplings must be measured from recorded spectra. When δ_{AB} (in Hz) is of the same order, or smaller than $^{n}J_{AB}$, computer analysis of the spectrum is generally required.[21] First order spectra, however, have δ_{AB} (in Hz) $>>$ any $^{n}J_{AB}$. The following case for first order spectra is considered: observed A nucleus coupled with high natural abundance (>90%) B nuclei. If no severe line broadening caused by relaxation or exchange effects is observed, the coupling pattern of A nucleus with m.B. equivalent nuclei is a multiplet; the number of lines is given by $2mI_B + 1$. The relative intensities of the multiplet components conform to a symmetric binomial distribution, and the separation between adjacent multiplet is equal to $^{n}J_{AB}$.

1.1.7 Relaxation Times[6,7]

Relaxation times cover a large range of values, being 0.1 ms to 1000 s for non-viscous liquids. The major factor differentiating T_1 for different nuclei is I.

Nuclei with $I = \frac{1}{2}$ tend to have large T_1 and T_2 values, while nuclei with $I > \frac{1}{2}$ (quadrupolar nuclei) tend to have small T_1 and T_2 values. Quadrupolar nuclei possess an electric quadrupole moment, and electric field gradients at the nucleus lead to efficient relaxation. Small T_1 relaxation times allow rapid pulse repetition in FT experiments, which

helps to improve the signal to noise ratio (S/N). However, small T_2 values lead to broad resonance lines and low resolution spectra.

The spin-lattice relaxation time can be viewed as the rate of energy transfer from the spin system to the lattice. For an isolated spin:

$$dM_z(t)/dt = -(M_z(t)-M_0)/T_1 \qquad ---(1.13)$$

The experimental measurement of T_1 is developed in section 1.2.11.2. Time constant T_2 characterizes the loss of phase coherence of a given spin system, after excitation in a plane perpendicular to B_o, which leads to a decrease in M_y or M_x. This is an entropy effect. For an isolated spin:

$$\text{(same for x comp.)} \quad dM_y(t)/dt = -M_y(t)/T_2 \qquad ---(1.14)$$

T_2 is directly related to the resonance line width. When inhomogeneity in B_o is negligible, the lineshape is Lorentzian, and for a single line

$$W_{\frac{1}{2}} = (\pi T_2)^{-1} \qquad ---(1.15)$$

where $W_{\frac{1}{2}}$ measures the line width at half height in Hz. Although measuring T_2 requires exact experimental conditions, there is; $T_2 \leq T_1$. In addition, the relaxation time in the rotating frame, $T_{1\rho}$, can be measured instead of T_2 since, in general, for the liquid state, $T_{1\rho} = T_2$, and $T_{1\rho}$ measurements are less sensitive to pulse missetting than T_2 ones.

1.1.8 Relaxation Mechanisms[7]

Any measured relaxation time for nucleus A is related to several potential relaxation pathways. In simple cases, relaxation rates are additive:

$$\frac{1}{T_i obs} = \frac{1}{T_i e} + \frac{1}{T_i dd} + \frac{1}{T_i q} + \frac{1}{T_i csa} + \frac{1}{T_i sc} + \frac{1}{T_i sr} \qquad ---(1.16)$$

where i stands for 1 or 2, obs is the observed parameter, and the various subscripts define the precise relaxation process.

The last three terms refer to chemical shift anisotropy (csa), scalar relaxation (sc) and spin-rotation (sr). These are of minor importance, and are only mentioned for the sake of completeness.

The electron-nuclear relaxation mechanism (e) occurs when paramagnetic species (or impurities) are present in the solution. It is an efficient mechanism that generally dominates the others.

In diamagnetic samples the most important mechanisms are usually the dipole-dipole (dd) and quadrupolar (q) mechanisms, which are reviewed in more detail.

1.1.8.1 Dipole-dipole Relaxation Mechanism[6,7]

Although the coupling energy between two magnetic dipoles at a fixed distance is averaged to zero by molecular rotations, it can still cause nuclear relaxation. This dipole-dipole (dd) mechanism is often dominant for spin $\frac{1}{2}$ nuclei. It involves interactions with other nuclei (or with unpaired electrons)

$$\frac{1}{T_i dd} = [\mu_0 \gamma_I \gamma_S h/4\pi]^2 \quad I_S (I_S+1)\, r^{-6}_{IS} f_i(\nu_I, \nu_S, \tau_c^I) \qquad ---(1.17)$$

$f_i(\nu_I, \nu_S, \tau_c^I)$ is a complex function of correlation time τ_c^I characteristic of the random motion of the IS vector and of the ν_I, ν_S resonance frequencies. In the extreme narrowing condition (e.n.c.): $\omega_I \tau_c^I << 1$ ($\omega = 2\pi\nu$) generally met in high resolution experiments, $T_{1dd} = T_{2dd}$.

Equation (1.17) with the cited forms of f is only valid for isotropic molecular motion. If preferred rotation about a given axis occurs (including internal rotation), then the rotational diffusion is not characterized by a single value of τ_c, and the equations for T_{1dd} need modification.[22] To illustrate this point, consider the ^{13}C NMR of monosubstituted benzenes.[23] Rotation about the C_2 axis of these molecules is usually much faster than around axes perpendicular to it. Since the former motion does not influence relaxation of the para ^{13}C nucleus, its value of T_1 is shorter than those of the ortho and meta ^{13}C nuclei. Note that in the range of short τ_c values imposed by the e.n.c., relaxation times are generally independent of B_o.

Now f (ν_I, ν_S, τ_c^I) reduces to

$2\ \tau_c^I$ if I and S are identical and belong to the same molecule.

$^4/_3\ \tau_c^I$ if I and S are different and belong to the same molecule.

These situations give rise to an intramolecular dipole-dipole relaxation mechanism. If I and S belong to different molecules (the function, f, is more complex) an intermolecular mechanism develops. Since τ_c decreases with temperature, T_{1dd} increases with temperature.

Two nuclei, I and S_i when close enough, can interact through space in a dipole-dipole mechanism. The irradiation of any one of these S nuclei can lead to a modification of the energy level distribution of the second, I. A modification of the intensity of the resonance line of the I nucleus ensues. This phenomenon, known as the nuclear Overhauser effect (NOE), depends on the observing field and the mobility in solution of the molecule in question. Simple guidelines for NOE measurement are given in section 1.2.11.1.

An enhancement factor, η characterizes the NOE:

$$\eta = \frac{A - A_0}{A_0} \qquad \text{---(1.18)}$$

where A_0 = a line integral without perturbation of nucleus I,
when A = a line integral of nucleus I when irradiating neighbouring S nuclei. Under the e.n.c.:

$$\eta_{max} = \gamma_S / 2\gamma_I \qquad \text{---(1.19)}$$

This enhancement aspect of the NOE is developed in section 2.1.2. An examination of the NOE can yield information on conformation or dynamic processes.[24]

A determination of the dipole-dipole relaxation contribution to the different relaxation mechanisms is afforded by

$$T_1dd = (\eta_{max}/\eta)T_1obs \qquad \text{---(1.20)}$$

1.1.8.2 Quadrupolar Nuclear Relaxation[5,6,7]

The quadrupolar relaxation mechanism (q) is often encountered in heteronuclei NMR because 87 of the 116 magnetically active isotopes posses a spin value $>\frac{1}{2}$, and have an electric quadrupole moment in addition to the magnetic dipole moment. The interaction of a nuclear quadrupole movement, eQ, with electric field gradient, eq, provides a very efficient process for nuclear relaxation via molecular rotation.

In the extreme narrowing limit, (τ_c is 1-10ps for non-viscous liquids) the relaxation rates T_{1q}^{-1} and T_{2q}^{-1} are identical, and are given by:

$$\frac{1}{T_{1q}} = \frac{1}{T_{2q}} = \frac{3\pi^2}{10}\,\frac{(2I+3)}{I^2(2I-1)}\,\chi^2\,(1+\eta_a{}^2/3)\tau_c \qquad ---(1.21)$$

where χ is the nuclear quadrupole coupling constant (NQCC measured in Hz if T_i and τ_c are in s). The NQCC is defined by

$$\chi = e^2 q_{zz} Q/h \qquad ---(1.22)$$

The largest component of the electric field gradient, q_{zz}, is a function of asymmetry at the site of the nucleus. The assymmetry parameter, η_a takes values between 0 and 1, and, is given by:

$$\eta_a = \frac{q_{yy} - q_{xx}}{q_{zz}} = \frac{\chi_{yy} - \chi_{xx}}{\chi_{zz}} \qquad ---(1.23)$$

In pulse FTNMR, linewidths are related to T_{2q} as in eq (1.15), (assuming the quadropolar mechanism is dominant) so that linewidths are given by

$$W_{\frac{1}{2}} = (3\pi/10)\, f(I)\, \chi^2\, (1+\eta_a^2/3)\, \tau_c \qquad ---(1.24)$$

where

$$f(I) = (2I+3)/[I^2(2I-1)] \qquad ---(1.25)$$

The full range of the asymmetry parameter leads to only a 33% change in T_{iq}. Some workers[25] define the NQCC:

$$\chi' = \chi(1+\eta_a^2/3)^{0.5} \qquad ---(1.26)$$

when χ' is determined but η_a is not known. The full range of η_a will only give a 16% change in the NQCC, which in some determinations of χ, is comparable to the total error in χ.

Correlation times of non-viscous liquids usually fall in the range 1-10ps, with larger or more bulky molecules generally giving larger τ_c values. 'Viscous' liquids can give larger τ_c values ($\tau_c \simeq 60$ps for aqueous Ca-EDTA complex).[25]

However, the dependence of T_{1q} upon q_{zz} leads to a very wide range of T_{1q} for different compounds containing the same isotope. Thus T_{1q} is strongly dependent on the symmetry at the site of the nucleus. In nitrogen compounds, q_{zz} for ^{14}N ($I=1$) varies from near zero ($\chi \simeq 0$) for NH_4^+(aq) to a large value ($\chi \simeq 4$MHz) for CH_3CN, yielding T_1 values of 50s and 22 ms[26] respectively. Relaxation in NH_4^+(aq) is controlled primarily by the NH dipole-dipole interaction.

In boron compounds, a similar situation occurs. For $^{11}B(I=3/2)$ in symmetric molecules like BH_4^-, $q_{zz} \simeq 0$ ($\chi \simeq 0$)[27] with $T_1 \simeq 10$s, and in the less symmetric molecules of three coordinate boron compounds, where $q_{zz} >> 0$ ($\chi \simeq 3$MHz), T_{1q} values are typically 10ms. An even greater range of T_{1q} values is found for chlorine and bromine. For ions with tetrahedral symmetry or higher, T_{1q} can be as much as several seconds, but in unsymmetric environments, T_{1q} can be smaller than several microseconds. These low values of T_{1q} are due to the large ($\chi \geq 100$MHz) values of the NQCC's.

However, a few isotopes have a predominance of chemically interesting compounds for which the isotope is in either a highly symmetric or unsymmetric environment. With a few exceptions, (eg. Me_2SO_2)[28] most organic sulphur compounds contain sulphur in sites of low symmetry for which $W_{\frac{1}{2}}$ is usually in the 0.1 to 5 kHz range.[8a] On the other hand, most chemically interesting compounds of germanium have this nucleus in

substituted tetrahedral sites where q_{zz} is relatively small. Germanium-73 T_{iq} values are discussed in chapter 5.

When comparing $W_{\frac{1}{2}}$ for different nuclides, (with constant electric field gradients) the factor of importance is:[29]

$$L = f(I)Q^2 \qquad ---(1.27)$$

Hence $|Q|$ for ^{2}H, ^{6}Li, and ^{133}Cs are small, ($<10^{-30}m^2$) and these isotopes tend to give rather small linewidths. The halogen series ^{35}Cl, ^{79}Br, ^{127}I have an increasing $|Q|$ and a corresponding marked increase in linewidths. Quadrupole moments for ^{35}Cl and ^{127}I are $-0.08m^2$ and $-0.8m^2$, with $W_{\frac{1}{2}}$ values of the isotopes in KCl and $KI_{(aq)}$ of 17 and 1,800 Hz, respectively. When there are two or more quadrupolar nuclei for a given element, the one preferred for NMR studies may sometimes be the one with the smaller $|Q|$, even if it has the lower receptivity. When high resolution spectra are required (δ studies) ^{6}Li may be preferred to ^{7}Li, for example.

Linewidths are related inversely to I. Table (1.1) lists the linewidths expected for the spins of chemically useful isotopes if a linewidth of 100 Hz is assigned to I=1 and all other relevant NMR parameters are the same.

An illustration of the relation between I and $W_{\frac{1}{2}}$ is provided by ^{121}Sb ($I=5/2$), and ^{123}Sb ($I=7/2$), which yield linewidths of 220 Hz and 160 Hz respectively[7], in close agreement with eq (1.27). (sample $SbCl_6^{2-}$).

l	1	3/2	5/2	3	7/2	9/2
f(l)	5	4/3	8/25	1/5	20/147	2/27
W(1/2)	100	26	12	6.4	3.2	1.4

TABLE 1.1 Relative line widths for the spins of chemically useful isotopes from $f(l) = (2l+3)/[l^2(2l-1)]$, W(1/2) in Hz .

Since the quadrupole interaction is usually the dominant one for quadrupolar nuclei (unless $\chi=0$ due to molecular symmetry), and since it is entirely an intramolecular interaction, a measurement of the relaxation times provides an excellent means of measuring simply and unambiguously the molecular correlation time if the NQCC can be determined independently. However, correlation times are assigned about each principal axis in an asymmetrical molecule, and the situation is more complex than outlined here.[30]

On the other hand, χ can be determined via eq (1.21) if τ_c can be determined from some other source. For instance, if the quadrupolar isotope is surrounded by ligands which contain protonated carbon atoms, the correlation time for the molecule can be estimated from the ^{13}C T_{1dd} value, an estimate of r_{CH} and eq (1.21).[25] In these cases, it is reasonable to assume that ^{13}C $T_{1obs} \simeq {}^{13}C$ T_{1dd}.

1.1.9 Nuclear Spin Properties of the Elements[6,8]

Several nucleus-dependent factors are of prime importance when starting multinuclear NMR. As far as I is concerned, the most important division is into nuclei with zero spin (no NMR signal), those with $I=\frac{1}{2}$ and those with $I>\frac{1}{2}$. As can be seen in the last section, when $I>\frac{1}{2}$, the relaxation mechanism is efficient, and the linewidths can be larger than for $I=\frac{1}{2}$, and dependent on Q and I.

The magnetogyric ratio for a nucleus is also of great importance, since it affects both the frequency and the intensity of the resonance. Its units (SI) are $rad.T^{-1}.s^{-1}$, and values range in magnitude from 0.357 x 10^7 (for ^{197}Au) to 28.5335 x 10^7 (for ^3H) giving a variation of nearly two orders of magnitude in NMR frequencies at constant field. Using the fact that natural abundance sensitivity at constant field (receptivity, R_I) is given by $\gamma_I{}^3N I_I(I_I+1)$, it is useful to define a relative receptivity R_I^H or R_I^C. The receptivity of isotope I is given as a fraction of the receptivity of ^1H (H) or ^{13}C (C). Putting in the relative parameters:

$$R_I^H = 6.9664\times10^{-28}\ R_I \qquad rad^3T^{-3}s^{-3}\% \qquad ---(1.28)$$

$$R_I^C = 3.9472\times10^{-28}\ R_I \qquad rad^3T^{-3}s^{-3}\% \qquad ---(1.29)$$

Up to date (1981-83) values of γ, N, R_I, Q, I and Ξ are given in references:[7,8]

In fact, multinuclear studies are usually directed towards a better understanding of the structural or dynamic properties of the compounds in question. Now the experimental S/N can be redefined in terms of spectrometer time compared to the information obtained during the allotted period of time.[8b] This leads to the definition of a new parameter; namely the detectability of a given isotope for a given compound:

$$D_I = R_I \, f(N_d, W_{\frac{1}{2}}^{-1}, T_{1I}^{-1}) \qquad ---(1.30)$$

for which N_d is the number of resonating spins in the detector coil.

The value of D_I is strongly dependent on $W_{\frac{1}{2}}^{-1}$. For linewidths $W_{\frac{1}{2}}'$ and $W_{\frac{1}{2}}$, and the corresponding number of scans to reach a constant S/N: s', s; the relationship for a Lorentzian line is:

$$s' = s \, (W_{\frac{1}{2}}^{1}/W_{\frac{1}{2}})^2 \qquad ---(1.31)$$

For instance, if $W_{\frac{1}{2}} = 1$ Hz, and $W_{\frac{1}{2}}' = 10$ Hz, then the broader line of the two requires a factor of 100 more scans to reach the same S/N.

This concept is very important when observing quadrupolar nuclei, for which $W_{\frac{1}{2}}$ can vary enormously.

Methods of increasing D_I are discussed later in section 2.1.1.

1.2 EXPERIMENTAL METHODS

1.2.1 Introduction[6]

Nuclear magnetic resonance spectroscopy was initiated by the successful attempts in 1946 to measure the magnetogyric ratio of the proton. Later, improvements in instrumentation led to the discovery of chemical shifts and coupling constants.

Commercial continuous wave proton spectrometers became available in the early 1960's, and quickly became widely used, particularly in structural organic chemistry. The major limiting factor of NMR is its low sensitivity by spectroscopic standards. Hence, studies concentrated on the several most sensitive nuclei and there was a steady progression to higher magnetic fields. In the early 1970's, the introduction of Fourier transform methods and decoupling techniques greatly increased NMR sensitivity, and led to an upsurge of interest in less sensitive but chemically very significant nuclei, such as ^{13}C. However, the electronic hardware was usually specific to one nucleus, so that studies of the currently 'more obscure' nuclei were quite limited. In the late 1970's commercial NMR instruments capable of studying a wide range of nuclei (multinuclear) became available. Now, truly multinuclear NMR studies are not uncommon. (The abbreviation NMR appeared in the abstracts of Chemical Abstracts Services about 11,000 times from 1982-1983, and the number of appearances per year has been growing since at least 1967.)

This section will give an outline of experimental methods required for proper use of this spectroscopic tool, and the reader is referred to the general NMR texts for complete coverage of this topic.[1,2,6,7] Only the simple pulsed (FT) NMR method will be discussed. The FT method is far more common in multinuclear NMR than the alternative continuous wave, stochastic, or tailored excitation methods.

1.2.2 The Fourier Transform Method[7]

The NMR phenomenon was outlined in section 1.1.3, but in order to gain insight into the FT method, a rotating frame of reference, OXYZ, is introduced. The set of OXYZ axes (FIG.(1.2(a))precesses at a frequency equal to the Larmor precession of the resonant nucleus with respect to the fixed laboratory frame. The equation of motion for $\underline{M}$ takes the same form as for eq (1.3):

$$(d\underline{M}/dt)_{rot} = \gamma\underline{M} \times \underline{B}_{eff} \qquad ---(1.32)$$

where the effective field, B_{eff} is now the resultant of B_o, B_1, and of a fictitious field $^{\omega}/_{\gamma}$ which accounts for the rotation of OXYZ about the z axis ($^{\omega}/_{\gamma}$ is in the opposite direction to B_o). Figure (1.2(b)) shows the generalized picture of the motion of $\underline{\mu}$ off resonance, and in the case of on resonance (FIG.1.2(c)). The on resonance picture is still valid when ν and ν_o are slightly different (a few kHz).

When applied over a short time, (t_p) B_1 forces the magnetic moments to precess around it, tilting the vector sum of these moments an angle α from its original position along B_o.

$$\alpha = (\gamma/2\pi)B_1 t_p \quad \text{(degrees)} \qquad ---(1.33)$$

The magnitude of a signal following a single pulse is sin α. Normally, B_1 is a constant for a given frequency range of a spectrometer (γ is constant for a given isotope). The desired tip angle is obtained by adjusting t_p. This pulse simultaneously produces a range of resonant frequencies and so affords the most efficient method of recording an NMR spectrum.

After a pulse excitation, a spin system tends to return to its equilibrium state, and a free induction decay (FID) is detected by the spectrometer receiver coil. The decay rate is governed by an exponential term exp ($-t/T_2^*$)

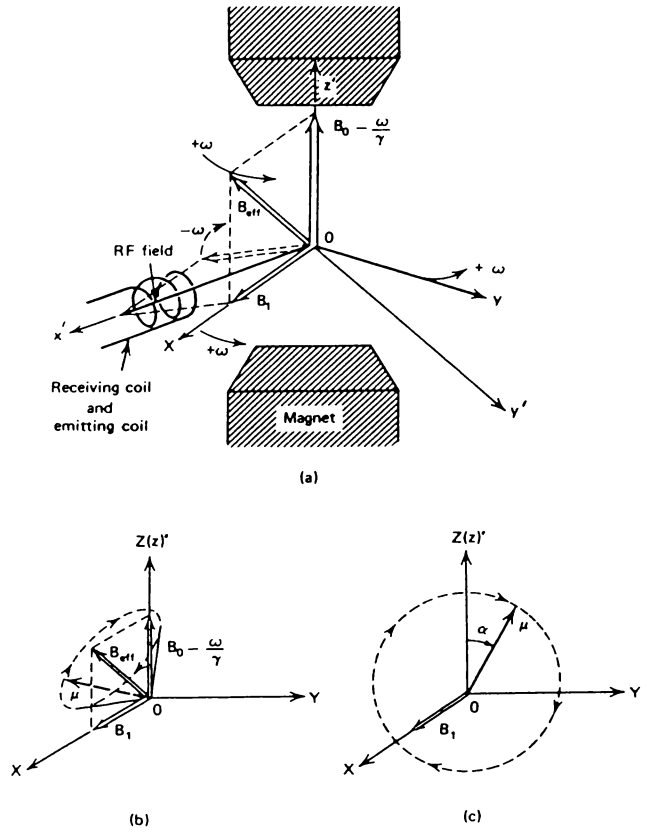

FIG. 1.2 The rotating frame and the resonance phenomenon: (a) The different magnetic fields in the lab. frame Ox'y'z' and the rotating frame OXYZ. (b) Motion of the nuclear magnetic moment, $\underline{\mu}$ in off resonance condition.(original position along OZ) (c) Motion of $\underline{\mu}$ in on resonance conditions. (original position along OZ : α , pulse angle.)

$$\frac{1}{T_2^*} = \frac{1}{T_{2_I}} + \frac{1}{T_2'} \qquad ---(1.34)$$

where T_{2_I} is the spin-spin relaxation time of isotope I, and T_2' characterizes an instrumental spin-dephasing process due to magnetic field inhomogeneities. Thus $T_2^* < T_1$, which means that the FID can disappear before the spin system reaches it thermodynamical equilibrium. The FID is detected and then amplified. In general the FID cannot be directly interpreted in terms of δ or $W_{\frac{1}{2}}$. Before Fourier transformation into the well known frequency domain, by a mini-computer, the analogue signal of the FID must be converted to a digital one by an analogue to digital converter (ADC). This process involves rapidly sampling the FID voltage at fixed time intervals, and storing a number proportional to this voltage in each memory location (called acquisition).

The total number of memory locations (POINT) used during the sampling process and acquisition time (ACQTM) are related to the observed frequency range (FREQU) by the Nyquist theorem:

$$\text{FREQU} = (\text{POINT})/[2(\text{ACQTM})] \qquad ---(1.35)$$

The ADC must work at twice the speed of the spectral width to unambiguously digitize the signals. Wordlength of the ADC determines the accuracy and the dynamic range it can handle.

Folding (or foldback) is an important artifact in the frequency domain that arises from this sampling process. There are two classes of this artifact, called 'folding' and 'arithmetic folding'. The second type arises because the detector cannot determine whether a resonance line is located at plus or minus $\delta\nu$ Hz from the carrier frequency ν_o. This gives rise, after the sampling process, to a folding back around ν_o.

There are two modes of detection, the single detection mode, and the quadrature detection mode, which has the carrier frequency in the centre

of the spectrum. This second mode gives a S/N gain of $\sqrt{2}$ compared to the single detection mode. Both types of detection have filtering and attenuation of any 'signal' outside the filter bandwidth. This reduces the foldback of noise into the spectrum.

A record of the FID is contained in POINT memory locations, and the resulting usable frequency separation will be displayed over (POINT)/2 data points. The frequency resolution for this experiment (Hz) is:

$$RES = 2(FREQU)/(POINT) \qquad ---(1.36)$$

Once the FID has been digitized, any addition of signals is usually carried out by the mini computer at this stage. The S/N of the added FIDs varies as the square root of the number of FIDs. Using a fast Fourier transform algorithm on data which has 2^{n+10} elements (n, a whole number) the same computer will convert the data into a mathematically complex frequency domain (FIG.1.3). Ideally, the real part of the transform gives the so-called υ mode, and the imaginary part, the u mode. In practice, phase shifts occur, so additional phase corrections are added before the final presentation of the spectrum.

Normally, the spectrum is recorded in the absorption mode (υ) which has a Lorentzian line shape proportional to the number of resonating spins, and is integrable. The other types of spectrum include the dispersion mode, the magnitude mode, and the power mode.

Having provided a basic guide to the fate of the NMR signal in a generalized spectrometer, attention will be turned more to the details of spectrum recording from an operators point of view.

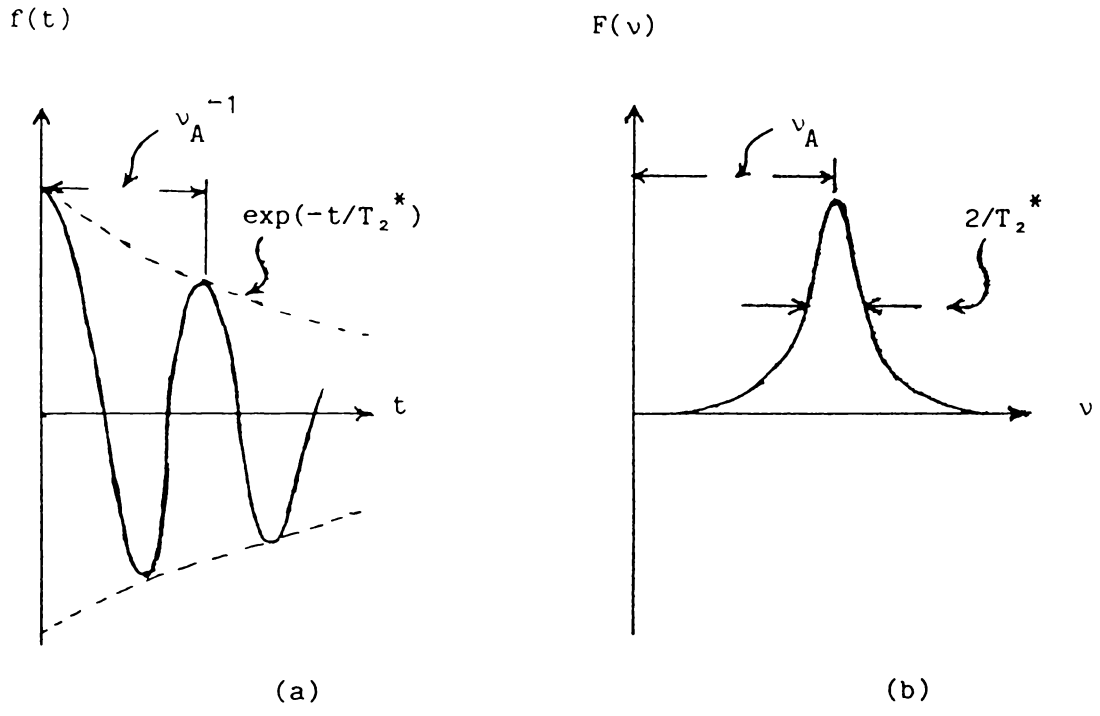

FIG. 1.3 Picture of a generalized FID (a) and the Fourier transformed spectrum (b), showing the real part of the absorption mode. The mathematical transform is:

$$F(\omega) = \int_{-\infty}^{+\infty} f(t) \exp(-i\omega t)\, dt$$

Note that when exactly on resonance, $\nu_A \rightarrow 0$. A FID decay envelope of $\exp(-t/T_2^*)$ yields a Lorentzian line of $W_{\frac{1}{2}} = 2/T_2^*$.

1.2.3 Sample Preparation[7]

Several guidelines are worth remembering when preparing a sample. The sample should be as concentrated as possible with a height in the sample tube about the same as the receiving coil. Avoid using a solvent which has large resonances near the solute resonances. The solution viscosity should be minimized in order to reduce linewidths.

In addition, when performing quantitative or dynamic measurements, solid particles and dissolved oxygen should be removed.

1.2.4 Lock System[7]

Field frequency lock systems maintain the B_o/ν_o ratio constant enough to facilitate high resolution NMR experiments. This is achieved by monitoring the frequency of a given NMR line. Any drift in this resonance position is fed back by an automatic control loop as a correcting voltage to the magnet power supply.

When the locking resonance is in the frequency range of the observed nucleus the lock is called a homonuclear one, otherwise it is called a heteronuclear lock. A heteronuclear lock using a deuterium isotope in a solvent is currently the most common situation.

The lock system can be internal, in which the locking isotope is furnished by the solvent, or external. An external lock of the first kind contains a locking substance in a tube concentric to the sample tube. An external lock of the second kind consists of a small ampoule containing the locking substance permanently located near the sample tube.

Detection of the lock is performed in a continuous wave mode, and so care must be taken to avoid lock-signal saturation arising from high amplifier gain.

1.2.5 Reference[7]

Several kinds of reference exist. The internal kind has an inert substance added to the solution to provide a unique resonance for referencing. Alternatively the external reference method uses a reference substance added to a capillary and placed in the NMR sample tube. The substitution method consists of recording the resonances of the sample, and then exchanging tubes and recording the reference using the same parameters. If the frequency of the reference line is outside the observed spectral region, an appropriate compound with a known chemical shift can be used as a secondary reference.

It is important to take account of the fact that the frequency of the reference line can be solvent or temperature dependent. Temperature dependent references ($\delta(^{59}Co)$ changes 3.5 ppm/°C) require a longer waiting time to attain thermal equilibrium and greater attention to sources of temperature gradients such as the decoupler power.

1.2.6 Chemical Shift Measurements[7]

Chemical shift data should be accompanied with the experimental conditions, including: the lock system and substance, the referencing system, the physical state of reference and solute, the temperature of the experiment, and the accuracy of the chemical shift or coupling constant.

When using substitution referencing, the chemical shift is simply given by equation (1.10) in the case of an identical sample and reference lock substance. This procedure avoids a volumic susceptibility correction or a knowledge of the reference-sample interactions. If a different sample and reference lock substance are used, a correction is applied.

$$\delta_i = \delta_{i(obs)} + \delta_{i(lock)} - \delta_{ref(lock)} \qquad ---(1.37)$$

where the $\delta_{(lock)}$ values refer to the chemical shifts (ppm) of the two locking substances.[7]

1.2.7 Spectrum Recording[7]

A brief description of the important parameters required to record the spectrum of an unknown compound are presented. More detail is given in section 1.3.2 when searching for a 'new' isotope on a specific spectrometer. However, here it is assumed that a spectrum of the reference has already been obtained.

The first requirement is to have the correct frequency and the appropriate frequency range to observe the resonances. It is often worth calculating the expected resonance positions.

Spectral resolution (eq (1.36)) is chosen by adjusting the memory size (POINT) since the frequency range is already chosen. A guideline is:

$$\text{POINT} > 2(\text{FREQU})/W_{\frac{1}{2}} \qquad \text{---(1.38)}$$

Alternatively, ACQTM should approximate $3T_2^*$ ($\sim W_{\frac{1}{2}}^{-1}$).

Otpimal pulse angle, α_o and the waiting time between pulses (including ACQTM), W, should be chosen according to the T_1 value of the signal:

$$\cos \alpha_0 = \exp(-W/T_1) \qquad \text{---(1.39)}$$

Thus long T_1 values require a small α_o and (or) a large pulse interval. Relaxants can be added to reduce T_1.[31] The smaller the pulse width (or angle), the greater the spread of frequencies produced (eg. a 10 μs pulse excites nuclei within ±25kHz from the pulse frequency with less than 2% change in power over the spectrum).

A knowledge of the pulse length corresponding to a pulse angle is often required, particularly when α=90°. In practice it is easier to find the null point of a signal at α=180°, since it is better defined than the signal maximum at α=90°. In this procedure, $W \geq 5T_1$, and ideally, the sample

height should match the receiver coil height to reduce diffusion and r.f. field inhomogeneity.

Rearrangement of equation (1.33) relating α to t_p leads to

$$t_{90}^{X} = t_{90}^{A} \gamma^{A}/\gamma^{X} \qquad ---(1.40)$$

where t_{90}^{X} is the 90° pulse width for isotope X, and t_{90}^{A} is the predetermined 90° pulse width of isotope A. This applies to isotopes with similar resonant frequencies, solutions of similar ionic strength[32] and with the same probe.

Receiver gain must be optimized so that it is high enough to allow the ADC to obtain digitized signals, and low enough to avoid the ADC 'clipping' the signal (a saturation effect on the memory giving distorted signals).

Finally, the delay before acquisition may need adjustment, to avoid pulse breakthrough or acoustic ringing especially in the case of low-γ nuclei. Without the introduction of a time delay, this results in spectra with 'rolling baselines'. Even more important is the loss of signal when this delay is introduced for a signal with a short T_2.

1.2.8 FID and Spectral Manipulations[7]

Commercially available spectrometers offer a software package that accommodates a variety of FID or spectrum manipulations.

Pulse breakthrough or acoustic ringing (section 1.2.7) results in saturation of the first 10 to 50 memory words in the FID. A flat baseline can be obtained by left shifting the FID, which is equivalent to adding a delay before the acquisition. This introduces a third order dephasing.

Alternatively, the first points of the FID can be zero filled. If too many points are zeroed, a new 'baseline distortion' is introduced and contains an over-emphasis of the $\sin x/x$ appearance of the peak.

Sensitivity enhancement can be achieved by multiplying each point of the FID with a decaying exponential exp (-t/k) such that k matches T_2* of the FID. This introduces some line braodening.

Resolution enhancement procedures include multiplying the FID by a weighting function, and this generally decreases signal intensity.

Software packages usually provide calculation of integrals, and contain subroutines to calculate the frequency and chemical shift of a chosen peak.

1.2.9 Decoupling Procedures[7]

Heteronuclear decoupling is the most frequently used form of decoupling, which consists of observing a given nucleus while irradiating another in a different spectral region. Several heteronuclear decoupling states can be chosen, notably including the broadband state, for which the entire chemical shift range of the irradiated nucleus is swept by a modulation scheme in the decoupling frequency.

Other common forms of decoupling include: heteronuclear selective (irradiation of a specific line) heteronuclear broadband or selective, off resonance (partial decoupling) and homonuclear decoupling (same observation and irradiation nuclei).

1.2.10 Pulse Sequences

An overview of some of the pulse sequences available is presented. However, pulse sequences involving polarization transfer are examined in chapter 2.

Acoustic ringing can be eliminated without destroying the information at the beginning of the FID by use of an echo sequence[33] 90-τ-180-τ-ACQU. When a residual anisotropic interaction exists, the sequence is modified to 90_x-τ-90_y-τ-ACQUIRE.[34] The observing pulse can be set to the Ernst angle[35] for optimum sensitivity by adding a second spin-echo.[36]

Making use of the fact that acoustic ringing behaves as if it has $T_1 \simeq 0$, the pulse sequence named ACOUSTIC[37] was designed: DELAY-θ-ACQUIRE(+)--DELAY-180-τ-θ-ACQUIRE(-). Real peaks add coherently, while acoustic ringing will cancel.

Unwanted lines can be eliminated by the following methods: unwanted peak saturation[38], selective pulse sequences[39], (a selective 90° or 180° pulse on the unwanted peak is followed by a non-selective 90° pulse) discrimination by T_1,[40] (using 180-τ-90-ACQUIRE) or discrimination by T_2[41] (using 90-τ-180-τ-ACQUIRE). For the last two methods, τ is adjusted to the null (or invert) the desired line, which is the broad line for the method using T_2.

The selective impulsion train, or DANTE sequence[42], consisting of a train of micropulses, has a variety of uses. It can be used for relaxation time measurement, exchange rate measurements, peak suppression, or for selectively picking out absorptions.

Amplitude modulation can be introduced into noise decoupled NMR spectra by heteronuclear J couplings.[43] This conversion of J coupling into sign and intensity information can be used as a test for multiplicity. In general the method is more sensitive, more selective and easier to interpret than single-frequency off-resonance decoupling experiments. These so-called J-modulated spin-echo (JMSE) type pulse sequences are discussed in section 2.2.2.

A number of sequences can be used to reduce the total accumulation time in cases where the nuclei have long T_1 values with the resulting long waiting times between acquisitions. Driven equilibrium Fourier Transform (DEFT)[44] and Spin Echo Fourier Transform (SEFT)[45] methods are based on echo type refocusing pulse sequences. The homo-spoil[46] method suppresses any magnetization left after the end of the acquisition period in the phase perpendicular to B_o by briefly spoiling one of the field homogeneity gradients.

Problems caused by pulse imperfections can be alleviated by the use of composite pulses instead of single pulses.[47,48] For instance, B_1 inhomogeneity can be reduced by using a $90°_x 180°_y 90°_x$ composite pulse instead of a $180°_x$ pulse.

1.2.11 Dynamic Measurements

This section presents a brief description of NOE measurement, followed by the techniques and methods in T_1 measurements. Descriptions of the measurement of T_2 are found in several general texts.[1,2,6,7]

1.2.11.1 Heteronuclear NOE[7]

A spectrum of nucleus I is recorded under continuous S nucleus broadband heterodecoupling. Then, a second spectrum is acquired with the decoupler gated on just before the acquisition, so that no NOE develops this time.[49] In order to allow the I spin system to be in equilibrium, $W \geq 9T_1$ is recommended. (The longest T_1 from I and S nuclei is chosen.) The precision in an NOE determination will never exceed a few percent[50] and the S/N is of major importance in the overall precision.

1.2.11.2 T_1 Measurements[7]

There are at least five principal methods devoted to the determination of longitudinal relaxation: saturation recovery (SRFT), inversion recovery (IRFT), progressive saturation (PSFT), variable nutation angle (VNAFT), and single scan (SSFT). Since the first method, and in particular, the second method are of relevance to later experimental work, they will be discussed.

In its basic version, the inversion recovery method rests on the following pulse sequence[51] DELAY-180-τ-90-ACQUIRE. The equilibrium magnetization is first inverted by a 180° pulse and is then allowed to recover during a period τ. The value of M_Z is then measured by acquiring the signal which follows a 90° pulse (FIG.(1.4)). A waiting time, $W \geq 5T_1$

is required before repeating the sequence so that the equilibrium magnetization may be restored. After Fourier transformation, signals are observed which relax individually as a function of τ between $-M_o$ ($-I_\infty$) and $+M_o$ ($+I_\infty$). Integration of eq (1.13) for the initial condition $M_z(t=o) = -M_o$ produces:

$$I_\tau = I_\infty[1-2\exp(-\tau/T_1)] \qquad ---(1.41)$$

Relaxation times are then easily obtained by a semilogarithmic or an exponential fit of the data. If an estimate of the T_1 value can be made, an experiment with about 10 τ values will span a range between $0.3T_1$ and $2T_1$.

Phase alternation (inverted every second scan) of the observing 90° pulse eliminates[52] echo formation at small τ values ($T_2^* \simeq T_1$).

When W becomes prohibitively long for long T_1 values, the fast inversion recovery (FIRFT) method is a useful modification. This modification allows relatively short waiting times, namely $W \geq 2T_1$. The signal intensity obeys:

$$I_\tau = I_\infty\{1-[2-\exp(-W/T_1)]\exp(-\tau/T_1)\} \qquad ---(1.42)$$

A dynamic steady state which requires the elimination of the first 10 scans must be reached before acquisition. Unfortunately the FIRFT method is sensitive to pulse value missetting and carrier offset position. A three parameter, direct exponential fit is strongly recommended[53] to estimate T_1.

The SRFT method has a pulse sequence similar to the IRFT method but with a 90° pulse (or 90° pulse train) replacing the 180° pulse:

$(90)_i$ -τ-90-ACQUIRE

Now the signal intensity is:

$$I_\tau = I_\infty[1-\exp(-\tau/T_1)] \qquad ---(1.43)$$

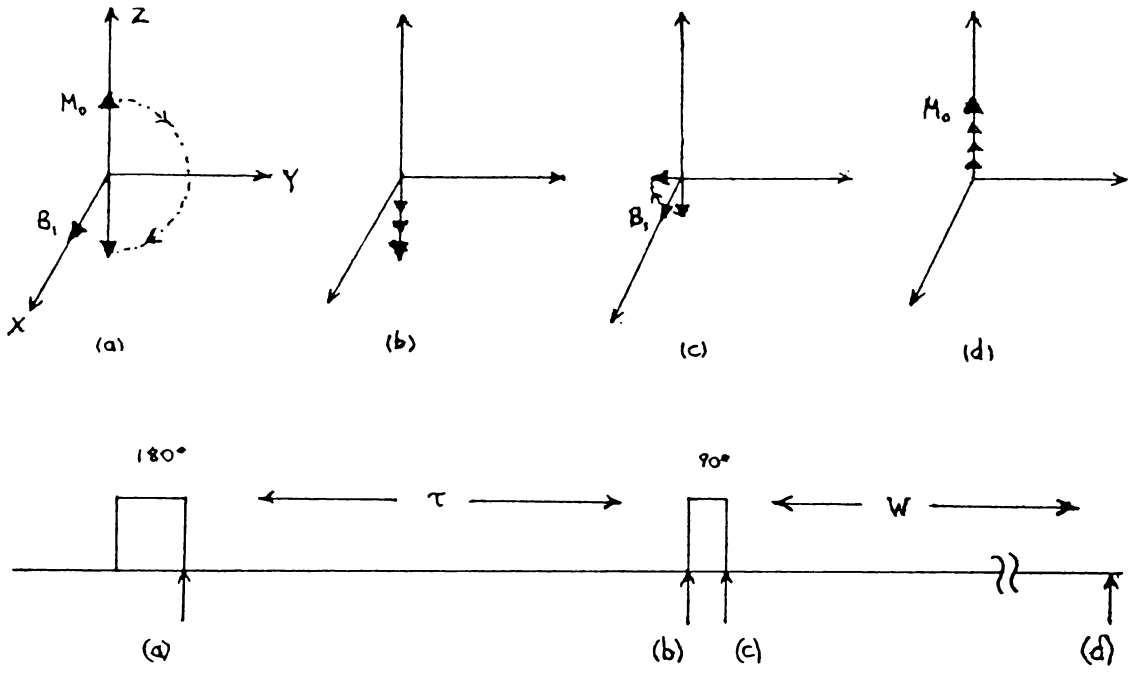

FIG. 1.4 Behaviour of the magnetization vector and the corresponding pulse sequence in an inversion recovery experiment. For short values of τ ,longitudinal magnetization is still negative, and an inverted FT signal is seen. For long values of τ,the signal is positive. The intensity, I_∞ which corresponds to the equilibrium magnetization is obtained from $\tau > 5T_1$.

An homospoil pulse can be inserted between the 90° pulse train $(90°)_i$ and the variable delay τ, and again after the FID acquisition to avoid the build up of echoes. A small, but non-trivial waiting time of up to 100 ms is required for good field homogeneity to be restored. This method is sensitive to pulse value missetting.

Accurate T_1 measurements require the observance of a number of experimental precautions and a knowledge of the possible sources of error. There should be good sample preparation (section 1.2.3) and accurate pulse angle adjustment. The offset condition, with respect to the carrier frequency will lead to systematic errors.[54] The IRFT method is the least sensitive to this effect. Systematic errors are also introduced by r.f. field inhomogeneities, but can be reduced by good

sample preparation or a multiparameter fit for the data.[54] In order to fully realize the available dynamic range, the receiver gain should be optimized.

Finally the T_1 value is obtained by fitting the measured signal intensities and the corresponding variable parameter (τ_i) to the theoretical variation of signal intensities. A semilog plot is warned against[55], but a least-squares fit is satisfactory. Multiparameter direct exponential fits are the best of the three fitting procedures.

Since the IRFT method appears to be the least sensitive to systematic errors (cf. all principal methods)[56,57,58] it will probably be preferred to the SRFT method, except in cases where the waiting time is prohibitively long for the former method. However, regardless of the method, it is prudent to first measure T_1 on a standard sample, and optimize the relevant parameters before measuring a new T_1 value.

1.3 FTNMR AT WAIKATO

This section contains a collection of experimental details pertaining to FTNMR at Waikato University.

1.3.1 Spectrometer Specifications

An abbreviated version of the specifications of the JEOL FX90Q spectrometer is listed.

Operating frequency ^{1}H 90 MHz

Magnet 2.11 T electromagnet, mass 0.9 tons, power consumption 8 kVA

Detection Quadrature Phase Detection (QPD)

Lock Int. or External, Auto or manual, heteronuc. ^{7}Li or ^{2}D

Probes Two broadband: 'Low frequency'(2.76-6.5 MHz) and 'Broadband'. also Dual $^{13}C/^{1}H$

S/N test ^{13}C, 180 (Dual probe plus QPD, 90° single pulse 90% ethylbenzene)

Minicomputer TI 980B 750 nsec/word, 16 bit, 56K (40K data storage)

Computer control Light pen on cathode ray tube screen

External memory Twin Floppy Disc drive

Pulse programmer PG200 programmable, 64 addresses (machine language),13 bit

ADC 12 bit, 2 channel (FREQU $\leq$ 30 kHz)

Foreground/Background System, Homospoil pulse system

Proton irradiation phase shifter, Spin-Lock unit, Var. temp. unit

Multinuclear observation is facilitated by two broadband probes, a broadband frequency synthesizer, and a broadband preamplifier. Any nucleus from ^{103}Rh at the low frequency limit, to ^{1}H, can be observed with the exception of nuclei resonating in the region of ^{205}Tl. To stabilize the input circuitry when using the high inductance low frequency (LF) probe the supply voltage is reduced, and so pulse widths are increased.

Light-pen control is probably faster than keyboard-type input of parameters.

The foreground-background system allows real-time monitoring of an accumulation, providing more efficient use of time, and less reliance on predictions of S/N based on the sample, compared to 'pre-set' accumulations.

This spectrometer has a small static field when compared to superconducting magnets which have fields typically up to 10 T. A lower B_o gives intrinsically lower S/N (section 2.1.1) and, in general, less signal dispersion. (Unlike 'superconducting magnet spectrometers', 'electromagnet spectrometers' cannot be run in the unlocked mode.)

On the other hand, the spurious acoustic ringing pulse at low frequencies[59] is proportional to B_o^2. As B_o is decreased, the narrowing condition becomes less stringent with respect to τ_c, and the NOE becomes more efficient for a given value of τ_c.[7a] The chemical shift anisotropy relaxation mechanism becomes less efficient as B_o decreases.[7b] Finally, the lower cost associated with a lower field spectrometer can allow more flexibility in its use for research purposes. For instance, lower cost machines are more accessible to research students, in general.

1.3.2 A Search Routine for NMR Isotopes

Following is a routine developed for the FX90Q spectrometer for finding a new NMR isotope.

Preparation Pick a reference compound with a known Ξ value. If such a reference is unavailable, choose a sample with a well defined δ value with respect to a reference which has a Ξ value, and use the following equation to obtain Ξ for the sample:

$$\Xi_{sample} = \Xi(1+\delta_{sample}/10^6) \qquad ---(1.44)$$

Use the same concentration and solvent as specified in literature, if possible. To obtain the exact resonant frequency on the FX90Q, multiply

LOCK	SAMPLE	k
D_2O in 10mm tube	5mm	0.89604052
D_2O in 5mm	10mm	0.89604050
$CDCl_3$ in 10mm	5mm	0.89603822
LiCl(sat.aq.) 5mm	10mm	0.89603956

TABLE 1.2 Factors,k for obtaining the resonant frequencies of a reference (or sample) in the JEOL FX90Q spectrometer, knowing Ξ (or Ξ_{sample}),for various locks.

Ξ (or Ξ_{sample}) by a factor k, giving the exact static field experienced by the sample. Table (1.2) shows a selection of these constants, which were obtained from the ^1H resonant frequencies of TMS under the appropriate lock conditions (Appendix 1).

Estimate, from literature, as many as possible of the following parameters for the chosen compound: $W_{\frac{1}{2}}$, T_1; from eq (1.40), section 1.2.7, and γ, estimate t_{90}, and estimate the number of scans to yield an identifiable signal.

Initial Instrument Parameters The frequency position is:

$$\underset{(MHz)}{\nu_{FX90Q}} = \underset{(MHz)}{(OBFRQ)} + \underset{(kHz)}{(OBSET)}/1000 \qquad ---(1.46)$$

where the constraints are that the 'primary frequency parameter', OBFRQ is an odd number with 2 decimal places (2.70-90.00 MHz), and the carrier offset, OBSET, is any number of up to 6 digits in the range 0-100 kHz. OBSET should be near 50 kHz to make sure the following condition is fulfilled:

$$\underset{(kHz)}{(OBSET)} + \underset{(Hz)}{(FREQU)}/2000 < \underset{(kHz)}{100}\ , \quad \underset{(kHz)}{(OBSET)} - \underset{(Hz)}{(FREQU)}/2000 > 0 \qquad ---(1.47)$$

where FREQU is about 30-10 kHz for broad signals or about 20-10 kHz for sharp signals.

Choose POINT to be small, 1K-4K, for broad signals or to be larger, 4K-16K for sharper signals.

The pulse time PW1 is translated into an approximate tip angle when t_{90} has been estimated. (Software automatically computes ACQTM from POINT and FREQU.) With reference to eg (1.39), section 1.2.7, have a small value of W, and adjust PW1 to give the optimum tip angle. The waiting time is simply the delay time, PD, plus ACQTM. For instance, for long T_1 values α_o can be 20°, and for short T_1 values, α_o can be about 90°.

Accumulations If no NMR signal is seen when the predicted number of scans to see a signal has been exceeded, repeat the accumulation with ν_{FX90Q} higher and/or lower by about (FREQU)/2. This procedure can be used in the 'automatic measurements' mode with OBFRQ or OBSET as the stacked parameter, provided that the frequency range allows the probe to be kept in tune.

If no NMR signals are seen now, /check for mistakes in the predictions (especially ν_{FX90Q}), or sample preparation and positioning, or instrument parameters. Failing this, check the literature (eg. Primary literature quoted a figure as a resonant frequency that was in fact an OBFRQ setting).

When a signal increases in S/N with the number of scans, find the frequency of the signal, ν_{signal}. The value of OBSET corresponding to the signal is found by the so-called IRSET spotting procedure. Repeat the accumulation with FREQU reduced by a factor of about 2 and OBSET adjusted to put ν_{signal} near the centre of the screen. If the signal disappears, or it changes its apparent frequency, then it is an artifact. The most common artifact is a folded signal, which behaves in a predictable way, (FIG.(1.5)) and so it can be accounted for.

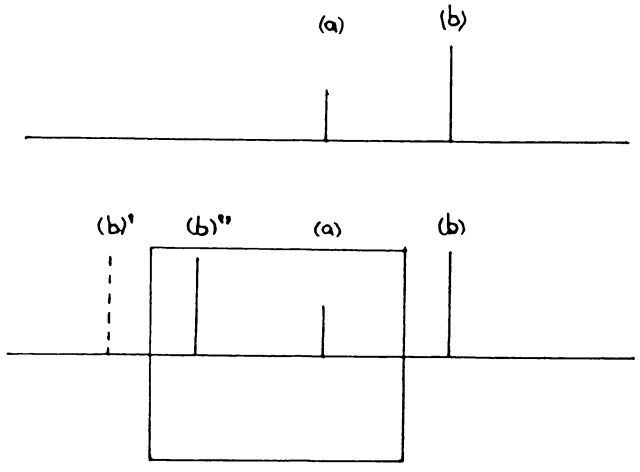

FIG. 1.5 Folded signal from the FX90Q spectrometer. Signal (a) appears in the spectral window in the correct frequency position, being just outside the window, but (b) acts as if it is reflected about the centre of the window to (b)' and then reflected about the end of the spectral window to appear in the window at (b)''. MAIN SOLUTION: Put window where the real signals (a) and (b) are.

If the signal passes the above tests, then the instrument parameters of the last accumulation should be kept, and another accumulation should be started, with only the lock material in the probe. When the same signal appears under these conditions, this is not an NMR phenomenon (eg. there is a non-NMR signal at 16.004 MHz). The non-appearance of the signal under these conditions means that the original signal was most probably an NMR signal. (Assuming the predicted parameters, especially ν_{FX90Q}, are close to the experimental ones.)

A useful feature of a broad line, when a sample is in the probe, is that if it disappears when only the lock is in the probe, it is very likely to be an NMR signal. On the other hand, sharp lines can be 'spikes' which change position the next time an accumulation is run,

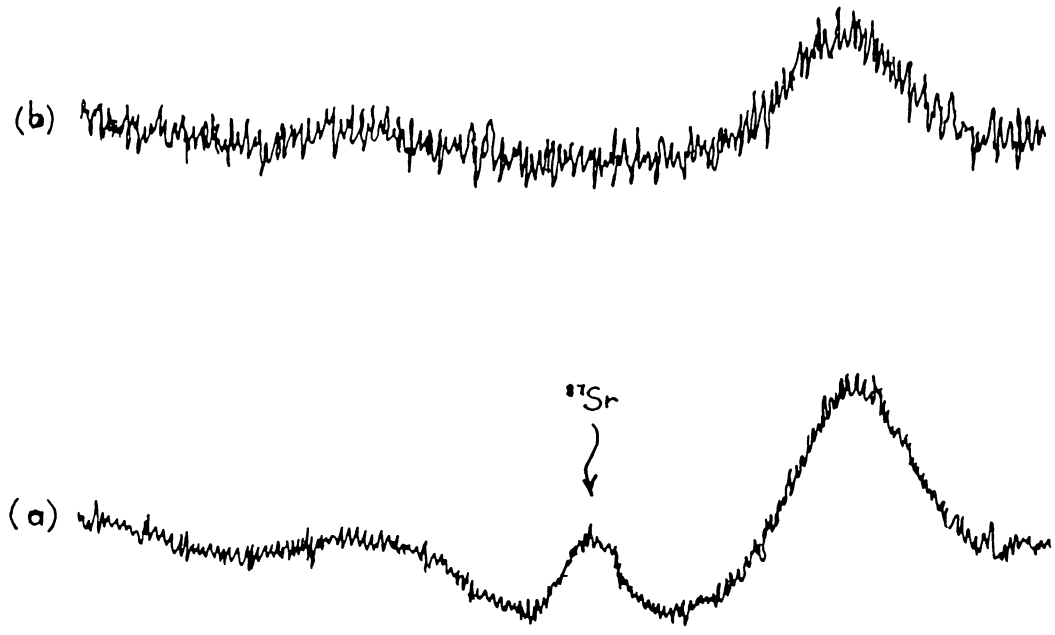

FIG. 1.6 Search for ^{87}Sr resonance in saturated aqueous $Sr(NO_3)_2$. (a) Sample plus lock. (b) Lock only. Broad peaks in (b) are due to acoustic ringing.

regardless of the existence of a sample. Thus a sharp line that is a candidate for a 'new' NMR signal is usually looked for in more than one accumulation.

Example of search operation

An example of one of the more difficult searches is provided by ^{87}Sr. From literature[7,60] a sample of $Sr(NO_3)_2$ saturated in water has: $T_1 < 10^{-2}$ (s), $W_{\frac{1}{2}} \sim 10^3$ (Hz), $t_{90} \sim 100\mu s$, δ (rel. to $SrCl_2$) = -50 ppm and about 10^3-10^4 scans are required to identify the signal.

Ξ ($SrCl_2/D_2O$) = 4.3338 (MHz), Ξ ($Sr(NO_3)_2$ /sat. H_2O) = 4.3337 (MHz)

ν_{FX90Q} = 3.8832 (MHz), OBFRQ = 3.83, OBSET = 53.20, PD = 5 ms

PW1 = 100 μs.

A signal is found at 3.8832 (MHz), with $W_{\frac{1}{2}}$ = 280 Hz, after 10^2 - 10^4 scans (FIG.(1.6(a))). Since the observed parameters are close to the expected ones, especially for ν_{FX90Q}, the signal is very likely to be

from ^{87}Sr. However, spurious signals from acoustic ringing are common at this low frequency. Repeating the accumulation without the sample (FIG.(1.6(b))) resulted in the non-appearance of this signal. (As a further check, ideally, the spectrum should be recorded with a smaller value of FREQU (and POINT), but the $W_{\frac{1}{2}}$ to FREQU ratio is already large, making it difficult to phase correctly.)

1.3.3 The Low Frequency Probe

Figure (1.6) exhibits an unfortunate feature of the LF probe, namely acoustic ringing. It arises from the electromagnetic generation of ultrasonic standing waves in the probehead. In the presence of B_o, acoustic energy is converted to an oscillating magnetic field which is sensed by the detection coil as a broad signal. The ringing pulse is proportional to B_o^2 and to the transmitter pulse amplitude for observation frequencies in the range 5 to 20 MHz.[59]

The major method (section 1.2.8) used to reduce acoustic ringing is zero filling the front of the FID, by setting the FID parameter, T2, to 1-6 (eg. FIG.(1.6)). When FREQU $\leq$ 5000 Hz, and POINT$\geq$4K the software pre-set delay between the pulse and the onset of acquisiton, DELAY, is at least 150 μs, and when used with FID zero-filling, acoustic ringing is not a problem for sharp lines. The higher the S/N per scan, the smaller the intensity of acoustic ringing (eg. more intense ^{73}Ge signals, with FREQU $\leq$ 3000 Hz show no acoustic ringing even with standard DELAY, T2 settings).

DELAY is often increased to about 200 μs when a large value of FREQU and/or a small value of POINT reduce the pre-set value of DELAY below 100 μs (section 1.2.7).

A 90-τ-180 echo sequence (section 1.2.10) has been found useful when long accumulations and large values of FREQU are routinely used (eg.^{17}O),

but otherwise, the previous techniques are similar in performance, and easier to use than this pulse sequence (eg. ^{73}Ge).

Sensitivity enhancement and multiplicity assignment sequences have the advantage of allowing negligible acoustic ringing.

1.3.4 NMR Isotope Parameters

A list of all the most important NMR parameters required for the observation of specific isotopes on the FX90Q is contained in appendix 1. Instrumental parameters were obtained from spectra of chosen samples.

Chemical shift referencing equations and resonant frequencies (Ξ) are also included. Experimental values of Ξ from the FX90Q are listed with two other independent sources, and for each isotope there is close agreement between experimental and literature values.

CHAPTER 2 POLARIZATION TRANSFER IN LIQUID STATE FTNMR

2.1 OUTLINE

An introduction to polarization transfer and a literature review are presented in sections 2.1.1 to 2.1.6. There is an emphasis on the most widely used method of PT, that is, the class of pulse sequences named INEPT.

Two dimensional spectroscopy using PT is not discussed, since, at the time of writing, 2D FTNMR at Waikato University is experimentally inaccessible or very limited in scope, due to a lack of disc storage space. However, attention is drawn to references on 2D PT experiments.[61-66]

Section 2.2 examines INEPT in more detail, giving calculations of the parameters for INEPT from the present work, and an overview of the scope of INEPT.

Methods and results of preliminary experimental work using INEPT are presented in section 2.3.

2.1.1 Sensitivity to the NMR Experiment

There is a very large range of sensitivity to the NMR experiment shown by spin species in the Periodic Table. Natural abundance sensitivity at constant field, (section 1.1.9) R_I, varies by 10^7, due to differences in N, γ and I.[6a] Alternatively, the magnetization[1a] can be shown to determine the eventual signal intensity:

$$M_0 = (\hbar^2/3k_B)\ (NB_0/T)\ [\gamma(I+1)]^2 \qquad ---(2.1)$$

Thus signal intensity is also proportional to magnetic field strength and inversely proportional to temperature, T. (A relative sensitivity can be defined, which is a function of B_o as well as N, γ, and I. This quantity is proportional[4a] to $(B_o)^{3/2}$.)

As mentioned in section 1.1.9, the experimental parameter of direct interest is the detectability, D_I, defined in eq (1.30).

An increase in sample tube diameter will lead to an increase in D_I via an increase in the number of spins which resonate in the detector coil, N_d. In fact D_I varies as the square of the sample tube diameter, so that going from a 5 mm to a 10 mm tube increases D_I fourfold. This improvement is somewhat attenuated by an increase in pulse imperfections, a lengthening of pulse times, and a reduction of T_2^* compared to T_1.[6b] Alternatively, N_d can be increased by isotopic enrichment. Although expensive for unusual isotopes, enrichment for some isotopes like ^{13}C or ^{17}O is not uncommon.

Reductions in correlation time for quadrupolar nuclei will result in an increase in D_I due to the important $W_{\frac{1}{2}}$ factor. Correlation time can be diminished by reducing the viscosity of the solution or by heating the solution.

Long $T_1(I)$ values are a significant factor in reducing D_I for some spin $\frac{1}{2}$ nuclei. Relaxants can be added to reduce $T_1(I)$ when dipole-dipole relaxation dominates. An intermolecular dipole-dipole interaction developed in the solution can also shorten $T_1(I)$ for some spin $\frac{1}{2}$ nuclei.

Detectability can be improved not only by physical methods, but also by increasing the receptivity of the nucleus I itself. This latter effect can be achieved by transferring spin polarization from another nucleus of higher receptivity to I.

2.1.2 Nuclear Overhauser Effect

In modern FTNMR spectroscopy, a factor of some importance is the nuclear Overhauser effect, NOE, which arises[67] in double-resonance experiments when say, nucleus I is observed while species S is irradiated. This effect is discussed in section 1.1.8.1, and 1.2.11.1. Under normal conditions, the NOE lies between 1 (no effect) and a maximum given by

$$(NOE)_{max} = 1 + \gamma_S/2\gamma_I \qquad ---(2.2)$$

For ^{13}C NMR under ^{1}H irradiation, a welcome enhancement of 3 is obtained, which is not far from the $(NOE)_{max}$. If either γ_S or γ_I is negative, the intensity of the double resonance signal can be zero or less than that of the single resonance. Most modern FT experiments are carried out under conditions of ^{1}H or ^{19}F irradiation, and so NOE diminuition of signals can be a problem for the observation of spin $\frac{1}{2}$ nuclei with negative magnetogyric ratios. Gated decoupling techniques are often used to remove the NOE in this case. For a given correlation time, the NOE generally diminishes as the observing field is increased.

Spin $\frac{1}{2}$ nuclei in proton solvents sometimes experience an intermolecular NOE, and an increase in signal intensity when the proton solvent resonance is irradiated.

These NOE effects, however, are rarely observed for nuclei with spin, $I>\frac{1}{2}$, because the dipole-dipole relaxation mechanisms that are necessary for the NOE are dominated by quadrupole interactions.

Hereafter, the common usage of polarization transfer (PT) is used, that is, any PT not including Overhauser polarization.

2.1.3 Polarization Transfer Via Spin-Spin Coupling

In the quest for increased detectability of NMR signals of insensitive nuclei, one good solution is the use of PT. Spin polarization is transferred from a nucleus, S with a large magnetogyric ratio (usually a proton) to the nucleus to be observed, I, which has a relatively small γ value. Heteronuclear spin polarization in the rotating frame is transferred via dipolar spin-spin coupling in solids, or scalar spin-spin coupling in liquids.[68] The maximum enhancement is approximated by;[69]

$$(PT)_{max} \cong \gamma_S/\gamma_I \qquad ---(2.3)$$

By comparison with the $(NOE)_{max}$ in equation (2.2), this PT maximum enhancement is greater, and there will be no reduction in signal due to $\gamma_S = -\gamma_I$. The third point making PT enhancement potentially superior to the NOE is that the recycle time for the PT experiment is, in general, faster than an NOE experiment. Workers[69,70] using spin $\frac{1}{2}$ nuclei report that the PT recycle time is governed by proton relaxation rates, $(T_1)^{-1}$, which are faster than the cross relaxation rates, $(T_{SI})^{-1}$, that dominate recycle times for the NOE experiment.

2.1.3.1 Selective Population Inversion

One method of PT is the selective population inversion experiment.[1b] Line intensities of coupled spectra can be enhanced.[71] However, the experimental requirements are rather stringent, being precise positioning of the double irradiation frequency upon usually unobservable S satellite transitions associated with I, and a large coupling constant, J (S,I). Only one line at a time in the proton (S) spectrum can be perturbed. (On the other hand, this experiment can be performed on any FT NMR spectrometer equipped for gated proton irradiation.)

2.1.3.2 Cross Polarization

Cross polarization (CP) via Hartmann-Hahn contact in the rotating frame is familiar in solid state NMR[68,72], and has been applied to liquid state high resolution NMR with considerable success.[73,74,75] For J-CP, a selective 90° pulse is applied to the S nucleus resonance and followed by a non-selective pulse in the I nucleus, with the Hartmann-Hahn condition fulfilled. That is;

$$\gamma_S B_2^S = \gamma_I B_1^I$$

where B_2^S and B_1^I are the strengths of the decoupling, and observing r.f. fields, respectively.

However, a disadvantage of this technique is its sensitivity to any mismatch between the S (usually protons) and the I r.f. coils, which makes necessary the construction of probe coils doubly tuned for protons and I, a procedure that generally reduces the basic I sensitivity. Improvements have been made,[76] notably adiabatic J-CP,[77] but the experimental conditions required for liquids are still hard to obtain on an ordinary modern FTNMR spectrometer.

2.1.4 Insensitive Nuclei Enhancement by Polarization Transfer

In early 1979 Morris and Freeman[69] reported a pulse sequence giving a differential PT without the need for special doubly tuned probe coils and their associated disadvantages. In fact, the only non-standard feature of the spectrometer for proton PT was the provision of a computer controlled 90° phase shift on the proton transmitter. There were minor modifications to improve timing stability, but later workers[70,78] have not found these necessary. Since the pulse sequence bears a superficial resemblance to the driven equilibrium FT method for sensitivity enhancement. Morris and Freeman adopted the acronym INEPT (Insensitive nuclei enhancement by polarization transfer).

This first paper on proton coupled ^{13}C INEPT reported a PT sensitivity enhancement over unenhanced proton coupled spectra of pyridine of 5 to 6. Enhancement arose partly from the spin population effect, (γ_H/γ_C) of about 4. It also came from a faster repetition time for the PT experiment compared to the normal NOE type experiment. The PT recycle time is governed by the relatively short proton spin-lattice relaxation time. In addition, the expected PT intensity ratios for multiplets, being -1:1 for doublets, -1:0:1 for triplets, and -1:-1:1:1 for quartets,[79,80] was confirmed for doublets. A differential PT generates these multiplet lines, which are polarized positively and negatively so that the total polarization of each multiplet vanishes. As a consequence of the multiplet intensity ratios, proton decoupling straight after the final I 90° pulse would collapse the antiphase signals, and hence lose any enhancement. A delay (Δ) between the final pulse and acquisition is required to allow the multiplet components to come into phase before the onset of decoupling.

Later, Morris[70] reported both proton coupled and decoupled ^{15}N NMR using INEPT. The original proton coupled pulse sequence was used, together with the modification of an appropriate delay between the final

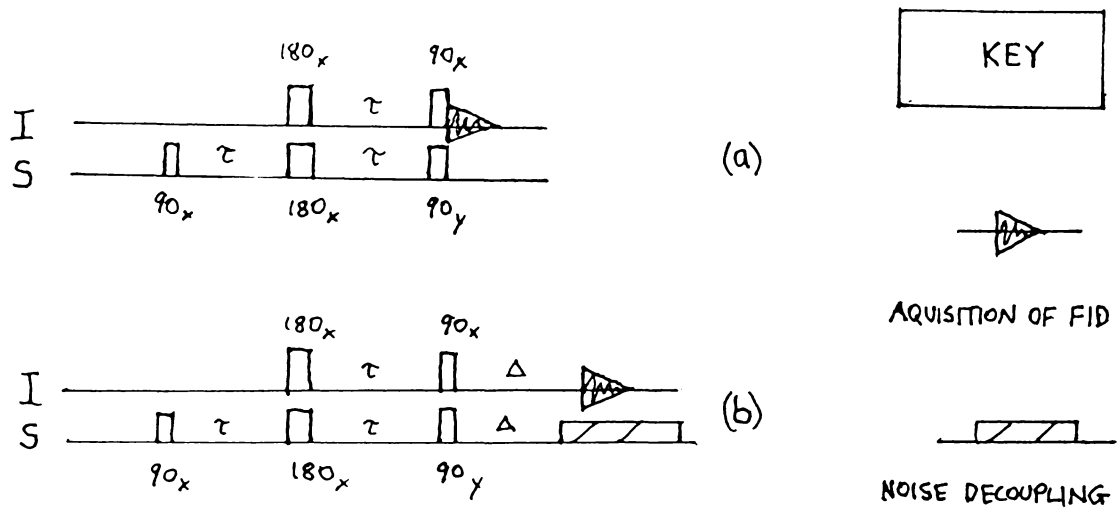

FIG. 2.1 INEPT pulse sequences proposed by Morris and Freeman[69,70] for S coupled (a), and S decoupled (b) spectra. Phase alternation of the final S pulse removes signals not due to PT. The irradiation channel, S, is usually for ^{1}H.

pulse and acquisiton to allow recording of the enhanced proton decoupled spectrum. The pulse sequences used are illustrated in FIG.(2.1), where the notation α_i indicates that, in the ^{1}H rotating frame, the r.f. pulse is applied along the i axis (x or y) to rotate spin magnetization α degrees (90 or 180) from its original position. When the observation nucleus, I, has a spin of $\frac{1}{2}$, the time, τ is $(4J)^{-1}$. An explanation of the operation of INEPT is given in section 2.1.4.1.

Using a sample of blocked glycylglycine, Morris procured sensitivity improvement factors for proton coupled and decoupled ^{15}N spectra of 15, and 8, respectively, over the unenhanced spectra, and 4, and 2, respectively, over the nuclear Overhauser enhanced spectra. The NOE enhancement is at its theoretical maximum of -4 for the sample chosen. Both spin population effects and recycle time effects contributed to the sensitivity improvement, and the signal enhancement was about 80% of that predicted.

Thus the utility of INEPT as a sensitivity enhancement tool was demonstrated. In the following review of literature, unless otherwise

specified, it is assumed that polarization is transferred from protons (S) to the observed nucleus (I).

Shortly after the Morris and Freeman work, another application of INEPT was proposed independently by Burum and Ernst[81] and by Doddrell and Pegg.[78] Doddrell and Pegg found that decoupled INEPT sequences allowed assignments of CH, CH_2, and CH_3 resonances in much shorter times than the conventional off resonance decoupling. Since different types of carbon have different intensity cycles with respect to Δ, by judicious alteration of this timing parameter, different carbon atoms can be identified. For CH doublets, at $\Delta=(2J)^{-1}$ there is a maximum, while CH_2 triplets and CH_3 quartets are zero. At $3(4J)^{-1}$, CH_2 and CH_3 groups are of maximum, and near maximum intensity, respectively, and of opposite sign. At $(4J)^{-1}$, CH_3 groups have the same relative phase as at $3(4J)^{-1}$. Finally, CH_2 groups have phase alternating maxima at $(4J)^{-1}$ and $3(4J)^{-1}$. This was demonstrated using cholesterol. However, the delay, Δ, introduces a large, linear, phase (LP) variation across the spectrum given by

$$LP \simeq 180^\circ \ (\Delta/DW)$$

where DW is the dwell time. Phase roll and baseline instability result from this LP variation. Doddrell et al further noted that although the spectra were recorded with the standard cross coil, high resolution probe system, which gives inhomogeneous ^1H r.f. pulses, this inhomogeneity results in a loss of signal to noise ratio (S/N) but no loss in phase information. They used essentially the same pulse sequence as Morris and Freeman.

Burum and Ernst[81] performed a similar study using ^{13}C INEPT as an assignment aid. In addition they computed the dependence of the decoupled enhancement factors on Δ, and gave experimental values, confirming the theory for CH, CH_2, and CH_3 groups in isobutyl chloride.

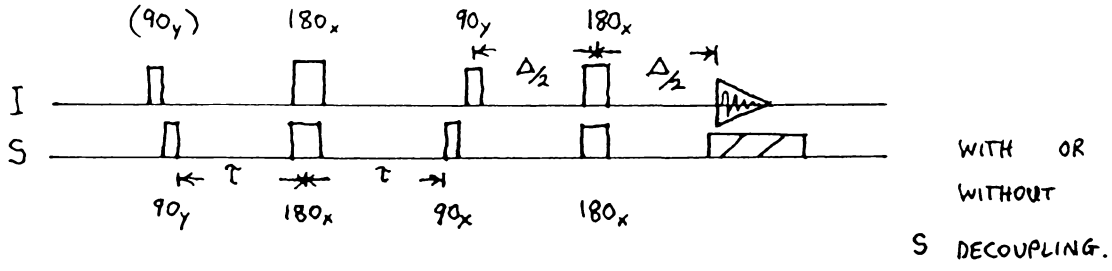

FIG. 2.2 INEPT pulse sequences used by Ernst and Burum.[81] When S decoupling is employed during detection, the initial 90°_y, I pulse is not necessary. 90° pulses are applied sequentially.

The coupled pulse sequence used (FIG.(2.2)) has a free precession time, Δ, before acquisition, giving a net PT rather than the differential PT evident in Morris and Freeman's sequence. Thus all non-zero signals are positive.

Another[81] discovery made was that the initial ^{13}C magnetization distorts the multiplet intensity ratios in coupled ^{13}C INEPT. This distortion can be removed by destroying this initial magnetization with an initial 90°_y ^{13}C pulse (FIG.(2.2)). Using coupled INEPT on $CHCl_3$, this effect was elegantly shown. A further reported advantage of INEPT over conventional pulse sequences is the minimal amount of sample heating in the case of INEPT.

Later, the INEPT sequence was shown to be useful for the determination of the ^{13}C NMR spectra of paramagnetic transition metal complexes when the relaxation times are long.[82] The relaxation pathway in paramagnetic T.M. complexes is dominated by electron-nuclear dipolar coupling, and so there is little NOE of the ^{13}C signal when proton broadband decoupling is applied. Thus P.T. enhancement via the ^{13}C-^{1}H scalar coupling is particularly welcome. Although PT enhancement is greater than NOE enhancement, the maximum P.T. enhancement (2.7) was only 68% of the theoretical maximum. This relaxation was attributed to the unsuitability

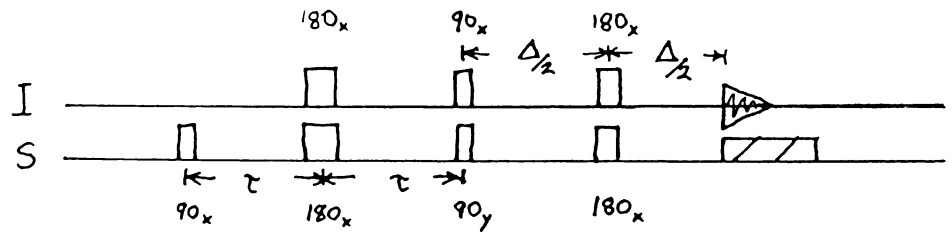

FIG. 2.3 Decoupled INEPT pulse sequence used by Doddrell et al.[82] There is phase alternation of the final $90°_y$ S pulse. (By implication 90° pulses are applied simultaneously.)

of the ^1H saddle coil and decoupling amplifier to produce ^1H r.f. pulses. Doddrell et al used the modified pulse sequence shown in FIG.(2.3). The addition of the two final 180° pulses eliminates phase roll and baseline instability.

Note that phase roll and baseline instability can be reduced also by the addition of only one final refocusing pulse, a 180° I pulse, at the onset of decoupling.[83] The final two time delays are now Δ rather than $\Delta/2$.

Enhancement of the NMR signal of a quadrupolar nucleus using INEPT was first demonstrated by Doddrell et al[84] using the ^{14}N nucleus, in ammonium nitrate. Following a discussion of the spin particle problem of a spin 1 particle scalar coupled to 4 equivalent spin $\frac{1}{2}$ particles, it was deduced that the optimum timing for the coupled ^{14}N INEPT spectrum was $\tau=(8J)^{-1}$ $(\Delta=0)$, with enhancement $(M_H\gamma_H)/\gamma_N$. Here $M_H = \Sigma m_H$ are the spin levels summed over the 4 protons of the molecule. In this case, M_H takes the 5 values ±2, ±1, or 0. For decoupled spectra, the maximum signal is with $\Delta = (6J)^{-1}$, with enhancement $[3/4 \sin(60)\gamma_H]/\gamma_N$. The pulse sequences used were (a) in FIG.(2.1) for coupled spectra, and that in FIG.(2.3) for decoupled spectra. It is useful to define;

$$E\% = \frac{\text{(EXPERIMENTAL ENHANCEMENT)}100}{\text{(THEORETICAL ENHANCEMENT)}} \qquad \text{---(2.4)}$$

The results were that decoupled spectra gave enhancements, E, of 7.1, E% = 79 allowing for the NOE, and for coupled spectra, $|M_H|$ = 1, 2, respectively gave E = 13.85, 27.9, E% = 98, 88.

A short time later,[85] the same research group reported the PT enhancement of ^{29}Si and ^{119}Sn NMR signals in the six compounds; MMe_mCl_{4-m} where M = Si, Sn, n = 2,3,4. They demonstrated the dependence of the enhancement on the number of scalar coupled protons, n. For spin $\frac{1}{2}$ nuclei, they derived the expression for the first maximum of decoupled enhancement as a function of n, with coupling constant J.

$$\Delta_{(opt)} = (\pi J)^{-1} \arcsin n^{-0.5} \qquad ---(2.5)$$

Also, the associated enhancement of (2.5) is given by

$$E_{d(opt)} = (\gamma_H/\gamma_I)n^{0.5}(1-1/n)^{0.5(n-1)} \qquad ---(2.6)$$

COMPOUND	DECOUPLED ENHANCEMENT	E%
$SnMe_4$	5.3	92
$SnMe_3Cl$	3.8	76
$SnMe_2Cl_2$	3.2	76
$SiMe_4$	9.2	85
$SiMe_3Cl$	8.5	90
$SiMe_2Cl_2$	5.0	64

TABLE 2.1 Proton decoupled enhancements of ^{119}Sn and ^{29}Si INEPT over reverse gated decoupled sequences.[85] The INEPT sequence in FIG.(2.3) is used.

Experimental results are tabulated in TABLE(2.1). Reductions in enhancement for the three compounds with the lowest E% values were attributed to short ^{119}Sn and ^{29}Si T_2 values for these compounds. Relative intensities of multiplets in the coupled PT spectrum of $SnMe_4$ (using a differential PT) showed the expected features, namely ratios of 3:30:132:330:495:396:0:-396:-495:-330:-132:30:3.

The workers concluded that enhancements are dependent on n, and the S/N gains measured represent a time saving factor of 10-100 for ^{29}Si and ^{119}Sn NMR spectra. Furthermore, they predicted that the PT sequence would be especially useful for obtaining metal $I=\frac{1}{2}$, NMR signals, provided there is a resolvable coupling constant, and that $(\Delta,\tau) < T_i^{-1}$.

A further pioneering publication for proton PT appeared in 1981. This article[86] by Pegg et al presented the first generalized theory of enhancement by INEPT for any nuclear spin quantum number, I, and for any number of coupled protons, n. The pulse sequences given by Morris and Freeman (FIG.(2.1(a))) and Doddrell et al (FIG.(2.3)) were studied theoretically.

Coupled enhancements, E, of the I multiplet were shown to vary with τ as:

$$E(M_H,I) = \frac{M_H\gamma_H}{\gamma_I} \frac{\sum m_I \dfrac{\sin(4\pi J m_I \tau)}{m_I^2}}{\sum m_I} \qquad ---(2.7)$$

Where $m_I = I, I-1, \ldots, -I$. Values of τ which result in maximum enhancement, $\tau(opt)$, were calculated, together with the associated maximum enhancements, E(opt).

Decouped enhancements, E_d, were shown to vary with Δ as:

$$E_d(n,I) = [E(M_H,I)/2M_H]\, n\cos^{n-1}(\pi J\Delta)\sin(\pi J\Delta) \qquad ---(2.8)$$

Again, values of Δ were calculated which yield maximum enhancement, $\Delta(opt)$, together with these maximum decoupled enhancements, $E_d(opt)$.

This theory is confirmed experimentally by studying proton PT spectra of the ^{10}B and ^{11}B resonances in $NaBH_4$. Allowing for relaxation effects, being mainly from the ^1H T_2, there was excellent agreement between theoretical and experimental functions of coupled enhancement with respect to τ. Actual enhancements reported for the $M_H = \pm 2$ transitions were the

following. For $I = {}^{3}/_{2}$, ^{11}B; $E_{(opt)} = 3.9$, E% = 90, and for $I = 3$, ^{10}B; $E_{(opt)} = 6.0$, E% = 85.

It was concluded that, using the present results for $I = {}^{3}/_{2}$, 3, and known results for $I = \frac{1}{2}$, the theoretical functional dependence of $E(M_H, I, \tau)$ upon τ is generally correct. In addition, the data given for $I = 1$[84] using the ^{14}N resonance in NH_4NO_3, together with $I = \frac{1}{2}$[78-82], using the ^{13}C resonances in CH, CH_2, CH_3 imply that the variation of $E(M_H, I, \tau_{(opt)})$ with Δ is correct, along with the calculation of $\Delta_{(opt)}$ for $E_{d(opt)}$ measurements.

2.1.4.1 Mechanism of INEPT pulse sequences

A summary of the mechanism of INEPT is then followed by a detailed non-mathematical description of the mechanism.

The nucleus to be observed is I, which is scalar coupled to a nucleus, S of higher sensitivity to the NMR experiment, usually a proton. Basically the notion is to 'transfer the higher sensitivity' of the S nucleus to the I nucleus via the coupling, J. To be more accurate, there is a polarization transfer. The 'process of transfer' can be summarized as follows. An I modulated spin echo of S is used to invert one I satellite of each S directly coupled to I. This leads to the full S Boltzmann spin polarization appearing across the connected I transitions.[70]

Although this basic mechanism requires only three 90° pulses, in practice 180° refocusing pulses are almost always added to compensate for chemical shift errors and phase errors. It is this type of INEPT sequence used in practice that will be explained later. A differential PT (observable without S decoupling, but no overall PT) is created by three 90° pulses when no free precession time is allowed after the pulses. A pair of 180° refocusing pulses midway between the three 90° pulses removes the off resonance effects from S (chemical shift errors). If a free precession time, Δ, is allowed after the final 90° pulse, a net

(overall) PT occurs, and a pair of 180° refocusing pulses removes the off resonance effects from I (the effect is to reduce instrumental phase error).

2.1.4.2 Explanation of INEPT Mechanism

For a mathematical description of INEPT in terms of the Heisenberg vector model the reader is referred to the references.[86,88]

A 'hand-waving' type mechanism, as used by Morris and Kowaleski,[87] will be used to show the working of INEPT pulse sequences. In FIG.(2.4) the S and the I magnetization vectors are depicted along with the corresponding timing in the INEPT pulse sequence. Hereafter, reference is made to this figure.

This time evolution is applied to the simple case of one S nucleus and one I nucleus, both spin $\frac{1}{2}$. Sections (a) to (g) show the disposition of the two S magnetization vectors, one attributable to molecules with I in the α state, and the other to those with I in the β state, viewed in a frame of reference at the S transmitter frequency. Similarly, sections (h) to (m) show the motion of the two I vectors, one derived from molecules with S nuclei in the α state, the other to nuclei in the β state, in a frame of reference rotating in synchronism with the I transmitter.

After the initial equilibration delay ....

(a) .... both S vectors are at Boltzmann equilibrium lying along the z axis.

The first $90°_x$ S pulse rotates these ....

(b) .... onto the +y axis ....

Precession takes place for a time $\tau = (4J_{SI})^{-1}$

(c) .... leaving the S vectors at right angles.

The 180° S pulse reflects these about the xz plane ....

(d) .... resulting in a new orientation in the xz plane.

The 180° I pulse ....

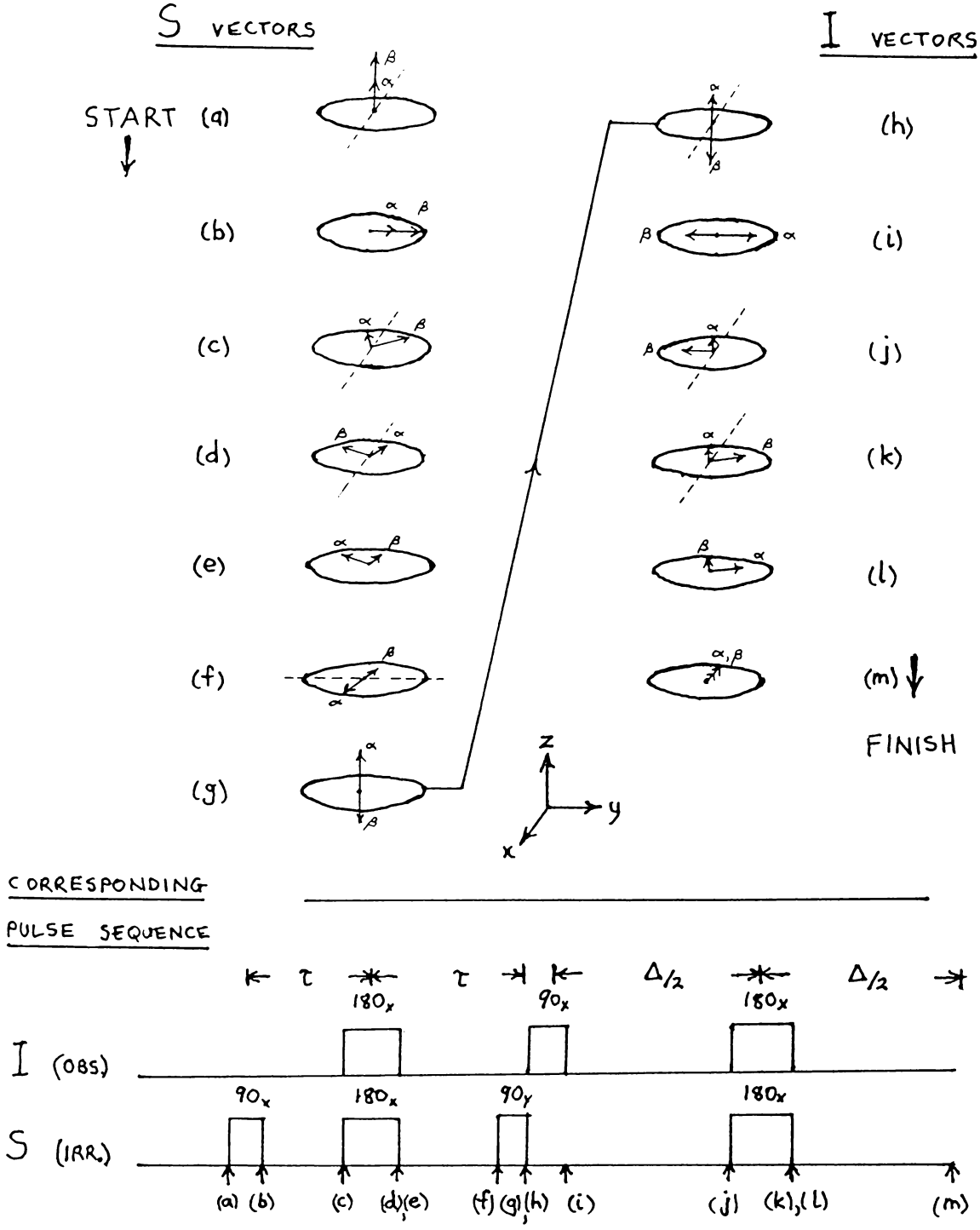

FIG. 2.4 Magnetization vectors at critical times for the pulse sequence shown. Acquisition of I at time (i) results in an S coupled spectrum with half the components enhanced, the others enhanced, but inverted. Acquisition at (m) with S decoupling results in an enhanced, S decoupled spectrum. (See text for full explanation.)

(e) .... leaves the labels α, β interchanged. The order of these last two operations is unimportant. Since the interchange of spin labels also interchanges their frequency, the two vectors continue to diverge until ....

(f) .... they arrive aligned in opposite directions along the x axis. An S 90° pulse is applied along the y axis ....

(g) .... leaving the α magnetiziation aligned along the +z axis, and the β magnetization along the -z axis. Hence, at this time in the sequence, the S part of the spin system has been prepared in a non-equilibrium state in which one I satellite has been inverted, and the other, restored to the +z axis.

IN FACT, THE POPULATION DIFFERENCES ACROSS THE CONNECTED I TRANSITIONS NOW EQUAL THOSE ACROSS THE S TRANSITIONS, if the small, initial I longitudinal magnetization can be neglected, CORRESPONDING TO LONGITUDINAL I MAGNETIZATIONS A FACTOR γ_S/γ_I GREATER THAN NORMAL.

(h) .... The I magnetizations are also aligned along the +z and -z axes, now using the I rotating frame of reference.

An I 90° pulse now rotates the two vectors.

(i) .... leaving these I vectors in opposite directions along the y axis. If acquisition of the I magnetization is applied now, (Δ=0) an S coupled I spectrum is procured, with half the signals enhanced, and the other half, enhanced, but inverted. The application of S decoupling at this point would result in mutual cancellation of the enhanced signal.

On the other hand, assuming threre is no acquisition .... after a further free precession time $\Delta/2 = (4J_{SI})^{-1}$....

(j) .... the two I vectors are at right angles.

The 180° I pulse reflects them about the xz plane ....

(k) .... resulting in a new orientation in the xz plane.

Finally, the 180° S pulse ....

(l) .... gives the I vectors interchanged labels. The order of these last two operations is immaterial.

After a final time delay of $\Delta/2$, the precession ....

(m) .... results in the two vectors coming back into phase.

When acquisition of the enhanced, transverse I magnetization is applied now, together with S decoupling, an enhanced, S decoupled spectrum of I is obtained. The unenhanced component of the signal is removed by phase alternation of the $90°_y$ S pulse with alternate signal addition and subtraction in the receiver.[86]

Similar arguments can be applied to IS_n ($n = 1,2,3...$) spin systems, but now for S decoupled spectra, Δ must be shortened, according to the equations given by Pegg et al.[86]

Again, analogous methods can be applied to IS_n for isotopes of I with spin higher than $\frac{1}{2}$, but τ must be shortened, according to the theories on INEPT timing parameters.[86]

For example, the value of Δ giving maximum enhancement, $\Delta_{(opt)}$, for $n = 4$ is $(6J_{SI})^{-1}$, and $\tau_{(opt)}$ for a nucleus I of spin $^3/_2$ is approximately $(11.32\ J_{SI})^{-1}$.

Strictly, the aforementioned general theories apply to the case of S being a proton. They can also apply to the case of S being any one type of spin $\frac{1}{2}$ nucleus, with as ^{19}F or ^{31}P.

2.1.5 Applications of INEPT

Brevard, van Stein, and van Coten[89] reported results which showed the possibilities offered by the INEPT sequence for the direct observation of ^{109}Ag and ^{103}Rh complexes where these nuclei have a ^{1}H resolved scalar coupling $^{3}J(M, ^{1}H)$. The potential for orders of magnitude reductions in accumulation time due to the INEPT spin population effect and the relatively fast INEPT recycle time, were, in part, realized. These features were demonstrated by ^{109}Ag and ^{103}Rh INEPT on a series of binuclear Ag and binuclear Rh complexes.

INEPT facilitated, for the first time, the structural study of a series of Ag complexes by ^{109}Ag NMR. However, by inspection of the spectra presented, the PT enhancements are somewhat smaller than those predicted by Pegg et al's equations.[86] Coupled enhancement ($M_H=\pm1$) for ^{109}Ag, ^{103}Rh is up to 43 and 64 , respectively. Experimental coupled enhancements were less than half of theory, by looking at the presented spectra, and allowing for the different probes used. Long free precession times from the small scalar coupling (2-10 Hz), and r.f. pulse inhomogeneity at the low observation frequencies could partly account for these reductions. Finally, the up down appearance of the coupled INEPT allowed more accurate determination of coupling constants, especially when resonances are broadened. For example, ^{109}Ag signals are broadened by ^{14}N quadrupolar relaxation.

A number of months later,[90] van Koten, Brevard, and van der Ploeg reported ^{109}Ag INEPT evidence for direct Pt to Ag bonding in a dinuclear AgPt complex. Unique information, which could not be obtained from ^{195}Pt NMR (linewidth 500 Hz) is provided by ^{109}Ag INEPT spectra. Specifically, INEPT allowed observation of a $^{1}J(^{195}Pt,^{109}Ag)$ of ±170 Hz, pointing to the presence of a direct Pt-Ag interaction. Also, the ^{109}Ag INEPT spectra of the complexes supported the data obtained from the ^{1}H

NMR spectra. Remember that ordinary ^{109}Ag NMR would probably have taken too much instrumental time to make this NMR study very practical.

Application[91] of ^{109}Ag INEPT and ^{1}H-$\{^{109}Ag\}$ NMR to a silver (I) complex allowed a study of its stereochemistry.

In early 1982, Helmer and West[92] submitted a note on the application of PT via INEPT to ^{29}Si NMR for a wide variety of silicon compounds. Significant PT decoupled enhancement was obtained for silicon bonded to H, Me, OMe, t-Bu, and Ph. The signal enhancement and relatively fast INEPT recycle times enable potential reductions in accumulation time of 30 to 300 times. INEPT has recycle times a factor of 3 to 6 shorter than conventional single pulse sequences, and E_d ranged from 3 to 9. A typical INEPT pulse sequence used was that given by Doddrell (FIG.2.3)).

Equations formulated by Pegg et al[86] were presented, predicting $\Delta(opt)$, and $E_{d(opt)}$. However, it was stated that $\tau(opt) = (4J)^{-1}$. This is only true for a spin quantum number of $\frac{1}{2}$.

For the compounds already studied by Doddrell et al and given in TABLE (2.1), Helmer and West procured similar values of E%. INEPT via the largest coupling constants, $^{1}J(Si,H)$, gave the largest E% values of about 100 to 72. One expects this result, since the larger ^{1}J constants give smaller free precession times in INEPT, resulting in less signal loss from spin-spin relaxation. Compounds containing Si-Cl bonds have E% ranging from 80 (Me_3SiCl) to 38 ($t\text{-}BuSiCl_3$). Spin-spin relaxation is very fast in these compounds, resulting in a loss of signal.

An interesting feature of the[92] data is the procurement of PT enhancement for three compounds with no resolved scalar coupling. All previous workers have stated that a resolvable scalar coupling is a prerequisite for obtaining PT. (Perhaps selective proton decoupling would result in faint, resolvable coupling for the silicon compounds.)

Some of the limitations of INEPT were highlighted in a paper by Bolton.[93] It was found that the PT method will not, in general, be applicable to macromolecules due to T_2 losses during PT, and since ^{13}C T_1 values will typically be shorter than those of the protons. This point was illustrated using a high molecular weight polynucleotide. However, the use of PT was superior to the NOE when observing protonated ^{15}N or ^{13}C in amino acids or nucleotides.

Hitherto, this review has included INEPT only using proton PT. INEPT using phosphorus PT was reported by Brevard and Schimpf.[94] The requirement is however, a ^{31}P irradiation channel, which is not standard for all commercial FTNMR instruments.

Several reasons are given for choosing ^{31}P. First, ^{31}P has a large γ, and is 100% abundant. Second, a vast range of organometallic compounds are stabilized by phosphine ligands. Finally, the ^{31}P T_1 values in organometallic compounds[1c] are in a reasonable range, although in some cases, an inert paramagnetic relaxation agent should be added to decrease the INEPT recycle time. In fact, ^{31}P T_1 values are 7 to 12 seconds for transition metal phosphine complexes. The workers studied ^{103}Rh, ^{183}W, and ^{57}Fe $\{^{31}P\}$ - INEPT on the metal phosphine complexes, and doped these complexes with 10^{-2} M $Cr(acac)_3$. Looking at ^{103}Rh INEPT, on $RhCOCl-[P(C_6H_5)_3]_2$, the recycle times were 1.5 and 80 seconds, respectively, with and without the addition of $Cr(acac)_3$. In this case, the PT enhancement was 6, giving E% = 47. This reduction was attributed to signal loss in the pulse sequence, since T_2^* is significant compared to the delay, Δ, and from an imperfect r.f. field profile because of strong ($90° \simeq 100$ μs) rhodium pulses.

In conclusion, $\{^{31}P\}$ - INEPT experiments are a good alternative to direct acquisition when observing low γ transition metal isotopes, as long as a resolvable metal phosphorus coupling exists. This method cannot

be compared directly with the Quadriga technique,[6c, 95, 96] which works on single line spectra, and requires spectrometer modification, unlike INEPT.

Furthermore, it was stated that complex phosphorus spectra can be easily used with INEPT, since one can use an average value of τ based on an average coupling constant $J(I,^{31}P)$. However, this insensitivity of τ with respect to J is lost as the spin quantum number of I increases, if one examines the functional forms of $E(M_H,1)$ with τ for different values of 1.[86]

Rinaldi and Baldwin[97] reported the use of PT from isotopically enriched deuterium to ^{13}C as a new NMR strategy for isotopic labelling studies. This strategy takes advantage of both the ^{13}C chemical shift dispersion and the expediency of ^{2}H incorporation.

The selectivity of enhancement was demonstrated for two deuterated aromatic compounds. Although enhancements were less than unity, as they predicted, the fast PT recycle time compared to the single pulse proton decoupled recycle time preserved the obtainable S/N for a given time.

It's interesting to note that the experimental value of $\tau_{(opt)}$ was $(4J)^{-1}$. This is identical with $\tau_{(opt)}$ used for an irradiated nucleus of spin $\frac{1}{2}$. However, $\Delta_{(opt)} = (2.66J)^{-1}$ for one attached deuterium, is different to $\Delta_{(opt)} = (2J)^{-1}$ for one attached proton.

Non-standard hardware modifications were necessary to achieve a deuterium irradiation channel.

2.1.5.1 Modifications of INEPT

Most of the modifications of INEPT are listed in TABLE (2.2). The first three modifications use INEPT with the measurement of T_1. Although modification (3) offers little advantage over conventional inversion-recovery experiments when the 'subject' is a protonated ^{13}C nucleus, considerable time savings were obtained for ^{29}Si and ^{15}N nuclei.

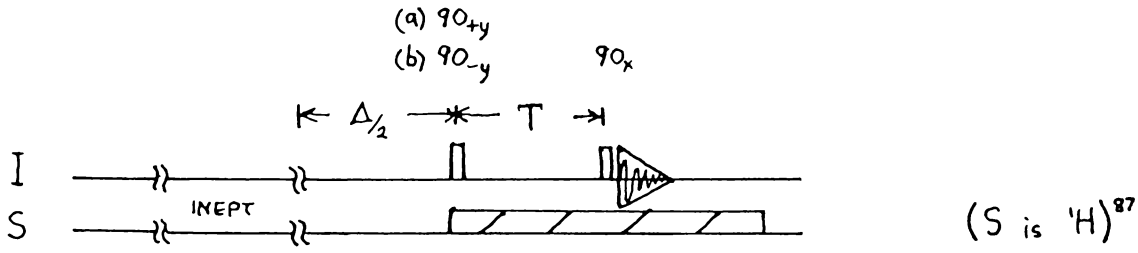

FIG. 2.5 Pulse sequence used for INEPT enhanced measurement of spin-lattice relaxation times for nucleus I. The first seven pulses are the same as the refocused INEPT sequence in FIG.(2.3). Depending on the phase of the penultimate I 90° pulse, either (a) (I has $\eta>-1$) enhanced -z magnetization or (b) (I has $\eta<-1$) enhanced +z magnetization for the I spins is generated. T is the relaxation period.

Any spectrometer equipped for gated proton irradiation can use the sequence SINEPT. However, there is a sine dependence of the ^1H transmitter offset from the individual ^1H chemical shifts.

SEQUENCE	PURPOSE	REFERENCES
(1) I.R. followed by ^{1}H M transferred to ^{13}C via INEPT	Proton T_1 values observed in well dispersed ^{13}C signals. Fast recycle times.	98
(2) INEPT followed by I.R.	Measure ^{15}N T_1 values with sensitivity enhancement.	99
(3) INEPT followed by "pseudo"-I.R.	Measure T_1 for low γ nuclei with sensitivity enhancement. Choice between enhanced I.R. and enhanced dynamic NOE experiment:being (a),(b) respectively in FIG. (2.5) .	87
(4) Presaturation of ^{13}C then INEPT , then INADEQUATE	Observation of ^{13}C-^{13}C coupling with sensitivity enhancment.	100, 101
(5) INEPT ,then 180° ^{1}H pulse	Editing INEPT spectra: easy differentiation of n=1 from n=3 .	102
(6) SINEPT ,INEPT without the first pair of 180° pulses	Can be used on (older) spectrometers without a proton phase shifter.	103

TABLE 2.2 An outline of the modifications to INEPT.
(I.R.=Pulse sequence for inversion-recovery T_1 experiment)
(INADEQUATE=A double quantum transfer sequence)

2.1.6 PT Pulse Sequences Subsequent to INEPT

Some of the PT pulse sequences subsequent to INEPT are listed in TABLE (2.3). The sequences DEPT and UPT are described in the next two sections.

Sørensen and Ernst (TABLE (2.3))[116] reported that a minimum of spectral distortion is introduced by the sequences INEPT+ and DEPT++, which are similar in qualitative performance. Quantitatively, DEPT++ is less susceptible than INEPT+ to having incorrect relative intensities between different spin multiplets, and to incorrect separability of subspectra arising from variations in J value.

2.1.6.1 Distortionless Enhancement by P.T.

A promising type of PT sequence, similar to INEPT, was reported by Doddrell, Pegg, and Bendall.[106,107] This sequence is illustrated in FIG.(2.7) and is called Distortionless Enhancement by P.T.(DEPT). In the special case of the final S pulse, flip angle, θ, being $\pi/2$, the sequence is called exclusive PT (EPT).[108,109,110] This EPT sequence applied to an IS group, both of spin $\frac{1}{2}$, shows a second period, $\tau=(2J)^{-1}$ that has no effect. If this period were omitted and refocusing pulses ignored, the result would still be the same, and the sequence would be a simple INEPT experiment. But, in general, the signals from IS_n groups oscillate during the second period as $\cos^{n-1}\pi J\tau$. For example, with $\tau=(2J)^{-1}$, IS_2 and IS_3 groups give zero signals. However, when $\theta\neq\pi/2$, the detailed analysis of the resulting superposition states is complex.[111] DEPT yields the same maximum enhancements as decoupled INEPT, the replacement of $\pi J\Delta$ by θ giving exact correspondence. The same enhancements for each and every multiplet in coupled spectra are found, each enhancement being equal to that found in the corresponding decoupled spectrum.

Three advantages over the INEPT sequence were outlined.[111]

SEQUENCE	PURPOSE	REFERENCES
SESET ,Semi-selective excitation by PT (Uses DANTES sequence)	Alternative to INEPT when only one I nucleus to be observed,or S nuclei bonded to I are in a narrow frequency range. Selective w.r.t. S chemical shifts.	104,105
DEPT ,Distortionless enhancement by PT	Alternative to INEPT for l=1/2, more "accurate" spectral editing than INEPT. Gives normal FT multiplet intensity ratios.	106,107 108,109 110,111
SEPT ,Selective enhancement by PT	Alternative to INEPT,DEPT for editing coupled spectra.	112
Inverse-INEPT	Observe weak S lines in I spectra. FIG. (2.6)	113,114
Inverse-DEPT	(Observe weak S lines in I spectra.)	115
INEPT+	Less distortion than INEPT, especially for coupled spectra. Gives normal FT multiplet intensity ratios.	116
DEPT+ , DEPT++	Less distortion than DEPT, especially for coupled spectra. DEPT++ better than DEPT+ .	116
UPT ,Universal PT	Multinuclear version of DEPT . (any l)	117

TABLE 2.3 Outline of the PT sequences subsequent to INEPT.

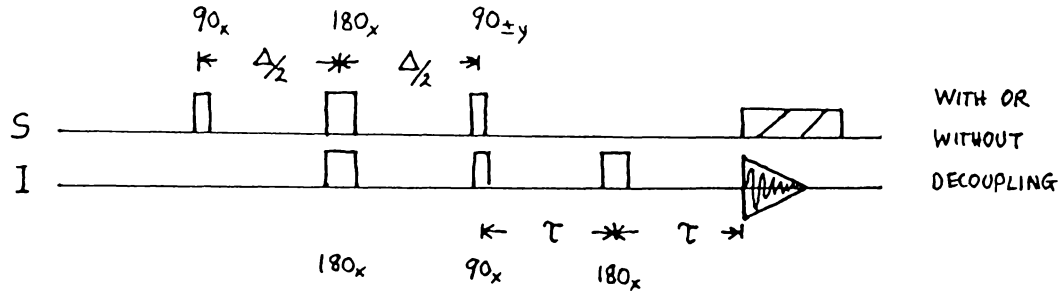

FIG. 2.6 Inverse INEPT sequence, which is used with $\tau=(4J)^{-1}$ for $\frac{1}{2}$ nuclei (TABLE (2.3)).[113,114] Phase alternation of the final I pulse is employed.

There are fewer pulses in DEPT than in seven-pulse INEPT, and so DEPT is less liable to variation from theoretical intensites due to r.f. inhomogeneity or misset pulses.

DEPT has the advantage of a reduced dependence on J, when used for decoupled spectra. Specifically, the parameter used for distinguishing signals with different n, is Δ for INEPT which is dependent upon J, but this parameter is θ for DEPT, which is independent of J. The dependence of intensities on the period $\tau=(2J)^{-1}$ is a second order effect for DEPT.

Ordinary FTNMR multiplet intensity ratios are preserved in the coupled spectra of DEPT, unlike INEPT. Instrumental phase errors were shown to be more serious for coupled seven-pulse INEPT than DEPT.

The utility of this pulse sequence was demonstrated by ^{13}C NMR on numerous compounds including 2-chlorobutane, cholesterol, and cholesteryl acetate.[106,111] The CH, CH_2 and CH_3 subspectra of these compounds were obtained by the linear combinations of $\theta_1=\pi/4$, $\theta_2=\pi/2$ and $\theta_3=3\pi/4$ that gave the greatest cancellation of unwanted spectra. Full spectra use $\theta_1=\pi/4$ only.

Clearly DEPT overcomes some of the limitations of INEPT, and can find widespread use in generating enhanced coupled spectra, spectral editing, and S/N enhancement.

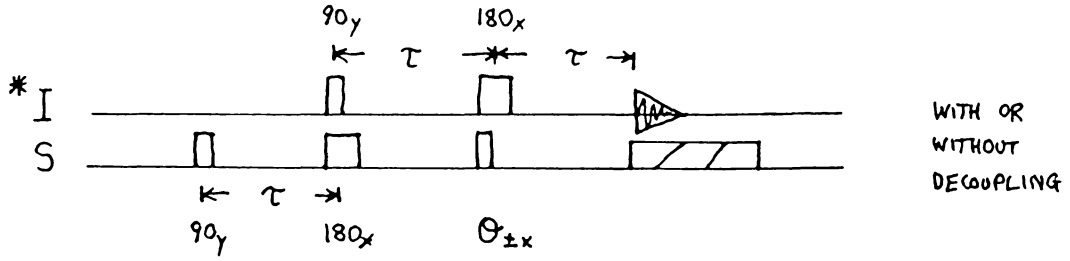

FIG. 2.7 Distortionless enhancement by PT (DEPT) sequence proposed by Doddrell, Pegg, and Bendall.[106] Phase alternation of the final S pulse is employed to cancel unenhanced I signals. *Both heteronuclei are spin-half species. $\tau=(2J)^{-1}$.

One can, however, qualify the stated advantages by the following points.

Zero enhancement of the central, largest multiplet when n is even, is compensated for by the larger enhancement of smaller, outer multiplets. In general, coupled INEPT gives larger enhancements than coupled DEPT for outer multiplets. Some examples for $I=\frac{1}{2}$ are shown in TABLE (2.4).

		COUPLED ENHANCEMENTS						
GROUP MULTIPLET	IH	IH_2		IH_3		IH_4		
	-	INNER	OUTER	INNER	OUTER	INNER	MIDDLE	OUTER
SEQUENCE								
DEPT	1.0	1.0	1.0	1.15	1.15	1.30	1.30	1.30
INEPT	1.0	0.0	2.0	1.0	3.0	0.0	2.0	4.0

TABLE 2.4 Coupled PT enhancements for DEPT and INEPT sequences when nucleus I has spin quantum number $\frac{1}{2}$. Enhancements are in units γ_H/γ_I.

Having five pulses, DEPT has fewer pulses than the usual INEPT sequence for decoupled spectra, which has seven pulses. However, the most commonly used coupled INEPT sequence has five pulses.

Examples of coupled INEPT and coupled DEPT were given,[106,111] and in these spectra, DEPT has less instrumental phase errors. However, coupled INEPT using net PT ($\Delta\neq o$) was used. Despite the up-down appearance

of spectra, the more commonly used coupled INEPT sequences using a differential PT ($\Delta \simeq o$) are less prone to instrumental phase errors.[116]

For compounds with a short T_2, total precession times in a sequence (T_t) can determine the PT enhancement. Coupled INEPT ($I=\frac{1}{2}$) using a differential PT has $T_t = (2J)^{-1}$ while decoupled INEPT has $T_t = (2J)^{-1}+\Delta$. Both coupled and decoupled DEPT have $T_t = 3(2J)^{-1}$. Signal loss due to r.f. inhomogeneity is similar overall for the coupled sequences, both having the same number and type of pulses, and so the shorter T_t, the smaller the signal loss, due to relaxation effects. Thus coupled INEPT gives less signal loss, due to relaxation effects, than coupled DEPT. Decoupled INEPT, generally having two more 180° pulses than DEPT will have a larger r.f. inhomogeneity, leading to more signal loss. On the other hand decoupled INEPT ($I=\frac{1}{2}$) still has shorter total precession times than decoupled DEPT, because Δ is always less than $2(2J)^{-1}$.
If T_2 is short enough, the loss of signal during T_t (for DEPT) will 'outweigh' the loss of signal by r.f. inhomogeneity (for INEPT). This last point is well illustrated by the smaller value of E_d for DEPT (3.2) compared to INEPT (4.2) from the ^{195}Pt spectra of $[Me_3Pt(H_2O)_2]_2SO_4$.[107] In a field of 2T the ^{195}Pt T_2 is short, being about 15 ms.

2.1.6.2 Universal PT

In contrast to INEPT, both EPT and DEPT are restricted to $I=\frac{1}{2}$ heteronuclei. By having two variable pulse angles, a sequence is created which can accommodate any spin quantum number for I.[117] The universality of the sequence suggests its name: Universal PT or UPT (FIG.(2.8)).

Analysis of UPT by a Heisenberg picture approach led to the conclusion that it gives equivalent results, including equivalent enhancements to general INEPT for $I(I)$, $S(I=\frac{1}{2})_n$ systems when $\phi=\pi J\tau$ and $\theta=\pi J\Delta$. This theory was verified for the case of the ^{10}B NMR spectra of $NaBH_4$.[117]

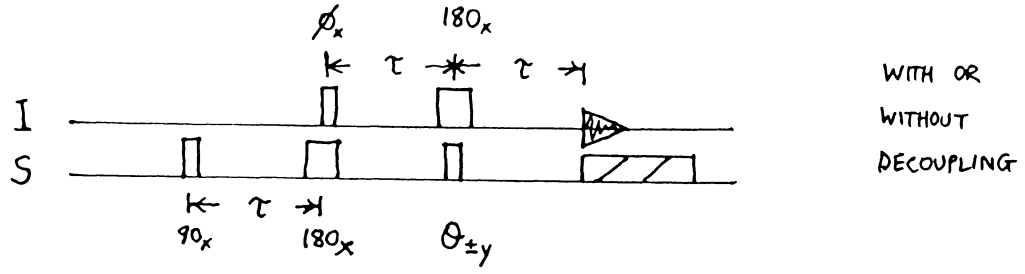

FIG. 2.8 Universal PT sequence[117] $\tau=(2J)^{-1}$. Phase alternation of the final S pulse is employed.

The theoretical curves of signal intensity versus θ and ϕ were compared to experiment, and deviations were attributed to r.f. pulse inhomogeneity.

Just as with DEPT for $S(\frac{1}{2})_n$ systems, UPT was shown to retain the 'normal' FT coupled multiplet ratios. It was predicted that UPT will also retain the insensitivity to missetting the delay periods in spectral editing exhibited by DEPT.

Pegg and Bendall presented a theoretical study of UPT, with experimental support, and showed that it can be used to transfer magnetization from S $(l_2)_n$ systems to other systems, I $(l_1)_m$, where n, m are the number of nuclei scalar coupled to spins l_2 and l_1 respectively, through a single coupling constant.[118]

Later, UPT was used to transfer nuclear magnetization from one quadrupolar nucleus, (deuterium) to another quadrupolar nucleus (boron in BD_4). This pulse sequence was also used to assign multiplicity on CD_n in a manner analogous to DEPT.[119]

2.2 EXAMINATION OF THE PULSE SEQUENCE INEPT

2.2.1 Calculation of INEPT Parameters

As mentioned earlier, Pegg et al[86] derived equations to predict enhancements E, E_d (equations (2.7), (2.8), respectively) and the associated timing parameters τ, Δ for a nucleus I of any spin quantum number, 1, with n scalar coupled protons. In the present work these equations have been necessary, for example with $1=^{9}/_{2}$ ^{73}Ge, to obtain the timing parameters $\tau(opt)$, $\Delta(opt)$ for maximum enhancement, $E_{(opt)}$, $E_{d(opt)}$.

In the light of the utility of these equations, computer programs were created to compute the relevant timing parameters. These programs were developed on the University of Waikato VAX 11/780 computer using BASIC, and are listed in appendix 2. The program INTIME calculates the optimum timing parameter, $\tau(opt)$ and the associated maximum coupled enhancement, E(opt), for any nucleus, I, of spin quantum number 1, proton total spin M_H, and magnetogyric ratio γ_I. Similarly, the timing parameter $\Delta(opt)$, and the associated decoupled enhancement, $E_{d(opt)}$ are calculated for any spin, 1, number of attached protons, n, and γ_I. Output of $\tau(opt)$ with respect to $\langle E_{(opt)} \rangle$ for a given 1, $\Delta(opt)$ with n, and $\langle E_{d(opt)} \rangle$ as a function of n and 1 is calculable. Tables of the aforementioned parameters are also given. The notation $\langle E_{(opt)} \rangle = k_1 E_{(opt)}$ and $\langle E_{d(opt)} \rangle = k_2 E_{d(opt)}$ is employed, where $k_1 = M_H^{-1}\gamma_H^{-1}\gamma_I$, and $k_2 = \gamma_H^{-1}\gamma_I$ are constants for a specific nucleus. The values of $\tau(opt)$ and $\Delta(opt)$ can be given as units of J by; $\tau(opt) = (T(opt)J)^{-1}$ and $\Delta(opt) = (D(opt)J)^{-1}$, or with given J values.

Plots of the coupled enhancements of a nucleus I, of given spin, $E(M_H,1)$, with respect to τ, yield trigomometric functions characteristic of the nuclear spin. Comparison of the experimental functional relation between $E(M_H,1)$ and τ for a given spin, with the theoretical relation is

a good way to check the theory.[86] (Ideally the theory should be checked for each spin.)

In the light of this, a program named FUNC was created, which yields an output of $E(\alpha)$ with respect to α, for a given spin. Here, following the example of Pegg et al;

$E(\alpha) = k_3 E(M_H, 1)$

For a specific nucleus, k_3 is a constant given by ...

$$k_3 = \gamma_I \sum_{m_I} m_I^2 / (2M_H\gamma_H) \qquad E(\alpha) = \sum_{m_I>0} m_I \sin m_I(\alpha) \qquad \text{---(2.9)}$$

$$\alpha = 4\pi J\tau$$

Decoupled INEPT can be used to show[78,81,85] how many protons, n, are attached to the nucleus, I, by the variation of $E_d(n, 1, \Delta)$ with Δ. Output of $E_d(n, 1, \Delta)$ with respect to Δ would assist in obtaining judicious values of Δ which will identify the value of n for I.

One expresses $E_d(n,1,\Delta)$ as $E_d(n,1) = k_4 E_d(\beta)$

Where
$$E_d(\beta) = n\sin(\beta)\cos^{n-1}(\beta)$$
$$\beta = \pi J\Delta \qquad \text{---(2.10)}$$

For a specific nucleus k_4 is a constant

$$k_4 = \gamma_H(2\gamma_I)^{-1} \langle E(opt)\rangle$$

The program PARITY gives output of $E_d(\beta)$ as a function of β, or $k_4E_d(\beta)$ as a function of β. Values of $\langle E(opt)\rangle$ required to evaluate k_4 have already been calculated from the program INTIME.

It is useful to remember that for maximum enhancements, coupled INEPT has $\Delta=0$ (or $\Delta=\Delta(opt)$) and decoupled INEPT requires that τ be set equal to $\tau(opt)$.

In order to calculate maximum coupled enhancements, one must know the $n+1$ values of the 'proton compound state' in the molecule, corresponding to the $n+1$ total proton spin quantum numbers of M_H. Now $M_H = \Sigma m_H$,

where m_H is the z-spin quantum number of a particular proton ($\pm\frac{1}{2}$) and the summation is over the n protons in the molecule.

Thus; $M_H = n/2,(n/2)-1,(n/2)-2,\ldots,-n/2$ ---(2.11)

2.2.1.1 Listing of INEPT Parameters

Given in TABLE (2.5) are the maximum enhancements and optimum timing for INEPT. Namely, T(opt) and E(opt) are given as functions of l, and D(opt) as a function of n, together with $\langle Ed(opt)\rangle$ as a function of n and l. $\tau(opt) = (T(opt)J)^{-1}$ and $\Delta(opt) = (D(opt)J)^{-1}$.

Next, in TABLE (2.6), the maximum $\{^1H\}$-INEPT enhancements are given for a selection of nuclei. Coupled enhancements are given in units of M_H, and decoupled ones, in units of $\langle Ed(opt)\rangle$. For example, maximum coupled enhancements using ^{13}C are 7.954 M_H and for decoupled enhancements are 3.977$\langle$(Ed(opt)$\rangle$. In the decoupled case, one can look at TABLE(2.3) in the part with $\langle Ed(opt)\rangle$, l=0.5, so that, for example when n=3 (CH_3), Ed(opt)$\simeq$3.977 x 1.15$\simeq$4.57. In the former coupled case, applied to the same example of n=3, one notes that $M_H = \pm\frac{1}{2}, \pm^3/_2$. Thus the inner two multiplets have E(opt) = $\pm\frac{1}{2}$ x 7.954 =$\pm$3.977, and the outer two multiplets, $\pm$11.93.

TABLE(2.7) was constructed to assist in the quest for the appropriate values of D needed to identify resonances of particular multiplicity. These calculations used the program PARITY to generate the function Ed with respect to timing, Δ, for the more widely used values of n (n = 1,2,3,4,6,9,12). A graph of these functions suggests the best timing available to distinguish one function from all others. In these calculations, $\tau=\tau(opt)$. By using this table, for example to distinguish n=1 from n$\neq$1 one can see that D=2 is used, which gives a positive maximum enhancement for n=1 and a zero signal for n$\neq$1.

PROTON COUPLED INEPT

1	$T_{(opt)}$	$< E_{(opt)} >$
0.5	4	2
1	8	1
1.5	11.32	0.70273
2	14.50	0.54716
2.5	17.62	0.44961
3	20.71	0.38222
3.5	23.78	0.33268
4	26.85	0.29466
4.5	29.90	0.26542
5	32.94	0.24002
6	39.02	0.20259
7	45.09	0.17530

PROTON DECOUPLED INEPT

n	1	2	3	4	5	6	9	12
$D_{(opt)}$	2.0000	4.0000	5.1043	6.0000	6.7758	7.4705	9.2444	10.7279
1				$< E_{(opt)} >$				
0.5	1.000	1.000	1.15	1.30	1.43	1.55	1.87	2.15
1	0.50	0.50	0.58	0.65	0.72	0.78	0.94	1.07
1.5	0.35	0.35	0.40	0.45	0.50	0.54	0.66	0.75
2	0.27	0.27	0.32	0.36	0.39	0.42	0.51	0.59
2.5	0.22	0.22	0.26	0.29	0.32	0.35	0.42	0.48
3	0.19	0.19	0.22	0.25	0.27	0.30	0.36	0.41
3.5	0.17	0.17	0.19	0.22	0.24	0.26	0.31	0.36
4	0.15	0.15	0.17	0.19	0.21	0.23	0.28	0.32
4.5	0.13	0.13	0.15	0.17	0.19	0.21	0.25	0.28
5	0.12	0.12	0.14	0.16	0.17	0.19	0.22	0.26

TABLE 2.5 Maximum enhancements and optimum timing for coupled and decoupled INEPT ,using the equations of Pegg et al[86] in the computer program INTIME. $\tau_{(opt)} = (T_{(opt)}J)^{-1}$, $\Delta_{(opt)} = (D_{(opt)}J)^{-1}$

ISOTOPE	SPIN I	MAX. COUPLED ENHANC. in units of M_H	MAX. DECOUPLED ENHANC. in units of $\langle E_{d6pt} \rangle$
^{13}C	0.5	7.954	3.977
^{15}N	0.5	-19.731	-9.865
^{29}Si	0.5	-10.067	-5.033
^{31}P	0.5	4.941	2.470
^{57}Fe	0.5	61.77	30.87
^{77}Se	0.5	10.487	5.243
^{89}Y	0.5	40.816	20.408
^{103}Rh	0.5	62.80	31.40
^{109}Ag	0.5	42.98	21.49
^{113}Cd	0.5	-9.018	-4.509
^{119}Sn	0.5	-5.363	-2.682
^{125}Te	0.5	-6.339	-3.170
^{183}W	0.5	48.005	24.003
^{195}Pt	0.5	9.319	4.659
^{199}Hg	0.5	11.167	5.583
^{207}Pb	0.5	9.589	4.794
^{2}H	1	6.514	6.514
^{6}Li	1	6.795	6.795
^{9}Be	1.5	5.001	7.117
^{10}B	3	3.558	9.308
^{11}B	1.5	2.191	3.118
^{14}N	1	13.838	13.838
^{17}O	2.5	3.317	7.377
^{27}Al	2.5	1.726	3.838
^{43}Ca	3.5	-4.944	-14.861
^{53}Cr	1.5	-12.432	-17.692
^{61}Ni	1.5	-7.864	-11.191
^{71}Ga	1.5	2.304	3.279
^{73}Ge	4.5	-7.584	-28.669
^{91}Zr	2.5	-4.837	-10.757
^{95}Mo	2.5	6.899	15.345
^{99}Ru	2.5	-9.744	-21.673

TABLE 2.6 Maximum enhancements using proton PT via INEPT on specific isotopes. Proton PT requires resolvable proton coupling and $T_2 \gtrsim (\tau, \Delta)$. Spin 0.5 isotopes usually fulfill the latter condition. (negative signs for negative γ values)

VALUES OF n TO DISTINGUISH	VALUES OF D, THE TIMING	SPECTRAL FEATURES
1 from others	2	n=1,↑ n≠1,zero
2 from 3	1.33-1.2436	n=3,90%↑ n=2,↓ ranging to n=3,↑ n=2,95%↓
4 from 3	1.2436-1.2	n=3,↑ n=4,95%↓ ranging to n=3,95%↑ n=4,↓
2 from 4	6 and then 3	n=2,85%↑ and then n=2,85%↑(same) n=4,↑ n=4,33%↑(smaller)
3 or 9 from 6 or 12	1.1545-1.1213	n=3,9,85%,95%↑,(respec.) n=6,12,100%,80%↓,(resp.) ranging to n=3,9,70%,100%↑,(resp.) n=6,12,95%,95%↓,(resp.)
3 from 9	9.244 and then 3.33	n=9,↑ and then n=9,7%↑(smaller) n=3,70%↑ n=3,70%↑(same)
6 from 12	10.728 and then 4	n=12,↑ and then n=12,8%↑(smaller) n=6,90%↑ n=6,50%↑(same)

TABLE 2.7 Timing and corresponding spectral features used to distinguish resonances with different numbers of protons,n. Decoupled INEPT sequences with $\tau_{(opt)}$ and $\Delta = (DJ)^{-1}$ timing are used. KEY..... ↑ means the positive maximum, having the same sign as the maximum signal using the smallest timing $\tau_{(opt)}$, $\Delta_{(opt)}$. 50%↓ means 50% of the negative maximum.

KEY
Number of protons in PT,n
FT intensity ratios
INEPT intensity ratios

n=0
1
0

n=1
1 1
-1 1

n=2
1 2 1
-1 0 1

n=3
1 3 3 1
-1 -1 1 1

n=4
1 4 6 4 1
-1 -2 0 2 1

n=5
1 5 10 10 5 1
-1 -3 -2 2 3 1

n=6
1 6 15 20 15 6 1
-1 -4 -5 0 5 4 1

n=7
1 7 21 35 35 21 7 1
-1 -5 -9 -5 5 9 5 1

n=8
1 8 28 56 70 56 28 8 1
-1 -6 -14 -14 0 14 14 6 1

n=9
1 9 36 84 126 126 84 36 9 1
-1 -7 -20 -28 -14 14 28 20 7 1

n=10
1 10 45 120 210 252 210 120 45 10 1
-1 -8 -27 -48 -42 0 42 48 27 8 1

n=12
1 12 66 220 495 792 924 792 495 220 66 12 1
-1 -10 -44 -110 -165 -132 0 132 165 110 44 10 1

TABLE 2.8 Multiplet intensity ratios from conventional FTNMR, and coupled INEPT via a differential PT,for various values of n.

Finally, tabulations of the multiplet intensity ratios from coupled INEPT are compared to the conventional binomial intensity ratios for various values of n. In TABLE (2.8) are given the intensities for a differential PT via coupled INEPT, which experimentally requires that $\Delta=0$. The absolute value of these recorded intensities gives the intensities for a net PT via coupled INEPT, which requires $\Delta=\Delta(opt)$. INEPT intensity ratios are gleaned by multiplying the binomial FT ratios by M_H, and dividing the result by the highest common factor.

2.2.1.2 Listing of UPT Parameters

The tabulation for INEPT can be used for the universal PT sequence UPT using the following equivalence:
$\phi = \pi J\tau$ and $\theta = \pi J\Delta$. Thus the pulse angles are variable, while the pulse delays are fixed at $(2J)^{-1}$ for UPT.

2.2.2 Summary of the Features of INEPT

There are two main advantages in the use of INEPT pulse sequences compared with simple single pulse sequences.

Sensitivity enhancement is the most obvious. For a given number of scans, INEPT sequences can give a signal E times larger in S/N than conventional sequences. By inspection of TABLE (2.6) it is evident that, in general, E is significantly larger than one. This PT enhancement is larger than the NOE enhancement. The ratio of the recycle times of INEPT to other sequences, r, is important when considering instrumental time saving, since INEPT can reduce the time to reach a given S/N by a factor E^2/r. Since, in general, proton T_1 values are shorter than cross relaxation times for spin $\frac{1}{2}$ nuclei, as a rule, r is smaller than one for spin $\frac{1}{2}$ nuclei. Nuclei with negative magnetogyric ratios and which give a zero signal due to the NOE effect can be observed using INEPT.

The other valuable use of INEPT is in identification. Coupled spectra with or without INEPT can identify the number, n, of scalar coupled spin $\frac{1}{2}$ nuclei (^{1}H or ^{31}P)[86,95] on a given nucleus. However since the intensity variation of E_d with Δ is different for a different n, by a judicious choice of Δ, decoupled INEPT can identify n in a relatively short time with much less chance of overlapping spectral lines. Decoupled PT spectroscopy is superior to off resonance decoupling in the assignment of ^{13}C spectra[78,81] in complex molecules, since the former techniques gives simpler first order spectra in a shorter time, and with far less chance of overlapping lines than the latter technique. Common values of n; 0, 1, 2, and 3 can be distinguished with decoupled INEPT. Simple two or three-pulse schemes (FIG.(2.9)) are used for the observation of proton broadband decoupled J-modulated spin-echo ^{13}C NMR spectra.[120,121] They can only easily distinguish n=0 from n$\neq$0 and n, odd from n, even. By careful examination of relative signal intensities, the n=1 resonance can be distinguished from the n=3 resonance, but this is experimentally more difficult to do than with INEPT. Namely, at a time $\tau=(3.288J)^{-1}$, there is a maximum intensity difference between n=1 and n=3, being 58% and 19% of maximum, respectively. The simple 2-pulse scheme (a) has the advantage of being accessible to the older and routine spectrometers.

The 'up-down' appearance of coupled INEPT (via differential PT) can allow the identification of broader spectral lines that would, in ordinary coupled spectra, be lost with overlapping lines.

A pulse sequence with qualitatively similar performance to INEPT, called DEPT, gives an analogous method of assignment by variations of the tip angle of the final ^{1}H pulse rather than by variation of the final precession time, Δ.[107] Two variable tip angles for the sequence UPT allow it to be truly multinuclear, like INEPT.[117]

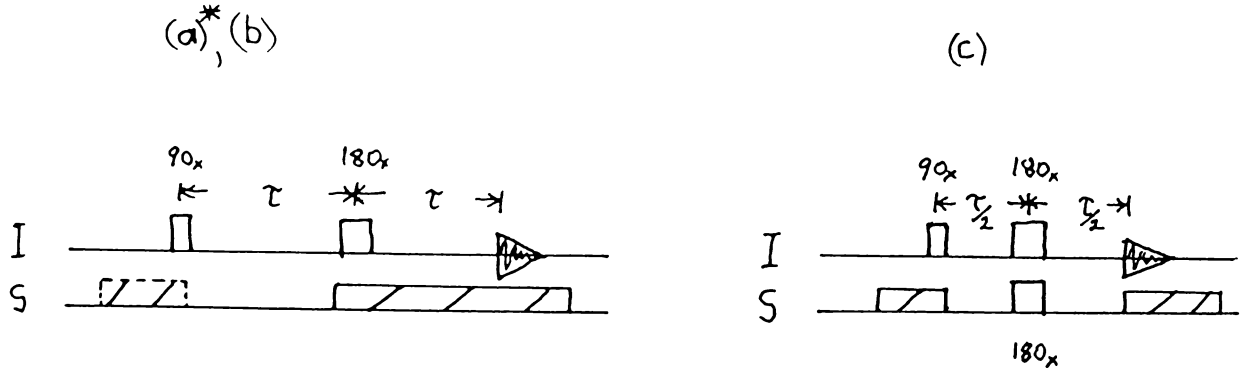

FIG. 2.9 Pulse sequences for the observation of proton broad-band, decoupled J-modulated spin-echo I (^{13}C) spectra.[120,121]
(a), (b) Delayed decoupled sequence with 180° I spin echo pulse.
(c) Heteronuclear J-modulated experiment with S (^{1}H) BB, decoupling during acquisition.
*Sequence (a) only has decoupling during and after the 180x pulse.

Disadvantageous features of INEPT related to the FTNMR instrument used, include the following. Enhancements are reduced by r.f. pulse inhomogeneity,[82] primarily in the irradiation channel. Irradiation coils and amplifiers are designed for decoupling rather than for generating r.f. pulses. (It is necessary to use composite pulses to reduce inhomogeneity before using INEPT in 2 dimensional NMR.) Pulse irreproducibility[87] can result in random errors larger than simple T_1 measurement pulse sequences if INEPT is used prior to relaxation measurement. Instrumental phase errors, and signals not due to PT are difficult to completely erradicate, complicating assignment-type experiments.

The complexity of the INEPT experiment and the associated increase in time and cost to 'get it working' are a disadvantage compared to the use of conventional pulse sequences. However, this experimental complexity for INEPT is less than for other classes of PT experiments. (With the exception of SINEPT, SPI sequences have less instrumental hardware requirements than INEPT.) There must be a prior knowledge of the correct 90° and 180° I and S pulses, an order of magnitude knowledge of J_{IS}, and a knowledge of the timing parameters T(opt) and D(opt). Pulse missetting or mistiming

results in phase errors and signal loss. The sinusoidal variation of intensities with timing means that mistiming is not a serious problem.

A judicious choice of sample is required for INEPT. This sample must have the nuclei of interest scalar coupled to a spin $\frac{1}{2}$ nucleus of large magnetogyric ratio (^{1}H or ^{31}P). With a few exceptions[92] J_{SI} must also be resolvable under the conditions that INEPT is used. Spin-spin relaxation times of I must not be short compared to the timing of the INEPT sequence, or a reduction in signal will ensue. This is a significant restriction to the application of INEPT to quadrupolar nuclei. In addition, spin-lattice relaxation times of S must not be long compared to I if one desires to have shorter recycle times for INEPT compared with simpler sequences. Addition of an inert paramagnetic relaxant[94] or use of a solvent that reduces the S T_1 value can circumvent this problem.

Finally, it should be noted that if n is even, most coupled INEPT sequences give zero intensity to the central line. This is partly compensated by the increased enhancement of the smaller, outer multiplets. Coupled DEPT and UPT give a non-zero central signal, however, as does the coupled INEPT sequence named INEPT^{+}.[116]

2.3 PRELIMINARY EXPERIMENTAL WORK ON INEPT

Experimental work with INEPT was performed on easily accessible isotopes with a view to gaining expertise before ^{73}Ge INEPT was perfected.

After the hardware modifications to facilitate proton PT, INEPT decoupled pulse sequences (a), (b), (d), (e) in FIG. (3.16) were tried on ^{13}C and ^{29}Si. Proton irradiation pulse widths for 90° tip angles were found for the standard broadband (BB) 10 mm diameter probe, NM-OBS1, to be 43±3 μs, and for the low frequency (LF) 10 mm probe, NM-IT10LF, 48±3 μs. The technique for finding these pulse widths is outlined in section 3.11.1.

In order to test INEPT on a quadrupolar nucleus with a low observation frequency like ^{73}Ge, a short study on ^{14}N was embarked upon. Nitrogen-14 can be observed on the present spectrometer either with the BB probe or the LF probe. Observation pulse widths are smaller than irradiation pulse widths for the BB probe, but for the LF probe this order is reversed. Thus two sets of INEPT pulse sequences were constructed to accommodate the different size pulse widths when using the BB and LF probes. A test sample of saturated, aqueous ammonium nitrate was used. (The lock was provided by a sealed tube of D_2O placed concentrically in the sample tube.)

Preliminary work on the BB probe yielded $E_d = 7.1$, $E\% = 79$. (This compares well with the results by Doddrell et al;[84] $E\% = 80$.) Using the LF probe, exploratory work revealed: $E_{AV} = 17.6$, $E_{AV}\% = 86$ and $E_d = 5.1$, $E\% = 57$ with $\tau\% = 8$ and $\Delta\% = 2$. (Compare with Doddrell et al: $E_{AV}\% = 95$. However pulse widths here for the LF probe are about double those used by Doddrell et al.) The reduction in enhancement from the BB to the LF probe is partly due to the increase in r.f. inhomogeneity associated with the increase in pulse widths. Utilization of coupled INEPT with a differential PT (Δ=o) should yield multiplet intensities of -1:-2:0:2:1. These intensities were similar to intensities found in the present work.

(τ% and Δ% are the % deviations between theoretical and experimental timing defined in equation (3.2).)

2.3.1 Proton PT on an Untested Spin-½ Isotope: ^{77}Se

In order to gain further expertise in the use of INEPT, this PT sequence was applied to a hitherto untested isotope: ^{77}Se. Reasonable enhancements were attained, (TABLE (2.9)) remembering that long range coupling with long precession times was used ($^2J(Se,C,H) \simeq 10.5$ Hz). The reduction in E% from 100 is partly attributable to PT signal loss during precession times. PT intensity ratios for Me_2Se were similar to the expected values of -1:-4:-5:0:5:4:1, except that the outermost two lines were only just higher than the noise. The recycle time of INEPT was equal to the recycle time of a single-pulse decoupled sequence for Me_2Se. Thus the instrument time saving is proportional to the square of the enhancement being a factor of 20 for decoupled INEPT and 14 to 40 for coupled INEPT.

	COMPOUND	MAX. ENHANCEMENT COUPLED	MAX. ENHANCEMENT DECOUPLED	AVERAGE E% COUPLED	AVERAGE E% DECOUPLED	TIMING τ%	TIMING Δ%
(A)	Me_2Se	3.8,≥6	4.6	≥ 33	57	-0.5	0
(B)	Me_3SeI	- , -	3	-	31	-	-

TABLE 2.9 ^{77}Se INEPT maximum enhancements and associated timing. (A) Neat (B) Neat, unpurified from (A).

This preliminary work shows that ^{77}Se INEPT is a potentially useful instrument time reduction tool when studying organoselenium compounds.

Dimethyl selenide (b.p. 60-70 °C, lit. 57 °C)[122] was prepared from the reaction of MeI and Na_2Se in aqueous base.[123] It was distilled under vacuum and sealed. The high boiling point and yellowish colour is probably explained by traces of yellow $(MeSe)_2$ (b.p. 152 °C) which

forms in the presence of moisture. However, the ^{13}C NMR shows essentially one singlet, so that impurities must be present in only trace amounts. Trimethylselenonium iodide was prepared by mixing cold diethyl ether solutions of Me_2Se (20% molar excess) with MeI.[124] (The lock for ^{13}C and ^{77}Se NMR was provided by a tube of D_2O placed concentrically with the sample tube.)

CHAPTER 3 APPLICATION OF PROTON PT TO A HIGH-SPIN NUCLEUS, GERMANIUM-73

3.1.1 Rationale

The inorganic chemistry group at Waikato University has a long-standing interest in germanium chemistry. FTNMR on the ^{73}Ge nucleus provides a possible tool for studying germanium chemistry. However, ^{73}Ge has a low receptivity to the NMR experiment, being 1.1×10^{-4} in natural abundance sensitivity relative to the proton.[6d] Before exploring the basic NMR parameters of ^{73}Ge, methods of sensitivity enhancement will therefore be developed in this chapter. Fortunately this isotope, having a very small, negative magnetogyric ratio (-0.9332×10^{7} rad.T.$^{-1}$.s^{-1})[6e] is a good candidate for sensitivity enhancement by PT.

NOE effects, which are expected to be small for quadrupolar nuclei such as ^{73}Ge ($I = {}^{9}/_{2}$)[6f] are unlikely to give rise to signal enhancement. Indeed, from present work, for $GeMe_4$, the nuclear Overhauser effect is approximately 0.7. Since germanium compounds containing hydrogen are numerous,[125] and resolvable $J(^{73}Ge, ^{1}H)$ coupling exists,[126,127,128] proton PT via J coupling is a good means of sensitivity enhancement. INEPT-type sequences are used since they are relatively accessible experimentally, their main requirement being pulse programmer control over the proton radio frequency (r.f.) channel.[78]

A further reason for interest in ^{73}Ge INEPT is that INEPT has not yet been tested on the 'higher-spin' nuclei. Although most INEPT work has been on spin $\frac{1}{2}$ nuclei, (sections 2.1.4-2.1.5.1) Doddrell et al have studied nuclei with $I=1$[84], $I = {}^{3}/_{2}$ and $I=3$.[86] All chemically useful nuclei have spin ${}^{9}/_{2}$ or less. Isotopes exist with spin greater than ${}^{9}/_{2}$ for the elements V, La, Lu, but they have more abundant isotopes of lower spin.

Germanium-73 has a quadrupole moment that is not large, $(-0.18 \times 10^{-28} m^2)$[129] and a spin quantum number that is large, resulting in ^{73}Ge spin-spin relaxation times that are not prohibitively small for INEPT, being 30-740 ms in GeR_4 compounds.[127]

Finally, ^{73}Ge has a low resonant frequency, being 3.4883 MHz in $GeMe_4$ with reference to ^1H T.M.S. resonance at 100.00 MHz.[7c] As a consequence, acoustic ringing is significant, and r.f. pulse widths are large and inhomogeneous. If INEPT works well under these unfavourable experimental conditions, then there is more hope for the extension of the range of quadrupolar nuclei that are candidates for this technique.

3.1.2 Outline

The application of the theory on INEPT[86] to the case of $I = {}^9/_2$ enables one to find the enhancement as a function of the timing parameters. The functional relation of the theoretical coupled enhancement with timing, (τ) was checked for $I = {}^9/_2$ by use of coupled ^{73}Ge INEPT on GeH_4.

INEPT is used to find the number of protons, n, J coupled to the observed nucleus, I. The functional relation of the theoretical decoupled enhancement with timing, (Δ), has been well documented for n = 1,2,3.[78,81] The first maxima have been looked at with n=4[84], 6, 9, and 12.[85] In the present work, this theoretical enhancement was checked for n=12 by using decoupled ^{73}Ge INEPT on $GeMe_4$.

Maximum enhancements were sought using coupled and decoupled ^{73}Ge INEPT on two compounds of T_d symmetry; GeH_4 and $GeMe_4$, and then on a compound in the C_{3v} point group;[130] $GeMeH_3$. Experimental enhancements, timing and multiplet intensity ratios were compared to theory.

Application of ^{73}Ge INEPT, using both the sensitivity enhancement and the assignment aid features available were shown in a number of different cases. Another application was found, namely use of the 'up-down' appearance of coupled INEPT to obtain a coupling constant accurately.

Next, the scope of ^{73}Ge INEPT was explored, with respect to ^{73}Ge relaxation times and the condition of a resolvable coupling constant. INEPT was then applied to a large number of 'organogermanium' compounds. To complete this section of work, the use of the PT sequences DEPT and UPT was compared to INEPT for ^{73}Ge NMR.

3.2 INEPT APPLIED TO SPIN $^{9}/_{2}$

Reference is made to the timing in the following general pulse sequence;

(90yS)-τ-(180xS)(180xI)-τ-(90yS)(90xI)-Δ-(ACQUIRE WITH OR WITHOUT S DECOUPLING)

By means of the computer program INTIME described in section 2.2.1, output of coupled enhancement with respect to τ was calculated. Thus the maximum coupled enhancement for a given spin, E(opt) , was found numerically, and the associated optimum time τ, τ(opt), was picked out. Lists of ⟨E(opt)⟩ and τ(opt) for various spin quantum numbers, I, are presented in TABLE (2.3). In the present case of $I = {}^{9}/_{2}$;

$\langle E(opt) \rangle = 0.26452 \qquad \tau(opt) = (29.90J)^{-1}$

Applied to coupled ^{73}Ge INEPT the maximum enhancement is;
$E(opt) = 7.583\ M_H$, where M_H is the total proton spin.
There are $n + 1$ values of M_H.

Following the example of Pegg et al[86] the variation of $E(M_H, I, \tau)$ given in equation (2.7) is re-expressed as $E(M_H, I) = k_3 E(\alpha)$, where $E(\alpha)$ and k_3 are given by equation (2.9). Here, $k_3 = -0.69493\ M_H$. The computer program FUNC, as described in the previous chapter, gave the output of $-k_3 E(\alpha)$ with α, depicted in FIG. (3.1) for $I = {}^{9}/_{2}$. Using coupled ^{73}Ge INEPT on GeH_4 one obtained the experimental relationship between coupled enhancement and τ for both $M_H = 1$ and $M_H = 2$.

Allowing for relaxation effects, there is excellent agreement between the form of the experimental and theoretical curves. This adds further credence to the theory presented by Pegg et al.

Note that in FIG.(3.1) the plot is of -E so that the larger portions are above the horizontal axis.

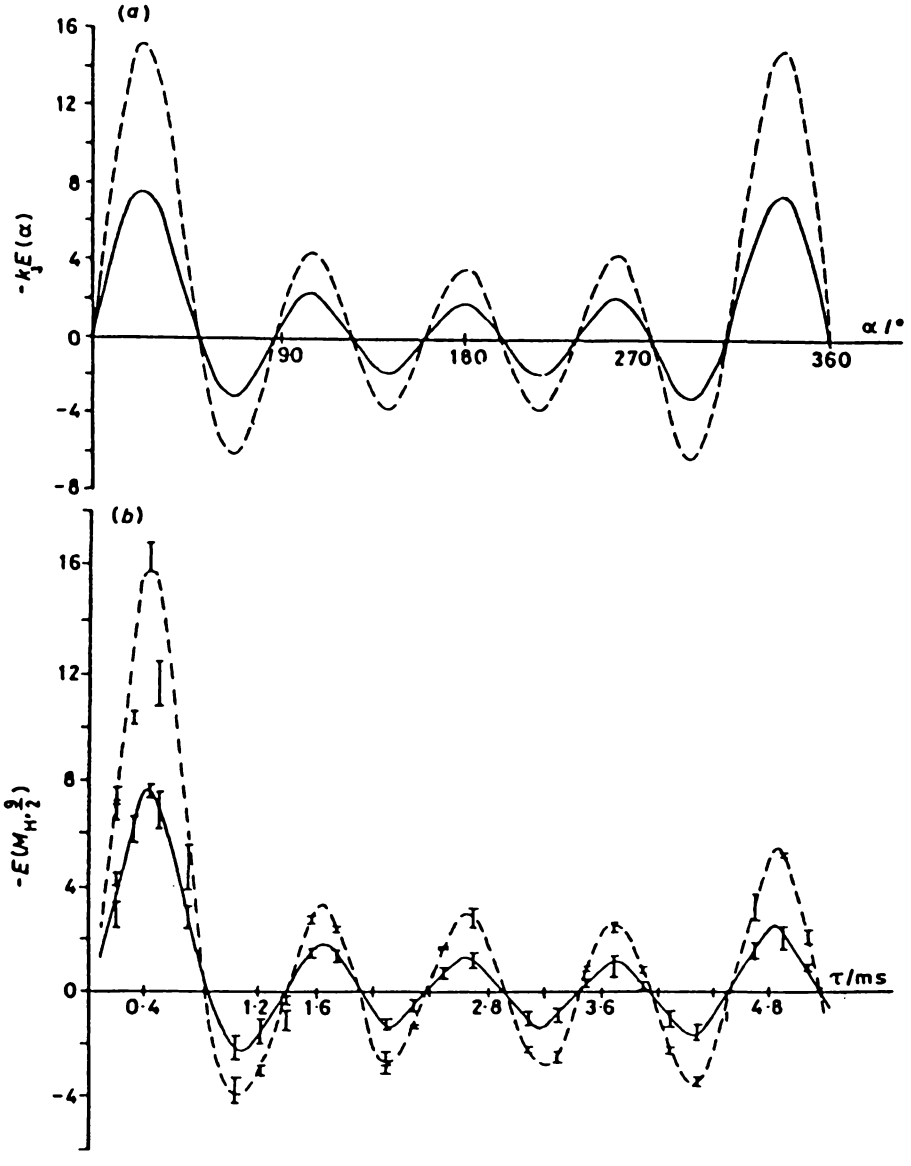

FIG. 3.1 (a) Plots of the trigonometric function

$$E(\alpha) = \sum_{m_I \neq \frac{1}{2}}^{9/2} m_I \sin(m_I \alpha)$$

for $0° \leq \alpha \leq 360°$ and $M_H = 1, 2$; $\alpha = 4\pi J\tau$; $m_I = \frac{1}{2}, 1, {}^{3}/_{2}, \ldots {}^{9}/_{2}$

(b) Experimental variation of $E(M_H, {}^{9}/_{2})$, $M_H = 1, 2$, with respect to τ, in milliseconds. This was procured from the coupled ^{73}Ge resonances in GeH_4. $^{1}J(Ge,H)$ was measured as -97.6±.3 Hz.

KEY $M_H = 1$ (——), $M_H = 2$ (---)

3.2.1 Discussion

Pegg et al observed relaxation effects in the experimental variation of $E(2, {}^{3}/_{2})$ and $E(2,3)$ with τ for the ^{11}B and ^{10}B resonances, respectively, in $NaBH_4$. They attributed these effects mainly to the ^{1}H T_2. Relaxation times for ^{11}B in $NaBH_4$ [6g] and for ^{73}Ge in GeH_4 (section 5.3.2) are both of the order of one second. Perhaps most of the relaxation effects observed in the present study on GeH_4 come from the ^{1}H T_2. By linewidth measurements, $T_2^*{}_{(H)}$ in GeH_4 was found to be about 0.1 second, probably being dominated by magnet inhomogeneity.

3.3 INEPT APPLIED TO 12 SCALAR COUPLED PROTONS

The first maximum of decoupled enhancement, Ed(opt), and the optimum timing, Δ(opt) were computed using the program INTIME. For the case of twelve protons scalar coupled to any nucleus, the timing and enhancement of the first maximum are;

$\langle Ed(opt) \rangle = 2.1466 \qquad \Delta(opt) = (10.7279J)^{-1}$

Applied to ^{73}Ge; $Ed(opt) = 8.139$.

Using arguments analogous to those in the previous discussion of $E(M_H, l, \tau)$, one reexpresses the variation of $E_d(n, l, \Delta)$ in equation (2.8) as $E_d(n, l) = k_4 E_d(\beta)$, where k_4 and $E_d(\beta)$ are given earlier by equation (2.10). The program PARITY, detailed in the preceding chapter, gave the variation of $E_d(\beta)$ with β for n=12, as shown in FIG. (3.2).

Experimental variation of $E_d(12, {}^{9}/_{2})$ with Δ, using τ(opt), is also depicted in FIG. (3.2). The decoupled ^{73}Ge resonance of $GeMe_4$ was used. In the present case, to compare experiment directly with theory, one uses; $E_d(12, {}^{9}/_{2}) = -3.7913\ E_d(\beta)$.

Looking at this figure, one sees that there is good agreement between the experimental and theoretical forms of the curves. This agreement must account for the finite experimental relaxation times.

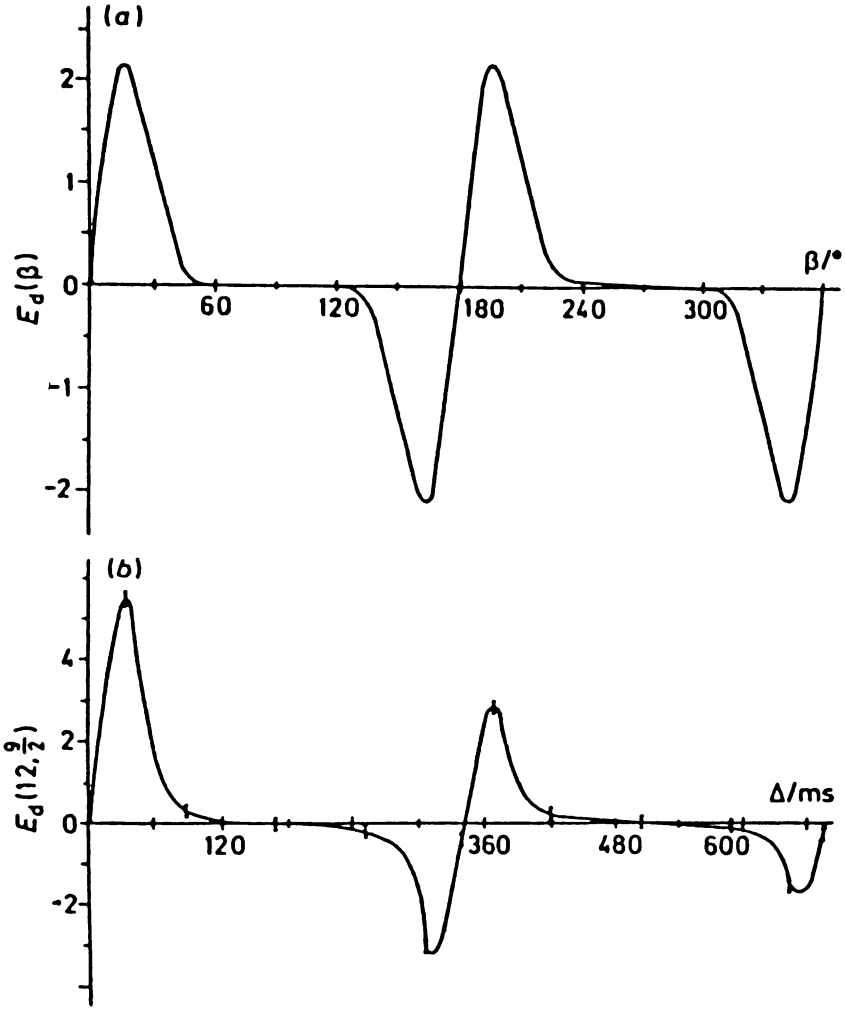

FIG. 3.2 (a) Plot of the trigonometric function $E_d(\beta) = 12 \sin(\beta) \times \cos^{11}(\beta)$ for $0 \leq \beta \leq 360°$, $\beta = \pi J \Delta$

(b) Experimental variation of $E_d(12, {}^9/_2)$ with Δ in milliseconds, obtained from the decoupled ^{73}Ge resonance in $GeMe_4$. $^2J(Ge,H)$ was measured as 2.95±.02 Hz.

Hence this study confirms that in the case of n=12, $l=^{9}/_{2}$, the functional form of $E_d(n,l,\Delta)$ with respect to Δ is correct. In theory this functional form will be independent of l.

3.3.1 Discussion

Doddrell et al[82] reported that the ^{13}C signal following a PT sequence decays with a time constant T_1^*, given by;

$$(T_1^*)^{-1} = (T_{1_H})^{-1} + (T_{2_C}^*)^{-1} \qquad ---(3.1)$$

, where T_{1_H} is the proton T_1 and $T_{2_C}^*$ is the carbon apparent spin-spin relaxation time. It is interesting to apply this equation to the apparent relaxation time for ^{73}Ge in $GeMe_4$ following the PT sequence. The PT decay of the signal fits an exponential decay quite well, yielding $T_1^* = 260\pm30$ ms. Using $T_2^*_{Ge} = 330\pm30$ ms and $T_{1H} = 9000\pm1000$ ms, (from the present work), then the theoretical decay is characterized by $T_1^* = 320\pm60$ ms. The observed and expected times, T_1^* are within experimental error. (This result does not discount the possibility that the final $90_x(I)$ pulse may not be the original[82] definition of the 'end' of the PT sequence, as it is used here.)

3.4 ^{73}Ge INEPT ON GeH_4 AND $GeMe_4$

This exploratory study used compounds with Ge in a site of tetrahedral symmetry, so that ^{73}Ge relaxation times due to quadrupolar mechanisms would be relatively long. Loss of P.T. signal will thus be minimized.

3.4.1 Coupled Spectra

Simple unenhanced proton coupled spectra from 90° ^{73}Ge pulses, (NON), were compared with spectra from proton coupled INEPT under the same experimental conditions. Several sets of spectra under similar experimental conditions were repeated, and representative samples are recorded in FIG.(3.3). These spectra form the main source of data for the coupled enhancements and multiplet intensity ratios shown in TABLE (3.1).

Non-zero enhancements in S/N for the same number of scans range from a factor of 5.8 to 20. Germane yielded enhancements about equal to those predicted by theory. However, tetramethylgermane showed enhancements about three quarters of the theoretical values. This reduction is due to the significant loss of P.T. during the pulse sequence. Time delays in the pulse sequence are about 40 times longer for the $GeMe_4$ than for GeH_4. Thus there is more opportunity for the P.T. signal to decay in the case of $GeMe_4$.

Maximum enhancements were found near the predicted value of $\tau = (29.90J)^{-1}$. Timing between the mid points of the proton pulses was $(23J)^{-1}$ for GeH_4 and $(29.8J)^{-1}$ for $GeMe_4$. It matters exactly how this value of τ is measured. Measuring τ as the time between the end of one proton pulse and the start of the next, then $\tau(opt) = (26J)^{-1}$ for GeH_4 and $(30.0J)^{-1}$ for $GeMe_4$. The timing for GeH_4 is subject to larger error than for $GeMe_4$ since in the former case, the smaller time delays are comparable to the actual r.f. pulse widths.

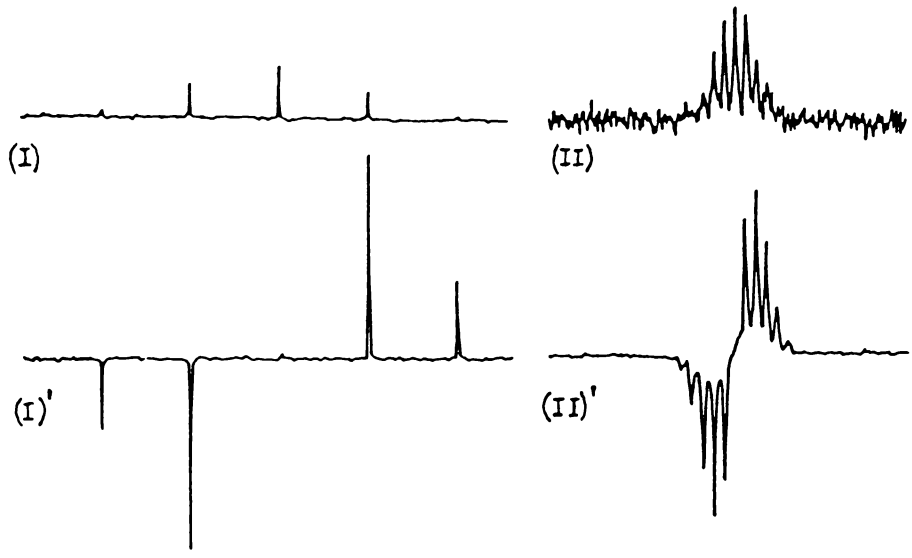

FIG. 3.3 Coupled ^{73}Ge INEPT on GeR_4 under the same experimental conditions as unenhanced proton coupled (NON) spectra. (I),(I)' GeH_4; NON, INEPT, respec. 100 scans, 2000 H_Z window, 4K data points, (II), (II)' $GeMe_4$: NON, INEPT, respec., 304 scans, 500 Hz, 8K.

COMPOUND	MULTIPLET $\lvert M_H \rvert$	EXPERIMENTAL ENHANCEMENT	% FRACTION OF THEORY, E%
GeH_4	2	16.3	107
	1	7.2	95
$GeMe_4$	5	(20)	(50)*
	4	(20)	(66)
	3	15.8	69
	2	11.3	74
	1	5.8	76

COMPOUND	MULTIPLET M_H	PT INTENSITY RATIO EXPTL.	PT INTENSITY RATIO THEORY	FT INTENSITY RATIO EXPTL.	FT INTENSITY RATIO THEORY
GeH_4	-2	0.8	1	0.4	1
	-1	2.0	2	3.2	4
	0	0	0	6.0	6
	1	-1.9	-2	3.9	4
	2	-0.7	-1	0.9	1
†$GeMe_4$	-6	3	1	-	1
	-5	16	10	23	12
	-4	48	44	76	66
	-3	116	110	220	220
	-2	171	165	517	495
	-1	132	132	814	792
	0	0	0	924	924
	1	-140	-132	800	792
	2	-174	-165	522	495
	3	-116	-110	267	220
	4	-48	-44	92	66
	5	-14	-10	26	12
	6	-3	-1	-	1

TABLE 3.1 Germanium-73 coupled INEPT on GeH_4 and $GeMe_4$. Enhancements (upper table) and multiplet intensity ratios (lower table) from theory and experiment are recorded. Data was mainly from FIG.(3.3) ,but * numbers in brackets required a long accumulation time FT spectrum ,and †for GeMe4 a long accumulation time PT spectrum was also required.

PT multiplet intensity ratios were generally as predicted. Differences between experimental and theoretical intensity ratios were similar for both P.T. and F.T. spectra. Use of an INEPT pulse sequence[81] which removes initial ^{73}Ge magnetization resulted in no significant change in absolute intensity ratios. It is probable therefore that pulse inhomogeneity is a significant factor contributing to the slight deviations from the theoretical multiplet intensities.

3.4.2 Decoupled Spectra

Spectra from single 90° ^{73}Ge pulses with gated proton decoupling were compared to spectra from INEPT with broad-band proton decoupling under the same experimental conditions. The simple pulse sequence allows essentially no nuclear Overhauser effect (NNE). Several sets of spectra under similar conditions were repeated, and samples are shown in FIG. (3.4). Enhancements are listed in TABLE (3.2). If care was not taken to degas the lock solvent and to obtain a high resolution lock, then the enhancements were typically 10% less than those recorded here. Maximum enhancements were almost at the theoretical value for GeH_4 and about three quarters of theoretical value for $GeMe_4$, following the trend for coupled enhancements.

Optimum choices of, Δ, as measured from the mid-point of the final 90° Ge pulse to the onset of decoupling were $(11\,J)^{-1}$ and $(6\,J)^{-1}$ respectively for $GeMe_4$, and GeH_4. Corresponding theoretical times were similar, being $(10.7\,J)^{-1}$ and $(6.0\,J)^{-1}$ respectively.

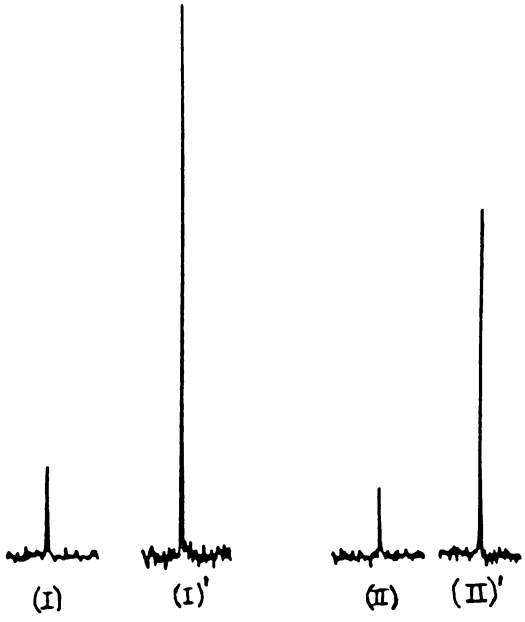

FIG. 3.4 Samples of spectra using gated decoupling (NNE) and INEPT with broad-band decoupling under the same experimental conditions for GeR_4 . (I), (I)' $GeMe_4$ using NNE, INEPT, respec., 10 scans 2000 Hz, 8K. (II), (II)' GeH_4 using NNE, INEPT, respec., 10 scans, 1000 Hz, 4K.

COMPOUND	EXPERIMENTAL ENHANCEMENT	% FRACTION OF THEORY, E%
GeH_4	4.8	98
$GeMe_4$	5.8	72

TABLE 3.2 ^{73}Ge decoupled INEPT on GeH_4 and $GeMe_4$. These enhancements were procured from the spectra in FIG. (3.4) but with the entire baseline recorded to accurately measure the noise.

3.4.3 Discussion

It is interesting to compare the maximum enhancements and optimum timing gleaned in this study, with work on other nuclei. This comparison is recorded in TABLE (3.3). Pulse sequences used for coupled INEPT are essentially the same, namely the 5-pulse sequence presented by Morris & Freeman,[69] and likewise the decoupled sequences all have two refocusing pulses added between the 90° pulses and acquisition. To assist in this comparison, one defines the % deviation of experimental timing T_{ex} from the theoretical timing T_{th} as;

$$T\% = \frac{| T_{ex} - T_{th} |}{(T_{ex} + T_{th})} \; 200 \qquad \text{---(3.2)}$$

Enhancements procured from ^{73}Ge INEPT on GeH_4 were slightly closer to theory than other work, but the % deviation of timing, τ, was also the highest in the work shown. Short time delays in this case contributed to a large E% and a large error in the timing.

Looking at $GeMe_4$, one sees that E% is lower than other work but T% values are similar to other work. Long time delays lead to small errors in the timing, but together with a short T_2, also contribute to the reduction of E%.

Present studies on GeR_4 revealed that the long recycle times can be rationalized by long proton T_1 values, yielding recycle times of $5T_{1H}$ to $10\ T_{1H}$. Further details are given in section 3.6.1.1. INEPT applied to ^{14}N in NH_4NO_3 was used with a recycle time of 6 seconds,[84] while INEPT on ^{10}B in $NaBH_4$ was used with a recycle time of 40 seconds.[86] Near room temperature $T_{1H} \simeq 6$ s in $NaBH_4$[27], so that the long ^{10}B INEPT recycle time can be explained by the long T_{1H}, amounting to $7T_{1H}$. Furthermore, recycle times were about $10\ T_{1p}$ for maximum enhancement in phosphorus PT using ^{103}Rh INEPT on a Rh complex.[94] This arose from waiting times of 80 s

NUCLEUS	COMPOUND	AVERAGE COUPLED	%ENH., E% DECOUPLED	% DEVIATION, TIMING τ	Δ	REF.
^{73}Ge	GeH_4	100	98	1.2	9	‡
	$GeMe_4$	75	72	0.3	-4	†
^{14}N	NH_4NO_3	95	80	-	-	84
^{11}B	$NaBH_4$	90	-	-	-	86
^{10}B	$NaBH_4$	85	-	-0.4	-	86
^{119}Sn	$SnMe_4$	-	92	-	2	85
^{29}Si	$SiMe_4$	-	85	-	-	85
^{13}C	C_5H_5N*	-	70	-	-	82

TABLE 3.3 Comparison of work yielding the % fraction of theoretical enhancements, E%, and the % deviation of timing from the theoretical optimum values. A positive timing deviation means the experimental timing is greater than the theoretical.
*Average E% of α,β,γ carbons is recorded. †Present work.

and a ^{31}P T_1 (T_{1P}) of 7.7 s. The ^{31}P spin system is similar to a $\{^1H\}$-I NOE measurement in terms of population requilibration for which the recommended waiting time is $10T_1$.[50] Hence the long ^{103}Rh waiting time is not surprising.

3.5 ^{73}Ge INEPT ON $GeMeH_3$

The germanium atom in $GeMeH_3$ (C_{3v} point group) [130]is in a site of lower symmetry, electronically and sterically, than germanium in GeH_4 or $GeMe_4$. Thus the larger quadrupolar interactions from the larger electric field gradient are expected to give smaller relaxation times. The fact that T_2* is only slightly shorter than that in GeH_4, (section 5.3.2), and that ^1J and ^2J coupling between germanium and protons was easily resolvable recommends this compound as a candidate for testing INEPT. It is interesting to attempt proton PT via both ^1J and ^2J coupling.

3.5.1 Coupled Spectra

A comparison of simple coupled spectra with spectra from coupled INEPT is shown in FIG. (3.5) and TABLE (3.4). Maximum enhancements were found at about $(25\ J)^{-1}$ and $(26\ J)^{-1}$ using ^1J and ^2J coupling respectively, yielding slightly over, and slightly under half of the theoretical enhancements, respectively.

CONDITIONS	†GROUP OF MULTIPLETS	AV. ENH.	% THEORY, E%
$GeMeH_3$ ^1J INEPT	Inner half	3.4	90
	Outer half	9.1	80
$GeMeH_3$ ^2J INEPT	Inner half	3.6	95
	Outer half	6.4	55

TABLE 3.4 Enhancements of coupled INEPT on $GeMeH_3$ using both ^1J and ^2J scalar coupling.
†For ^1J INEPT, the inner half means the inner 2 groups of 4 multiplets. For ^2J INEPT, the inner half means the middle 2 lines in each of the groups of 4 multiplets.

The single pulse coupled spectrum (NON) showed the expected binomial distribution of intensity ratios due to both ^1J (quartet) and ^2J (quartet) scalar coupling to protons. INEPT via ^1J coupling showed the expected differential PT intensity ratios[80] from ^1J (-1, -1, 1, 1) and FT intensity ratios from ^2J (1, 3, 3, 1). INEPT via ^2J coupling showed 'approximately' PT intensity ratios from ^2J and 'approximately' FT intensity ratios from ^1J coupling. The outer two groups of four multiplets showed a greater deviation from the expected ratios than the inner two groups, lacking a one to one correspondence between observed and expected signs. There was also a greater reduction in E% for the outer groups of multiplets as defined in TABLE (3.4) . However, the overall

FIG. 3.5 Coupled ^{73}Ge INEPT via ^{1}J and ^{2}J coupling; both under the same experimental conditions as the unenhanced coupled experiment (NON). The spectra were from a sample of $GeMeH_3$ for which ^{1}J (Ge,H) = $-94.3\pm.1$ Hz and ^{2}J (Ge,H) = $3.48\pm.1$ Hz.
(I) (I)' using NON and ^{1}J INEPT, respec., with 482 scans, 1000 Hz, 8K
(II)' using ^{2}J INEPT with 482 scans, 1000 Hz, 4K.

spectrum has the 180° rotational symmetry about the centre point expected for coupled INEPT spectra using differential PT.

CONDITION	PT INT. RATIOS EXP.	THEORY	CONDITION	PT INT. RATIOS EXP.	THEORY	CONDITION	FT INT. RATIOS EXP.	THEORY
INEPT	-1.1	-1	INEPT	-1.4	-1	single*	1.1	1
via	-2.8	-3	via	-3.2	-1	pulse	2.6	3
^1J	-2.7	-3	^2J	-1.2	1	coupled	2.8	3
coupled	-0.7	-1	coupled	0.4	1	(NON)	1.2	1
	-1.2	-1		-4.0	-3		3.6	3
	-3.0	-3		-5.9	-3		9.2	9
	-2.7	-3		1.3	3		8.9	9
	-0.7	-1		3.0	3		3.2	3
	0.9	1		-3.0	-3		4.1	3
	2.8	3		-1.9	-3		8.9	9
	3.3	3		5.5	3		9.0	9
	1.3	1		4.2	3		2.9	3
	1.0	1		-0.4	-1		1.4	1
	2.9	3		0.6	-1		2.8	3
	3.0	3		2.8	1		2.0	3
	1.0	1		1.5	1		0.5	1

TABLE 3.5 Multiplet intensity ratios for ^{73}Ge INEPT via ^1J and ^2J coupling and single pulse coupled experiments on $GeMeH_3$.
* All data were taken from FIG. (3.5) ,with the exception of the FT intensity ratios. These FT intensities were obtained from a larger number of scans of the same accumulation used to give NON in FIG. (3.5)

3.5.2 Decoupled Spectra

Spectra from $GeMeH_3$ using gated decoupling and INEPT with broadband decoupling are presented in FIG.(3.6), together with the enhancements (TABLE (3.6)). Enhancements were evident for ^1J and ^2J INEPT but E% was smaller here than decoupled INEPT was for GeH_4 or $GeMe_4$. Optimum values of Δ were, approximately, $(4.7\ J)^{-1}$ and $(4.5\ J)^{-1}$ via ^1J and ^2J coupling, respectively. In both cases the theoretical optimum time is $(5.1\ J)^{-1}$.

3.5.3 Discussion

Coupled enhancements for $GeMeH_3$ (TABLE (3.4)) were slightly reduced from the theoretical values. Using ^1J coupling, $GeMeH_3$ had similar precession times to GeH_4, but in view of the shorter relaxation times of the former, lower average coupled E% values of the former compared to the latter compound were not surprising. Similarly, using ^2J, $GeMeH_3$ has similar precession times to $GeMe_4$, and in view of the similar T_1 and T_2 values of these particular samples, the similar average coupled E% values of these two compounds was not unexpected. Furthermore, the lower overall enhancement from INEPT via ^2J rather than ^1J coupling is rationalized by the longer time delays used via ^2J compared to ^1J. This result reinforces the statements made by the originators of INEPT[69] recommending the use of one bond couplings in INEPT in preference to long range coupling.

Experimental values of τ(opt) and Δ(opt) using $GeMeH_3$ were not as close to the theoretical values as were these experimental parameters for $GeMe_4$ and GeH_4. This is partly due to the less scrupulous search for the maxima in the present study.

Intensity distortions have been reported[111] in coupled PT spectra when using long range J_{IS}. If I is coupled to two or more S spins, which, in turn, have homonuclear couplings J_{SS}, then intensity modulations may occur for the I multiplet when $J_{IS} \simeq J_{SS}$. In the present case of $GeMeH_3$,

this form of distortion probably occurs since $^{2}J(Ge,H) \simeq {}^{3}J(H,H)$, being 3.5 and 4.1 Hz, respectively.

The unexpected PT intensity ratios for INEPT via ^{2}J coupling could be due not only to the homonuclear proton coupling, but also to factors including; an inaccurate theory on intensity ratios, pulse missetting, incomplete removal of unenhanced signal components, r.f. inhomogeneity and initial ^{73}Ge magnetization.

Lower values of E% in decoupled spectra compared to coupled spectra can be partially explained by the large free precession times, Δ, in the decoupled sequence giving further opportunity for decay of the PT signal.

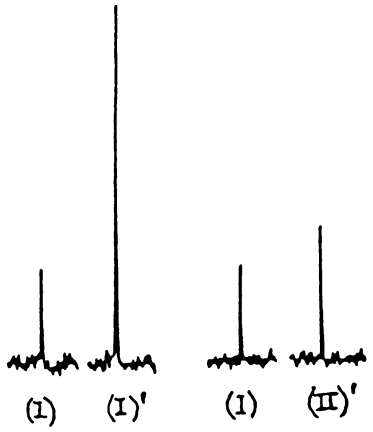

FIG. 3.6 Spectra of decoupled ^{73}Ge INEPT via ^{1}J and ^{2}J coupling both under the same experimental conditions as the spectra that uses gated decoupling (NNE). The sample is $GeMeH_3$. (I), (I)',(II)' are NNE, ^{1}J INEPT, ^{2}J INEPT, respec., each have 10 scans, 2000 Hz, 4K.

CONDITIONS	ENHANCEMENT	% OF THEORY, E%
$GeMeH_3$ ^{1}J INEPT	3.3	75
$GeMeH_3$ ^{2}J INEPT	1.5 (2.0)	34 (46)

TABLE 3.6 Enhancement of decoupled INEPT on $GeMeH_3$ via ^{1}J and ^{2}J, using the data in FIG.(3.6). (Data from single scans are in brackets.)

3.6 APPLICATIONS OF ^{73}Ge INEPT

From the ^{73}Ge INEPT applied to GeH_4, $GeMe_4$, and $GeMeH_3$, one can see that there are possible uses in ^{73}Ge NMR for INEPT in terms of sensitivity enhancement and as an assignment aid.

3.6.1 Sensitivity Enhancement

Clearly, useful S/N enhancements for germanium compounds with resolvable ^1J(Ge, H) or ^2J (Ge, H) coupling are attainable. Coupled enhancements of 3.6 to 20, and decoupled enhancements of 1.5 to 5.8 have been demonstrated so far. However, the practical use of INEPT in sensitivity enhancement must take account of the different recycle times of INEPT and the standard pulse sequences. Accordingly, the time saving factor of INEPT is E^2/r, where r is the ratio of the recycle time of INEPT, r_1 to the recycle time of the standard pulse sequence, r_o. One must also note that time saving is more strongly dependent on E, being proportional to E^2, than it is on r.

3.6.1.1 Recycle Times

All spectra from INEPT thus far have been recorded with the minimum r_1 that gave the maximum signal, and then using $r_1 = r_o$. However, this procedure has made r_o unnecessarily long. To illustrate this point, decoupled spectra, with and without INEPT were recorded for different recycle times. The same samples of $GeMe_4$ and GeH_4 employed earlier were used here. Tetramethyl germane has very small amounts of n-dibutyl ether, while germane gas is dissolved in this solvent (FIG.(3.7)). There was a large signal loss if $r_1 < 30$ s, but there was little signal loss for the conventional pulse sequence unless r_o was smaller than several seconds.

Recycle times of sequences such as the reverse-gated decoupled one (NNE) are largely governed by the T_1 of the observation nucleus.[73b] In fact, ^{73}Ge T_1 values for GeH_4 and $GeMe_4$ were of the order of one second,

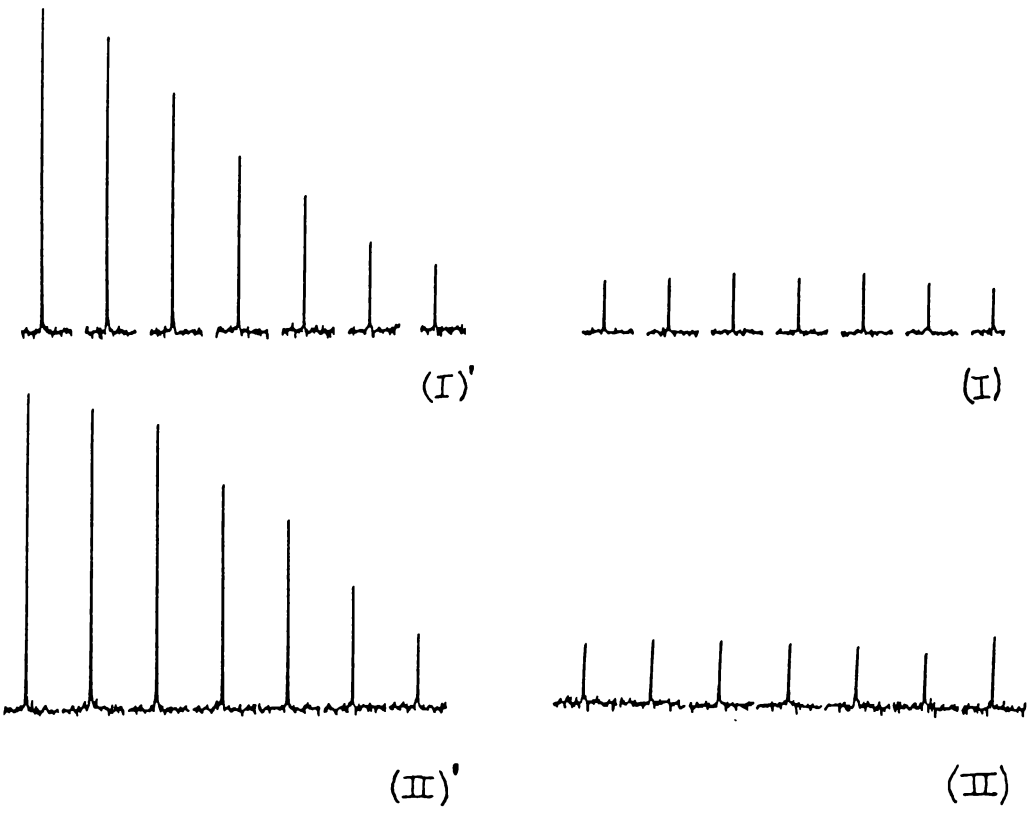

FIG. 3.7 Decoupled ^{73}Ge spectra using INEPT or reverse gated decoupling under the same experimental conditions, but with variable recycle times. For each set of four spectra, recycle times decrease from left to right; 120*, 60, 30, 15, 10, 5, 1 sec., respec. (I) (I)' for GeH_4 , NNE, INEPT, respec., 10 scans, 1000 Hz, 4K, (II) (II)' for $GeMe_4$, NNE, INEPT, respec., 10 scans, 1000 Hz, 4K, *(longest recycle time is 90 s for $GeMe_4$).

and half a second, respectively (section 5.3.2). Hence, signal loss by saturation effects is likely for simple pulse sequences with 90° observation pulses when r_o is shorter than several seconds, so that r_o is $2T_1$ to $4T_1$. For accurate intensity measurements waiting times of at least $5T_1$ are recommended.[7e]

In the case of INEPT, recycle times are governed by the proton T_1 (T_{1H}). Proton T_1 measurements of the same samples used with INEPT yielded T_{1H} values of 16 ±5 and 9 ±1 s, respectively for GeH_4 and $GeMe_4$. These relaxation times, although long compared with most T_{1H} values,[6h] are not beyond the realm of possibility. A factor contributing to the lengthening of T_{1H} would be the very small dipole moment on the GeH bonds.[131] Vacuum line techniques used in sample handling and degassing further assist in the lengthening of relaxation times by the removal of paramagnetic impurities such as oxygen. Thus the long recycle times for ^{73}Ge INEPT on the present GeR_4 samples ($5T_{1H}$ to $10\ T_{1H}$) can be rationalized by the long proton T_1 for these samples.

3.6.1.2 Reduction of Recycle Times

Experimentally, the recycle times r_1 and r_o consist of;

$r_1 = AQ_1 + PD_1$, $r_o = AQ_o + PD_o$

Now, when comparing PT and FT spectra, the acquisition times (AQ) are equal, $AQ_1 = AQ_o = AQ$. The pulse delay parameters (PD) are, in general, different; $PD_1 > PD_o$, so that $r_1 > r_o$ and $r > 1$. Reductions in r in order to increase sensitivity enhancement are important when r is large, which in turn, occurs when $AQ << PD_1$. For example, in coupled INEPT spectra; $AQ \simeq 8$, $PD_1 \simeq 20$, $r \simeq 3$ but in decoupled INEPT spectra; $AQ \simeq 1$, $PD_1 \simeq 30$, $r \simeq 15$. So, in general, a quest for the reduction in recycle times to increase sensitivity enhancement is applicable to the routine decoupled spectra which do not require high resolution. (AQ is small).

To reduce recycle times, one reduces T_{1H}. In principle, this can be attained by using solvents[8c] which have more intermolecular dipole interactions with the protons of the germanium compound than the solvent presently used, n-dibutyl ether. More dilute samples may also allow shorter relaxation times by allowing more dipole interactions. Finally, one can also add an inert paramagnetic relaxant agent to reduce T_{1H}.[7f]

Using the sample of $GeMe_4$ with very small amounts of n-dibutyl ether as the reference, the following information was found from ^{73}Ge INEPT.

The solvents benzene and chlorobenzene with $GeMe_4$ reduced recycle times to a small extent. Small amounts of $Cr(acac)_3$ in n-dibutyl ether ($<10^{-3}M$) greatly reduced recycle times, and so did the more usual concentrations of $Cr(acac)_3$ in C_6H_6 ($10^{-2}M$).

This information was derived from a comparison of the maximum S/N attainable using NNE and INEPT sequences for a constant experimental time (TABLE (3.7)). PT enhancement ranged from about one and a half for the almost neat compound, to two for the compound in chlorobenzene, to about four in the case of compounds with $Cr(acac)_3$. With the exception of chlorobenzene as a solvent, all these $GeMe_4$ samples gave similar maximum enhancements as the almost neat $GeMe_4$, provided r_1 was long enough. Thus the present amounts of $Cr(acac)_3$ reduced T_{1H} without significantly reducing ^{73}Ge T_2 values for the purposes of INEPT.

A further measure of the recycle times is the approximate minimum time that still retains maximum enhancements. These values were 90, 60, 40, 25, 10, seconds (±30%), for samples (a), (b), (c), (d), and (e), respectively. Good sensitivity enhancement was found at about a half to a third of these times.

More polar solvents, like DMSO or acetone, would probably shorten r_1 further, but they may also decompose some germanium hydrides. Addition of small amounts ($<10^{-3}M$) of $Cr(acac)_3$ effectively reduced r_1 so that ^{73}Ge

SAMPLE	OPTIMUM RECYCLE TIME (s) (±20%)	MAXIMUM ENHANCEMENT (±10%)	TIME SAVING (±40%)
(a) $GeMe_4$, 80% vol. in $n\text{-}Bu_2O$	19	1.6	2.6
(b) $GeMe_4$, 15% vol. in C_6H_6	14	1.7	2.9
(c) $GeMe_4$, 15% vol. in C_6H_5Cl	14	1.9	3.6
(d) $GeMe_4$, 15% vol. in $n\text{-}Bu_2O$ $< 10^{-3}$ M $Cr(acac)_3$	7	3.6	13
(e) $GeMe_4$, 15% vol. in C_6H_6 $< 10^{-2}$ M $Cr(acac)_3$	4	3.6	13

TABLE 3.7 Optimum recycle times and maximum enhancements of decoupled INEPT compared to NNE for various $GeMe_4$ samples. Both pulse sequences have maximum S/N for the constant instrument time of 112s . All spectra were 8K,2000Hz ,.... ,with an NNE recycle time of 2.8s or $4T_{1Ge}$. Similar relative enhancements ,but all slightly reduced,were found at half the acquisition time used above. This smaller acquisition time corresponds to $3T_2^*$,the minimum time to accurately define a line.[7d]

INEPT is an effective sensitivity enhancement tool for $GeMe_4$. This small amount of relaxant might decompose some germanium hydrides, but if it does, the amount of decomposed hydride will probably be negligible compared to the total amount of sample in an NMR sample tube. Although substantial amounts (10^{-2}M) of $Cr(acac)_3$ decreased r_1 slightly more, the larger amounts of this chemical are more likely to decompose a significant amount of some types of germanium hydrides.

Preliminary studies on the use of a homogeneity spoiling pulse preceding the INEPT sequence showed that it offered no useful reduction in recycle times. This technique is designed to shorten T_2^* rather than T_1 in any case.[7g]

3.6.1.3 Sensitivity Enhancement of Coupled Spectra

Sensitivity enhancement has been shown for the most difficult case, namely that of decoupled spectra without long acquisition times. A good example of practical sensitivity enhancement using coupled spectra with longer acquisition times is shown in FIG.(3.8). Overnight accumulations of the same instrumental times on neat $GeMe_4$ yielded 8000 scans from the unenhanced coupled sequence and 900 scans from coupled INEPT. The INEPT sequence gave S/N gains of 3 to 13 times, corresponding to a potential time saving of at least nine. In addition, all 12 out of the 12 possible multiplets were resolved using PT, while 10 out of the 13 possible multiplets were resolved using conventional FTNMR.

The same experiment, repeated with a sample of $GeMe_4$ doped with $Cr(acac)_3$ (sample (d)) gave 30% higher S/N gains with INEPT compared to neat $GeMe_4$ (sample (a)) with INEPT. An increase in sensitivity enhancement due to faster recycle times was predicted earlier to be smaller for the present experiments with its relatively long acquisition times. However in this case, the increase is less than expected. Remembering that S/N gains for a given instrumental time are proportional to $E/\sqrt{r}$, and noting that r(a) = 9, r(d) = 2, then if $E_{(a)} = E_{(d)}$ the S/N gain of (d) should be larger than (a) by a factor of $\sqrt{(9/2)} \simeq 2.1$. ($E_{(i)}$ = Enhancement for compound i in TABLE (3.7).) A factor of 1.3 is found, so that $E_{(d)}$ may really be about $(0.6)E_{(a)}$. Probably $E_{(d)}$ is reduced by 'saturation effects' since r(d) is small. A slight reduction in resolution for (d) compared to (a) may also point to saturation effects or arise from the $Cr(acac)_3$ reducing ^{73}Ge relaxation times.

Sensitivity enhancement has also been procured for germane. Using the same instrumental time, coupled PT S/N gains of 1.5 and 5 were found for inner and outer multiplets, respectively (FIG.(3.3)). This represents potential time saving factors of 2 to 20.

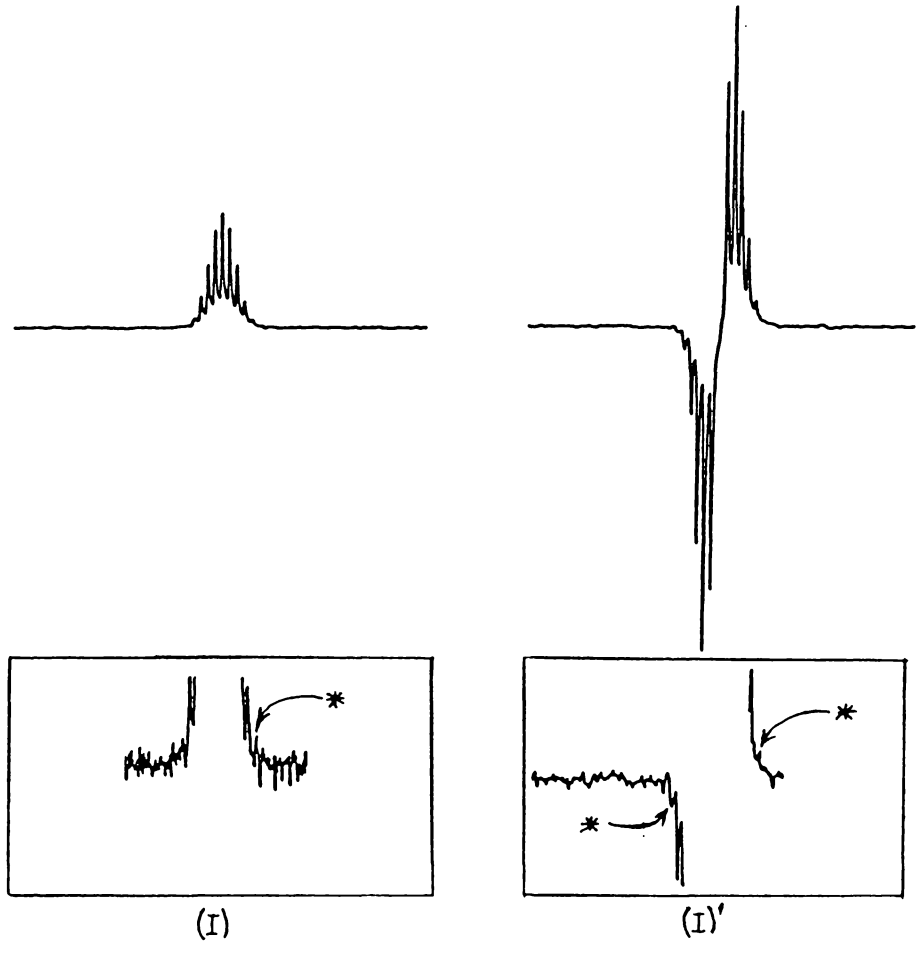

FIG. 3.8 Demonstration of sensitivity enhancement from coupled ^{73}Ge INEPT, (I)' on $GeMe_4$, over unenhanced coupled spectra, (I). Spectra were accumulated over the same instrumental time (both 700 Hz, 8K) with recycle times of 7 s, (I) and 60 s, (I)'. Figures in boxes are portions of the spectra above them with an expansion of the vertical axis.
* = outer multiplets

3.6.2 Assignment Aids

As demonstrated for the compounds $GeMe_m H_{4-m}$ m = 0,1,4, the experimental values of Δ(opt) in decoupled INEPT correspond closely to the theoretical values. Using $\Delta(opt) = (D(opt)J)^{-1}$, one finds that D(opt) is essentially a function of the number of protons used in P.T., n. Thus decoupled INEPT can be used as an assignment aid for ^{73}Ge NMR in a similar fashion to its current use in ^{13}C NMR.

In order to streamline this technique of assignment, use is made of TABLE (2.7) in which are calculated the values of D used to distinguish a specific value of n from all other values of n. A common problem is that one does not know if resonances have n = 1,2, or 3. Using D = 2 one knows that any non-zero positive signal is a singlet. Finally, using any timing about in the range D = 1.33 to 1.2436 gives n = 2 resonances negative (max. to 95% max., respectively) and n = 3 resonances positive (90% max. to max., respectively).

The usefulness of this assignment technique is demonstrated in ^{73}Ge NMR for germanium hydrides. The self reaction of germyl iron tetracarbonyl complexes; $Fe(CO)_4$ $(GeMe_xH_{3-x})$ $(GeMe_yH_{3-y})$ x,y = 0, 1, 2,or 3; results in the production of carbonyl complexes containing the Ge_2Fe_2 ring with elimination of germanium hydrides characteristic of the starting material.[132] These hydrides are $GeMe_mH_{4-m}$ (m = 0, 1, 2 or 3) and can be readily observed by ^{73}Ge NMR, while ^{73}Ge signals were not found from any Ge-Fe species. Proton and ^{13}C NMR spectra of these simple hydride products are complicated by solvent signals, vacuum tap grease signals, and signals from the mononuclear and dinuclear germyl iron carbonyls. Thus the ^{73}Ge NMR spectra are the most informative for the study of the hydrides in these reaction mixtures. As an example, $Fe(CO)_4(GeMe_2H)$ $(GeMeH_2)$ in C_6H_6 was allowed to self react at room temperature, and the ^{73} Ge INEPT via $^1J(Ge, H)$ coupling of 95 Hz was used. Now the number of

protons attached to germanium, n, can be 1, 2, 3, or 4. Firstly, D = 4 was used as the reference for phasing, and two signals were found as depicted in FIG.(3.9). Secondly, D = 1.24 was employed to reveal n = 1,3 in a positive direction and n = 2,4 in the other direction. Next, D = 2 gives a non-zero signal for n = 1 only. Since no signal was seen, signal (i) was identified as n = 3 ($GeMeH_3$). Finally, two experiments were performed to find if signal (ii) was n = 2 or n = 4. Using D = 6 followed by D = 3 will show n = 2 signals unchanged, but the final experiment leaves n = 4 signals reduced by a factor of 3 compared to D = 6. Since these two experiments left signal (ii) unchanged, it was shown to be n = 2 ($GeMe_2H_2$). Instrumental time for this INEPT experiment was similar to the proton decoupled J modulated spin echo (JMSE) experiment, despite the faster recycle time of the latter experiment.

Although these particular products can be identified by chemical shift comparisons, using samples of the neat hydrides, the system shown illustrates the usefulness of ^{73}Ge INEPT as a practical tool in the assignment of multiplicity. However, decoupled INEPT will be a very useful tool in the assignment of multiplicity of more complex germanium hydrides. Chemical shift comparisons will, in general, give little or no information about multiplicity in polynuclear germanium hydrides.

As an example, the compound GeH_3 $GeMe_2H$ was studied by ^{73}Ge INEPT using ^1J coupling. In a convenient instrument time (a half hour), one ^{73}Ge resonance was observed. Using D = 2, no signal was observed, from which one deduces that the resonance is not from a GeH group. Following this, D = 1.2 was employed to differentiate n = 3 from even multiplicities. The positive intensity signal indicated the expected multiplicity of 3. Thus the single ^{73}Ge resonance found here for GeH_3 $GeMe_2H$ was from the GeH_3 group. One could not receive this knowledge from chemical shift comparisons. With difficulty, one could differentiate GeH groups from

FIG. 3.9 Demonstration of ^{73}Ge INEPT as an assignment aid. Decoupled spectra of the products of the self reaction of $Fe(CO)_4$—$(GeMe_2H)(GeMeH_2)$ in C_6H_6. (a) Phasing reference, $n \neq 0$ (↑) (positive); (b) n = 1 and 3 (↑), n = 2 and 4 (↓); (c) n = 1 (↑), $n \neq 1$ (zero). Thus signal (i) has n = 3 and arises from $GeMeH_3$; (d) n = 2 has same intensity in the two experiments, while n = 4 has intensity reduced by a factor of three for $\Delta = (3J)^{-1}$. Thus signal (ii) has n = 2 and arises from $GeMe_2H_2$. For comparison, (e) is a standard 90° pulse sequence with reverse gated decoupling, and (f) a J-modulated spin echo sequence both with the same number of scans as INEPT.

GeH_3 groups using JMSE pulse sequences.[120] (There is some doubt regarding the assignment of the $GeMe_2H$ group which has a very low S/N compared to the GeH_3 group, see 3.4.8.2.) Finally, an overnight scan using coupled INEPT revealed a -1, -1, 1, 1 'quartet', confirming the GeH_3 assignment.

3.6.3 Other Applications

Use was made of the 'up-down' appearance of coupled INEPT (Δ=o) and the null $M_H = 0$ multiplet to separate the signals of two compounds that have accidentally overlapping proton coupled ^{73}Ge resonances.

The case in question is a mixture of GeH_4 and Ge_2H_6 in di-n-butyl ether. Digermane is synthesized either from germane or with germane, and it is difficult to remove all of the germane from samples of digermane. In a quest for the coupling constant $^1J(Ge,H)$ in digermane, the unenhanced coupled ^{73}Ge spectrum was obtained, and it was found that the signals of the two compounds were accidentally overlapping (FIG.(3.10 (a))). Hence, this coupling constant is not accurate.

Using coupled ^{73}Ge INEPT, with a factor of 1.4 less in instrumental time, and a factor of 21 less in the number of scans, one procured the spectrum in FIG.(3.10 (b)). Despite the smaller instrumental time using INEPT, the S/N from its spectrum was larger than from the unenhanced coupled spectrum. The expected P.T. multiplet ratios were attained, being close to -1:-2:0:2:1 for GeH_4 and -1:-1:1:1 for Ge_2H_6. Now the Ge_2H_6 multiplet in the same position as the zero multiplet for GeH_4 has no overlapping GeH_4 resonance. In addition, the remaining Ge_2H_6 multiplets were more readily distinguished from the GeH_4 ones, in the case of the PT spectrum compared to the FT one. This allowed a coupling constant of digermane from the PT spectrum to be found, (-95.5±0.5 Hz) with much lower random error than from the FT spectrum (-95±10 Hz).

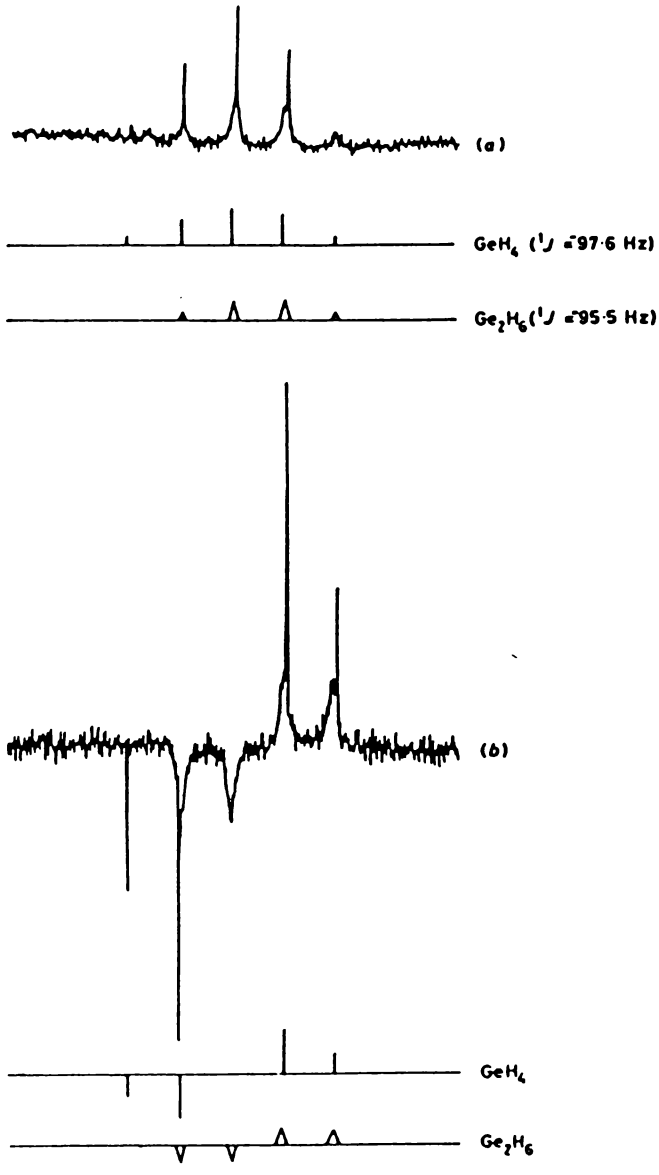

FIG. 3.10 Application of coupled ^{73}Ge INEPT to resolve accidentally overlapping signals. The FT (a) and PT (b) coupled ^{73}Ge spectra of a mixture of GeH_4 and Ge_2H_6 in n-Bu_2O. Stick diagrams below the experimental spectra show the theoretical spectral components. Spectrum (a) is the average of 18,000 scans and (b) the average of 860 scans. Both have a 2000 Hz window and 8K data points.

3.7 THE SCOPE OF ^{73}Ge INEPT

Several examples follow to give some indication of the boundaries of ^{73}Ge INEPT with respect to the relaxation time of the germanium nucleus and the condition of a resolvable germanium hydrogen coupling constant. Finally, the use of INEPT on further germanium compounds is presented.

3.7.1 INEPT on Compounds with Short Relaxation Times

The aforementioned example of GeH_4/Ge_2H_6 exhibited a sensitivity enhancement from INEPT using the same instrumental time as the unenhanced coupled pulse sequence. This enhancement is substantial for GeH_4 since it has a relatively long T_2. Digermane, however, has a short ^{73}Ge T_2 compared to germane, since the former compound has a greater deviation from spherical symmetry than does germane. In fact T_2* for Ge_2H_6 is much shorter than T_2* for $GeMeH_3$ (section 5.3.2). It is interesting to note that although digermane has a short T_1 and T_2*, being in the vicinity of 20 ms, significant PT still occurs. For constant scans, coupled ^{73}Ge enhancement was 4 and 10, respectively for the inner and outer multiplets (FIG.(3.10 (b))), and the decoupled enhancement was about 2 (FIG.(3.11)). These parameters represent 90%, 80% and 40%,respectively of the theoretical values.

Already mentioned in the assignment aid section is the compound GeH_3GeMe_2H. Having a similar environment to GeH_3GeH_3, the present GeH_3 group would have similar, short relaxation times (T_2* $\simeq$ 35 ms). Nevertheless, INEPT on this GeH_3 group does give S/N enhancements over conventional pulse sequences. For example, E_d = 3 and, E% = 70.

Thus INEPT 'works' even on germanium compounds with a relatively short T_2* value (<50 ms), albeit with a reduction in the PT signal.

FIG. 3.11 ^{73}Ge INEPT on a compound with short relaxation times; Ge_2H_6. Both the FT (left spectrum) and the PT spectrum are the average of 40 scans.

3.7.2 INEPT via Unresolved Scalar Coupling

So far, all the compounds studied have had a resolvable Ge-H coupling under the same experimental conditions as INEPT was applied successfully. There was no resolvable GeH coupling from $GeEt_4$ in $CDCl_3$ at, or just below room temperature in unenhanced ^{73}Ge coupled spectra. Selectively decoupled spectra were inconclusive, yielding a 'faint' indication of coupling of the order of several hertz. Despite this lack of resolvable coupling, both coupled and decoupled INEPT yielded maximum enhancements of 2.2 when using timing for an 'assumed' coupling constant of about 3.5 to 4 Hz.

The deduced coupling constant gleaned from coupled INEPT (for τ) ($J = 3.8\pm.4$ Hz) is in closer agreement with the deduced constant from decoupled INEPT (for Δ) if one assumes the 8 methylene protons give PT ($J = 4.0\pm.4$ Hz) rather than the 12 methyl protons ($J = 3.2\pm.4$ Hz). Here, the theory of Pegg et al is used to derive coupling constants from the timing at maximum enhancements, being $J = (29.9\ \tau(opt))^{-1}$ for coupled spectra and $J = (8.7\ \Delta(opt))^{-1}$, and $J = (10.7\ \Delta(opt))^{-1}$ at n = 8 and 12 respectively for decoupled spectra. Polarization transfer is more likely to occur via $^2J(Ge,H)$ than $^3J(Ge,H)$, since the former values are larger than the latter, being in the vicinity of 3 Hz for the former and 2 Hz for the latter.[6i]

Larger scalar coupling constants mean, in general, less loss of PT signals during the pulse sequence.

Coupled INEPT on $GeEt_4$ in $CDCl_3$ showed no resolved GeH coupling, but did manifest a partition into two signals, up and down, according to the sign of the magnetization at acquisition. This partition is expected for the present coupled INEPT sequence, which uses differential PT.[81]

Neat, pure $GeEt_4$ has some resolvable GeH scalar coupling as seen in coupled spectra, and a further study on this is mentioned in section 3.8.2.

3.7.3 Comparison

Doddrell et al[85] attributed significant reductions in ^{119}Sn and ^{29}Si INEPT enhancements from the theoretical maximum to short T_2 values. The compounds were $SnMe_3Cl$, $SnMe_2Cl_2$ and $SiMe_2Cl_2$. In these cases, where $60 < E\% < 80.$, T_2 values were not given, but they are not likely to be smaller than for Ge_2H_6. ($40 \leq E\% \leq 90$, $T_2^* \simeq 20$ ms)

Other workers have found enhancements using INEPT even when the relevant scalar coupling is not resolved. Namely, Helmer and West[92] list three compounds with unresolved coupling for which ^{29}Si INEPT gave enhancements over ^{29}Si 90° pulses with gated decoupling to remove the NOE. These three compounds had $35 < E\% < 80$.

3.8 ^{73}Ge INEPT ON FURTHER GERMANIUM COMPOUNDS

Following is a tabulation of most of the maximum enhancements and optimum timings obtained on organogermanes and hydrides. Compounds mentioned earlier in this chapter are included in these tables to facilitate comparisons. Scalar coupling used to transfer spin polarization has magnitudes of 85-98 Hz for $^{1}J(Ge,H)$ coupling and 2.7-3.5 Hz for $^{2}J(Ge,H)$ coupling. Discussion of the tabulated data includes a rationale for deviations of enhancement, timing, and intensity ratios from the theoretical values. Utilization of INEPT as an assignment aid is discussed.

3.8.1 Methylgermanes, $GeMe_xH_{4-x}$

3.8.1.1 Decoupled Enhancements

E_d ranged from 5.8 to 1.5, and E% from 89 to 33.

Tetramethylgermane had an NOE of 0.7, whereas the PT enhancement was 5.8. Long precession times associated with the long range coupling present allow the PT signal to decay and so reduce E%. When tetramethylgermane is in a dilute solution of C_6H_6, $C_6H_6/Cr(acac)_3$, or $n\text{-}Bu_2O/Cr(acac)_3$, E_d is still similar to the above figure, but when the solvent is C_6H_5Cl, E_d is significantly smaller. All the measured line widths of the $GeMe_4$ solutions were 1.0-1.5 Hz, but the 'natural' line widths were only about 0.5 Hz, assuming $T_1 = T_2$ and that all T_1 values are similar to that in 85% by volume $GeMe_4$ in $n\text{-}Bu_2O$. Thus magnetic field inhomogeneity may mask an increase in T_2 for the case of C_6H_5Cl as the solvent. Viscosity may be one factor accounting for differences in T_2, knowing that C_6H_5Cl has a greater viscosity than C_6H_6.[133a]

Trimethylgermane exhibited a ^{2}J INEPT E% value 2.7 times smaller than the corresponding ^{1}J value, due to the loss of signal during the longer precession times concomitant with the use of long range coupling. Thus nine protons attached via three carbon atoms to germanium gave less enhancement (2.3) than one directly attached to germanium (3.4).

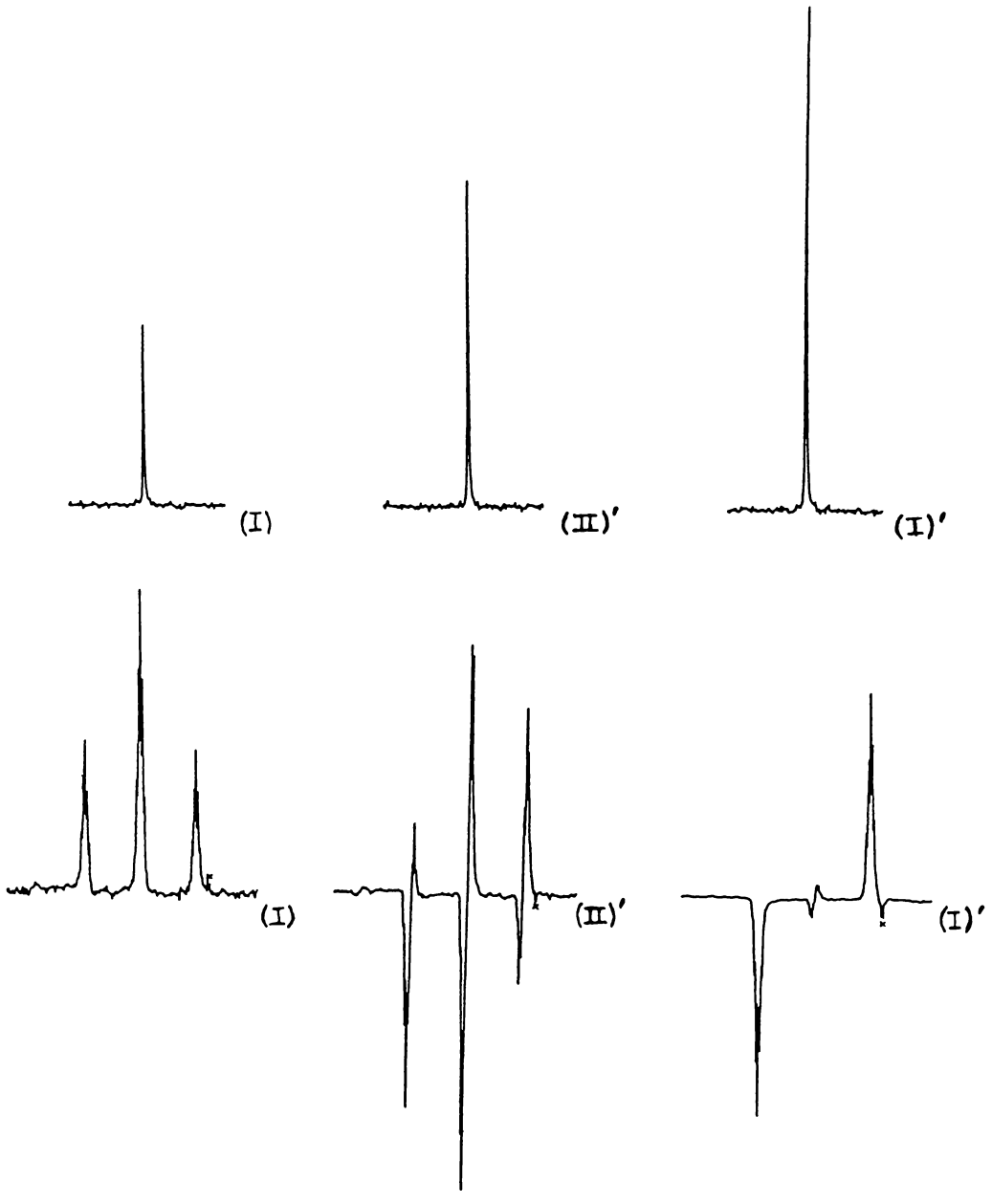

FIG. 3.12 Decoupled (top) FT (I) and germanium-73 INEPT via ^{2}J (II)' and via ^{1}J (I)' spectra of $GeMe_2H_2$. Similarly for coupled (bottom) spectra (x = small signal from $GeMeH_3$). Conditions are, for all decoupled spectra; 10 scans, 1000 Hz, 4K, coupled; 300 scans, 3000 Hz, 8K.

COMPOUND	MAX. ENHANCEMENT COUPLED	DECOUPL.	AVERAGE E% COUPL.	DEC.	AVERAGE T% τ	Δ
(A) $GeMe_4$	5.8,20	5.8	75	72	0.3	-4
(B) $GeMe_4$	5.2,12	5.4	73	67	0.3	-4
(C) $GeMe_4$	-	5.4	-	67	0.3	-4
(D) $GeMe_4$	-	5.2	-	65	0.3	-4
(E) $GeMe_4$	_	3.7	-	39	0.3	-4
(F1) $GeMe_3H$	-	3.4	-	89	-0.7	-1.8
(F2) $GeMe_3H$	-	2.3	-	33	6.0	6.5
(G1) $GeMe_2H_2$	7.8	2.8	103	73	4.0	-0.1
(G2) $GeMe_2H_2$	2.2	2.0	30	35	13	13
(H1) $GeMeH_3$	3.4,9.1	3.3	85	75	4.8	7.3
(H2) $GeMeH_3$	3.6,6.4	1.5	76	34	15	16

TABLE 3.8 Maximum experimental enhancements and associated timing of ^{73}Ge INEPT compared to theory, for **Methylgermanes.** Coupled enhancs. are for the smallest (left), and largest $|M_H|$. (A)80% by vol. in n-Bu_2O (B)15% v. n-Bu_2O with $Cr(acac)_3$ (C)15% v.C_6H_6 with $Cr(acac)_3$ (D)15% v.C_6H_6 (E)15% v.C_6H_5Cl (F1),(F2) the same sample ,dilute in C_6H_{14} using ^1J,^2J coupling respec. (G1),(G2) similarly,a neat sample with Ge_2MeH_5 (H1),(H2) in solution in n-Bu_2O .

Dimethylgermane also showed a reduction in E% when using long range coupling. This reduction in E% is such that E_d from ^2J INEPT was only slightly smaller than E_d from ^1J INEPT. There was a large positive deviation in timing, and by its sign, indicates that it is not a loss of PT signal via T_2* processes over the precession times. Note that the highest S/N obtained for ^{73}Ge NMR in this thesis was procured by 1383 scans of ^1J INEPT on $GeMe_2H_2$, leading to a S/N of 805.

Similar observations to those made on dimethylgermane can be made on methylgermane regarding E% for ^1J and ^2J INEPT, and the large, positive deviation in timing for ^2J INEPT.

COMPOUND	MAX. ENHANCEMENT COUPLED	DECOUP.	AVERAGE E% COUP.	DEC.	AVERAGE T% τ	Δ
(I) $GeEt_4$	5.5†	4.3	43	64	-38*	-30
(J) $GeEt_4$	2.2†	2.2	20	33	-20*	-28
(K) $GeEt_3H$	-	1.4	-	37	0.5	0.1
(L1) $GeEtH_3$	2 ,4	3.0	44	69	-4.3	14

TABLE 3.9 Max. exp. enhancements and associated timing of ^{73}Ge INEPT compared to theory, for **Ethylgermanes.**
(I),(K),(L1)neat (J)30% v.in $CDCl_3$ (L1)uses ^1J coupling .
†There is only partially resolved coupling,so this is an average enh.
*For the purposes of calculation, the coupling is assumed to be $^2J(Ge,H)$ rather than $^3J(Ge,H)$.

In the absence of relaxation effects, one methyl group will theoretically give the same E_d value as three hydride ligands. Averaging the experimental results for methylgermanes, and noting that $E_d(GeMe_4) > E_d(GeH_4)$, one obtains the rough rule of thumb that two methyl groups are 'worth' one hydride ligand in terms of actual decoupled enhancement.

3.8.1.2 Coupled Enhancements

E ranged from 20 to 2.2, and average E% values, from 103 to 30.

In almost every case, E% was larger than the corresponding E% using decoupling. Reductions in E% for decoupling are due to the introduction of the long free precession times of the Δ periods.

Coupled enhancements for tetramethylgermane were, on average, three-quarters of the theoretical, and the PT intensity ratios are close to the theoretical values. There is no proton-proton coupling of a similar

COMPOUND	MAX. ENHANCEMENT COUPLED	MAX. ENHANCEMENT DECOUP.	AVERAGE E% COUP.	AVERAGE E% DEC.	AVERAGE T% τ	AVERAGE T% Δ
(M) GeH_4	7.2,16.3	4.8	101	98	1.2	9
(N) GeH_4	-	2.9*	-	59	5.6	14
(O) Ge_2H_6	4 , 10	2	85	40	0.5	7
(P) Ge_2H_6	-	2.2	-	50	2.2	-5.5
(Q) Ge_3H_8	-	2.2	-	50	1.8	-5.8
(Q)' Ge_3H_8	-	2	-	50	-2.6	-34

TABLE 3.10 Max. exp. enhancement and associated timing of ^{73}Ge INEPT compared to theory, for **Polygermanes** . (M),(O)in solution in n-Bu_2O (N),(P),(Q) neat mixture of the three polygermanes. (Q) GeH_3 signal (Q)' GeH_2 signal . *τ not optimized .

magnitude to $^2J(Ge,C,H)$, and so no distortion to intensity ratios from proton coupling.

Dimethylgermane revealed an average E% of 100%, within experimental error when using ^1J coupling (FIG.(3.12)). Intensity ratios were also close to theoretical values in this case. The use of long range coupling gave a reduction in E% and some intensity distortions. One expects three groups of multiplets separated by ^1J in the FT ratio 1:2:1, with each group having the PT ratios -1:-4:-5:0:5:4:1. All the expected signs were found, but the multiplets, especially the outer two groups of multiplets, contain unexpected ratios. Methylgermane gave a coupled ^2J spectrum not only distorted in absolute intensity but also in sign. By comparison, ^2J coupled INEPT on silylgermane gave only distortion in absolute intensities, the distortion increasing for the outer multiplets. To a first approximation, the amount of distortion should be inversely proportional to fractional differencesbetween $^2J(Ge,X,H)$ and $^3J(H,Ge,X,H)$. These values as percentages:

COMPOUND	MAX. ENHANCEMENT COUPLED	DECOUPL.	AVERAGE E% COUPL.	DEC.	AVERAGE T% τ	Δ
(R1) GeH_3GeMeH_2	-	2.4*	-	55	0.1	42
(R1)' GeH_3GeMeH_2	-	1.6	-	42	-0.6	17
(S1) $(GeMeH_2)_2$	-	1.6	-	42	-0.6	17
(T1) $(GeMeH_2)_2$	-	2	-	50	-0.6	17
(U1) GeH_3GeMe_2H	-	3.0	-	69	-11	-4.4
(V1) GeH_3GeMe_3	-	2.8	-	64	-11	-4.4
(W1) $(GeMeH_2)_2GeMeH$	-	1.4†	-	37	-	-
(X1) GeH_3SiH_3	3.0,8.3	4.2	77	96	1.8	4.2
(X2) GeH_3SiH_3	1.8,4.6	2.7	44	62	-26	-28
(Y1) $GeMeH_2SiH_3$	-	2.6†	-	69	-	-

TABLE 3.11 Max. exp. enhancs. and associated timing compared to theory with ^{73}Ge INEPT,on **Methylpolygermanes and Silylgermanes.** (R1),(R1)',(S1)neat mixture of GeH_3GeMeH_2 and $(GeMeH_2)_2$ (R1) GeH_3 signal (R1)' $GeMeH_2$ signal. (T1),(U1),(V1),(W1)all neat (X1),(X2)in solution in n-Bu_2O (Y1)in solution in C_6H_6.All via ^1J, except (X2),via ^2J . *Δ not optimized †Rough comparison between INEPT,$\Delta=(1.4J)^{-1}$,and a standard JMSE sequence,time delay $\tau=(J)^{-1}$ between pulses.

$GeSiH_6$, (43), $GeMe_2H_2$, (17), and $GeMeH_3$, (15), provide a limited rationale for the 'greater distortion' of $GeMeH_3$ compared to the two other compounds. However, this rationale wrongly predicts a far greater distortion for $GeMe_2H_2$ compared to $GeSiH_6$.

There is a trend for outer multiplets to have smaller E% values than inner multiplets. That is, as the absolute value of M_H increases, E% decreases, and for a given M_H, the outer multiplets show a decrease in E%.

3.8.1.3 Assignments

The utility of INEPT as an assignment aid has already been demonstrated for methylgermanes with the example of a methylgermane/dimethylgermane mixture in iron carbonyls (section 3.6.2).

When a sample labelled $GeMe_2H_2$ was initially examined, ^1J PT was used with D = 1.3 to check that the main signal was n = 2. The main signal was negative, confirming the expectation, and by comparison with the JMSE sequence used in section 3.6.2, there was a 2·6 fold enhancement. (Since $GeMe_2Cl_2$, the starting material for $GeMe_2H_2$, is often contaminated by $GeMeCl_3$ and $GeMe_3Cl$, $GeMe_2H_2$ frequently contains some $GeMeH_3$ and $GeMe_3H$.)[132]

Similarly, on the same sample, the timing D = 1.3 also showed 2 weak signals with n = 1 or n = 3, having the same chemical shifts as previous samples with $GeMe_3H$ and $GeMeH_3$. This supports the expectation that these weak signals are from $GeMe_3H$ and $GeMeH_3$, with the added bonus of a 2.7 and a 2.9 fold enhancement, respectively, compared to theJMSE sequence.

3.8.2 Ethylgermanes, $GeEt_xH_{4-x}$

3.8.2.1 Decoupled Enhancements

Here, E_d ranged from 4.3 to 1.4, and E% from 69 to 33.

Neat tetraethylgermane exhibited a small NOE of 0.9, whereas INEPT gave $E_d \leq 4.3$. Significant PT enhancements for $GeEt_4$, neat and in $CDCl_3$ solution were attained in spite of a lack of any well resolved Ge,H coupling.

Decoupled enhancements for $GeEt_4$ were halved when $CDCl_3$ was added, and this is partly accounted for by a corresponding increase, almost 2-fold, in T_2*. The larger sample volume of the $GeEt_4/CDCl_3$ sample compared to that of $GeEt_4$ (10 mm c.f. 5 mm o.d. tube) tends to reduce[6j] T_2*, and also the solvent may provide a more efficient relaxation pathway

for $GeEt_4$. Although, in both cases, the experimental optimum timing was 20% to 40% smaller than the theoretical, these calculations were not very significant since the coupling constants used were not well defined.

Long range Ge,H coupling was unresolved in tri-ethylgermane, but ^1J(Ge,H) coupling was well resolved. Nevertheless, E_d via ^1J was still small due to the small relaxation times ($T_1 \simeq T_2 \simeq T_2^*$) of 13 ms.

Again, using ^1J coupling, there was a significant three fold enhancement for ethylgermane. Relaxation times are intermediate in value between neat $GeEt_4$ and neat $GeEt_3H$ (Section 5.3.2).

3.8.2.2 Coupled Enhancements

Proton coupled INEPT yielded one broad negative signal and one broad positive signal for $GeEt_4$ (section 3.7.2.).

Coupled INEPT on $GeEtH_3$ gave the expected PT intensity ratios of -1:-1:1:1, each separated by ^1J(Ge,H).

3.8.3 Polygermanes, Ge_xH_{2x+2}

3.8.3.1 Decoupled Enhancements

Polygermanes yielded values of E_d in the range 4.8 to 2, and E% from 98 to 40. Since germane has considerably longer relaxation times than the other polygermanes, its enhancements are expected to be closer to the theoretical than the other polygermanes. An inspection of E% values supports this view.

Germane in solution in n-Bu_2O has an NOE of 0.6, while INEPT gave $E_d \leq 4.8$. When a sample of polygermanes had INEPT parameters optimized for digermane and trigermane, E_d dropped to 2.9 for germane.

Decoupled enhancements for digermane and the two signals of trigermane were about 2, and E% was about 50. In spite of the short T_2^* value of GeH_2 in trigermane (11 ms) half the theoretical enhancement was obtained.

3.8.3.2 Coupled Enhancements

These enhancements ranged from 16.2 to 4, corresponding to E% from 101 to 85. Only ^1J coupling was used, and all the expected PT intensity ratios were found.

The absence of long precession times in coupled INEPT increased E% markedly for compounds with short T_2^*, such as digermane. Thus E% for coupled and decoupled INEPT was 85 and 40, respectively.

No coupled enhancement factors are listed for trigermane because no spectra from 90° single-pulse sequences were recorded. (The trigermane sample contains digermane, and germane, and purification is difficult.) INEPT spectra were recorded instead because of the simplified spectrum obtained: namely the absence of the large central GeH_4 peak and the central GeH_2 peak, and the 'up-down' appearance of peaks. This idea has already been discussed in section 3.6.3 when finding the coupling constant of digermane. Coupled INEPT was also used to find the coupling constants of trigermane.

3.8.3.3 Assignments

The chemical shifts of polygermanes are more dependent on the solvent or medium than on the chemical structure (section 4.7.3) so that chemical structure assignment on a chemical shift basis alone is not very reliable.

A mixture of germane, digermane and trigermane (N), (P), (Q) gave one sharp signal, two broad signals, and one weak, broad signal. Using D = 1.3 (FIG.(3.13)) the sharp signal became negative, so n = 2 or n = 4. Using D = 6 followed by D = 3, the S/N decreased by a factor of 3.5. In theory, this S/N reduction factor is about 3 for n = 4, and so this sharp signal is n = 4 (GeH_4). This assignment is also predicted by the small linewidth of the germane signal.

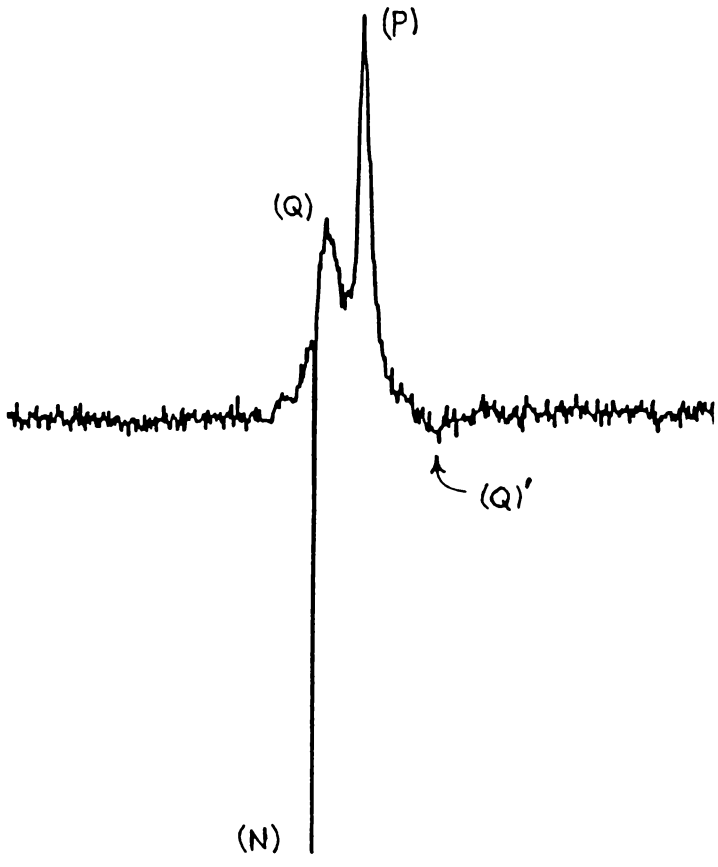

FIG. 3.13 Spectrum of decoupled INEPT used 'in the assignment mode', D = 1.3, on a neat mixture of (N) germane, (P) digermane, and trigermane. (Q) terminal, (Q)' central trigermane signal.

Since the largest of the three broad signals was positive using D = 1.3, n = 1 or n = 3. Branched isomers of polygermanes (n=1) are rare with the methods of synthesis and purification used on the present sample, and in any case, ^1H NMR shows no doublets (n=1). Hence this signal is assigned to n = 3 (GeH_3). Furthermore, it had the same linewidth as digermane in other samples, so it is assigned as digermane.

By similar arguments, the other signal is assigned as n = 3. It had a larger linewidth than digermane signals, so this signal is assigned to the terminal trigermane groups.

Finally, the weak, broad signal was negative with D = 1.3, showing that n = 2 or n = 4. Using D = 6 followed by D = 3, the S/N increased slightly, so the signal has n = 2. In addition the signal is too broad to be n = 4. This signal is assigned to the central GeH_2 group in trigermane.

The above assignments result in the closest conformity to the expectation that the area under the terminal GeH_3 signals are twice that of the central GeH_2 signal. However, intensity measurements are not quantitative, due to the varying amounts of signal loss during INEPT precession times from the variation in T_2^* values.

3.8.4 Methylpolygermanes, $GeMe_wH_x(GeMe_yH_z)_m$ and Silylgermanes, $GeSi_xMe_yH_z$

3.8.4.1 Decoupled Enhancements

For these classes of compounds, E_d was in the range 4.2 to 1.4, and E% from 96 to 37.

Even though Δ for the GeH_3 signal of methyldigermane was not optimized, it gave a larger E% value than the $GeMeH_2$ signal for which Δ was in fact optimized. This is not surprising in view of the larger relaxation times of the former group compared to the latter.

In line with previous trends, INEPT via ^1J coupling on $GeSiH_6$ gave larger E% values compared to ^2J due to short precession times. Short precession times together with 'long' relaxation times similar to tetramethylgermane resulted in ^1J E_d values very close to the theoretical maximum.

3.8.4.2 Coupled Enhancements

E ranged from 8.3 to 1.8 and E% from 77 to 44.

Although the assignment of decoupled signals of 1-1 dimethyldigermane is discussed in the earlier section on assignment aids, the coupled ^1J INEPT spectrum warrants further discussion. This spectrum (FIG.(3.14)) of GeH_3 showed the expected -1:-1:1:1 PT intensities, each multiplet superimposed with the 1:1 FT intensities from the hydride ligand in the neighbouring $GeMe_2H$ group. These FT intensity ratios are an additional aid in distinguishing the present compound from the similar compound, methyldigermane. Also, a new class of ^2J coupling constant was gleaned, namely $^2J(Ge,Ge,H)$.

It is somewhat surprising that E% was lowered from decoupled (96) to coupled (77) INEPT via ^1J on $GeSiH_6$. This difference is not due to PT Loss during precession times or obvious pulse missetting. The experimental optimum timing for ^2J INEPT on $GeSiH_6$ was about 30% lower than the theoretical figure. Since the value of $^2J(Ge,Si,H)$ is well defined, this deviation is probably due to a significant loss of the PT signal even during the τ precession time (9.2 ms each). Intensity ratios were as expected using short range coupling, but using long range coupling, ratios were somewhat altered from the expected values of: four groups of multiplets separated by ^1J in the FT ratio 1:2:2:1, each multiplet is in the PT ratio -1:-1:1:1. Intensity distortions here are compared to those found with other compounds in section 3.8.1.2.

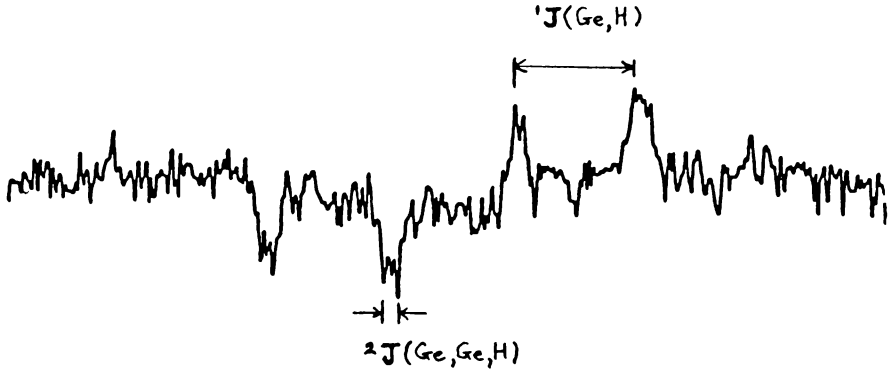

FIG. 3.14 Coupled ^{1}J INEPT on the GeH_3 group of (U1) GeH_3GeMe_2H.

3.8.4.3 Assignments

Utilization of INEPT with D = 1.3 on a sample containing methyldigermane, together with methylgermanes, revealed one positive and one weak negative signal in addition to the three methylgermane signals as discussed in 3.8.1.3. The positive and negative signals are therefore assigned to the GeH_3 and the $GeMeH_2$ groups, respectively, of methyldigermane. Enhancements were slightly above unity compared to a JMSE sequence.

A sample of methyldigermane mixed with 1,2 dimethyldigermane gave one 'slightly broader' negative signal and one sharp, positive signal using D = 1.3. Since the slightly broad signal had a linewidth too great for GeH_4 (n=4) and a chemical shift far removed (nearly 100 ppm) from GeH_4, it is assigned to the $GeMeH_2$ (n=2) groups. Almost no signal was observed with D = 2, so the sharp signal must be a GeH_3 group from methyldigermane.

Similarly, a neat sample of 1,2 dimethyldigermane gave the expected single negative signal with D = 1.3, and the possibility of n = 4 is discounted by linewidth and chemical shift values.

It should be noted that the $GeMeH_2$ group in methylpolygermanes has almost the same chemical shift as, and a similar linewidth to, the compound $GeMeH_3$ (section 4.3). INEPT offers the quickest way of distinguishing these two different 'groups'.

A neat sample of 1,2,3 trimethyltrigermane gave one negative signal using D = 1.4, with E_d = 1.4 compared to a JMSE sequence. Discounting the possibility of n = 4 from the chemical shift, the signal is assigned to the terminal $GeMeH_2$ groups. An overnight accumulation gave sufficient S/N to show the central GeMeH signal using a JMSE sequence, but not using INEPT. The former sequence also identified the signal as coming from a GeMeH (n=1) group rather than from the compound $GeMe_2H_2$ which has an almost identical chemical shift.

In a similar fashion, the use of the PT sequence confirmed that the large signal in two further samples of 1,2,3 trimethyltrigermane is due to the terminal $GeMeH_2$ groups.

Single-pulse sequences show one sharp, and one broad signal for GeH_3GeMe_3. INEPT via ^1J using D = 1.3 gave only one sharp, positive signal (n=1 or n=3). Proton NMR showed only singlets, and so the sharp signal is assigned to (n=3)GeH_3 and the broad signal not observed by INEPT in the assignment mode is (n=0) $GeMe_3$, as expected.

This leads to a discussion on the limitations of multipulse sequences arising from rapid signal decay. The $GeMe_3$ group (T_2^* $\sim$11 ms) on $GeMe_3GeH_3$ was not observed by JMSE sequences, probably because the signal had decayed significantly during precession times. Thus the lack of signal when INEPT is used in the assignment mode on a broad signal can be due either to n = 0 or to rapid signal decay during precession times. However in the present case, the ambiguity was removed by the appearance of two singlets in proton NMR in the $GeMe_3$ and GeH_3 regions.

The broad signal ($T_2^* \sim 8$ ms) found with the signals from GeH_3GeMe_2H has been tentatively assigned to a high molecular mass methylpolygermane. Both single-pulse sequences and INEPT used with short precession times (max. delay 2 ms) gave this broad peak. However, JMSE sequences (max. delay 11 ms) and INEPT with long precession times D = 1.4 (max. delay 4 ms) did not reveal this peak. Thus the signal could be n = 0, 1, 2, or 3. (Proton spectra showed unassigned signals in the GeH and GeMe regions.)

On the other hand, an overnight accumulation did reveal the broad GeH_2 signal ($T_2^* \sim 11$ ms) in trigermane even though INEPT was used with the long precession times associated with 'the assignment mode of use'.

Silylgermane has a ^{73}Ge signal uniquely defined by its extreme low frequency position and small linewidth (section 4.3).

Methylgermyl-silane ($GeMeH_2SiH_3$), however, has a chemical shift near to methylgermane, and so INEPT with D = 1.4 was used to check this signal. The negative signal indicates n = 2 as expected for $GeMeH_2SiH_3$. Although not optimized for Δ the enhancement was 2.6 compared to a single 90° pulse sequence without a NOE.

3.9 ^{73}Ge DEPT AND UPT

Distortionless enhancement by PT (DEPT)[106] and universal PT (UPT)[117] were discussed in section 2.1.6 on pulse sequences subsequent to INEPT. This literature appeared during the course of ^{73}Ge INEPT experiments. Although DEPT is not strictly applicable to quadrupolar nuclei, a time delay 'analogous' to that used for τ with INEPT was tried, together with tip angles corresponding to Δ with INEPT. Universal PT was designed for use with any NMR isotope, however.

Work with DEPT was merely exploratory, and it is not claimed that the 'optimum' timing and maximum enhancements were found for this sequence. The standard $(2J)^{-1}$ time delays in DEPT were replaced with the same total τ precession times used in ^{73}Ge INEPT, namely $(14.95\,J)^{-1}$. The variable tip angle in the final pulse (FIG.(3.17)) was set equal to $\pi J\Delta$.

On the sample of germane (M), the largest coupled and decoupled enhancements were about 1.5 and 2, respectively. Coupled DEPT gave positive multiplets close to the expected ratios of 1:4:6:4:1. The lowest frequency multiplet had a nearby negative signal of similar intensity and a further negative signal appeared to lower frequency, separated by $^{1}J(Ge,H)$.

Since UPT has a theoretical basis for optimum timing and maximum enhancements, E% values can be recorded (TABLE (3.12)).

Using $^{1}J(Ge,H)$, enhancements were 'reasonable', but always lower than the corresponding values from decoupled INEPT. When experimental conditions for UPT and INEPT were made as similar as possible, and spectra are run consecutively, UPT delivered up to 80% of the S/N of INEPT.

Long range coupling used with ^{73}Ge UPT gave no enhancements of practical use, except possibly when precession times are greatly reduced from the theoretical values. For instance, tetramethylgermane yielded the greatest enhancement when precession times were about a quarter of the theoretical value ($\tau\% = -120$).

	COMPOUND	MAX. ENHANCEMENT COUPLED	MAX. ENHANCEMENT DECOUPLED	E% VALUES COUPLED	E% VALUES DECOUPLED	T% τ
(A)	$GeMe_4$	-	0.13	-	1.6	0
(A)	$GeMe_4$	-	1.0	-	12	-66
(A)	$GeMe_4$	-	1.7	-	21	-120
(A)	$GeMe_4$	-	0.43	-	5.3	-156
(H1)	$GeMeH_3$	-	2.4	-	55	0
(M)	GeH_4	2.4,3.0	3.4	56	71	0

TABLE 3.12 Max. enhancements and associated timing using ^{73}Ge UPT. The samples are the same as those presented for ^{73}Ge INEPT. In each case θ and ϕ were very close to the theoretical optimum values, and all accumulations were the average of 10 scans.

Coupled ^{73}Ge UPT revealed the expected binomial pattern of multiplets.

A rationale for the reduction in E% using ^{73}Ge UPT compared to ^{73}Ge INEPT is based on the longer precession times of the former compared to the latter. The total precession time for UPT is $(0.66J)^{-1}$ for all nuclear spins, I, and for any number of attached protons, n. Total free precession times for INEPT when, n varies from 1 to 12 are, for instance, $I = \frac{1}{2}$: $(J)^{-1}$ to $(1.69J)^{-1}$, and $I = {}^{9}/_{2}$: $(1.77J)^{-1}$ to $(6.25J)^{-1}$. For n = 1 to 12, the relative precession times of UPT divided by INEPT are:

$I = \frac{1}{2}$ 1.50 to 2.53

$I = 1$ 2.00 to 4.37

$I = \frac{9}{2}$ 2.65 to 9.37

When INEPT is used in the assignment mode, Δ can be as large as $(1.24J)^{-1}$, fixing the limit of the minimum relative precession times:

$I = \frac{1}{2}$	1.15
$I = 1$	1.42
$I = \frac{9}{2}$	1.72

Reductions in E_d for INEPT have been ascribed to short T_2 values of the observed nucleus, I,[85] while reductions in E have been ascribed to short proton T_2 values.[86]

In cases where $T_2^*(^1H) \simeq T_2^*(I)$, the rather gross approximation that PT signal intensity $A_{(PT)}$ is attenuated within the sequence as:

$$A_{(PT)} \approx A^{\circ}_{(PT)} \exp[-T_i/T_2^*(I)] \qquad ---(3.3)$$

leads to an expression for the relative signal intensity of UPT and INEPT if signal loss occurs only by relaxation effects within the sequence:

$$A_{(UPT)}/A_{(INEPT)} \approx \exp[JT_2^*(I)/(1.5-\{0.5T\}^{-1}-D^{-1})] \qquad ---(3.4)$$

where $A^{\circ}_{(PT)}$ is the PT signal intensity when $T_2^*(I) \rightarrow \infty$, T_i is the total precession time, and $\tau = (TJ)^{-1}$ and $\Delta = (DJ)^{-1}$ have been defined in section 2.2.1.

Most organogermanium compounds with ^{73}Ge linewidths less than several Hz have $T_2^*(^1H) \simeq T_2^*(^{73}Ge)$. The simple hypothesis correctly predicts the order of UPT to INEPT relative signal intensities, but does not account for the large difference between intensities using short and long range coupling (TABLE (3.13)). In each case, there is more signal loss than predicted, especially when using long range coupling. This is not accounted for by the larger pulse inhomogeneity of INEPT compared to UPT. However, the predictions are based on a rather gross approximation.

	COMPOUND	$100\ A_{(UPT)}/A_{(INEPT)}$ EXPERIMENT	SIMPLE HYPOTHESIS
(A)	$GeMe_4$	2.2	21
(H1)	$GeMeH_3$	73	93
(M)	GeH_4	80	95

TABLE 3.13 Signal intensities of UPT relative to INEPT. The samples are the same as those presented for ^{73}Ge INEPT.

3.10 CONCLUSIONS

Proton polarization transfer using the INEPT class of pulse sequences is useful in ^{73}Ge NMR.

Theories[86] used to obtain optimum timing parameters are applicable to this 'high spin' case of $I = {}^{9}/_{2}$. The theoretical functional form of E with respect to τ,and E_d with respect to Δ (n=12),were in good agreement with experiment, thus extending the verification of these theories.

Despite the low observation frequency, and concomitant long, inhomogeneous 90° ^{73}Ge pulses (of width about 100 μs) on the NMR machine used, significant PT enhancements are attained. Coupled and decoupled enhancements from about 50% to almost 100% (GeH_4) of the theoretical maximum are attained for compounds with ^{73}Ge spin-spin relaxation times that are not relatively short. Most mononuclear germanium hydrides and some tetraalkyls fall into this category. Compounds with relatively short relaxation times (say, $T_2^* < 50$ ms) can give enhancements up to about half of the theoretical maximum values. All compounds exhibit more reduction from the maximum enhancement when the long free precession times concomitant with decoupling are added. P.T. enhancements are reduced by short ^{73}Ge T_2 values, by long free precession times when long range coupling is used, and by coupling which is not well resolved ($GeEt_4$).

There are substantial signal to noise enhancements afforded by INEPT, being 2 to 6 and 3 to 20 compared to unenhanced decoupled and coupled spectra, respectively. Long ^{1}H spin-lattice relaxation times and concomitant long INEPT recycle times limit the significant instrument time saving to compounds with a high ^{73}Ge T_1 to ^{1}H T_1 ratio or to accumulations with long acquisition times. However, by the addition of very small amounts of $Cr(acac)_3$, ^{73}Ge INEPT can be a useful sensitivity enhancement tool for both decoupled and coupled spectra. Potential time

saving factors of 2 to 10 and 2 to 100 have been demonstrated for decoupled and proton coupled conditions, respectively.

Coupled INEPT using differential PT has the advantage of less spectral crowding than single-pulse sequences (or 'net-PT' sequences) when observing mixtures of polygermanes. This is a useful technique, since polygermanes are difficult to free from traces of their homologues, and they all have similar chemical shifts.

Decoupled INEPT as a multiplicity assignment aid is quite useful when used via $^{1}J(Ge,H)$ coupling. Although almost all germanium compounds with GeH bonds have been given multiplicity assignments using INEPT, assignments are most useful in yielding signal identification when used with polygermanes, methylpolygermanes and methylgermyl-silanes. The limitation of signal loss during precession times is at least as great in standard JMSE type sequences as with INEPT when used in the 'assignment mode'.

In general, INEPT is the most appropriate PT sequence to use in ^{73}Ge NMR, because the limitation of short relaxation times compared to pulse sequence times is least critical for INEPT. INEPT gave significantly larger enhancements for ^{73}Ge NMR than the other multinuclear PT pulse sequence, UPT.

Therefore, proton PT to ^{73}Ge using INEPT is a useful tool in ^{73}Ge NMR, remembering that the chemistry of germanium together with hydrogen is quite extensive.[125] Moreover, germanium hydrogen coupling need not be ^{1}J (Ge,H) or resolvable in coupled spectra in order to furnish significant PT enhancements.

More extensive studies may be profitable on the use of solvents and the optimum concentrations of $Cr(acac)_3$ in order to reduce T_{1H} values without significant reduction of T_{2Ge} values or significant decomposition

of the germanium compounds. This may lead to a reduction in recycle times for INEPT, and so increase the usefulness of ^{73}Ge INEPT as an instrument time saving tool.

Since proton PT via INEPT works on a 'high-spin' nucleus of significant quadrupole movement, and low observation frequency, this result may be an incentive for the application of PT via INEPT to other quadrupolar nuclei. New candidates for proton or phosphorus PT could include ^{99}Ru, ^{95}Mo, ^{91}Zr, ^{47}Ti and ^{43}Ca. The limitation of PT signal loss during precession times is less important if INEPT rather than UPT is used.

3.11 EXPERIMENTAL DETAILS

3.11.1 Instrumentation

All NMR spectra were recorded on a JEOL FX90Q operating in the Fourier transform mode at a probe temperature of 27 °C. Germanium-73 NMR spectra were collected at 3.13 MHz using the standard low frequency probe NM-IT10LF with 10 mm outside diameter sample tubes.

A PG200 programmable pulse generator was used to create the pulse sequences. The installation of a cross polarization modification kit, stock number 19331, allowed the ^{1}H irradiation pulse to be applied along the Y axis in the ^{1}H rotating frame. This modification allowed the INEPT pulse sequences to operate.

Using the low frequency probe with the maximum amplitude on the probe tune meter, the 90° ^{73}Ge observation pulse is 130±3 μs and the 90° ^{1}H irradiation pulse is 48±3 μs. Reduction of the amplitude on the probe tune meter by detuning did not significantly alter the 90° ^{73}Ge pulse width. This 90° pulse was found by finding the null point of the 180° ^{73}Ge pulse. A pulse sequence based on one by Doddrell et al[134] is used to find the 90° ^{1}H pulse; (90° ^{n}X) -τ-(θ° ^{1}H)(ACQUIRE ^{n}X). When $\theta = \pi/2$ a null is observed in the coupled spectrum. The doublet signal of $GeEt_3H$ was used with $\tau = (2J)^{-1}$. Fine adjustments to the 90° ^{1}H pulse width were made by maximizing the PT enhancements, as used by Thomas et al.[61]

Representative lists of the instrument parameters used for ^{73}Ge NMR, including INEPT are given in appendix 3.

3.11.2 Sample Handling

Most germanium compounds in this study are water and air sensitive. Thus, in most cases, sealed 5 mm outside diameter cylindrical glass tubes were used to contain the samples, although in a few cases, sealed 3 mm and 8 mm tubes were used. These tubes were placed concentrically in a 10 mm NMR tube using two spacers. Degassed, fresh D_2O was placed in the 10 mm tube to provide the lock signal (FIG.(3.15)). The D_2O was replaced regularly, and degassed, since it slowly exchanges with atmospheric water vapour. A significant loss in PT was noted whenever the D_2O contained air bubbles. In almost all cases, there was insufficient sample to mix with deuterated solvent and seal in the largest size 10 mm tube. Moreover, since for the same sample, line broadening due to magnet inhomogeneity increased noticeably changing from a 5 mm to an 8 mm tube, no concerted effort was made to use sealed 10 mm sample tubes. For most of the compounds, the best trade off between sensitivity and magnetic field homogeneity appeared to be found in the use of 5 mm diameter sealed tubes. One sample of air stable $GeEt_4$ was mixed with $CDCl_3$ and placed straight into a 10 mm NMR tube.

With the exception of the sample of $GeEt_4$ in $CDCl_3$, all manipulations on the germanium samples were performed on vacuum lines. These samples were all degassed by freeze-thaw cycles before sealing into 5 mm or 8 mm glass tubes.

3.11.3 Materials

The solvents C_6H_6, C_6H_{14}, and n-Bu_2O were dried over sodium wire and degassed by freeze-thaw cycles in a vacuum line. At room temperature, GeH_4, Ge_2H_6, $GeMeH_3$, and $GeSiH_6$ are gases, and so they were distilled into the solvent until there was about one atmosphere pressure of gas in the sealed tube.

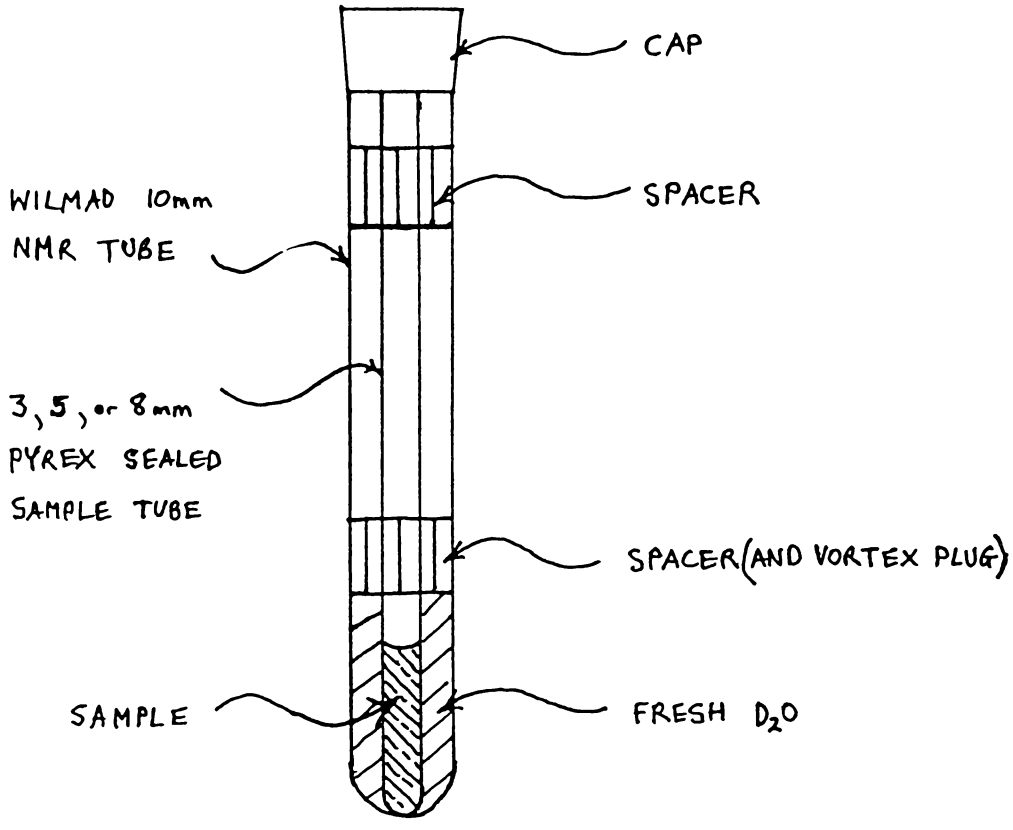

FIG. 3.15 Standard sample handling system used for ^{73}Ge NMR work. Spacers used were polypropylene for accurate work, and layers of masking tape otherwise.

Tetraethylgermane samples were used as supplied by the Germanium Research Committee. Tetramethylgermane,[135] methylgermanes,[132,136,137] and ethylgermanes were prepared by reduction of the corresponding alkyl halides. (Trimethylgermane was a decomposition product of $Fe(CO)_4(GeMe_3)_2$ and $Fe(CO)_4(GeH_3)_2$.) Polygermanes[138,139] and silylgermane[140] were prepared with standard techniques by students within Waikato University.

Methylpolygermanes with one methyl group per germanium, namely: GeH_3GeMeH_2, $(GeMeH_2)_2$, and $(GeMeH_2)_2GeMeH$, were prepared by the action of a silent electric discharge on $GeMeH_3$ followed by separation with g.c. or vacuum line distillations.[136] The compound GeH_3GeMe_2H was isolated as a minor product from the following reactions. Digermane was

chlorinated by $SnCl_4$ and this initial product was methylated with MeMgI.[136] Preparation of $GeMeH_2SiH_3$ was afforded by the addition of iodine to silylgermane followed by the addition of MeMgI in Bu_2O.[141] The compound GeH_3GeMe_3 was prepared by several research students at Waikato University, including the reference.[142]

All samples were checked for purity by use of ^{13}C and ^{1}H NMR, (^{29}Si NMR where appropriate) and some samples were also checked using infrared spectroscopy ($GeSiH_6$, $GeMe_mH_{4-m}$, m = 0, 1, 4).

3.12 PULSE SEQUENCES

All pulse sequences were created by the PG200 programmable pulse generator. The physical operation of INEPT sequences was checked using the pulse sequence INECHK, supplied by JEOL, together with an oscilloscope. It is important to disconnect the spin-lock unit before INEPT experiments, since it alters phase relationships so that INEPT will not work.

The decoupled INEPT pulse sequence employed is substantially the same as that used by Ernst and Burum.[81] Coupled pulse sequences used presently are essentially those given by Morris and Freeman[69] except that all the 90° pulses have the x and y axes of rotation in the ^{1}H frame interchanged. Essential spectral features from decoupled pulse sequences[81,82] which differ by this x and y interchange, are not significantly different. In addition, for coupled ^{73}Ge INEPT, this interchange gives no significant change in spectra. Thus, for all INEPT sequences presently used, the initial ^{1}H 90° pulse rotates magnetization about the y axis. The DEPT[106] and UPT[117] sequences are substantially the same as those recorded in the literature by Bendall, Doddrell, and Pegg.

3.12.1 Decoupled INEPT Sequences

Initially, the 6-pulse sequence (d) (FIG.(3.16)) with one final 180° observation channel refocusing pulse was used, as recommended by JEOL engineers.[144] However, the 7-pulse sequence, (e), with 180° refocusing pulses on both irradiation and observation channels was used in the present study. In the case of ^{73}Ge INEPT, (e) gave slightly higher S/N than (d) under the same conditions. Thus pulse sequence (e) was used for ^{73}Ge decoupled INEPT. Since (e) has half the total time delay (Δ) between the ^{73}Ge 90° pulse and acquisition, compared to (d), the former pulse sequence will give less PT signal loss during this free precession time than the latter. In practice, the delay Δ for (e) was found to be

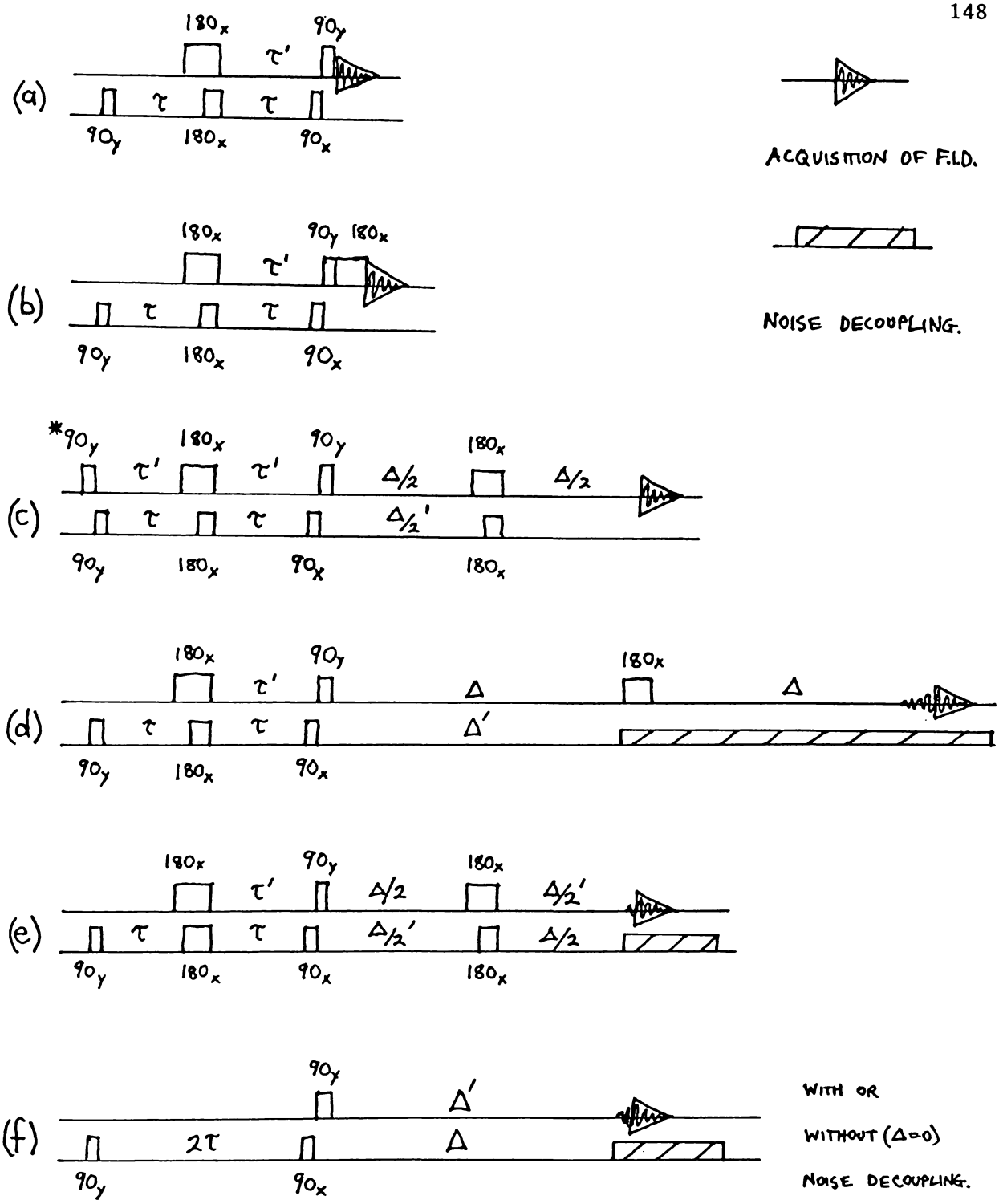

FIG. 3.16 The class of INEPT pulse sequences applied to ^{73}Ge NMR. Phase alternation of the final sequential pair of 90° pulses is employed.[143] (x,y, then -x,-y,...) R.f. pulses are applied along the x or y axis to rotate the magnetization 90° or 180° in the ^{1}H rotating frame. The top channel is observation, (^{73}Ge) and the bottom channel, irradiation (^{1}H). Note that $\tau' \geq \tau$, $\Delta' \geq \Delta$. *This 90° pulse has a constant phase throughout the experiment.

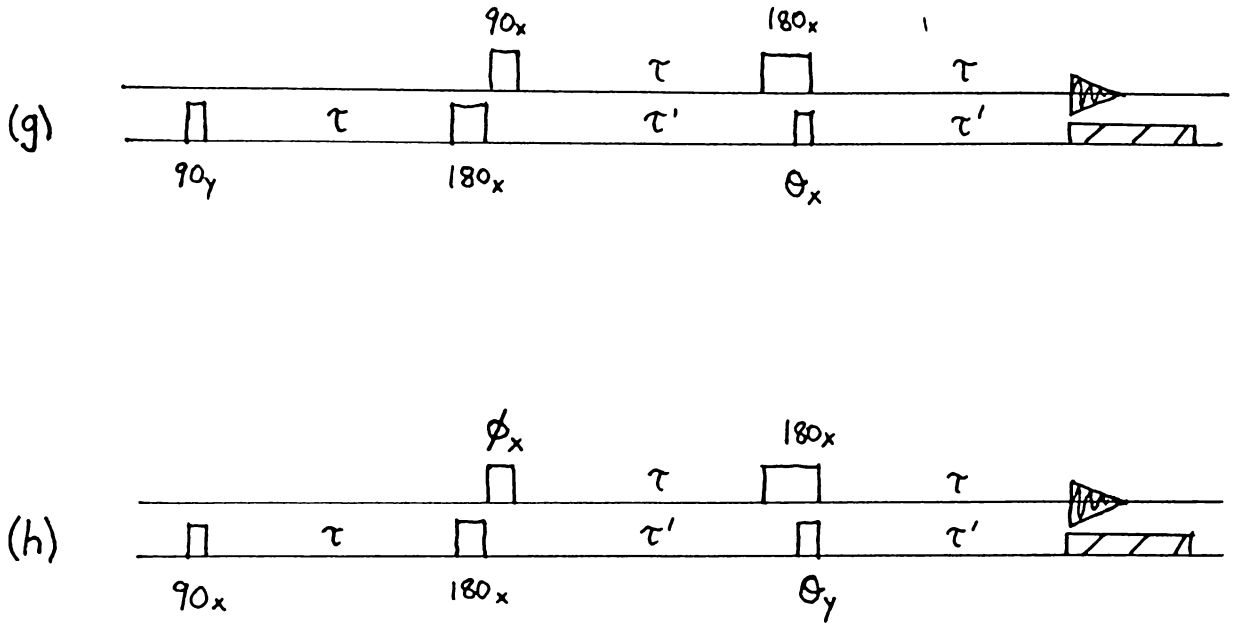

FIG. 3.17 Pulse sequences used subsequent to INEPT. Both DEPT (g) and UPT (h) can be used with or without noise decoupling. Phase alternation of the final pair of pulses for DEPT is used (x, x, then -x, -x), and phase alternation of all but the first pulse in UPT is used (180(S)x, ϕ(I)x, 180(I)x, θ(S)y then 180(S)-x, ϕ(I)x, 180(I)y, θ(S)-y). R.f. pulses are applied along the x or y axis to rotate the magnetization 90° or 180° in the ^{1}H rotating frame. The top channel is observation (^{73}Ge) and the bottom channel, irradiation (^{1}H). Note that $\tau' \geq \tau$.

defined as; between the midpoint and the endpoint of the 90° ^{73}Ge pulse, to the onset of decoupling. Maximum S/N was gained by using the theory on INEPT parameters to find D, having prior knowledge of J, preferably, and adjusting time parameters so that Δ equalled the delay defined above.

3.12.2 Coupled INEPT sequences

In the first instance, the decoupled pulse sequence received from JEOL engineers, (d), was modified to the minimum degree in order to procure a coupled INEPT sequence, (b). Specifically, the decoupler channel was left off during acquisition, and Δ was set to the smallest attainable value of 1 μs. Later,the simpler pulse sequence (a), was created. A comparison of the performance of these two sequences applied to ^{73}Ge NMR showed that they were the same, within experimental error, for S/N, phase characteristics, and multiplet intensity ratios. Spectra herein, from coupled ^{73}Ge INEPT are obtained with (b).

Since the final pair of 90° pulses are applied sequentially, (FIG.(3.16)) and ^{73}Ge pulses are longer than ^{1}H pulses, the delay τ between ^{73}Ge pulses cannot be set accurately at the same time as τ between ^{1}H pulses. Signal to noise ratios were maximized when the two delays, τ in the irradiation as opposed to the observation channel are critically set to be equal to each other and to the theoretical values. Experimental values of τ were measured from between the midpoint and the endpoint of the first ^{1}H pulse to a point between the midpoint and the endpoint of the second ^{1}H pulse.

Instrumental phase errors were not a significant problem with the two pulse sequences (a), (b), which use differential type PT.

3.12.3 Further Pulse Sequences

Experimental multiplet intensity ratios show a small distortion from the expected PT ratios. One reason could be the initial ^{73}Ge magnetization, by analogy with Ernst's ^{13}C experiments.[81] The pulse sequence (c) removes initial magnetization by the use of an initial 90° observation pulse. Since this coupled INEPT sequence has free precession times, Δ, giving net PT rather than differential PT as in (a), (b), (f), all non-zero signals are positive.

Initial work on GeH_4 showed the expected positive signals, but with no reduction in the slight distortion of intensity ratios. In fact, this sequence gave much larger instrumental phase errors than (b).

Because of the long, inhomogeneous ^{73}Ge pulses, an attempt to reduce inhomogeneity was made by using a pulse sequence, (f), with no 180° pulses.[145] One must sit on the ^{73}Ge and ^{1}H resonances to better than 1 Hz. However, the S/N of this type of sequence is slightly smaller than the other sequences, and the accurate prior knowledge of ^{73}Ge and ^{1}H resonances add to the experimental complexity.

Figure (3.17) presents the pulse sequences DEPT (g) and UPT (h) used for ^{73}Ge NMR.

Plans have been made to replace the final 180° ^{1}H refocusing pulses in INEPT with a composite pulse[61] to reduce r.f. inhomogeneity.

On hindsight, it would be advantageous to exchange all x and y axes in the coupled INEPT sequences, so that the instrumental phasing of single-pulse coupled sequences is similar to that of coupled INEPT. Instrument phasing from the present decoupled INEPT is similar (±10°) to single-pulse decoupled sequences.

Appendix 4 contains printouts of PT pulse sequences in machine language.

CHAPTER 4 GERMANIUM-73 BASIC NMR PARAMETERS

4.1 INTRODUCTION

Having established sensitivity enhancement and assignment aids in the previous chapter, attention is now turned toward exploring the basic NMR parameters of ^{73}Ge. This chapter is concerned with values of δ, J and $W_{\frac{1}{2}}$.

Group IV elements in the periodic table exhibit the unique property of having stable spin $\frac{1}{2}$ isotopes for most of the group. The exception is germanium. In general, spin $\frac{1}{2}$ species yield sharp lines and good spectral dispersion, but quadrupolar species yield broad lines and poorer dispersion. However, ^{73}Ge has a small to moderate linewidth factor compared to quadrupolar nuclei (TABLE (4.1)). Of the 29 isotopes listed, only 7 have a smaller linewidth factor ('sharper lines') than ^{73}Ge, although ^{73}Ge has a value midway between the extreme values. Germanium-73 has a moderate sized quadrupole moment ($-0.18 \times 10^{-28} m^2$)[129] but a large spin quantum number ($^9/2$). Furthermore, the tetravalency with tetrahedral coordination the norm, also serves to reduce linewidths.

In comparison with other Group IV elements, (TABLE (4.2)) ^{73}Ge has a low magnetogyric ratio, leading to a low receptivity and a low observation frequency.

This latter quality has meant that until the recent advent of 'wide-range' multinuclear FTNMR machines, this isotope has been experimentally inaccessible. In fact, γ for ^{73}Ge is one of the lowest in the periodic table, ^{57}Fe and ^{103}Rh being the only 'well-known' isotopes with lower γ values.

ISOTOPE	L (10^{-60} m^4)	ISOTOPE	L (10^{-60} m^4)
^{2}H	0.37	^{61}Ni	340
^{6}Li	0.03	^{71}Ga	167
^{9}Be	36	^{73}Ge	24
^{10}B	1.1	^{75}As	1200
^{14}N	13	^{87}Sr	96
^{17}O	2.2	^{91}Zr	128
^{23}Na	190	^{93}Nb	30
^{27}Al	71	^{95}Mo	46
^{33}S	40	^{99}Tc	67
^{35}Cl	85	^{99}Ru	18
^{39}K	40	^{115}In	510
^{43}Ca	3.4	^{187}Re	21600
^{49}Ti	78	^{209}Bi	120
^{51}V	37		
^{55}Mn	970		
^{59}Co	200		

TABLE 4.1 Line broadening factors, $L = f(I)Q^2$ for selected quadrupolar nuclei.

ISOTOPE	NUCLEAR SPIN	NATURAL ABUNDANCE N/%	MAGNETOGYRIC RATIO $\gamma/10^7$ $radT^{-1}s^{-1}$	NMR (a) FREQUENCY Ξ MHz	RELATIVE (b) RECEPTIVITY
^{13}C	1/2	1.11	6.725	25.145004	0.18
^{29}Si	1/2	4.67	-5.314	19.867184	0.37
^{73}Ge	9/2	7.76	-0.9332	3.488315	0.11
^{119}Sn	1/2	8.60	-9.971	37.290662	4.5
^{207}Pb	1/2	22.6	5.597	20.920597	2.0

TABLE 4.2 Nuclear spin properties of the Group IV elements.
(a) Value for the tetramethyl-group IV standard in a magnetic field such that the protons in Me_4Si resonate at 100.00 MHz.
(b) Receptivity relative to the proton = 1000 .

4.2 REVIEW OF ^{73}Ge NMR

In the light of the experimental inaccessibility of this isotope, it is not surprising that there is a scarcity of literature on this technologically important element. There are only three sources of ^{73}Ge NMR to 1983, including the most extensive ^{73}Ge NMR study, on a selection of GeR_4 compounds, by Kaufmann, Sahm, and Schwenk,[127] a ^{73}Ge NMR study on germanium tetrahalides by Kidd and Spinney,[146] and a ^{73}Ge INDOR study on germatranes by Pestunovich et al.[147] This work spans the time 1971 to 1980.

Studies involving ^{13}C are very large in number.

By comparison, from 1978-80, ^{29}Si, ^{119}Sn and ^{207}Pb were the 7th, 18th, and 26th most popular nuclei respectively, for chemical NMR studies with at least 85, 28, and 9 publications, respectively (including solid state studies).[8d] (Solid state ^{73}Ge studies included one of $Ge(Co_2)O_4$ by Saji[148] and of Ge and Ge alloys by Murakami et al,[149] over 1973-1982.) Several 'common nuclei' studies have yielded ^{73}Ge J values[126,128,150,151 152], and one study yielded an estimate of the ^{73}Ge NQCC[153] for GeF_6^{2-}. There is one study on the relation between ^{73}Ge δ values and CNDO/2 charges in germanium tetrahalides.[154]

NMR work on ^{73}Ge has been reviewed in 1978,[6k] as part of a review on less common quadrupolar nuclei[129] and as a minor part of a review on solution state NMR studies of Group IV elements other than carbon.[8d]

4.2.1 Chemical Shifts

A collection of all the δ and J ^{73}Ge parameters is given in TABLE (4.3) and (4.4). Chemical shifts are to high frequency of neat $GeMe_4$, the chosen reference material.[6k] Since the resonance frequency in $GeCl_4$ has been compared with those of a number of other nuclei,[155-159] it is possible to deduce that $\Xi(^{73}Ge)$ = 3,488,315±10 Hz in neat $GeMe_4$.

COMPOUND	SAMPLE	δ(Ge)	^{n}J(Ge,A) (a)	REFERENCE
$GeMe_4$	neat	0	2.99±.03 (2,H)	127
$GeMe_4$	-	-	-18.7 (1,C)	150
$GeEt_4$	neat	18.1±.7	-	127
$Ge(n\text{-}Pr)_4$	neat	2.1±.8	-	127
$Ge(n\text{-}Bu)_4$	neat	5.5±.8	-	127
GeH_4	-	-	-97.6 (1,H)	126
$Ge(SMe)_4$	50% v.CH_2Cl_2	153±3 (b)	-2.5 (3,H)	128
$Ge(OMe)_4$	neat	-36.0±.7	-1.9 (3,H)	127
$Ge(OR)(OR')_3N$	R=$SnMe_3$	-53.4	-	147 (c)
$Ge(OR)(OR')_3N$	R=H	-55.2	-	147
$Ge(OR)(OR')_3N$	R=$GeMe_3$	-55.2	-	147
$Ge(OR)(OR')_3N$	R=Me	-60.6	-	147
$Ge(OR)(OR')_3N$	R=Pr	-63.4	-	147
$Ge(OR)(OR')_3N$	R=$SiMe_3$	-73.8	-	147

TABLE 4.3 ^{73}Ge chemical shifts(ppm) and coupling constants(Hz) in **halogen-free Germanium compounds .**

(a)Extra figures in brackets are (n,A) for J values.
(b) $\Xi(^{73}Ge)$=3.488850 MHz by $^{1}H\text{-}\{^{73}Ge\}$ double resonance, δ derived by assuming $\Xi(^{73}Ge)$=3.488423 MHz in $GeCl_4$. (c) R'=CH_2CH_2 for germatranes.

COMPOUND	SAMPLE	δ(Ge)	$^nJ(Ge,A)$ (a)	REFERENCE
$(NH_4)_2GeF_6$	-	-	98±.5 (1,F)	152
GeF_4	-	-	178.5 (1,F)	151
$GeCl_4$	neat, CS_2	30.9±.5 (b)	-	127,146
$GeBr_4$	neat, CS_2	-312.1±.8 (b)	-	127,146
GeI_4	CS_2	-1080.7±1	-	127
GeI_4	C_6H_6	-1108.1±1	-	127
$GeCl_3Br$	CS_2 (c)	-47±4	-	146
$GeCl_2Br_2$	CS_2 (c)	-130±4	-	146
$GeClBr_3$	CS_2 (c)	-219±4	-	146
$GeCl_3I$	CS_2 (d)	-231±4	-	146
$GeCl_2I_2$	CS_2 (d)	-518±4	-	146
$GeClI_3$	CS_2 (d)	-808±4	-	146
$GeBr_3I$	CS_2 (e)	-513±4	-	146
$GeBr_2I_2$	CS_2 (e)	-708±4	-	146
$GeBrI_3$	CS_2 (e)	-901±4	-	146
$GeCl_2BrI$	CS_2 (f)	-316±4	-	146
$GeClBr_2I$	CS_2 (f)	-407±4	-	146
$GeClBrI_2$	CS_2 (f)	-601±4	-	146

TABLE 4.4 ^{73}Ge chemical shifts and coupling constants in **germanium tetrahalides.** (a)Extra figures in brackets are (n,A) for J values. (b)No change on dilution in CS_2. (c)Present in a 1:1 mixture of $GeCl_4$ / $GeBr_4$ (d)Present in 1:1 mixture of $GeCl_4$ / GeI_4 (e)Present in 1:1 mixture of $GeBr_4$ / GeI_4 (f)Present in 1:1:1 mixture of $GeCl_4$ / $GeBr_4$ / GeI_4 .

Chemical shifts have been obtained by pulsed FT techniques on a home-built spectrometer,[127] by CW techniques,[146] or by INDOR methods.[147,128] The chemical shift range of ^{73}Ge (∿1,250) is intermediate between ^{29}Si (∿500) and ^{119}Sn (∿2,180), and much smaller than ^{207}Pb (∿3,400). Shielding ranges increase with atomic number for these Group IV elements, reflecting the increasing numbers of electrons and the increasing atomic polarizabilities. The most shielded compounds are the tetraiodides. This shows the well recognized 'heavy atom effect', which has been shown[160] to involve spin-orbital interactions on the heavy atom. Surprisingly, GeI_4 affords two separate resonances in reference[127], but not in reference[146]. The second peak is tentatively ascribed to a species containing less iodine, since iodine is evolved from the solution.

Trends in ^{73}Ge chemical shifts parallel those of ^{119}Sn. Hence there is a roughly linear relationship for chemical shifts.

$$\delta(GeX_4) = 0.71\ \delta(SnX_4) \quad (X = Cl,Br) \qquad ---(4.1)$$

A better correlation between chemical shifts of the tetrahalides in general is found by using the first order additivity model,[146] although this can be improved still further by the inclusion of 'pairwise' additivity parameters. The same workers found all twelve possible mixed halides upon mixing the neat tetrahalides GeX_4 (X=Cl,Br,I). ^{73}Ge NMR in this case turned out to be a unique method for identifying and characterizing these compounds. In addition, these compounds also follow the δ patterns already established for ^{27}Al, ^{69}Ga, and ^{71}Ga in the tetrahalogeno complexes, ie I > Br > Cl.

CNDO/2 calculations[154] have shown that charge densities at the germanium atom change in a parallel manner to δ (Ge) values in the tetrahalide complexes. However, the extrapolation of this idea, namely that there is a direct relation between charge density and germanium shielding in general, does not explain the chemical shift of $GeMe_4$.

By comparison with ^{119}Sn, the other compounds examined gave the results expected, except that the value of $GeEt_4$ is larger than expected by a comparison with $Ge(n\text{-}Pr)_4$ and $Ge(n\text{-}Bu)_4$.

The shifts of the six germatranes reflect the Ge←N transannular interaction.[147]

A slight temperature dependence for the chemical shifts was found[127] for $Ge(OMe)_4$ (0.026 ppm/°C) and $GeBr_4$ (0.059 ppm/°C) while no such detectable variations were found for $GeCl_4$, $GeEt_4$, $Ge(n\text{-}Pr)_4$ and $Ge(n\text{-}Bu)_4$ at least in the range of 20 °C to 40 °C.

4.2.2 Coupling Constants

The only ^{73}Ge NMR parameter for non-tetravalent germanium appears to be the $^1J(Ge,F)$ constant[152] in $(NH_4)_2\ GeF_6$. Absolute values of reduced coupling constants involving germanium are larger than the analogous ones for silicon and smaller than the analogous constants for tin. For instance, $^1K(M,H)$ values, $(10^{20}NA^{-2}m^{-3})$ are SiH_4 (8.5)[161], GeH_4 (23.3)[126], and SnH_4 (43.1)[162], and $^1K(M,C)$ values are for $SiMe_4$ (-8.4)[163], $GeMe_4$ (-17.8)[127], and $SnMe_4$ (-30.2).[164] Coupling constants increase with atomic mass due to an increase in s electron density. In all cases the signs of the coupling constants are based upon comparison with those in compounds of other group IV elements rather than upon double resonance experiments.

Schwenk et al[127] provide the only values of J which come from direct ^{73}Ge observation.

4.2.3 Linewidths

Schwenk et al[127] recorded the linewidths corrected for magnetic field inhomogeneity. They are, in Hz, for GeR_4: R = Cl (2.02), Br (1.76), I (2.2), Me (0.58), Et (15.6), n-Pr (13.3), n-Bu (13.8), and OMe (17.7). Errors are about 5% - 10%. With the exception of $GeMe_4$, the linewidths for

organogermanium compounds are the widths of the absorption curves of the unresolved spectrum. However, to obtain the experimentally observed line widths, up to 0.4 Hz is added on to each value from inhomogeneity effects. (eg. $W_{\frac{1}{2}}$ ($GeMe_4$) $\leq$ 1.0 Hz). The corrected line width of the second peak from the GeI_4 sample has the largest value, namely 32 Hz. Linewidths for the tetraalkyl derivatives were dominated by unresolved coupling to protons, (except for $GeMe_4$)[127] and linewidths for the mixed tetrahalides were probably dominated by magnetic field inhomogeneity.[146] In the latter case, $W_{\frac{1}{2}} < 25$ Hz for neat tetrahalides and no accurate linewidth measurements could be made for mixed tetrahalides.

4.3 ^{73}Ge BASIC NMR PARAMETERS

Germanium-73 chemical shifts, linewidths and coupling constants, J (Ge,H) are presented in tabular form. Relevant diagnostic ^{1}H, ^{13}C, or other NMR data are also presented. Data are presented according to the class of compound.

Samples ranged in concentration from 8.6M ($GeCl_4$) to about 0.1M, and to recognize the signal (S/N > 2.5) several scans to several thousand scans were averaged, respectively.

The following units, nomenclature,and conventions are contained in tables 4.5-4.18: Default temp. 27±1 °C. COMPOUND column: An asterisk means that the multiplicity assignment was checked by ^{73}Ge INEPT. SAMPLE column: % by volume (v) in a solvent, ratios refer to mole ratios, δ column: ^{73}Ge δ in ppm to high frequency of neat $GeMe_4$. $W_{\frac{1}{2}}$, (J) column: linewidth at half height in Hz, in brackets are recorded ^{1}J(Ge,H) values in the range 80-100 Hz and ^{2}J(Ge,H) values in the range 2-10 Hz. OTHERS column: isotope observed H(^{1}H), C(^{13}C), Si(^{29}Si), Sn(^{119}Sn) is followed by δ values, using the conventions recorded in appendix 1 on multinuclear NMR parameters. Brackets following the ^{1}H δ value record the multiplet d (doublet), t (triplet), q (quartet), p (pentet), s (sextet), h (heptet), o (octet), n (nonet), d (decet) and ^{3}J (H,H). An asterisk by C means that the multiplicity assignment was checked by a JMSE sequence.

COMPOUND	SAMPLE	δ	W1/2,(J)	OTHERS
$GeMe_4$	80% v $n\text{-}Bu_2O$	0.73±.5	1.1±.1 (2.95±.03)	H 0.54 C 0.2
	75% v $n\text{-}Bu_2O$	0.57±.5	1.0±.1 (2.9±.1)	H 0.04 C 0.0
	75% v $n\text{-}Bu_2O$	0.50±.5	1.3±.1 (2.9±.1)	C 0.1
	15% v $n\text{-}Bu_2O$ traces $Cr(acac)_3$	0.64±.2	1.2±.2	H 0.31 C -0.5
	15% v C_6H_6 traces $Cr(acac)_3$	-0.3±.5	1.5±.2	H -0.01 C -0.6
	15% v C_6H_6	-0.3±.5	1.2±.1	H 0.06 C -0.5
	15% v C_6H_5Cl	0.0±.5	1.5±.2	H 0.23 C -0.1
$GeEt_4$	neat	17.8±.2	0.9±.1	C 9.5,4.4*
	dil. in $GeEt_3H$	17.7±2	-	C 9.4,4.3
	70% v $CDCl_3$	19±2	1.6±.1 (3.0±.6)	C 9.0,3.8*
	1:1 with $GeCl_4$	18.2±.1	1.2±.2	C 9.7,4.5
	75% v $n\text{-}Bu_2O$	17.8±.1	1.1±.05	C 9.3,4.1
	25% v $n\text{-}Bu_2O$	17.7±.1	1.3±.1	C 9.2,4.1
	6% v $n\text{-}Bu_2O$	17.8±.1	1.2±.05	C 9.2,4.0
	6% v C_6H_{12}	17.8±.1	0.9±.05	C 9.2,4.0

TABLE 4.5 Germanium-73 basic NMR parameters for low molecular mass **Germanium Tetraalkyls.**

COMPOUND	SAMPLE	δ	W1/2,(J)	OTHERS
$Ge(n\text{-}Pr)_4$	neat	2.4±.6	3.3±.2	C 19.6,19.0, 16.4 *
$Ge(n\text{-}Bu)_4$	neat	6.0±.6	5.1±.5	C 28.4,27.6, 14.4,13.3 *
$Ge(n\text{-}Pn)_4$	neat	6.0±.6	9.5±.5	C 36.9,25.8, 23.2,14.7, 13.5 *
$Ge(n\text{-}Hx)_4$	neat	5.6±.6	18±2	C 34.4,32.6, 26.2,23.7, 14.9,13.6 *

TABLE 4.6 Germanium-73 basic NMR parameters for high molecular mass **Germanium Tetraalkkyls.** (n-Pn = $n\text{-}C_5H_{11}$, n-Hx = $n\text{-}C_6H_{13}$)

COMPOUND	SAMPLE	δ	W(1/2),(J)	OTHERS
$GeMeH_3$ *	0.7 atm. in n-Bu_2O	-209.2±.6	1.3±.1 (-94.3±.1) (3.48±.1)	H 3.56(q,4.2) 0.42(q,4.1) C -1.2 *
	dil. in C_6H_6	-207.5±1	2.1±.2	H 3.35(q,4.1) -0.05(q,4.1) C -0.9
*	with $GeMe_2H_2$, Ge_2MeH_5, traces $GeMe_3H$	-209.2±.1	1.5±.2 (-94.5±.5) (3.5±.3)	H 3.24(q,4.0) C -11.9 *
	dil.in C_6H_6 fr. $F(GeH_3)(GeMeH_2)$ (traces GeH_4)	-206.9±1	6±1 (-96±1)	H 3.34(q,4.) -0.06(q,4.1) C -11.6 *
*	dil.in C_6H_6 fr. $F(GeMe_2H)(GeMeH_2)$ (some $GeMe_2H_2$)	-207.1±1	7±3	C -2.4 *
*	dil.in C_6D_6 fr. $GeMeH_2Br/(SiMe_3)_2Hg$	-206.8±2	2.4±.1	C 2.3
*	dil.in n-Bu_2O with Ge/Si hydrides	-207.0±.8	4.0±.5	
$GeMe_2H_2$ *	neat with Ge_2MeH_5 (some $GeMeH_3$)	-127.6±.1	1.8±.2 (-92.3±.5) (3.42±.2)	H 3.81(s,3.8) 0.37(t,3.8) C -7.2 *
	~15% v C_6H_6	-126.3±.2	3.3±.1	H 3.63(s,3.9) -0.01(t,3.9) C -7.1
	very dil. < 5% v n-Bu_2O	-125.3±2	10±4	C -6.3
*	dil.in C_6H_6 fr. $F(GeMe_2H)(GeMeH_2)$ (some $GeMeH_3$)	-126.1±2	8.5±1 (-93.7±1)	C -7.0 *
	in $SiCl_4$ (with $Co_2(CO)_8$)	-126.7±.8	1.8±.5	H 4.13(s,3.8) 0.69(t,3.8) C -6.5
	v.dil. in C_6H_6 with Si/Ge hydrides	-125.8±.8	5.0±.5	H 3.60(s,3.9) -0.07(t,3.7)

TABLE 4.7 Germanium-73 basic NMR parameters for low molecular mass **Methylgermanes.** (F = $Fe(CO)_4$)

COMPOUND	SAMPLE	δ	W(1/2),(J)	OTHERS
$GeMe_3H$ *	dil. in $GeMe_2H_2$ and Ge_2MeH_5 (some $GeMeH_3$)	-57.2±.2	1.8±.2	C -3.4 *
	dil. fr. $F(GeMe_3)(GeMe_2H)$ (some $GeMe_2H_2$)	-57.0±.8	4.0±.5 (-92.8±2)	H 4.23(broad) 0.53(broad) C -3.0 *
	dil. in C_6H_6 fr. $F(GeMe_3)(GeMeH_2)$	-56.5±2	10±2 (-87.9±5)	H 3.57(broad) 0.04(d,3.4) C -3.3
	dil.in C_6H_{14} fr. $F(GeMe_3)_2$ + $F(GeH_3)_2$ (some $GeMe_2H_2$)	-56.9±.2	4.0±.5	H 4.23(o,3.9) 0.50(d,2.9)

TABLE 4.8 Germanium-73 basic NMR parameters for a **Methylgermane.** (F = $Fe(CO)_4$)

COMPOUND	SAMPLE	δ	W(1/2),(J)	OTHERS
$GeEtH_3$	neat (traces $GeEt_2H_2$)	-186.4±.6	3.4±.2 (-92.4±.5) (~3±1)	C 12.6,(12.2) 1.5
$GeEt_2H_2$	v.dil. in $GeEtH_3$	-87.7±1	23±8	
$GeEt_3H$	neat (traces $GeEt_4$)	-15.7±.8	20±2 (-88±2)	C 10.5,4.2 *
	neat (some $GeEt_4$)	-16.4±.9	23±2 (-85±2)	C 10.4,4.1 *

TABLE 4.9 Germanium-73 basic NMR parameters for **Ethylgermanes.**

COMPOUND	SAMPLE	δ	W(1/2),(J)	OTHERS
GeH_4	* 1.2 atm. in $n\text{-}Bu_2O$	-298.7±.7	1.1±.1 (-97.6±.3)	H 3.20 (-97.5±.3)
	dil.in $n\text{-}Bu_2O$ with Ge_2H_6	-297.7±.7	1.5±.5 (-97.6±.5)	
	v.dil.in Et_2O with Ge_2H_6	-301.5±2	< 5	
	* with Ge_2H_6 and Ge_3H_8	-283.7±.6	1.5±.5	H 3.75
	dil. with Ge_4H_{10}	-298.8±1	< 2 (-97.7±.3)	
	in C_6H_{14} fr. $Ge_2H_6/Co_2(CO)_8$	-301.4±1	3±1	H 3.15
	in C_6D_6 fr. GeH_3Cl/Na	-296.7±.3	2.5±.5 (-97.7±.3)	H 3.04
Ge_2H_6	* 0.2 atm.,$n\text{-}Bu_2O$ (some GeH_4)	-311.8±.7	12.7±.5 (-95.5±.5)	
	0.6 atm.,$n\text{-}Bu_2O$ with GeH_4	-313.4±1	17±5	
	1:36 , $Ge_2H_6:Et_2O$	-316±2	15±5	H 3.18
	1:8,$Ge_2H_6:C_6H_6$ with $GeCl_4$	-308.9±1	18±2	H 3.22
	* with GeH_4 and Ge_3H_8	-300.5±.8	15±2 (-94.4±.5)	H 3.82
	with $SnMe_yCl_{4-y}$ (y=1,2,3)	-303.5±.5	12.7±.5	H 3.71 (broad)

TABLE 4.10 Germanium-73 basic NMR parameters for low molecular mass **Polygermanes.**

COMPOUND	SAMPLE	δ	W(1/2),(J)	OTHERS
Ge_3H_8	30% v C_6H_{12}	-297.6±1 (GeH_3)	25±5	H 3.55 (t,5) 3.46 (broad, shoulder)
*	with Ge_2H_6 and GeH_4	-287.7±1 (GeH_3)	25±8 (-94.1±.5)	H 3.95 (t,3.3) 3.84 (broad)
*		-324±2 (GeH_2)	30±10 (-90±10)	
Ge_4H_{10}	with some GeH_4	-284.3±1 (GeH_3)	76±5 (-96±3)	H 4.07 (t,- broad, distorted)
		-300±5 (GeH_2?)	100±20	

TABLE 4.11 Germanium-73 basic NMR parameters for high molecular mass **Polygermanes.**

COMPOUND		SAMPLE	δ	W(1/2),(J)	OTHERS
GeH_3GeMeH_2	*	with $GeMe_2H_2$ some $GeMeH_3$	-306.2±.2 (GeH_3)	2.0±.2	C -8.9 *
	*		-211.0±.2 ($GeMeH_2$)	4±1	
	*	1:1 with $(GeMeH_2)_2$	-300.4±1 (GeH_3)	2.9±.3	H 4.0 (-,4)
			(GeH_3)	(-90.0±.5)	3.53(t,3.8)
			(GeH_3)	(-4.7±.2)	0.83(t,4.4)
	*		-208.3±1 ($GeMeH_2$)	7±2 (-89.4±.5)	C -7.6
		dil. in GeH_3GeMeH_2	-296±2 (GeH_3)	7±1	H 3.49(t,2.5) 0.53(t,-)
			-208.5±1 ($GeMeH_2$)	13±1	
$(GeMeH_2)_2$	*	neat	-208.7±.6	7.0±.5	H 0.7 (broad) C -9.3
	*	1:1 with GeH_3GeMeH_2	-208.3±1	7±2 (-89.4±.5) (-4.5±2)	H 3.89(q,4.5) 0.77(t,4.4) C -8.7
GeH_3GeMe_2H	*	neat with some $(GeMeH_2)_2$	-295.9±.8 (GeH_3)	7±1	H 3.94(d,1.8)
			(GeH_3)	(-85±2)	1.29(d,2)
			-127.2±.1 ($GeMe_2H$?)	(-9.5±2) 3±1	
GeH_3GeMe_3	*	neat (some Ge hydrides)	-295.6±.7 (GeH_3)	11±1 (-90.7±1)	H 3.36 0.70
			-39±5 ($GeMe_3$)	30±10	C 1.4
		neat (some Ge hydrides)	-294.6±.8 (GeH_3)	2.0±.5	H 4.06 1.40 C 8.9
		v.dil. in C_6H_6	-297±2 (GeH_3)	6±2	H 3.08 0.14 C 0.2

TABLE 4.12 Germanium-73 basic NMR parameters for low molecular mass **Methylpolygermanes.**

COMPOUND	SAMPLE	δ	W(1/2),(J)	OTHER
$(GeMeH_2)_2GeMeH$	with traces	-206.2±.8	2.0±.5	H 4.5(broad)
*	Ge hydrides	($GeMeH_2$)		3.8(broad)
		-125 ±2	8 ±4	3.1(broad)
		(GeMeH)		C -3.9
				-9.8
*	dil. in $(GeMeH_2)_2$	-205.9±.6 ($GeMeH_2$)	<5	H 0.7(broad)
*	dil. in $(GeMeH_2)_2$, GeH_3GeMeH_2	-205.9±.6 ($GeMeH_2$)	<5	
$(GeMe_xH_y)_4$	neat,v.small sample	-298±2 (?)	30±10	H (v. broad)
$(GeMe_xH_y)_m$	with GeH_3GeMe_2H	-277±2 (?)	40±10	H 4.4(broad)
	with GeH_3GeMe_3	-279.3±1 (?)	35±2	

TABLE 4.13 Germanium-73 basic NMR parameters for high molecular mass **Methylpolygermanes** . (m = 2, or 3, ...)

COMPOUND	SAMPLE	δ	W(1/2),(J)	OTHERS
GeH_3SiH_3	0.7 atm. in $n\text{-}Bu_2O$	-324.6±.7	1.2±.2 (-91.5±.1) (-2.7±.1)	H 3.50 (q,4.7) 3.16 (q,3.7) Si -98.0±.1 W(1/2) 1.0 ±.2
	v. dil. in $SiCl_4$ with $GeMeH_2SiH_3$	-324±2	<5	H 3.9 , (shoulder) 4.7 (q,3.8)
GeH_3SiMeH_2	dil.in C_6H_6 (some $GeMeH_2SiH_3$)	-316.4±1	4±2	H 3.60 (t,4.1) 3.13 (-,3.8) -0.18 (t,4.7)
$GeMeH_2SiH_3$	30% v. C_6H_6 (traces $n\text{-}Bu_2O$)	-229.7±.8	4.0±.5	H 3.5 (complex) 3.22 (t,4.1) 0.00 (t,4.5) C -9.9 Si -95.1±.1 W(1/2) 4.0 ±.5
	v. dil. in C_6H_6 (mainly GeH_3SiMeH_2)	-230±2	4±2	H 2.62 2.11 -0.05
	v. dil. in $SiCl_4$ with GeH_3SiH_3	-230.1±1	4±2	H 4.07 (-) 3.80 (t,3.5) 0.89 (t,4.8)

TABLE 4.14 Germanium-73 basic NMR parameters for **Silylgermanes .**

COMPOUND	SAMPLE	δ	W(1/2)
$GeCl_4$	neat	30.9±.1	2.1±.1
	neat (BDH)	30.9±.1	1.8±.1
	neat,traces HCl	30.8±.1	2.2±.1
	with 1 atm. HCl	30.9±.5 31.2±.8	2.2±.3 <5 (a)
	20% v. $MeNO_2$	30.9±.5	7.8±.5
	1:1 pyHCl in 50% v. $MeNO_2$	30.7±1 30.8±.5	8±2 3.0±.5 (a)
	1:1.7 C_6H_5N in 60% v. CCl_4	27.6±.7	7.0±.6
	1:1 $GeEt_4$	31.1±.1	2.2±.1
	with $GeMe_mCl_{4-m}$	30.5±.4	6.0±1
$GeBr_4$	neat	-311.3±.1 -311.5±.1	2.2±.1 3.4±.2 (a)
	v. dil. fr. $GeBr_2H_2$	-310±2	4.0±.5
	with 1 atm. HCl	-311.5±.1 -311.4±.4	3.1±.3 4.0±.5 (b)
GeI_4	0.6M CS_2	-1081.8±.2	4.1±.2
	0.4M CS_2 (traces I_2)	-1084.3±.2	4.2±.2
	0.5M CS_2 some I_2	-1087±2	3.5±1
	v. dil. in C_6H_6 with $GeMeI_3$	-1106±4	10±4

TABLE 4.15 Germanium-73 basic NMR parameters for **Germanium Tetrahalides .**
(a) Moved in a vacuum line.(b) After 1 week sunlight.

COMPOUND	SAMPLE	δ	W(1/2)
$GeCl_3Br$	(a)	-47.8±.1	2.2±.1
	(d1)	-48.2±.3	<5
	(d2)	-47.0±.5	4.0±.6
	(d3)	-48.1±.3	4.0±.6
$GeCl_2Br_2$	(a)	-131.3±.1	2.2±.1
	(d1)	-131.0±.3	2.4±.6
	(d2)	-131.0±.3	3.6±.1
	(d3)	-130.9±.3	4.0±.6
$GeClBr_3$	(a)	-219.4±.1	2.2±.1
	(d1)	-218.1±.3	3.7±.6
	(d2)	-218.1±.3	3.0±.5
	(d3)	-217.9±.3	3.0±.6
$GeCl_3I$	(b)	-235.9±.2	23±4
$GeCl_2I_2$	(b)	-523.7±1	23±4
$GeClI_3$	(b)	-809.9±1	22±4
	(d1)	-804±2	25±5

TABLE 4.16 Germanium-73 basic NMR parameters for **Mixed Germanium Halides** .

Mole fractions of mixtures of neat tetrahalides GeX_4 are in near saturated solutions of CS_2 (except (a) neat tetrahalides only), follow with X : (a) 0.49:0.51,Cl:Br (b) 0.43:0.57,Cl:I (d1) 0.28:0.25:0.47,Cl:Br:I (d2) 0.17:0.53:0.30,Cl:Br:I (d3) 0.30:0.47:0.23,Cl:Br:I

COMPOUND	SAMPLE	δ	W(1/2)
$GeBr_3I$	(c)	-509.3±1	22±4
	(d1)	-510±2	20±4
	(d2)	-511±3	20±4
	(d3)	-511.3±1	15±3
$GeBr_2I_2$	(c)	-707.4±1	29±6
	(d1)	-705±3	15±3
	(d2)	-710±3	20±4
	(d3)	-711±5	25±5
$GeBrI_3$	(c)	-899.8±1	20±4
	(d1)	-900±3	17±4
	(d2)	-903±3	20±4
	(d3)	-902.9±1	10±3
$GeCl_2BrI$	(d1)	-326±3	7±3
	(d3)	-326±3	14±3
$GeClBr_2I$	(d1)	-418±2	19±4
	(d2)	-418±3	20±4
	(d3)	-416.7±1	15±3
$GeClBrI_2$	(d1)	-610.6±1	27±5
	(d2)	-615±3	20±4
	(d3)	-614.6±1	15±3

TABLE 4.17 Germanium-73 basic NMR parameters for **Mixed Germanium Halides** .

Mole fractions of mixtures of neat tetrahalides, GeX_4, are in near saturated solutions of CS_2, given with X : (c) 0.50:0.50, Br:I (d1) 0.28:0.25:0.47, Cl:Br:I (d2) 0.17:0.53:0.30, Cl:Br:I (d3) 0.30:0.47:0.23, Cl:Br:I

COMPOUND	SAMPLE	δ	W(1/2)	OTHER
(0)	$GeCl_4$ with	30.5±.1	2.5±.2	Si -18.2±.1
(1)	$SiBr_4$	-47.6 "	2.8 "	W(1/2) 8 ±1
(2)	0.57:0.43	-131.0 "	2.7 "	($SiCl_4$)
(3)	mole	-219.3 "	2.2 "	
(4)	fraction	-311.5 "	2.2 "	
(0)	$GeBr_4$ with	29.7±.1	2.9±.5	Sn -636±1
(1)	$SnCl_4$	-48.1 "	2.9 "	W(1/2) 180±20
(2)	0.48:0.52	-131.2 "	3.0 "	($SnBr_4$)
(3)	mole	-219.2 "	3.0 "	Sn -505±1
(4)	fraction	-310.9 "	2.5±.2	W(1/2) 300±30
				($SnBr_3Cl$)
(0)	$GeBr_4$ with	29.8±.2	2.6±.5	
(1)	$HgCl_2$ (solid)	-48.0 "	4.3 "	--
(2)	0.60:0.40	-131.5 "	4.5 "	
(3)	mole	-219.3 "	4.1 "	
(4)	fraction	-311.3±.1	3.7 "	
(0)	$GeBr_4$ with	30.3±.2	2.3±.5	
(1)	$HgCl_2$ (solid)	-47.4 "	4.8 "	--
(2)	0.55:0.45	-130.1 "	4.3 "	
(3)	mol. frac.	-217.2 "	4.0 "	
(4)	30% v. in CS_2	-308.2 "	2.6 "	

TABLE 4.18 Germanium-73 basic NMR parameters for **Mixed Germanium Tetrahalides from mixed nucleus systems** at equilibrium .

(0) $GeCl_4$ (1) $GeCl_3Br$ (2) $GeCl_2Br_2$ (3) $GeClBr_3$ (4) $GeBr_4$

4.4 OVERVIEW OF CHEMICAL SHIFTS

The chemical shift range is bounded by GeI_4 (-1081.8) and $GeCl_4$ (30.9). Halogen-free germanium compounds have a low frequency bound of -324.6 for $GeSiH_6$, (far lower than in the literature review) and a high frequency bound of 17.8 for $GeEt_4$. A pictorial summary of approximate chemical shift values follows in FIG.(4.1).

Germanium tetraalkyl δ values are clustered together at the high frequency bound of halogen-free germanium compounds, while polygermane δ values are clustered together near the low frequency bound for halogen-free germanium compounds. Chemical shifts of GeH_3 groups fall in about the same range. Methylgermanes, ethylgermanes, and methylated germyl groups ($GeMe_{3-x}H_x$- , x = 0,1,2, -GeMeH-) have δ values intermediate between tetraalkyls and polygermanes.

The ordering of chemical shifts for halogen-free germanium compounds is quite well predicted by the electronegativity and group electronegativity of the ligands (TABLE (4.19)). Using the ideas in section 1.1.5, a more electronegative ligand will cause the δ value to move to higher frequency by local shielding effects. Changes in δ accompanying changes in the atom M at a ligand are reflected by changes in M electronegativity (TABLE (4.20)). For instance, in the series GeH_3MH_3, M = Si,Ge,C, changing M from Si to Ge has a corresponding change in δ of 13 ppm, and changing M from Ge to C gives a change of 103 ppm. These correlate with differences in electronegativity of 0.1 and 0.6, respectively, both in sign, and in approximate magnitude. This correlation is found for the other compounds in TABLE (4.20).

Replacing Si with Ge in a ligand causes the adjacent Ge nucleus to have a change in δ of 13-21 ppm, and, similarly, replacing Ge with C in a ligand gives a change of 114-39 ppm.

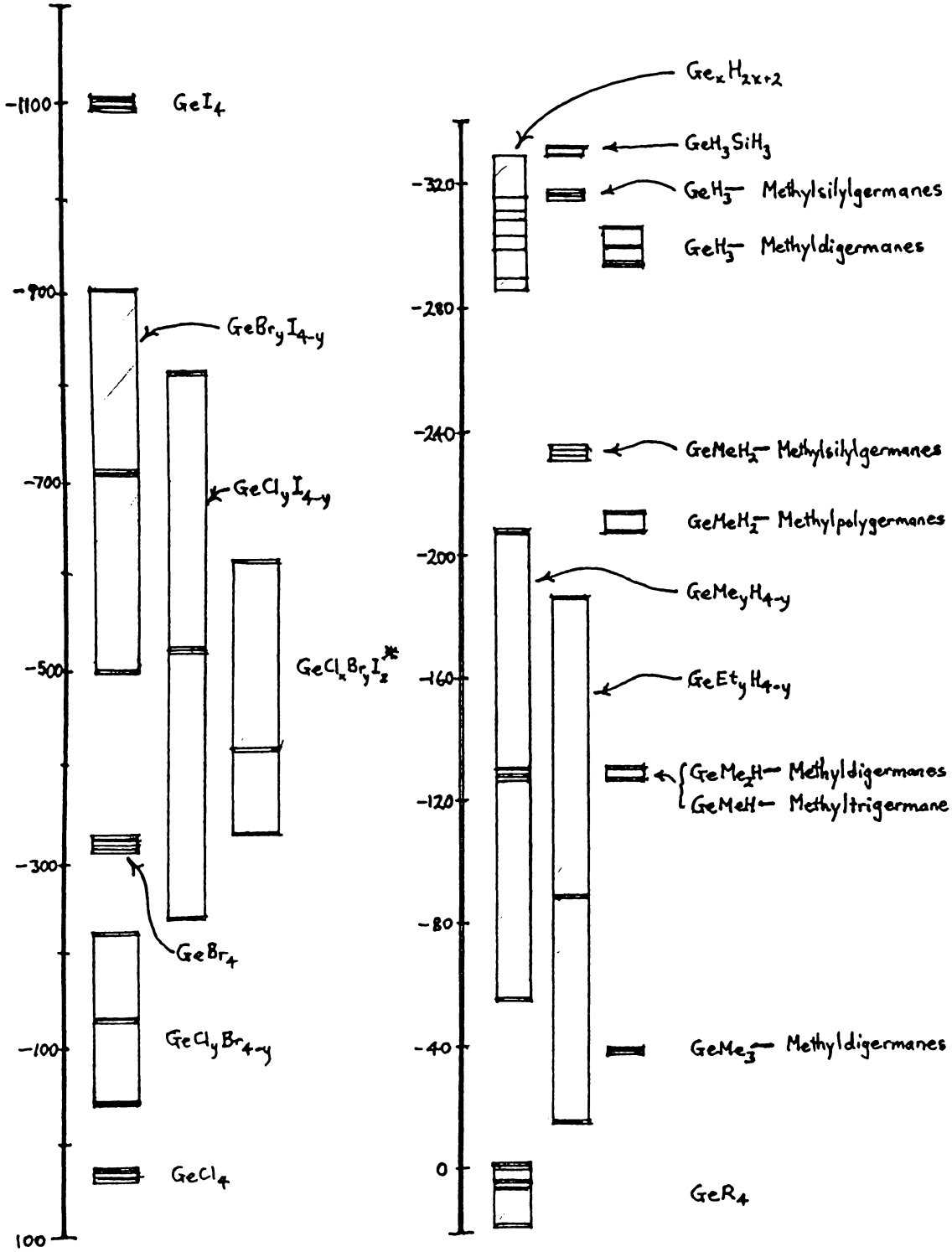

FIG. 4.1 Overview of ^{73}Ge chemical shifts. R = n-alkyl group, x = 1, 2, 3 or 4, y = 1, 2, or 3. Horizontal bands represent actual measurements.

*$GeCl_2BrI$, $GeClBr_2I$, and $GeClBrI_2$.

ELEMENT	ELECTRONEGATIVITY	ELEMENT or GROUP	ELECTRONEG. or GROUP ELECTRONEG.
I	2.7	Si	1.9
Br	3.0	Ge	2.0
Cl	3.2	SiH_3	2.2 - 1.9
		GeH_3	2.2 - 2.0
		H	2.2
		CH_3	2.3
		CH_2CH_3	≳ 2.3
		C	2.6

TABLE 4.19 Electronegativities and group electronegativities. They are average values on the Pauling scale from thermochemical data by Allred [165].

Tetraalkyl δ-values are correctly predicted to be to high frequency relative to hydrides, with $GeEt_4$ to high frequency of $GeMe_4$. However, the prediction of higher δ-values as the chain length increases above Et is not correct. Replacing Me or Et groups on methyl or ethylgermanes with hydride ligands gives a shift to low frequency, and replacing all Et groups with Me groups gives a shift to low frequency (by about 30 ppm) as predicted.

Methylpolygermanes have δ-values similar to methylgermanes, namely: $GeMeH_3$ is very close to $GeMeH_2$- groups in methyldigermanes and in 1,2,3 trimethyltrigermane, $GeMe_2H_2$ is very close to $GeMe_2H$- groups in methyldigermanes and to -GeMeH- in 1,2,3 trimethyltrigermane, $GeMe_3H$ is similar to $GeMe_3$- groups in methyldigermanes. This behaviour can be rationalized by the following for ^{73}Ge δ-values of the 'other' Ge nucleus: an -H ligand behaves like a $-GeH_3$ group, or a -GeMeH- group. It is likely that this ligand, and these groups are similar in electron withdrawing capacity relative to germanium. However, the chemical shift of $GeMe_3$- in $GeMe_3$-GeH_3 is to high frequency of $GeMe_3H$ by a significant amount (18 ppm). Simple electronegativity models would predict a reversal of this order.

COMPOUND	M(initial)	M(final)	Δδ
GeH_3MH_3	Si	Ge	13
	Ge	C	103
GeH_3MMeH_2	Si	Ge	16
	Ge	C	114
$GeMeH_2MH_3$	Si	Ge	21
	Ge	C	80
$GeMe_2HMH_3$	Si	Ge	-
	Ge	C	70
$GeMe_3MH_3$	Si	Ge	-
	Ge	C	39

TABLE 4.20 Changes in germanium-73 δ values (ppm) accompanying changes in the atom at one of its ligands , M .
$\Delta\delta = \delta$ [M(final)] - δ [M(initial)]

Germyl (GeH_3) groups on $GeH_3GeMe_{3-x}H_x$, x = 0,1,2 all fall in a narrow range of chemical shifts (-295 to -306), so one can postulate for ^{73}Ge δ-values of the 'other' Ge nucleus: a $-GeMeH_2$ groups behaves like a $-GeMe_2H$ and a $-GeMe_3$ group. In addition, δ-values of GeH_3GeH_3 fall within the range of shifts for the germyl groups of methyldigermanes when comparable solvents are used. Thus, when comparable solvents are used, for ^{73}Ge δ-values of the 'other' Ge nucleus: $-GeMe_{3-x}H_x$, x = 0,1,2,3 behave similarly.

When GeH_3-H and GeH_3-GeH_3 appear in the same sample, they have similar δ-values, as predicted, but germane is always slightly shifted to low frequency (by 14 to 16 ppm) as expected from simple electronegativity ideas. However, when GeH_3GeH_3 and GeH_3 in $GeH_3GeH_2GeH_3$ appear in the same sample, digermane is slightly shifted to high frequency (by 13 ppm). The order of chemical shifts is the opposite to the

prediction from the simplest electronegativity idea which assumes that a $-GeH_2GeH_3$ group has a slightly lower group electronegativity than a $-GeH_3$ group.

The ordering of chemical shifts is correctly predicted in twelve of the fifteen tetrahalides and mixed tetrahalides, if the 'combined electronegativity' assumes the simple linear combination:

$2.7x(I) + 3.0x(Br) + 3.2x(Cl)$ where the coefficients are simply the electronegativities in TABLE (4.19) and x(i) is the number of ligands of halogen i.

When heavy atoms are present in a molecule, δ is modified by anisotropic induced fields.[160] Only the bromides and iodides among the compounds listed in TABLES (4.15)-(4.18) are likely to show anisotropic contributions to δ. This is the basis for separating discussions on δ and electronegativity into halogen and halogen-free compounds.

It is informative to compare ^{73}Ge chemical shifts with other Group IV isotope chemical shifts.

There are a large number of silicon analogues of halogen-free germanium compounds, and the ^{29}Si and ^{73}Ge δ values of these compounds are recorded in FIG.(4.2). This plot is linear, revealing that similar nuclear shielding mechanisms are operating. Germanium has a chemical shift range about three times larger than silicon for halogen-free compounds. There is a marked degree of correlation, (better than δ (^{207}Pb) plotted against δ (^{119}Sn)).[6k] When tetrahalide and mixed tetrahalide compounds are included, the plot becomes curved upwards at lower frequency when 3 or 4 iodine ligands are used. Iodine ligands often give anomalous results in NMR, partly because the iodine atom, being large, has a large induced circulation.

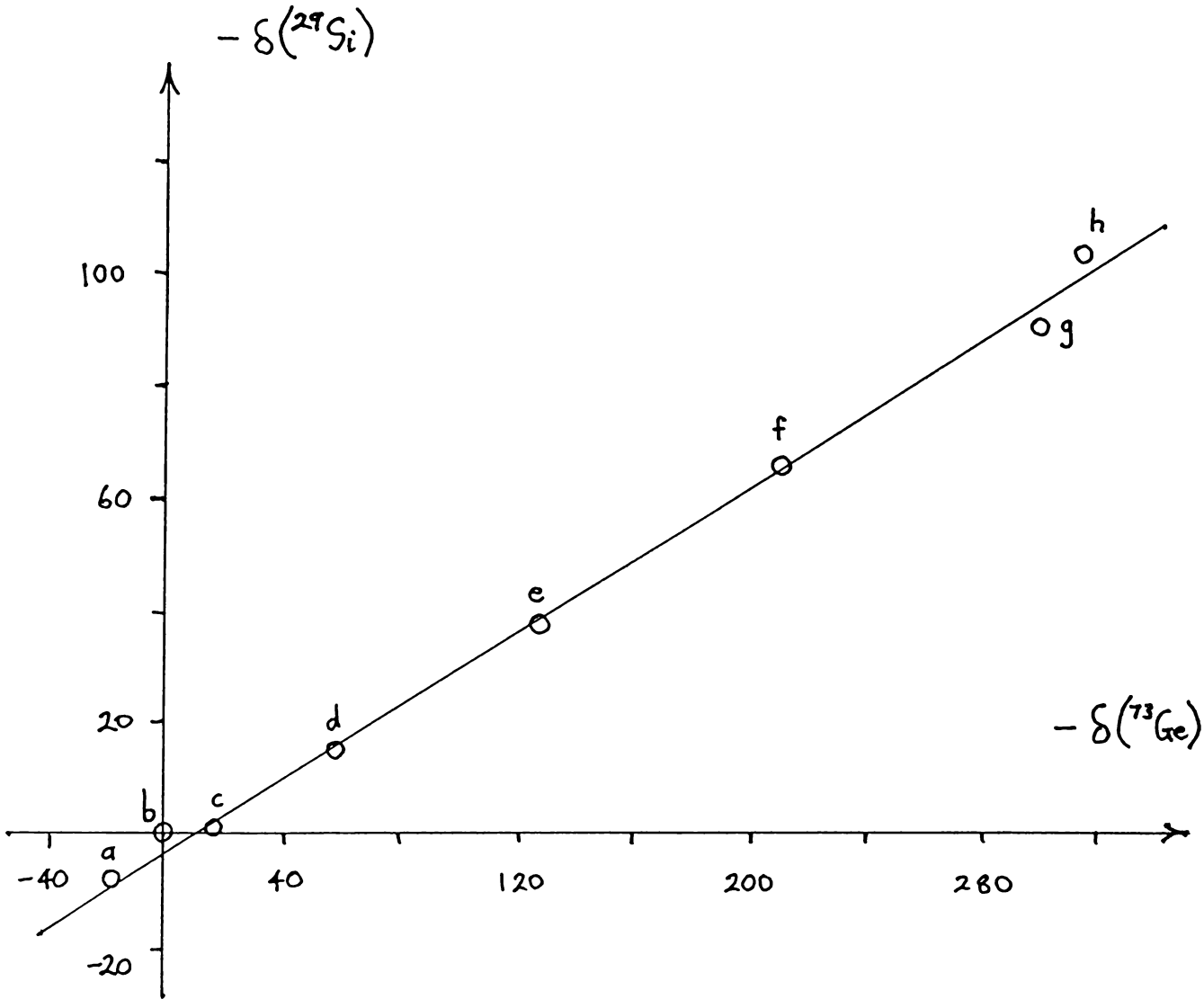

FIG. 4.2 Chemical shifts of ^{29}Si versus ^{73}Ge for halogen-free compounds. (All ^{73}Ge data are from the thesis, references given below are for ^{29}Si) M = Ge or Si. Both isotopes are referenced to MMe_4.

(a)[166] MEt_4 (b) MMe_4 (c)[167] MEt_3H (d)[168] MMe_3H

(e)[168] MMe_2H_2 (f)[168] $MMeH_3$ (g)[168] MH_4 (h)[168] M_2H_6.

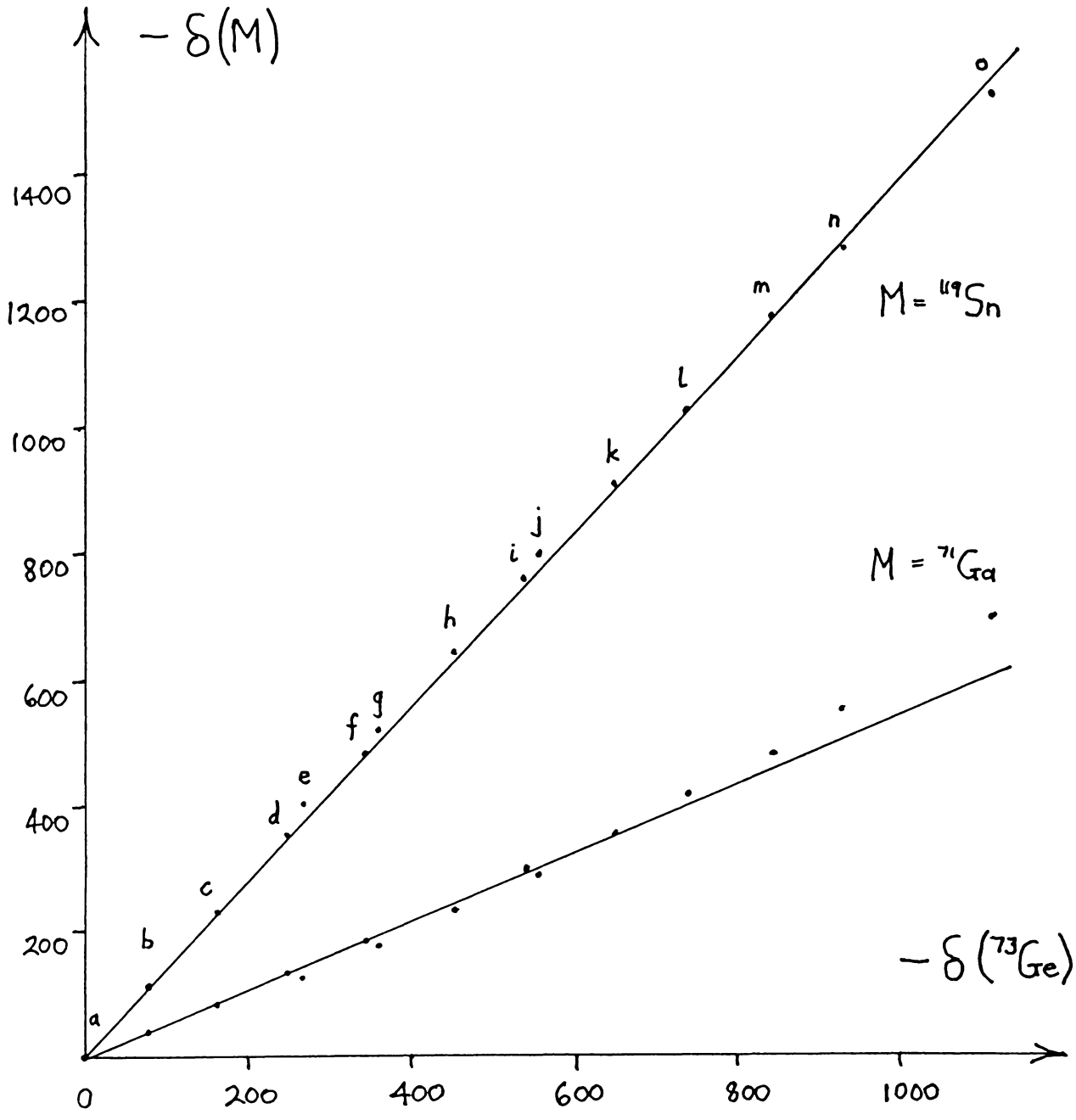

FIG. 4.3 Chemical shifts of M versus ^{73}Ge for tetrahalides and mixed tetrahalides. M = ^{119}Sn or ^{71}Ga. (All ^{73}Ge data are from the thesis, ^{119}Sn data from reference[169] and ^{71}Ga data from reference[170].) A = Sn, Ga, or Ge. All Ga data uses singly charged anions, referred to $GaCl_4^-$, and Sn, Ge data are referred to ACl_4.

(a) ACl_4, (b) ACl_3Br, (c) ACl_2Br_2, (d) $AClBr_3$, (e) ACl_3I, (f) ABr_4, (g) ACl_2BrI, (h) $AClBr_2I$ (i) ABr_3I, (j) ACl_2I_2, (k) $AClBrI_2$, (l) ABr_2I_2, (m) $AClI_3$, (n) $ABrI_3$, (o) AI_4.

A linear plot of ^{119}Sn and ^{73}Ge δ-values for tetrahalides and mixed tetrahalides (FIG.(4.3)) shows that similar nuclear shielding mechanisms are operating. The germanium chemical shift range is about one and a half times smaller than the tin range. Halogen-free compounds also form a linear plot, with a slope equal to that using tetrahalides in the plot, but with an intercept on the Sn axis 170 ppm to higher frequency.

The chemical shifts of ^{119}Sn and ^{29}Si have been explained[6k] by use of semi-empirical calculations involving the use of the Jameson-Gutowsky[171] formulation for the 'local' paramagnetic shielding term using the valence p-orbitals (for four coordinate compounds). Since ^{73}Ge chemical shift values parallel both ^{119}Sn and ^{29}Si, a similar theoretical treatment was applied to ^{73}Ge. In particular, the local paramagnetic term is proportional to the mean value of r^{-3}: $\langle r^{-3} \rangle_{np}$, where r is the orbital to nucleus distance, and n is the principal quantum number for the valence orbital. If the theory is a good model for Si, Ge, and, Sn, then

$$\frac{\Delta\delta(M)}{\Delta\delta(Ge)} = \frac{\langle r^{-3}(M) \rangle_{np}}{\langle r^{-3}(Ge) \rangle_{4p}} \qquad M=Si,Sn, \quad n=3,5,\text{respec.} \qquad \text{---(4.2)}$$

Using tabulated values[171] of $\langle r^{-3} \rangle_{np}$, it was found:

M	$\frac{\Delta\delta(M)}{\Delta\delta(Ge)}$	$\frac{\langle r^{-3}(M) \rangle_{np}}{\langle r^{-3}(Ge) \rangle_{4p}}$
Si	$0.32 \pm .02$	$0.3 \pm .05$
Sn	$1.41 \pm .05$	$1.3 \pm .1$

Theoretical and experimental values are close. The slope of the Sn/Ge plot is slightly larger than the predicted value, but this is common when chemical shift patterns for lighter and heavier elements of the same group are compared, and can be attributed to greater electronic sensitivity to the effects of substituents on the heavier elements. (Analogous plots

of δ (^{207}Pb) and δ (^{119}Sn) give a slope of 3.0 and a theoretical slope of 1.4.)[6k]

A plot of ^{71}Ga and ^{73}Ge chemical shifts for the isoelectronic gallium tetrahalide anions and germanium tetrahalide molecules has a curve at the low frequency end when there are 3 or 4 iodine ligands (FIG.(4.3)). This is qualitatively similar to the Si/Ge plot for tetrahalides. The chemical shift range of ^{73}Ge is larger than the range of ^{71}Ga by a factor of 1.8 for these compounds.

Since the chemical shift range of germanium is greater than for carbon[8d] as expected from the aforementioned theories, the germanium signal dispersion in halogen-free germanium compounds is larger than the carbon signal dispersion in the same compounds. For example, the ^{73}Ge and ^{13}C δ values, respectively, for methylgermanes in non-polar media is: $GeMeH_3$(-209.2, -11.9) $GeMe_2H_2$(-126.7, -6.5), $GeMe_3H$(-57.2, -3.4). Solvent type and concentration affect ^{73}Ge δ-values much less the ^{13}C values, partly because the former atoms are generally shielded more from intermolecular influences by other atoms in the same molecule. The range of ^{73}Ge and ^{13}C δ values, respectively, for methylgermanes in a variety of media is: $GeMeH_3$ (2.4, 14.2), $GeMe_2H_2$ (1.8, 0.7), $GeMe_3H$ (0.7, 0.4). Thus methylgermanes are easily distinguished from each other by ^{73}Ge δ value alone, while ^{13}C δ values can only distinguish methylgermanes when the medium is specified. Carbon NMR provides a useful check on sample purity and signal identification when used with germanium NMR.

Proton signal dispersion is even smaller than carbon signal dispersion in halogen-free germanium compounds, however, the normally well resolved multiplets with ^{3}J(H,H) separation in the former case often allow signal identification. (eg. Although the chemical shift range for ^{1}H in Ge_xH_{2x+2} is very small, being $\sim$1 ppm, informative second order signals are obtained for tetragermane and higher members.) Unfortunately, many

of the higher molecular mass halogen-free germanium compounds are synthesized in such small amounts that inhomogeneity from the sample size becomes a problem for proton NMR. When the sample volume was very small compared to the detector coil, multiplets from proton NMR were broadened so that the signal identification capabilities were greatly reduced. (Once ^{73}Ge and ^{13}C NMR spectra have been obtained from a small sample, it could be diluted, using vacuum line techniques, and the ^{1}H NMR obtained.) In most cases, after a ^{73}Ge spectrum had been obtained, it was easier to use ^{73}Ge INEPT to identify the multiplicity than to change probes and lock signals and use ^{1}H (or ^{13}C) NMR as an assignment aid. Thus ^{73}Ge NMR is a better tool than ^{1}H NMR for halogen-free compounds, provided there is sufficient sample concentration.

4.5 OVERVIEW OF LINEWIDTHS

Linewidths varied from 0.9 Hz for $GeEt_4$ to 100 Hz for the broadest signal in Ge_4H_{10}. Tetrahalides and mixed tetrahalides had linewidths ranging from 1.8 Hz for $GeCl_4$ to 29 Hz for $GeBr_2I_2$ (FIG.(4.4)).

Since ^{73}Ge has a small to medium line broadening factor compared to most other quadrupolar nuclei (TABLE(4.1)), linewidths are generally smaller than for analogous compounds of other quadrupolar nuclei (eg. $W_{\frac{1}{2}}$ ^{27}Al tetrahalide anions: 3-60 Hz[61], $W_{\frac{1}{2}}$ ^{71}Ga tetrahalide anions: 180-340 Hz[170]).

Linewidths increase with increased viscosity and increase with reduced symmetry at the germanium atom (section 1.1.8.2). Thus compounds having all four ligands identical yield the smallest linewidths (eg. GeH_4 (1.1), $GeCl_4$ (1.8), $GeEt_4$ (0.9), in Hz).

Compounds with dissimilar ligands give the largest linewidths (eg. $GeEt_3H$,23 Hz). Whenever a relatively large iodine ligand was present with other halogens, the linewidth was typically 10-25 Hz, otherwise linewidths were 2-3 Hz.

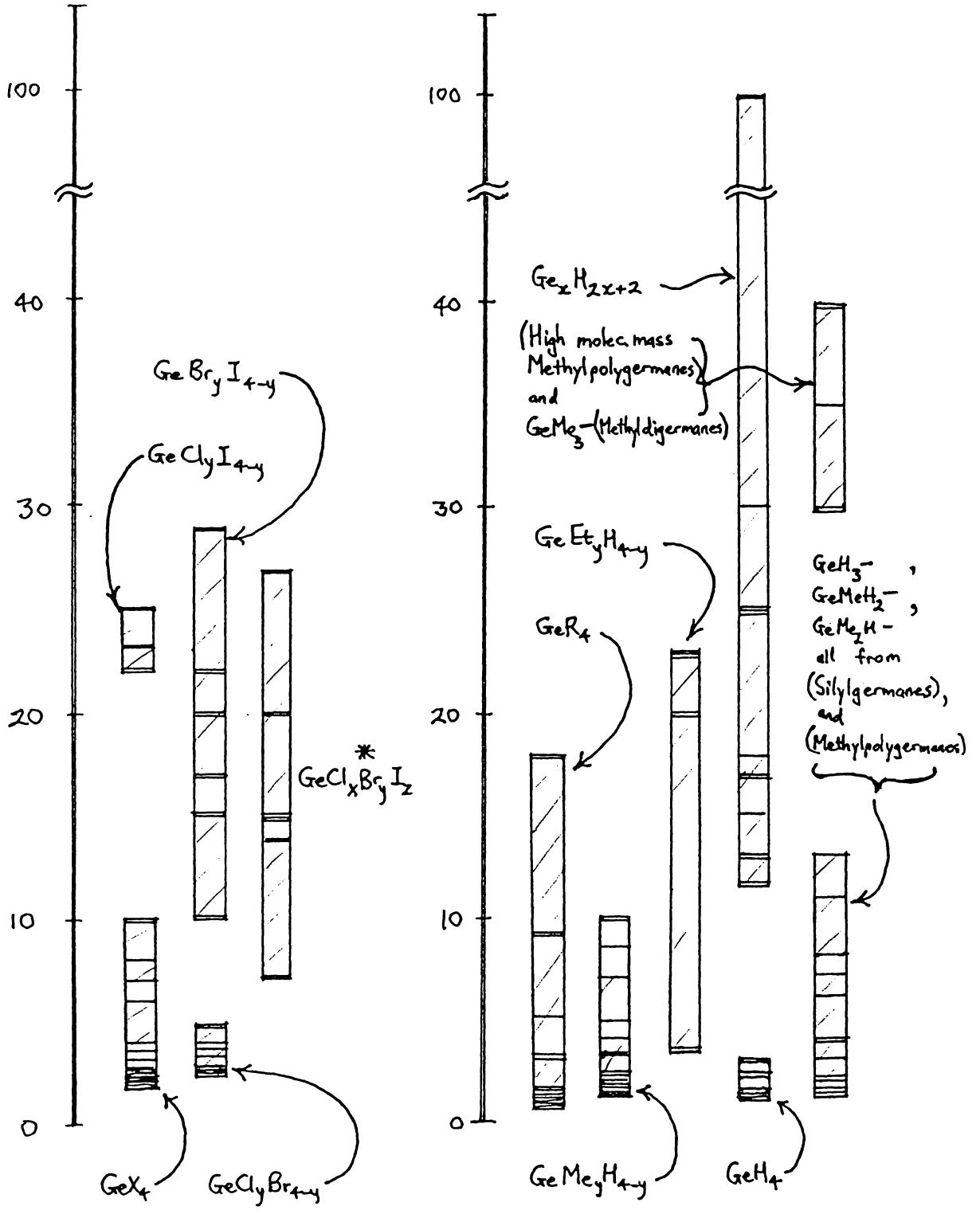

FIG. 4.4 Overview of ^{73}Ge linewidths.
R = n-alkyl grpup, X = Cl,Br, or I, x = 2,3, or 4,
y = 1,2, or 3.
Horizontal bands represent actual measurements *$GeCl_2BrI$, $GeClBr_2I$, and $GeClBrI_2$.

As viscosity and molecular mass increase, $W_{\frac{1}{2}}$ increases (eg. $Ge(n\text{-}Pr)_4$ (3.3), $Ge(n\text{-}Bu)_4$ (5.1), $Ge(n\text{-}Pn)_4$ (9.5), $Ge(n\text{-}Hx)_4$ (18), in Hz, all neat).

Replacing hydride ligands on GeH_4 with GeH_3 groups gives a large increase in $W_{\frac{1}{2}}$ as expected (eg. Ge_3H_8 25 Hz, 30 Hz), but replacing hydride groups on polygermanes with methyl groups, gives a large decrease in $W_{\frac{1}{2}}$, which is not expected from simple viscosity and symmetry arguments (eg. Ge_2H_6 (11.7), Ge_2MeH_5 (2, 4), $(GeMeH)_2GeMeH$ (2, 8), in Hz).

4.6 OVERVIEW OF COUPLING CONSTANTS

Scalar coupling from germanium to protons ranged from 97.6 Hz to 85 Hz for $|^1J(Ge,H)|$ and 9.5 Hz to 2.7 Hz for $|^2J(Ge,M,H)|$, where M is C, Si or Ge. Signs shown in section 4.3 are deduced from coupling constants in analogous Group IV compounds. In line with the literature in section 4.2.2, (^1H NMR yielded no satellites for Ge_2H_6)[172] proton NMR only yielded $^nJ(Ge,H)$ values when all four ligands attached to the germanium were the same.

The magnitude of these coupling constants generally increases with increasing s character at the germanium proton bond. This is expected whenever the contact term is dominant.[6m] For instance, as methyl groups or ethyl groups replace hydride ligands, the s character of the Ge-H bond decreases, (eg. angles for HGeH decrease from GeH_4 (109.7°)[173] to GeH_3CH_3, (109.25°)[174]) and the $^1J(Ge,H)$ values decrease in magnitude (FIG.(4.5)). Using the simple idea that replacement of H by Me, GeH_3, or SiH_3 leads to less s character at the adjacent Ge, there is a fair correlation of s character with the magnitude of coupling constants for alkylgermanes (^2J), polygermanes, methyldigermanes, and silylgermane. (TABLE (4.21)).

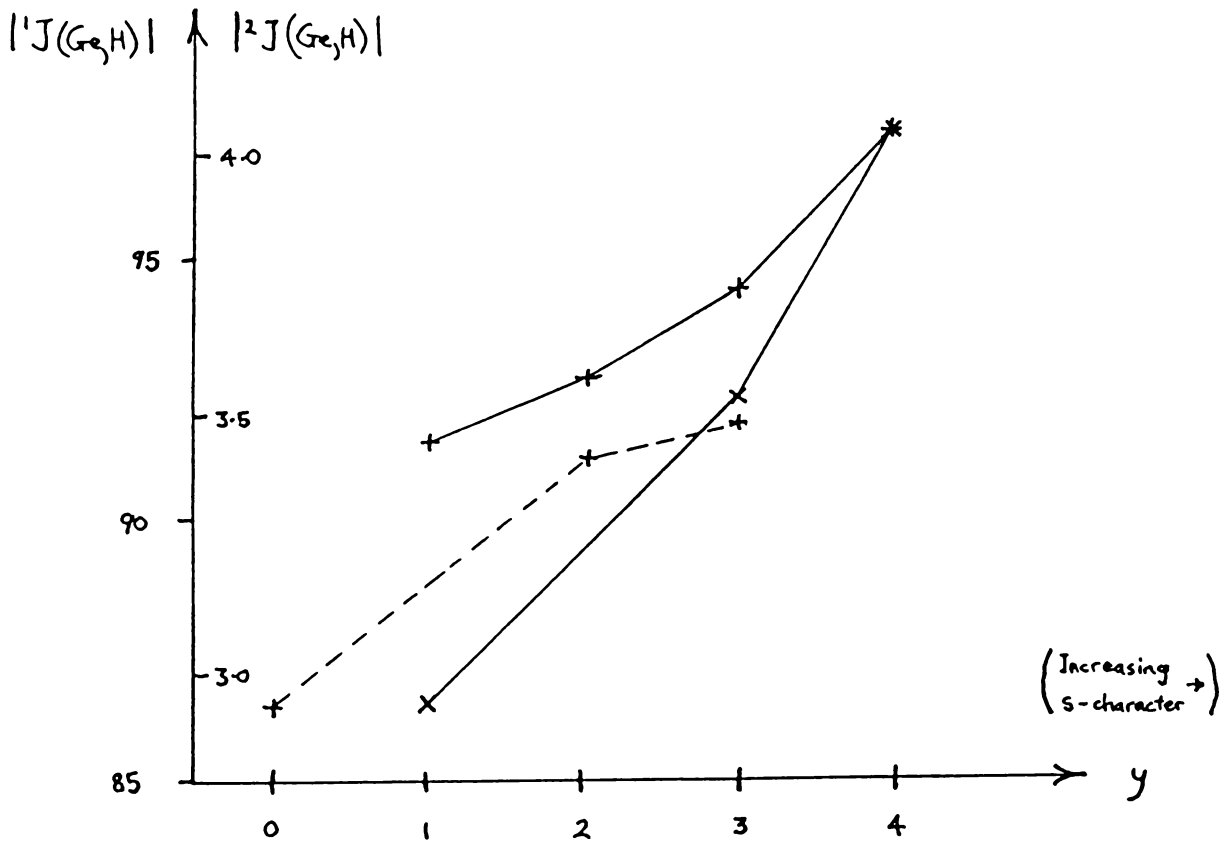

FIG. 4.5 $|^1J(Ge,H)|$ (— lines) and $|^2J(Ge,H)|$ (--- lines), Hz for Methylgermanes(+) and Ethylgermanes(×) versus y, the compound formula: $GeR_{4-y}H_y$.

$\|^2J\|$				(2.7)	-
$\|^1J\|$				91.5	97.6
COMPOUND				GeH_3SiH_3	GeH_4
$\|^1J\|$	90.0	96	94.0	95.0	97.6
COMPOUND	$(GeH_3)_2GeH_2$	$(GeH_3GeH_2)_2$	$(GeH_3)_2GeH_2$	GeH_3GeH_3	GeH_4
$\|^2J\|$	(4.5)		(9.5)	(4.7)	
$\|^1J\|$	89.4	90.7	85.0	90.0	95.0
COMPOUND	$(GeMeH_2)_2$	GeH_3GeMe_3	GeH_3GeMe_2H	GeH_3GeMeH_2	GeH_3GeH_3

TABLE 4.21 $|^1J(Ge,H)|$ and $|^2J(Ge,H)|$,Hz,of halogen-free germanium compounds in approximate order of increasing s character at the observed Ge(underlined) left to right.(valid for a given row)

The value of $^2J(Ge,Ge,H)$ for GeH_3GeMe_2H (GeH_3 group) is rather high compared to $^2J(Ge,Ge,H)$ values for other methyldigermanes. Even if this $^2J(Ge,Ge,H)$ value is disregarded, long range couplings follow the order:

$|^2J(Ge,M,H)|$: for M: Si < C < Ge.

4.7 FURTHER ^{73}Ge NMR DATA

4.7.1 Tetraalkyls

There is very little change in ^{73}Ge chemical shift with change in concentration or solvent (TABLE (4.5)). Chemical shifts tend to approach a constant (5-6) as the chain length on the alkyl ligands is increased. Indeed, adding one more CH_2 group on to each ligand should have less effect on the central Ge atom as the total length of each ligand is increased. Tetraethylgermane does not fit into this simple expectation, being to a significantly higher frequency than all other tetraalkyls. A similar, anomalously high frequency shift is found for R = Et, in a plot of $\delta\,^{29}Si$ versus chain length in SiR_3H compound.[167] Chemical shifts approach a constant as the chain length increases.

The linewidth for $Ge(n\text{-}C_6H_{13})_4$ (TABLE (4.6)) may be increased by the presence of nearby resonances from branched isomers. Carbon NMR shows that there is a 0.1 mole fraction of a branched isomer. (Using JMSE sequences, it was found that the ^{13}C signal of the terminal CH_3 group was always at the second lowest frequency position for tetraalkyls, $R_4 \neq Me_4$.)

4.7.2 Alkylgermanes

A plot of chemical shift versus the number of hydride ligands gives a so-called 'sagging pattern' (FIG.(4.6)). Such patterns are usually found for compounds of the type $MX_{4-y}Y_y$ ($M = {}^{29}Si$, ^{119}Sn, ^{207}Pb) when shielding is plotted as a function of y[8d], and are related to the way in which p electron 'imbalance'[171] affects the paramagnetic shielding term.

Before the $GeEt_2H_2$ resonance was found, all other members of this series were known, and a pairwise additivity model (section 4.7.5) predicted a δ value of -87.7. Later, the experimental value was found to be -87.7 Both alkylgermane series have δ values closely fitting the pairwise model but deviating significantly from a so-called first order model (section 4.7.5).

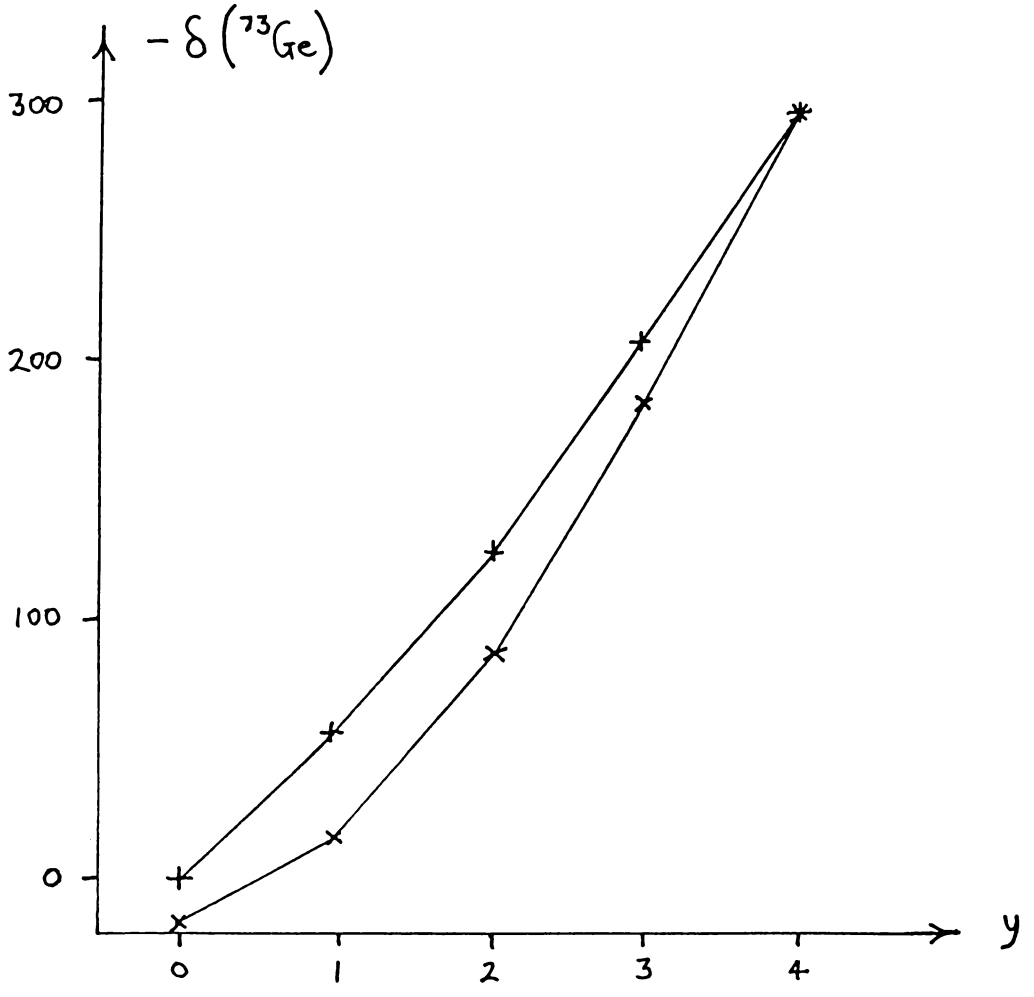

FIG. 4.6 ^{73}Ge chemical shift, -δ, (ppm) versus y, the number of hydride ligands attached to $GeR_{4-y}H_y$, R = Me (+) or Et (x).

4.7.3 Polygermanes

Unlike the other germanium compounds studied, polygermanes exhibit a chemical shift dependence upon the medium which is large compared to the δ range of the compounds (TABLE (4.10)). The total range for polygermanes is 40 ppm, and changing from a polar (Et_2O) to a non-polar (Ge hydrides) medium gave about a 16 ppm shift to high frequency for either GeH_4 or Ge_2H_6.

From ^1H NMR it was found that Ge_4H_{10} (TABLE (4.11)) contained mainly the n-isomer, with a 0.07 mole fraction of the iso-isomer. The large linewidth for this Ge_4H_{10} sample may be caused partly by an overlapping of the signals from the isomers.

4.7.4 Methylpolygermanes and Silygermanes

All the methylpolygermane samples were synthesized by previous research students well before the arrival of the FTNMR machine, so there was a limited knowledge of the purity of these samples.

A neat mixture of $(GeMeH_2)_2$ and GeH_3-$GeMeH_2$ gave two ^{73}Ge signals, one broad and one sharp. Using INEPT, the sharp signal was assigned to GeH_3 and the broad signal to $GeMeH_2$. Both ^1H and ^{13}C NMR showed 2 methyl signals in a 2:1 ratio. Since the assignment for ^1H Me groups was not known, the mole ratios of the two compounds could not be determined. (^{13}C NMR data does not unambiguously define this mole ratio either.) However, a 2.6:1 ratio in ^{73}Ge peak area for the broad to the sharp signal gave an unambiguous result: the mole fraction of $(GeMeH_2)_2$ is about 0.44±.05.

The $GeMe_2H$ assignment for GeH_3GeMe_2H is a tentative one (TABLE (4.12)). Although it fits in with other chemical shift trends, the S/N of this signal is much lower than the S/N of the GeH_3 group, even allowing for relaxation effects.

Assignments for the compounds $(GeMe_xH_y)_n$ are also tentative, due to the low S/N, and fast relaxation which stops the use of multipulse assignment sequences. The proton signal was too broad and the ^{13}C signal too low in S/N, to aid in assignment.

4.7.5 Tetrahalides and Mixed Tetrahalides

Chemical shifts of the mixed germanium tetrahalides can be calculated using the three single halogen shielding parameters δ (X)' (X = Cl,Br,I) obtained from δ' (X) = 0.25 δ (GeX_4). The shifts calculated using this first order approach, listed under the heading δ (first order) in TABLE (4.22), give deviations from observed values as large as 11.4 in magnitude with an average magnitude of deviation of 6.5. (This compares well with 1973 ^{73}Ge NMR data: deviations, max. 18, av. 10.)[146] These deviations lie outside the typical experimental error of ±1 and indicate the presence of a second-order effect upon the germanium shielding resulting from halogen-halogen interaction.

This second order effect is accommodated by using the pairwise additivity model.[175] The model allows the calculation of δ for a central atom by summing pairwise interaction parameters for all substituents taken as adjacent pairs. Pairwise additivity calculations (method[176]) show a maximum magnitude of deviation of 8.8, and an average of 2.5. (This compares well with 1973 data treated in the same way: deviations, max. 9, av. 4.4.)[146]

In the time between mixing the germanium tetrahalides in vacuo and obtaining a spectrum (>1 day) an equilibrium distribution of products had been established. (For a neat equimolar mixture of $GeCl_4/GeBr_4$, the time $t_{\frac{1}{2}}$ for the $GeCl_4$ signal to decrease intensity two-fold was 250 min.)[146]

Preliminary studies of mixed nucleus systems $GeX_4 : MY_y$; near equimolar ratios; M = Si,Sn, y = 4; or Hg, y = 2; X,Y = Cl, or Br, by NMR gave information

COMPOUND	δ (exptl.)	δ (first order)	Devn.	δ (pairwise add.)	Devn.
$GeCl_3Br$	-47.8	-54.7	-6.9	-48.1	-0.3
$GeCl_2Br_2$	-131.3	-140.2	-8.9	-131.4	-0.1
$GeClBr_3$	-219.4	-225.8	-6.4	-219.2	0.2
$GeCl_3I$	-235.9	-247.3	-11.4	-244.7	-8.8
$GeCl_2I_2$	-523.7	-525.5	-1.8	-522.1	1.6
$GeClI_3$	-809.9	-803.6	6.3	-801.1	8.8
$GeBr_3I$	-509.3	-503.9	5.4	-511.9	-2.6
$GeBr_2I_2$	-707.4	-696.6	10.8	-707.2	0.2
$GeBrI_3$	-899.8	-889.2	10.6	-897.2	2.6
$GeCl_2BrI$	-326.2	-332.8	-6.6	-329.4	-3.2
$GeClBr_2I$	-417.6	-418.4	-0.8	-418.5	-0.9
$GeClBrI_2$	-613.5	-611.0	2.5	-612.5	1.1

TABLE 4.22 Experimental and theoretical ^{73}Ge δ values for mixed germanium tetrahalides. Exptl. values are from TABLES (4.16),(4.17), and have a max. average error of ±1ppm
Devn. = δ(theory) - δ(exptl.) .

on the rates of redistribution (TABLE (4.18)). In each case, ^{73}Ge NMR proved to be the most useful NMR probe.

When M = Hg, the system came to equilibrium at room temperature within several days. No ^{35}Cl or ^{199}Hg NMR could be detected, probably because $HgCl_2$ solid is highly insoluble in $GeBr_4$ or CS_2. It is interesting that relatively rapid redistribution occurred under mild conditions in spite of the apparent insolubility of Cl^- in the medium ($HgCl_2/HgBr_2$ exchange is very fast).[6n]

When M = Sn, redistribution is slow, reaching equilibrium after several weeks at temperatures up to 75 °C. ($SnCl_4/SnBr_4$ exchange has $t_{\frac{1}{2}} < 10$ s when moisture is present.)[169] Tin-119 NMR was not very useful because of the very large line widths, being 400-50 times greater than for ^{73}Ge NMR.

When M = Si, redistribution is very slow, reaching equilibrium after several months at temperatures up to 75 °C. Silicon-29 NMR only showed one signal (compared to five for ^{73}Ge NMR) at any one time, for instance showing $SiCl_3Br$ at a half way stage from equilibrium, with twice the linewidth of ^{73}Ge NMR.

The very slow redistribution times when M = Sn, Si can be partly explained by the present experimental methods which included the rigorous exclusion of moisture and of HCl, HBr which can catalyze such reactions.[169] In contrast, there is relatively fast equilibration for the homonuclear systems MX_4:MY_4, M = Ge[146], Sn.[169]

4.7.5.1 Intensity Measurements

An equimolar mixture of $GeCl_4/GeBr_4$ gave an equilibrium mixture very close to the expected binomial distribution 1:4:6:4:1.[177] Near equimolar mixtures of $GeCl_4/GeI_4$ and $GeBr_4/GeI_4$ showed significant deviations from the expected distribution, having more signal intensity for the outer GeX_4 signals than expected. (A similar result was found for analogous Ga compounds, and GaI_4^- was suggested to be the most kinetically stable GaX_4^- anion.)[170] Low S/N precluded accurate intensity measurements for $GeCl_4/GeBr_4/GeI_4$ mixtures.

Equilibrium ^{73}Ge intensity distributions for mixed nucleus systems were compared with the appropriate binomial distributions. The calculations show the equilibrium distribution expected if the change in enthalpy for the redistribution of halogens was zero (TABLE (4.23)). Binomial distributions are weighted according to the exact mole fraction of halogen present (eg. Binomial probability is 0.5 only if the mole fraction of halogen is 0.5).

Each system shows an equilibrium distribution which has redistributed halogen more than predicted. It is quite likely that the change in enthalpy is positive, since there is the driving force of a heavier

SYSTEM		COMPOUND				
		$GeCl_4$	$GeCl_3Br$	$GeCl_2Br_2$	$GeClBr_3$	$GeBr_4$
(Si)	EXP.	*3.1	12.5	28.8	34.4	21.3
	TH.	*10.5	32.6	33.7	19.0	4.2
(Sn)	EXP.	44.1	36.9	15.2	3.8	0 *
	TH.	7.7	27.7	36.9	22.6	5.1*
(Hg)	EXP.	2.8	9.1	25.3	37.7	25.1*
	TH.	0.4	4.8	21.0	42.2	31.7*
(Hg)'	EXP.	6.8	18.9	32.4	29.7	12.2*
	TH.	0.8	7.6	26.5	40.9	24.2*

TABLE 4.23 Equilibrium ^{73}Ge intensity distributions for several mixed nucleus halide systems. (Si) $SiBr_4/GeCl_4$, (Sn) $SnCl_4/GeBr_4$,(Hg) $HgCl_2/GeBr_4$,(Hg)' $HgCl_2/GeBr_4/CS_2$, as shown in TABLE (4.18).Intensities are as proportions,totalling 100. The initial reactants have an asterisk * .

nucleus 'preferring' to have a heavier halogen in each case. For example the $SnCl_4/GeBr_4$ system reaches an equilibrium that has no $GeBr_4$ remaining.

Quantitative calculations based on average bond energies or chemical bond strength are not useful because of the large errors in these quantities. However, the change in enthalpy (av. bond energy and chem. bond strength) for the Si system is consistently smaller than for the Sn system, correctly predicting that the Si system will redistribute halogen to a smaller extent.

When CS_2 is added to the Hg system,halogen redistributes to a greater extent. There is probably more opportunity for Cl^- to move through CS_2 plus the reactant,than through the neat reactants.

4.8 CONCLUSIONS

The application of ^{73}Ge NMR has been extended significantly. Most of the compounds studied directly by ^{73}Ge NMR in the literature have been observed, and the total number of compounds studied directly by this method has been doubled.

This spectroscopic tool is useful in germanium chemistry, especially for the identification of halogen-free germanium compounds.

Moreover, a relatively 'low field' multinuclear FTNMR spectrometer is adequate for the study of this rather unreceptive NMR isotope.

4.9 EXPERIMENTAL DETAILS

4.9.1 Methods

Chemical shift referencing used the method of substitution. Tetramethylgermane was the reference for which Ξ = 3,488,318±10 Hz but since it was hard to obtain in high purity, the pure tetrachloride was used as a secondary reference, for which Ξ = 3,488,323±10 Hz. Both resonance frequencies are very close to literature values (section 4.2.1).

An external lock of the first kind was used (section 3.11.2).

Coupling constants were measured directly from ^{73}Ge NMR spectra, and in the case of GeH_4, also from ^{1}H NMR.

Linewidths were obtained directly from high resolution spectra, recorded under conditions where magnetization recovered fully between scans.

All NMR used the referencing shown in appendix 1.

4.9.2 Instrumentation

Instrumentation is outlined in section 3.11.1.

4.9.3 Materials and Sample Handling

Materials not already listed in section 3.11.3 are given below. Tetragermane was recovered with the lower molecular mass polygermanes from a silent electric discharge on GeH_4, and $H(GeMeH)_mH$ similarly from $GeMeH_3$. Other methylpolygermanes were byproducts in the synthesis of GeH_3GeMe_2H and GeH_3GeMe_3.

Methylsilygermane, GeH_3SiMeH_2 was produced by the action of $SnCl_4$ on GeH_3SiH_3 followed by excess MeMgI in Bu_2O.[141]

Germanium tetraalkyls, with the exception of $GeMe_4$ and $GeEt_4$, were used as supplied by the Organisch Chemical Institute, J.N.O.

Traces of HCl and HBr were removed from $GeCl_4$ (BDH chemicals) and $GeBr_4$ (Koch-Light Lab.) respectively, by vacuum distillation. Germanium tetraiodide was prepared by standard procedures,[178] and purified by vacuum sublimation at 110 °C.

All volatile chemicals, including CS_2, which was dried over molecular sieve type 3A, were stored under vacuum and moved in vacuo. Drybox techniques were used with involatile compounds like $GeBr_4$.

CHAPTER 5 GERMANIUM-73 NUCLEAR RELAXATION

5.1 INTRODUCTION

Relaxation times for quadrupolar nuclei are important in determining the overall scope of the NMR experiments. For these nuclei, the limits of observability are often determined by relaxation times,[127] and the signal intensity following multipulse sequences is quite dependent on these quantities (section 3.8.4.3).

5.2 REVIEW OF GERMANIUM-73 NUCLEAR RELAXATION

Schwenk et al[127] provide the only study on ^{73}Ge nuclear relaxation, giving ^{73}Ge T_2 values for tetrahedral compounds which have the same four ligands in a compound. The non-existence of a ^{73}Ge signal from $GeMeCl_3$ was attributed to small relaxation times, and yielded an upper limit for the relaxation time, $T_2 < 100$ μsec.

Linewidths, relaxation times calculated from line widths, and measured by the Carr-Purcell spin-echo method[179] are listed in TABLE (5.1). Measured linewidths were corrected[180] for magnetic field inhomogeneity and these corrected values are recorded, and used to calculate T_2 via equ. (1.15). Observed values of T_2 from the Carr-Purcell method were corrected for inhomogeneity in B_1.[181]

Values of T_2 attained by the two methods show agreement within the limits of error for $GeCl_4$, $GeBr_4$, $GeMe_4$, and $Ge(OMe)_4$. (The linewidth of $Ge(OMe)_4$ must be calculated using a fitting routine.) Relaxation times of the other tetraalkyls do not correspond with the linewidths since these compounds have unresolved proton coupling.

Germanium methoxide showed an inverse dependence of $W_{\frac{1}{2}}$ on the temperature, decreases in $W_{\frac{1}{2}}$ being 0.16 Hz/°C in the range 0 to 50 °C. In the range 20-40 °C linewidths of the tetraalkyls did not show a dependence on temperature.

COMPOUND	$W_{(1/2)}$ (Hz) (corrected for inhomogeneity)	T_2 (ms) (from $W_{(1/2)}$)	T_2 (ms) (from Carr-Purcell method)
$GeMe_4$	0.58±0.16	550±200	740±80
$GeEt_4$	15.6±0.4 †	(20.4±0.5)	140±20
$Ge(n\text{-}Pr)_4$	13.3±0.2 †	(23.9±0.4)	100±12
$Ge(n\text{-}Bu)_4$	13.8±0.5 †	(23.1±0.8)	65±7
$Ge(OMe)_4$	17.7±0.8 †	(18.0±0.9)	-
$Ge(OMe)_4$	12.2±1.5 (a)	26±3	30±3
$GeCl_4$	2.02±0.10	158±8	163±20
$GeBr_4$	1.76±0.14	181±15	196±30
GeI_4	2.2±0.3	145±23	-
GeI_4'	32	10	-

TABLE 5.1 Linewidths and ^{73}Ge spin-spin relaxation times for compounds which have all four ligands the same. [127] Measurement temperature 40 °C for GeI_4,GeI_4', 30 °C otherwise. Errors for linewidths and related T_2 values are 3 times the r.m.s. error plus a systematic error of ±0.04, and the max. error of the Carr-Purcell method are given. NMR linewidths of GeI_4 and the weaker line , GeI_4' , in CS_2 and C_6H_6 are the same. (a)= width of a single line calculated from a fitting routine. †= width of absorption curve of unresolved spectrum.

According to the general theory for longitudinal and transverse relaxation behaviour of spin $^5/_2$ and $^7/_2$ systems,[182,183] for rapid exchange of the nucleus between two sites or in the absence of exchange, relaxation behaviour can be described in terms of the superposition of three ($I=^5/_2$) or four ($I=^7/_2$) exponentially decaying contributions. However, T_1 for spin $^5/_2$ or $^7/_2$ may always be regarded as a single exponential due to the large contribution of one exponential compared to the others.[183] When the extreme narrowing condition (e.n.c.) is not obeyed, T_2 becomes a superposition of three ($I=^5/_2$) or four ($I=^7/_2$) exponentials.

One expects that for $I = ^9/_2$ the same principles apply, but that T_2 is a superposition of more than four exponentials when the e.n.c. is not obeyed.

Schwenk et al[127] used an observation frequency of 2.7 MHz, so that the e.n.c. is obeyed (and the lineshape is Lorentzian) if $\tau_c \ll 60$ nsec. This condition will probably be obeyed for the small molecules used in Schwenk's study.[5a] In addition, all single lines, with the exception of lines with unresolved proton coupling, were Lorentzian in shape.

However, thirteen years after this study, the calculation of T_2, especially using the Carr-Purcell method, is experimentally demanding and can easily contain systematic errors.[7h]

5.3 GERMANIUM-73 RELAXATION TIMES

All ^{73}Ge absorption lineshapes are Lorentzian, with the possible exception of lineshapes from compounds with unresolved proton coupling, setting an upper limit on $\tau_c << 50$ nsec, at the observation frequency of 3.13 MHz via the e.n.c. Thus T_1 and T_2 are equal, and for ^{73}Ge are given by (from section 1.1.8.2)

$$1/T_1 = 1/T_2 = (\pi^2/45)(\chi')^2 \tau_c \qquad ---(5.1)$$

All ^{73}Ge T_1 experiments using the inversion recovery techniques exhibited a single-exponential decay, supporting the expected extrapolation to $I = {}^9/_2$ on the theory of T_1 applied to $I = {}^5/_2$ and $I = {}^7/_2$ isotopes.[183]

5.3.1 The Quadrupolar Relaxation Mechanism

Germanium-73 nuclear relaxation has not been explicitly tested to ensure the dominance of the quadrupolar relaxation mechanism (although $W_{\frac{1}{2}}$ $Ge(OMe)_4$ decreases with temperature).[127]

A test, suggested by Marks[184] is based on the usual observation that $\tau_c \propto \bar{\eta}/T$, where $\bar{\eta}$ is the macroscopic viscosity of the solution and T is the absolute temperature. Since T_1 and τ_c are the only variables for a given compound, changes in τ_c effected through dilution or temperature will affect T_1 values. Data in TABLE (5.2) and selected data in TABLE (5.3) demonstrate that T_1 increases on dilution for an inert solvent, and increasing the sample temperature, as expected for a quadrupolar relaxation mechanism.[4b] The selected data in TABLE (5.3) refer to T_1, neat $GeEt_4$ (510) and T_1, 5.5% vol. $GeEt_4$ in C_6H_{12} (905).

Apparent spin-spin relaxation times were calculated from observed linewidths. Within the limits of error, the condition $T_1 \geq T_2^*$ is obeyed for all the present ^{73}Ge measurements. When T_1 is larger than about 100 ms, it becomes significantly larger than T_2^* as the effect of magnetic field inhomogeneity becomes more obvious. The largest T_2^* values ($W_{\frac{1}{2}} \sim 0.8$ Hz) are observed for GeH_4 and $GeMe_4$ at 30-40 °C.

COMPOUND	SAMPLE	T_1 (ms)	T_2* (ms)	T (°C)
GeH_4	1.2 atm.	863±90	290±30	-14.5
	$n\text{-}Bu_2O$	1300(40)	290±30	27.0
		1290±130	400±40	34.3
$GeMe_4$	75% v.	459±50	(>160)†	-14.8
	$n\text{-}Bu_2O$	597(12)	320±30	27.0
		662±70	400±40	41.3
$GeEt_4$	neat	284±30	(>160)†	-14.5
		510(15)	350±40	27.0
		526±50	(>160)†	34.2
		598±60	(>160)†	47.8
		731±70	(>250)†	67.5
$Ge(n\text{-}Pr)_4$	neat	113(2)	96±10	27.0
		(153±10) (a)	133±10	50.0
$GeCl_4$	neat	823±80	110±20	-14.8
		1020(10)	150±20	27.0
		1300±130	110±20	59.0
$GeEt_3H$	neat	7.4±.7	8±1	-14.5
		9.9±1	10±2	-1.0
		12.6(0.8)	12±1	27.0
		18.4±2	17±2	47.9
		21.4±2	16±3	59.0

TABLE 5.2 Germanium-73 nuclear relaxation at varying temperatures. Error in temp. is ±0.2°C . T_1 values at 27.0 °C have the standard deviation of the mean (random errors) in brackets, other figures are estimated max. random errors. † lower limit on T_2* , imposed by the low resolution of the spectrum , (a) T_1 based on the calculation: $T_1 \approx 1.177T_2$* obtained from several RT determinations of T_1 and T_2 for this compound.

5.3.2 Compilation of Germanium-73 Nuclear Relaxation Data

Lists of germanium-73 nuclear relaxation times at ambient probe temperature are given in TABLES (5.3) and (5.4), and a representative stacked plot of a T_1 calculation on a mixture of $GeCl_4$ and $GeBr_4$ is shown in FIG.(5.1).

Relaxation times increase with an increase in symmetry at germanium or a decrease in viscosity, as expected for the quadrupolar mechanism.

Examples of increases in symmetry (left to right) while keeping the viscosity comparable, include: $GeEt_3H$ (12.6) => $GeEt_4$ (510), $GeMeH_3$ (340) => $GeMe_4$ (597), $GeCl_3Br$ (337) => $GeCl_4$ (520), $GeClBr_3$ (278) => $GeBr_4$ (337). In all cases, the expected increase in T_1 (in brackets) from left to right was observed. The low T_1 value of $GeEt_3H$ is probably due to low symmetry at germanium caused by the large size difference in the ligands.

Examples of decreases in viscosity (left to right) while keeping the symmetry at germanium about constant, include:
$GeBr_4$ [neat] (206) => $GeCl_4$ [neat] (1020), $GeCl_4$ [with $GeBr_4$] (520) => $GeCl_4$ [neat] (1020), $GeBr_4$ [neat] (206) => $GeBr_4$ [with $GeCl_4$] (337), Ge (n-Hx)$_4$ (18.7) => Ge(n-Pn)$_4$ (30.6), => Ge(n-Bu)$_4$ (71.7) => Ge(n-Pr)$_4$ (113) => $GeEt_4$ (510), $GeEt_4$ [n-Bu_2O] (398) => $GeMe_4$ [n-Bu_2O] (597), GeH_3SiH_3 (570) => $GeMeH_3$ (374). In almost all cases, the expected increase from left to right was observed. However, the reverse trend was seen for silylgermane (b.p. 7 °C)[185] and methylgermane (b.p. -35 °C)[186], both in n-Bu_2O. There is likely to be lower effective symmetry at germanium for $GeMeH_3$ since there is a larger electronegativity difference between Ge and C than between Ge and Si (TABLE 4.19). A considerable viscosity difference exists between $GeCl_4$, which is a volatile liquid at RT, and $GeBr_4$, which melts at RT.

COMPOUND	SAMPLE	T_1 (ms)	T_2* (ms)	n
$GeMe_4$	75% v. n-Bu_2O	597(12)	320±30	5
	80% v. n-Bu_2O	560±100	290±30	1
$GeEt_4$	neat	510(15)	350±40	10
	neat,not degassed	510±50	320±30	1
	75% v. n-Bu_2O	367(6)	290±30	3
	25% v. n-Bu_2O	298(5)	240±20	3
	5.5% v. C_6H_{12}	905(24)	370±40	3
$Ge(n\text{-}Pr)_4$	neat	113(2)	96±10	3
$Ge(n\text{-}Bu)_4$	neat	71.7(6)	62±6	3
$Ge(n\text{-}Pn)_4$	neat	30.6(2)	29±3	3
$Ge(n\text{-}Hx)_4$	neat	18.7(0.7)	19±2	3
$GeMe_3H$	dil. in $GeMe_2H_2$, Ge_2MeH_5	340(60)	190±20	3
	dil. fr. decomp. $F(GeMe_3)(GeMeH_2)$	200±100	(>80)	1
$GeMe_2H_2$	with Ge_2MeH_5, some $GeMeH_3$	294(6)	180±20	3
	dil. fr. decomp. $F(GeH_3)(GeMe_2H)$	90±20	(>37)	1
$GeMeH_3$	dil. in $GeMe_2H_2$, Ge_2MeH_5	575(12)	220±20	3
	0.8 atm. n-Bu_2O	374(11)	250±30	4
$GeEt_3H$	neat	12.6(0.8)	12±1	3
$GeEtH_3$	neat	95.0(1)	94±10	5

TABLE 5.3 Germanium-73 nuclear relaxation (27°C) for **Germanium Tetraalkyls and Alkylgermanes .**

n-Pn = n-C_5H_{11} , n-Hx = n-C_6H_{13} , F = $Fe(CO)_4$.

COMPOUND	SAMPLE	T_1 (ms)	T_2* (ms)	n
GeH_4	1.2 atm. $n\text{-}Bu_2O$	1300(40)	290±30	4
Ge_2H_6	0.3 atm. $n\text{-}Bu_2O$	22.2(1)	20±2	3
GeH_3GeMeH_2	with $GeMe_2H_2$ some $GeMeH_3$	264(8) (GeH_3)	160±20 (GeH_3)	3
	1:1 with $(GeMeH_2)_2$	195(4) (GeH_3)	110±10 (GeH_3)	6
		50.5(2) † ($GeMeH_2$)	45±5 † ($GeMeH_2$)	6
$(GeMeH_2)_2$	1:1 with GeH_3GeMeH_2	50.5(2)	45±5	6
$GeSiH_6$	0.6 atm. $n\text{-}Bu_2O$	573(6)	270±30	3
$GeCl_4$	neat	1020(10)	150±20	4
	(a)	520(5)	140±10	3
$GeBr_4$	neat	206(6)	140±10	3
	(a)	337(40)	140±10	3
$GeCl_3Br$	(a)	233(5)	140±10	3
$GeCl_2Br_2$	(a)	217(4)	140±10	3
$GeClBr_3$	(a)	278(6)	140±10	3

TABLE 5.4 Germanium-73 nuclear relaxation times (27°C) for **Polygermanes, Methyldigermanes, Silylgermane, Tetrahalides and Mixed Tetrahalides.**

(a) One sample of $GeCl_4/GeBr_4$ in 1:1.03 mole ratio, respec. †This peak overlaps with the $(GeMeH_2)_2$ peak, but most (2/3) of the area under the peak is due to $(GeMeH_2)_2$.

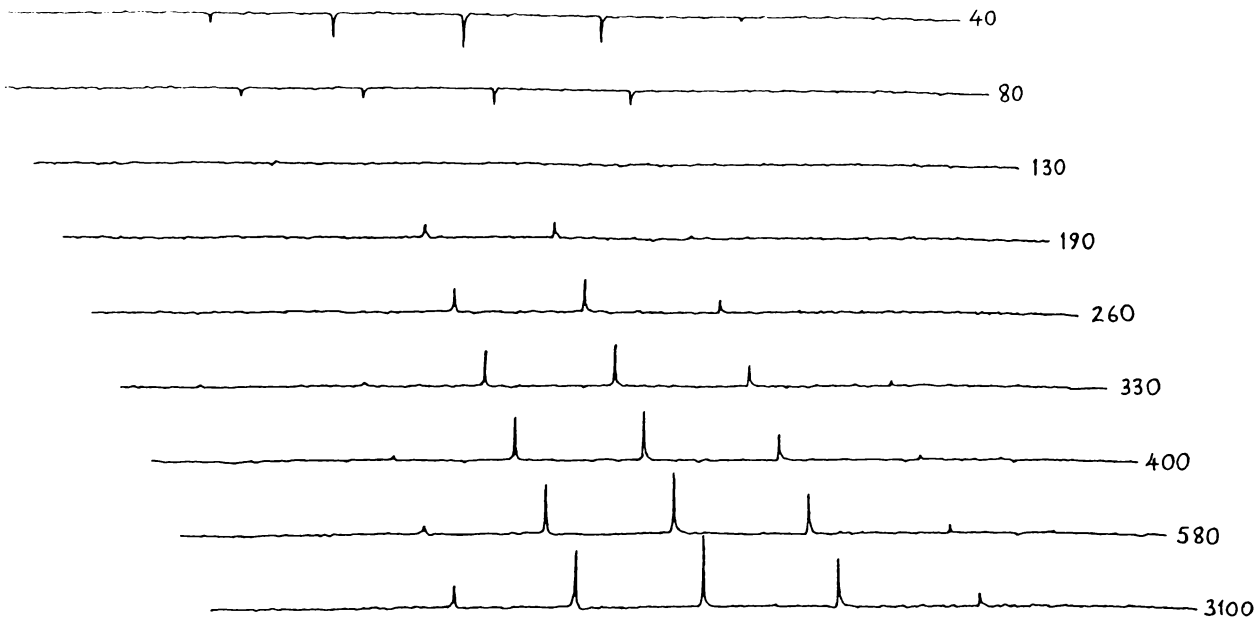

FIG. 5.1 Inversion-recovery spectra for the ^{73}Ge resonances of a 1:1.03 mole ratio of $GeCl_4/GeBr_4$ at ambient probe temp. (27 °C). The resonances, from left to right, are $GeCl_4$, $GeCl_3Br$, $GeCl_2Br_2$, $GeClBr_3$, and $GeBr_4$, and the numbers shown are values of the pulse sequence recovery time τ, in ms.

Examples of increases in symmetry and decreases in viscosity (left to right) include: $GeMe_2H_2$ (294) => $GeMeH_3$ (575), $GeEt_3H$ (12.6) => $GeEtH_3$ (95.0), Ge_2H_6 (22.2) => GeH_4 (1300), GeH_3GeMeH_2 (195, 50.5) => GeH_3GeH_3 (12.6). In all but one case, the expected increase in T_1 from left to right was seen. A reverse trend was seen comparing methyldigermane with digermane. The former molecule is probably more viscous (b.p. 54.7 °C, 1 atm)[187] than the latter, (b.p. 29.0 °C, 1 atm)[133b] and from an 'electronic' point of view, germanium in the former molecule may have a lower effective symmetry. (A Me group probably has a larger electronegativity difference with Ge than a H group, TABLE (4.19).) With the possible exception of the $GeMe_3$- group, all T_2* values from the linewidths (TABLES (4.10)-(4.13)) are smaller for digermane and trigermane than their methylated versions.

There is a large 60 fold increase in T_1 from Ge_2H_6 to GeH_4 which can be explained intuitively from symmetry and viscosity arguments (b.p. GeH_4-88.5 °C, 1 atm).[188] It is easy to selectively reduce the GeH_4 signal in a mixture of polygermanes by using a small waiting time between scans.

All samples were degassed except one sample of $GeEt_4$, which exhibited the same T_1 as a degassed sample of $GeEt_4$. Either oxygen is fairly insoluble in $GeEt_4$, and/or there may be no significant Ge-O interaction. Only the tetraalkyls can be tested in this way, since they are the only compounds which are air stable.

The dilution of $GeEt_4$ with n-Bu_2O leads to a decrease in T_1 which is the opposite of the expected trend for an inert solvent. There is probably a significant Ge-O interaction which reduces the electric field gradient at germanium. The possibility of a Ge-O interaction from n-Bu_2O is significant in the chemistry of organogermanium compounds since this ether is a frequently used solvent.

A similar rationale, just used for $GeEt_4$, could be used to explain the lower T_1 value of $GeMeH_3$ when an ether solvent is used, compared to a non-polar hydride medium. Similarly, the T_1 value of $GeMe_4$ in n-Bu_2O is lowered from the expected value for neat $GeMe_4$ when compared to neat $GeEt_4$ and n-Bu_2O solutions of $GeEt_4$, and the same rationale could be used here.

5.3.3 Information Derived from Nuclear Relaxation Times

5.3.3.1 Activation Parameters

Activation parameters for molecular reorientation can be obtained from the expression:[189]

$$T_1 = T_1^{\circ} \exp(-Ea/RT) \qquad ---(5.2)$$

Using the data of TABLE (5.1), plots of $\ln T_1$ vs 1/T were obtained with slopes -Ea/R where Ea is an activation energy for molecular reorientation, and the $\ln T_1$ intercept, T_1°, the value of T_1 at infinitely high temperature. Activation energies, together with Pearson's product moment correlation coefficient, r, are listed in TABLE (5.5).

As expected, these Arrhenius activation energies increased as the size of the molecule increased (eg. $GeMe_4$ (4.3) => $GeEt_4$ (8.4) => Ge (n-Pr)$_4$ (10)). This simple rationale would predict that Ea for GeH_4 would be smaller than $GeMe_4$, but they are similar within the limits of error. Intuitively, it is expected that as the ligands become more different in size, it will be harder for the molecule to reorientate. This idea correctly predicts that E_a for $GeEt_3H$ is larger than for $GeEt_4$.

Although the data for each compound fits a straight line with a negative slope ($r \simeq -1$) as expected for quadrupolar relaxation, the data

COMPOUND	SAMPLE	Ea ($kJmol^{-1}$)	T_1° (s)	r
$GeMe_4$	75% v. $n\text{-}Bu_2O$	4.3±0.9	3.4±1	-0.997
$GeEt_4$	neat	8.4±0.6	14±2	-0.999
$Ge(n\text{-}Pr)_4$	neat	(10±2)†	(7±1)†	-
GeH_4	1.2 atm. $n\text{-}Bu_2O$	5.2±0.7	10±2	-0.989
$GeCl_4$	neat	4.4±0.4	6.1±0.9	-0.983
$GeEt_3H$	neat	11.3±0.9	1.4±0.4	-0.990

TABLE 5.5 Activation energies for molecular reorientation derived from ^{73}Ge T_1 data.r is a correlation coefficient.
† = estimate based on two data points.

for $GeEt_3H$ has a larger apparent discontinuity (FIG.(5.2)) than the other compounds. Experimental error was too large to determine if this discontinuity between 0 and 25 °C was real, implying some change in structure, or an artifact. Since the apparent change in slope is very small, any change in structure would involve a very small change in E_a of less than 1 $kJmol^{-1}$, perhaps exhibiting a locked to free rotation situation. Experimental constraints from the probe and the sample hindered an extension of the temperature range of the measurements.

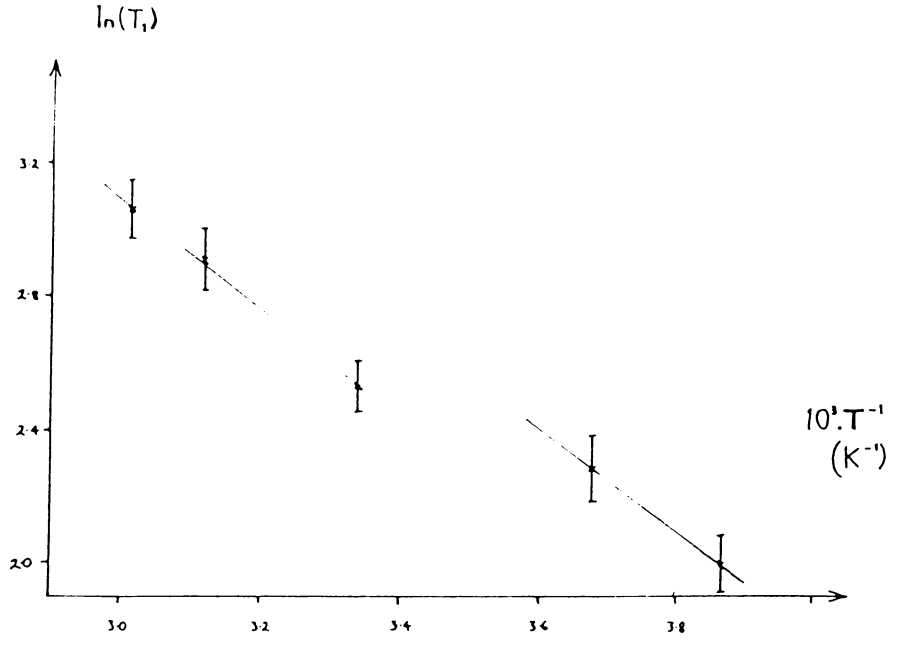

FIG. 5.2 Temperature variation of T_1 for Ge Et_3H.

5.3.3.2 Spectral Editing

A knowledge of T_1 values allows signals to be inverted, diminished or nulled (section 1.2.10).

Figure (5.3) shows a reaction mixture of all three methylgermanes and methyldigermane. There was a weak signal appearing as a shoulder on the $GeMeH_3$ signal whose chemical shift suggested a $GeMeH_2$ group. Using the known T_1 value of $GeMeH_3$ in this medium, it was possible to diminish and invert this resonance, verifying the existence of the underlying $GeMeH_2$ resonance.

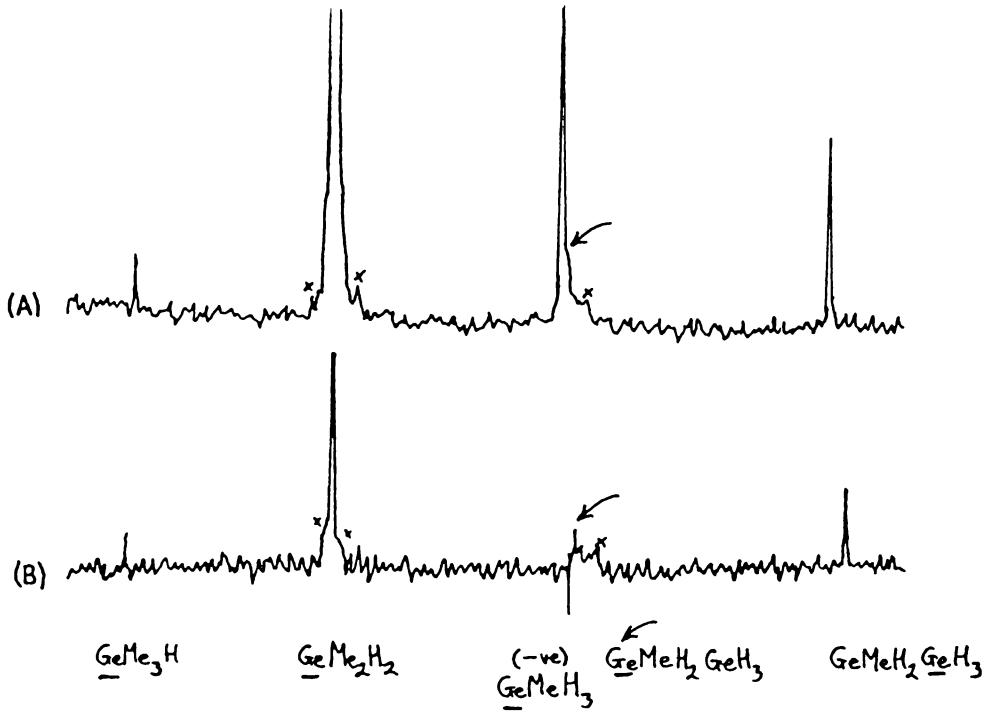

FIG. 5.3 Use of ^{73}Ge T_1 values in spectral editing for a mixture of three methylgermanes and GeH_3GeMeH_2 . (A) Single-pulse sequence (B) 180-τ-90 sequence adjusted to reduce and change sign of $GeMeH_3$ signal.

COMPOUND	SAMPLE	COMPOUND	SAMPLE	COMPOUND	SAMPLE
$GeMeCl_3$	neat	GeH_2ClSiH_3	CCl_4	$F(GeMeH_2)_2$ #	neat
$GeMe_2Cl_2$	"	$GeMeI_3$	C_6H_6	$F(Ge_2H_5)_2$	
$GeMe_3Cl$	"	GeI_2	"	$F(GeH_3)(Ge_2H_5)$	
$GeMe_2HBr$	C_6H_6	$GePh_4$	$CHCl_3$	$F(GeH_3)(SiH_3)$	C_6H_6
$GeMeH_2Br$	neat	$GeCl_4py_2$ †	CCl_4	$GeH_3Co(CO)_4$	
$GeMeH_2Cl$	C_6H_6	$(GeCl_6^{2-})$*	pyHCl	$GeCo_4(CO)_{14}$	CH_2Cl_2
GeH_3Br	neat	$Ge(OH)_6^{2-}$	$NaOH/GeO_2$	$GeCo_4(CO)_{13}$	"
GeH_2Br_2		$(GeH_3)_2Te$	CS_2	$Me_2GeCo_2(CO)_8$	C_6H_{14}
$GeBu_2Cl_2$	neat	$(GeH_3)_2F$	neat	$[Me_2GeCo(CO)_3]_2$	"
$GeMe_2ClGeH_3$	"	$F(GeH_3)(GeMeH_2)$	"	$(Ge_2H_5)Mn(CO)_5$	
$GeMeHClGeH_3$		$F(GeH_3)(GeMe_2H)$	"	$[GeH_2Mn(CO)_5]_2$	

TABLE 5.6 Germanium compounds giving no ^{73}Ge signal. (non-appearance not due to low concentration, except possibly sample *) †py = pyridine ,# F = $Fe(CO)_4$.

5.3.4 Limitations of Germanium-73 Observation

When relaxation times are very short compared to delay times between the observation pulse and acquisition,no NMR signal is detected. A list of some germanium compounds whose non-appearance in ^{73}Ge NMR is not due to low concentrations, is given in TABLE (5.6).

Most of the samples showed ^{13}C and ^{1}H signals diagnostic of the expected compound (eg. $GePh_4$, $GeMe_yCl_{4-y}$). Some of the smaller molecules were examined at higher temperatures where quadrupolar relaxation times will be longer.(eg. $GePh_4$ 50 °C).

The germanium hexachloride anion was prepared from $GeCl_4$ and pyHCl, but although the anion has been detected under these conditions by infrared spectroscopy,[190] only $GeCl_4$ was detected by ^{73}Ge NMR. It is possible that $GeCl_6^{2-}$ was present in low concentrations.

In a number of cases, paramagnetic impurities may have stopped NMR detection (eg. cobalt carbonyls).

Most compounds probably had very short relaxation times, precluding ^{73}Ge observation. Delay times between acquisition and observation pulses when searching for resonances were typically 0.1 ms, giving a probable upper limit on T_2^* of 0.1 ms. Thus there is a large gap between theoretically observable resonances ($T_2^* \geq 0.1$ ms, $W_{\frac{1}{2}} \leq 3000$ Hz) and the experimentally observed resonances ($T_2^* \geq 3$ ms, $W_{\frac{1}{2}} \leq 100$ Hz).

However, observation of broad lines is made difficult by their inherently low S/N. For instance, by eq. (1.31), keeping N_d constant, a line with $W_{\frac{1}{2}}$ = 3000 Hz requires 900 fold more scans to reach the same S/N as a 100 Hz line.

5.4 GERMANIUM-73 NUCLEAR QUADRUPOLE COUPLING CONSTANTS †

By inspection of eq. (5.1) it is seen that χ' can be calculated if T_1, and an independent estimate of τ_c are available. Using the method in section 1.1.8.2, the dipole-dipole relaxation of ^{13}C provides an estimate of τ_c via eq. (1.17), giving, for organogermanium compounds:

$$\tau_c = (4.42)10^{-11}/T_{1C} \qquad ---(5.3)$$

thus:

$$\chi'(^{73}Ge) = 0.321[T_{1C}/T_{1Ge}]^{0.5} \qquad ---(5.4)$$

where the units are τ_c (ps), χ' (MHz), and T_1i are the dipole-dipole and quadrupolar relaxation times of ^{13}C and ^{73}Ge, respectively (s).

Assumptions inherent in this method include: (a) there is no preferred axis[6p] of rotation about a given axis sensed by the carbon atoms, (b) τ_c for carbon is about the same as for germanium, (c) the dipole-dipole mechanism dominates for ^{13}C. Using the additional assumptions that: (d) τ_c is taken from the average of ^{13}C T_1 values and (e) r_{CH} assumes a single value taken from $GeMeH_3$ (1.083×10^{-10} m)[130], values of χ' were calculated. (TABLE (5.7)).

Assumptions (b), (c), and (d) are reasonable for fairly small molecules which have CH bonds (section 1.1.8.2)[191] although, strictly, (b) should be checked by establishing that Ea for ^{13}C is similar to Ea for ^{73}Ge.[191,192] Assumption (e) is also reasonable, since the small variations in r_{CH} will introduce errors small compared to errors in T_1 calculations (eg. $r_{CH} = 1.095 \times 10^{-10}$m for $GeMe_3Br$).[193]

However, assumption (a) is not strictly valid for compounds which have different ligands around germanium (section 1.1.8.1). Nevertheless, within this group of compounds, χ' reflects the expected symmetry at germanium. Hence the largest value of χ' is for $GeEt_3H$ which would have

† See back pocket

COMPOUND	SAMPLE	T_{1C} (av)	τ_c (av)	χ' (^{73}Ge)
$GeMe_4$	75% v. $n\text{-}Bu_2O$	18.6	2.4	1.79
$GeEt_4$	25% v. $n\text{-}Bu_2O$	11.5	3.8	1.99
	75% v. $n\text{-}Bu_2O$	10.7	4.1	1.73
	neat	10.6	4.2	1.46
$Ge(n\text{-}Pr)_4$	neat	4.06	11	1.92
$Ge(n\text{-}Bu)_4$	neat	2.03	22	1.69
$Ge(n\text{-}Pn)_4$	neat	1.41	31	2.16
$Ge(n\text{-}Hx)_4$	neat	1.11	40	2.45
$GeMe_3H$	(a)	10.3	4.3	(1.77)
$GeMe_2H_2$	(a)	22.9	1.9	(2.83)
$GeMeH_3$	(a)	28.8	1.5	(2.27)
	0.7 atm. $n\text{-}Bu_2O$	25.0	1.8	(2.62)
GeH_3GeMeH_2	(a) , (GeH_3)	18.7	2.4	(2.70)
	(a) , ($GeMeH_2$)	18.7	2.4	(5.28)
$GeEt_3H$	neat	15.2	2.9	(11.1)

TABLE 5.7 Germanium-73 nuclear quadrupole coupling constants and correlation times for **Organogermanium compounds .**

T_{1C},(s) and τ_c (ps) are averages in multiline spectra, χ' (MHz),values in brackets are rough estimates. Max. random errors: χ' (20%) , T_{1C} , τ_c (10%) , (a) Sample of $GeMe_2H_2$,Ge_2MeH_5 ,some $GeMeH_3$, $GeMe_3H$. n-Pn = $n\text{-}C_5H_{11}$, n-Hx = $n\text{-}C_6H_{13}$.

low symmetry (larger electric field gradient) at the germanium due to the different size ligands. Methylgermanes have similar χ' values, since they have Ge in a similar environment, and they are on average smaller than χ' for methyldigermane.

Neat tetraalkyls have a small range of χ' values that generally increase as chain length increases. Thus, as chain length increases, the large reduction in T_1(Ge) is mainly due to an increase in viscosity (τ_c) rather than a decrease in effective symmetry at germanium.

For the same medium, $GeMe_4$ and $GeEt_4$ have similar symmetry at the germanium. However, the addition of n-Bu_2O to $GeEt_4$ lowers the effective symmetry at Ge, supporting the earlier rationales for the unusual variations (5.3.2) of T_1 for $GeEt_4$ in solutions of n-Bu_2O. It is likely that there is a significant Ge-O interaction in this case. Assuming the same interaction occurs for $GeMe_4$, then χ' (neat $GeMe_4$) < χ' (75% v. $GeMe_4$ in n-Bu_2O)

Although the tetrahedral symmetry of simple molecules like GeH_4, $GeCl_4$, and $GeMe_4$ suggests a near zero electric field gradient, and a near-zero χ' value, this is not observed. The field gradient may be increased by vibrational distortion of the molecule.[194,195] On the other hand, since there is a fair correspondence between χ' and molecular structure, for the organogermanium compounds (including $GeMe_4$), rotational reorientation is probably the dominant time process, and vibrational processes don't contribute significantly to T_1.[196]

5.5 GERMANIUM-73 NUCLEAR OVERHAUSER EFFECTS

Germanium-73 nuclear Overhauser effect measurements yielded η, and via eq. (1.20), the % contribution of the dipole-dipole mechanism to nuclear relaxation, R%.(TABLE (5.8)).

COMPOUND	SAMPLE	η	T_1dd (Ge)	R%
GeH_4	1.2 atm. $n\text{-}Bu_2O$	-0.4	47	3
$GeMe_4$	75% v. $n\text{-}Bu_2O$	-0.3	29	2
$GeEt_4$	neat	-0.06	120	0.4

TABLE 5.8 Germanium-73 Nuclear Overhauser effects (±20%), dipole-dipole relaxation times (±25%, s), and % contribution to relaxation rates. (±30%)

The NOE is expected to be a maximum for a small mobile molecule, like GeH_4. Even in this case, R% is only about 3, being the same as the figure for the typical random error in the average of T_1 determinations. For $GeEt_4$, the dipole-dipole mechanism is almost negligible.

(Although the spin-rotation mechanism (section 1.1.8) can compete with the quadrupolar mechanism when $\chi < 3$ MHz,[197] it must be small for ^{73}Ge since it is proportional to γ^2. In addition T_1(Ge) increased with temperature, contrary to manifestations of the spin-rotation mechanism.)[7i]

5.6 COMPARISON

A comparison of the T_2 values measured from the Carr-Purcell method[127] with the present T_1 values of the neat compounds: GeR_4, R = Cl, Br, Et, n-Pr, n-Bu, shows that the former values are slightly lower than the latter, but the same within the limits of error, except for R = Cl, and Et. For $GeCl_4$ and $GeEt_4$, the Carr-Purcell method gives T_2 values 6.3 and 3.6 fold smaller, respectively, than the present T_1 values. While the apparent absence of degassing samples[127] could explain the slightly smaller values of T_2 compared to the present T_1 values (degassed samples), the very large differences are not explained. In addition, the present study

revealed that degassing had no significant effect on T_1 for samples of $GeEt_4$. A larger discrepancy is found if T_2 values measured from linewidths are compared with present T_1 values. Bearing in mind that n-Bu_2O used with the present sample of $GeMe_4$ will probably lower its T_1 value compared to the neat state, then the present T_1 value for $GeMe_4$ is similar to the T_2 values.[127] (Calculation of T_1 for neat $GeMe_4$ using the same fractional changes observed in neat and n-Bu_2O solutions of $GeEt_4$, give $T_1 \sim 800$ ms.)

Linewidths of the tetraalkyls showed a small inverse dependence on temperature at 20-40 °C, whereas Schwenk et al[127] observed no temperature dependence under these conditions.

Activation energies of 5.6 and 5.8 $kJmol^{-1}$ for ^{47}Ti and ^{49}Ti, respectively, in $TiCl_4$ (80% v. in toluene)[189] are not very different from Ea = 4.4 $kJmol^{-1}$ for neat $GeCl_4$, obtained using the same techniques. The linearity of the present $\ln T_1$ vs 1/T plots, as measured by r (-0.999 to -0.983) compare favourably with the study on $TiCl_4$ (-0.995 to -0.977).[189] In the present study, the largest Ea values are not unbelievable when compared with other work (eg. Ea $\sim$ 50 $kJmol^{-1}$ for Na^+ in crown ethers).[198]

Phase transitions involving Et ligands, somewhat similar to transitions postulated for $GeEt_3H$, have been found in other studies.(eg. transitions probably involving orientational disordering of the NEt_4^+ cation have been found at -78 °C and -13 °C).[199]

The non-existence of resonances from quadrupolar nuclei in asymmetrical environments is a fairly common situation for isotopes with medium to large line broadening factors (eg. no ^{71}Ga resonance was observed from the salts of $Ga_2X_6^{2-}$, X = Cl, Br).[170] In comparison with compounds that gave ^{73}Ge resonances, most compounds that gave no resonance were either relatively viscous or contained Ge in an asymmetrical environment.

NQCC's for tetravalent organogermanium compounds were typically 3 MHz, whereas χ for GeF_6^{2-} was estimated as 5.8 MHz by Tarasov and Buslaev.[153] McGlinchey et al calculated χ' (^{49}Ti) in TiF_6^{2-} as 1.6 MHz,[189] and felt that their value was more reliable than the larger value of 4.5 MHz given by Tarasov and Buslaev, due to their more direct measurement of relaxation and correlation times. This same argument could be used when comparing the present χ' values with those of Tarasov and Buslaev.

5.7 CONCLUSIONS

A detailed analysis of several small germanium molecules revealed that the quadrupolar relaxation mechanism dominates, and the dipole-dipole mechanism was a minor one in small organogermanium compounds.

Near room temperature, spin-lattice relaxation times measured by inversion recovery techniques ranged from 12.6 ms to 1300 ms, while T_2^* values calculated from linewidths ranged from 3 ms to 370 ms. Relaxation times could be rationalized in terms of the symmetry at germanium and the approximate viscosity of the solution.

A knowledge of T_1 values can be useful in spectral editing for mixtures of organogermanium compounds.

Activation energies for molecular reorientation varied from 4.3 to 11.3 $kJmol^{-1}$, and can be partly rationalized by the approximate size and overall symmetry of the molecule. A possible discontinuity in the $\ln T_1$ vs 1/T plot for $GeEt_3H$ may indicate some minor structural change near room temperature.

The decrease in T_1 and χ' for $GeEt_4$ for increasing dilution with n-Bu_2O shows that n-Bu_2O interacts with $GeEt_4$, increasing the electric field gradient at germanium.

Germanium in the tetraalkyls experiences a narrow range of electric field gradients, with χ' values being about 3 MHz. Changes in ^{73}Ge T_1 values for tetraalkyls are largely due to changes in correlation times.

There is still a large gap between the theroetically detectable ^{73}Ge resonances ($T_2^* > 0.1$ ms) and the observed resonances ($T_2^* \geq 3$ ms) which warrants further exploration.

5.8 EXPERIMENTAL DETAILS

5.8.1 Methods

All recorded ^{73}Ge and ^{13}C T_1 values were obtained from a phase alternated inversion recovery sequence (section 1.2.11.2) with $W \geq 5\ T_1$. Typically, a T_1 experiment required five τ measurements spanning 0.1 T_1 to 1.4 T_1. Standard JEOL software[200] was used to calculate T_1 from a least squares fit to a plot of ln (Mo - M (τ)) vs τ. Most T_1 determinations used the average of three (^{73}Ge) or two (^{13}C) independent stacked accumulations with at least two data reductions per accumulation.

The inversion-recovery method was tested by finding ^{13}C T_1 values on ethyl benzene, and comparing these with literature.[201] There was good agreement between the present values (p— 12.6, m— 16.7, o— 18.5, C_1— 57.3, CH_2— 18.3, CH_3— 10.7, sec) and literature.

Longer ^{73}Ge T_1 values were also extracted by the fast inversion recovery sequence (section 1.2.11.2) with $W \geq 3\ T_1$, using a linear iterative, two parameter fit to the data.[202] Software was written into a University of Waikato VAX11/780 computer using BASIC language. Germanium-73 T_1 values were systematically lower using this method, by 9-11%, compared to the inversion recovery method.

Preliminary experimentation with the saturation recovery method (section 1.2.11.2) was performed with a view to using this to determine longer ^{13}C T_1 values. (Standard JEOL software was used.)[200] Carbon-13 T_1 values obtained on ethyl benzene were similar for the saturation recovery and inversion recovery methods.

Germanium-73 nuclear Overhauser effects were found by comparing signal intensities using reverse gated decoupling to remove the NOE, with intensities using complete decoupling (section 1.2.11.1). Typically, several determinations were averaged, all using long waiting times: $W > 9\ T_{1H}$.

Proton T_1 values were estimated with the same methods used for all recorded ^{13}C and ^{73}Ge T_1 values.

5.8.2 Instrumentation and Materials

Nuclear relaxation studies used the same instrumentation (with the addition of a variable temperature unit JEOL-JES-VT-3) and materials (all degassed and sealed under vacuum) as found for chapter 4.

APPENDIX 1

NMR ISOTOPE PARAMETERS

N.M.R. ISOTOPE PARAMETERS

All the most important NMR parameters required for the observation of specific isotopes are contained in this section. The data applies specifically to the FTNMR spectrometer used at Waikato University, namely the JEOL FX 90Q model.

Chemical shift referencing equations and resonant frequencies are also included. Resonant frequencies are compared with two other independent sources. This catalogue is referred to on the basis of the atomic mass of the isotope.

Following is an explanatory section, and a list of the isotopes available to date.

+¦

This catalogue provides the basic NMR parameters for all the commonly observed isotopes. In addition, a large number of other isotopes are included. For each isotope, parameters are divided into two sections ,delineated by a dashed line.

The first section gives actual experimental parameters used by P.J.Watkinson on the FX 90Q spectrometer to observe an isotope in a given sample. The majority of samples are accepted NMR standards. In most cases, the tilt angle is not known accurately but the recorded parameters allow practically full recovery of T1 magnetization during the WAIT time between scans. (WAIT=PD+ACQTM) Probes of 10mm diameter are used. Line width at half height is denoted by W1/2 .

The second section gives data derived from the actual N.M.R. experiments. Included first is an equation giving chemical shifts referred to an accepted NMRstandard.(Not always the given sample)
X is the value of OBSET (KHz) of the unknown signal .
Y is the value of OBFRQ (KHz) . By default Y is the value recorded for the sample in the first section .
Finally, three line (or resonance) frequencies are recorded for the accepted NMR standard of the isotope. They refer to a field corresponding to exactly 100 MHz for the protons of TMS . The value on the far left is the present work derived from the sample in the first section. The middle and right hand values are from, respectively, HANDBOOK OF HIGH RESOLUTION MULTINUCLEAR NMR by Brevard and Granger, and NMR AND THE PERIODIC TABLE , by Harris and Mann. All line frequencies use the same NMRstandard unless shown otherwise. The nomenclature: (From x), means a chemical shift adjustment has been made using sample x .
The nomenclature: ? ,indicates a value of dubious reliability.
The temperature is 27 degrees Celcius throughout.
The present work uses the method of substitution for chem.shifts.

+¦

	1H	2H			6Li	7Li		
10B	11B		13C	14N	15N	17O		19F
			23Na					29Si
	31P				35Cl	37Cl		39K
			43Ca					
	51V				55Mn			59Co
			73Ge			77Se		
						87Sr		
					95Mo	97Mo		
						117Sn		119Sn
			183W					
					195Pt			199Hg
						207Pb		

+¦

(MHz)	(KHz)	(Hz)	(K)			(us)	(deg)	(s)
OBFRQ	OBSET	FREQU	POINT	SCANS	IRMOD	PW1	TILT	WAIT
89.55	53.9	600	8	1	0	10	40	10

```
********************
* 1H Hydrogen      *
********************

SAMPLE: TMS 5mm  ¦ D20          10mm ....(A)
SAMPLE: TMS 5mm  ¦ CDC13        10mm ....(B)
SAMPLE: TMS 10mm ¦ D20           5mm ....(C)
SAMPLE: TMS 10mm ¦ LiClsat.aq.   5mm ....(D)
W1/2     0.4 Hz
```

```
CHEM SHIFT
TMS           ==   ( X   54.0517 ) 11.160209     ...(A)

              ==   ( X - 53.8222 ) 11.160238     ...(B)

              ==   ( X - 54.0504 ) 11.160209     ...(C)

              ==   ( X - 53.9555 ) 11.160221     ...(D)

RES. FREQ.
MHz           100.00000       100.00000       100.00000
```

+¦

+¦

(MHz)	(KHz)	(Hz)	(K)			(us)	(deg)	(s)
OBFRQ	OBSET	FREQU	POINT	SCANS	IRMOD	PW1	TILT	WAIT
13.71	44.8	750	8	1	0	10	40	1

```
********************
* 2H Deuterium     *
********************

SAMPLE: D20 100% 10mm ¦ LiCl sat.H20 5mm
W1/2     1.0 Hz
```

```
CHEM SHIFT
D20           ==    ( X   44.8239 ) 72.701766

RES. FREQ.
MHz           15.350688      15.3507         15.351
                             (D20 in H20)    (no ref.)
```

+¦

(MHz)	(KHz)	(Hz)	(K)			(us)	(deg)	(s)
OBFRQ	OBSET	FREQU	POINT	SCANS	IRMOD	PW1	TILT	WAIT
13.13	56.2	3000	16	300	0	18	40	9

****
* 6Li Lithium *
****

SAMPLE: LiCl 1.0M H20 5mm ¦ D20 10mm
W1/2 0.7 Hz

CHEM. SHIFT
LiCl 1M aq. (X 56.1612) 75.837082

RES. FREQ.

MHz	14.716032	14.7160 (in D20)	14.716 (Lit inf. dil.)

(MHz)	(KHz)	(Hz)	(K)			(us)	(deg)	(s)
OBFRQ	OBSET	FREQU	POINT	SCANS	IRMOD	PW1	TILT	WAIT
34.77	53.6	750	8	1	0	13	80	1

****
* 7Li Lithium *
****

SAMPLE: LiCl 1.0M H20 5mm ¦ D20 10mm
W1/2 0.3 Hz

CHEM. SHIFT
LiCl 1M aq. == (X - 53.5600) 28.71619

RES. FREQ.

MHz	38.863822	38.8637 (in D20)	38.864 (Lit inf. dil.)

(MHz) OBFRQ	(KHz) OBSET	(Hz) FREQU	(K) POINT	SCANS	IRMOD	(us) PW1	(deg) TILT	(s) WAIT
9.57	56.4	1000	4	50	4	50	90	2

****
* 10B Boron *
****

SAMPLE: NaBH4 sat. 0.1M NaOH 5mm ; D2O 10mm
W1/2 3.0 Hz

CHEM SHIFT
Et2O.BF3 (X 56.3605) 103.88142 43.6

RES. FREQ.
MHz 10.74369 ---------- 10.743698
(from NaBH4)

(MHz) OBFRQ	(KHz) OBSET	(Hz) FREQU	(K) POINT	SCANS	IRMOD	(us) PW1	(deg) TILT	(s) WAIT
28.69	57.4	1000	8	10	4	8	45	4

****
* 11B Boron *
****

SAMPLE: NaBH4 sat. 0.1M NaOH 5mm ; D2O 10mm
W1/2 < 14. Hz

CHEM SHIFT
Et2O.BF3 (X 57.3642) 34.785797 43.6

RES. FREQ.
MHz 32.08406 ---------- 32.084093
(from NaBH4)

+¦

(MHz)	(KHz)	(Hz)	(K)			(us)	(deg)	(s)
OBFRQ	OBSET	FREQU	POINT	SCANS	IRMOD	PW1	TILT	WAIT
22.49	40.9	500	8	50	1	12	45	10

```
*******************
* 13C Carbon      *
*******************
```

SAMPLE: TMS 5mm ¦ D2O 10mm ... (A)
SAMPLE: TMS 5mm ¦ CDCl3 10mm ... (B)
W1/2 0.5 Hz

CHEM SHIFT			
TMS	== (X 40.9423) 44.38341	...(A)	
	== (X 40.8841) 44.38352	...(B)	
RES. FREQ.			
MHZ	25.145002 ...(A)	-------	25.145004
	25.145004 ...(B)	-------	25.145004

+¦

+¦

(MHz)	(KHz)	(Hz)	(K)			(us)	(deg)	(s)
OBFRQ	OBSET	FREQU	POINT	SCANS	IRMOD	PW1	TILT	WAIT
6.41	65.1	2000	4	4	1	45	90	2

```
*******************
* 14N Nitrogen    *
*******************
```

SAMPLE: MeNO2 5mm ¦ D2O 10mm
W1/2 13. Hz

CHEM SHIFT			
MeNO2	== (X 65.0722) 154.43843		
RES. FREQ.			
MHz	7.22632	7.2263	(7.224) (No ref. comp.)

+¦

(MHz)	(KHz)	(Hz)	(K)			(us)	(deg)	(s)
OBFRQ	OBSET	FREQU	POINT	SCANS	IRMOD	PW1	TILT	WAIT
9.03	52.9	3000	8	500	4	15	30	10

****
* 15N Nitrogen *
****

SAMPLE: NH4NO3 sat. H2O 10mm ¦ D2O 5mm
W1/2 1.0 Hz (NO3-)

CHEM SHIFT
MeNO2 == (X 52.9218) 110.09673 4.0

RES. FREQ.
MHz 10.13677 10.1367 10.136783

(MHz)	(KHz)	(Hz)	(K)			(us)	(deg)	(s)
OBFRQ	OBSET	FREQU	POINT	SCANS	IRMOD	PW1	TILT	WAIT
12.09	57.1	5000	8	3000	4	23	90	0.8

****
* 17O Oxygen *
****

SAMPLE: H2O 5mm ¦ CDCl3 10mm
W1/2 30.0 Hz

CHEM SHIFT
H2O == (X 57.1460) 82.323864

RES. FREQ.
MHz 13.55650 13.5564 (fr. D2O) 13.557 (no ref. given)

+¦

(MHz)	(KHz)	(Hz)	(K)			(us)	(deg)	(s)
OBFRQ	OBSET	FREQU	POINT	SCANS	IRMOD	PW1	TILT	WAIT
84.27	28.0	200	8	1	0	10	(45)	10

```
********************
* 19F Fluorine     *
********************
```

SAMPLE: C6F6 5mm ¦ D20 10mm
W1/2 0.5 Hz

CHEM. SHIFT
CFC13 == (X 28.0180) 11.862675 162.9

RES. FREQ.
MHz 94.09368 ---------- 94.093795

(Do NOT 1H decouple.)

+¦

+¦

(MHz)	(KHz)	(Hz)	(K)			(us)	(deg)	(s)
OBFRQ	OBSET	FREQU	POINT	SCANS	IRMOD	PW1	TILT	WAIT
23.65	52.0	5000	8	1	0	30	45	1

```
********************
* 23Na Sodium      *
********************
```

SAMPLE: NaCl 1M H20 5mm ¦ D20 10mm
W1/2 6.1 Hz

CHEM. SHIFT
NaCl aq. 1m == (X 51.9926) 42.190545

RES. FREQ.
MHz 26.45192 26.4519 (26.451)
(NaBr 9.8M in D20) (Na+ inf. dil.)

+¦

(MHz) OBFRQ	(KHz) OBSET	(Hz) FREQU	(K) POINT	SCANS	IRMOD	(us) PW1	(deg) TILT	(s) WAIT
17.75	51.8	500	8	100	4	10	45	9

****
* 29Si Silicon *
****

SAMPLE: SiMe4 5mm ; D20 10mm
W1/2 0.7 Hz

CHEM. SHIFT
SiMe4 == (X 51.8001) 56.17410

RES. FREQ.
MHz 19.867182 (19.8671) 19.867184
(4.2M in C6D6)

(MHz) OBFRQ	(KHz) OBSET	(Hz) FREQU	(K) POINT	SCANS	IRMOD	(us) PW1	(deg) TILT	(s) WAIT
36.23	42.4	1000	8	10	4	10	45	9

****
* 31P Phosphorus *
****

SAMPLE: 85% H3PO4 H2O 2mm ; D2O 10mm
W1/2 34. Hz

CHEM. SHIFT
85% H3PO4 == (X 42.3987) 27.569171

RES. FREQ.
MHz 40.48076 40.4807 40.480720
(in D2O)

(MHz)	(KHz)	(Hz)	(K)			(us)	(deg)	(s)
OBFRQ	OBSET	FREQU	POINT	SCANS	IRMOD	PW1	TILT	WAIT
8.73	49.4	2000	4	24	0	30	45	1

****
* 35Cl Chlorine *
****

SAMPLE: NaCl 1M H2O 5mm ¦ D2O 10mm
W1/2 7.8 Hz

CHEM. SHIFT
NaCl 1M H2O == (X 49.3736) 113.90334

RES. FREQ.

MHz			
	9.79796	9.7979 (KCl 2.21M in D2O)	9.798 (Cl- inf. dil.)

(MHz)	(KHz)	(Hz)	(K)			(us)	(deg)	(s)
OBFRQ	OBSET	FREQU	POINT	SCANS	IRMOD	PW1	TILT	WAIT
7.25	57.9	5000	8	200	0	30	40	1

****
* 37Cl Chlorine *
****

SAMPLE: NaCl 1M H2O 5mm ¦ D2O 10mm
W1/2 7.3 Hz

CHEM SHIFT
1M NaCl H2O == (X 57.9023) 136.83817

RES. FREQ.

MHz			
	8.15577	8.1557 (2.21M KCl in D2O)	8.156 (Cl- inf. dil.)

(MHz) OBFRQ	(KHz) OBSET	(Hz) FREQU	(K) POINT	SCANS	IRMOD	(us) PW1	(deg) TILT	(s) WAIT
4.13	51.3	3000	4	20	0	80	60	1

****
* 39K Potassium *
****

SAMPLE: KBr sat.(6M) H2O 5mm ¦ D2O 10mm
W1/2 5. Hz

CHEM SHIFT
K+ inf. dil. (X - 51.2929) 239.16047 + 7.8

RES. FREQ.			
MHz	4.66637	4.6664 (KBr sat. in D2O)	4.666

(MHz) OBFRQ	(KHz) OBSET	(Hz) FREQU	(K) POINT	SCANS	IRMOD	(us) PW1	(deg) TILT	(s) WAIT
5.99	40.4	2000	8	200	0	50	45	2

****
* 43Ca Calcium *
****

SAMPLE: CaCl2 sat. H2O 10mm ¦ D2O 5mm
W1/2 4.9 Hz

CHEM SHIFT
Ca2+ inf. dil. == (X - 40.4177) 165.82599 + 50.

RES. FREQ.			
MHz	6.72974	6.7294 (CaCl2 sat. in D2O)	6.728 (?)

(MHz)	(KHz)	(Hz)	(K)			(us)	(deg)	(s)
OBFRQ	OBSET	FREQU	POINT	SCANS	IRMOD	PW1	TILT	WAIT
23.51	45.9	5000	4	1000	0	20	45	1

****
* 51V Vanadium *
****

SAMPLE: Na3VO4 pH 14 sat.H2O 5mm ¦ D2O 10mm
W1/2 25. Hz

CHEM SHIFT
VOCl3 == (X 45.8864) 42.452233 536.2

RES. FREQ.
MHz 26.30297 26.3029 (VOCl3 90% in C6D6) 26.29

(MHz)	(KHz)	(Hz)	(K)			(us)	(deg)	(s)
OBFRQ	OBSET	FREQU	POINT	SCANS	IRMOD	PW1	TILT	WAIT
22.13	82.2	1000	8	1	0	10	40	4

****
* 55Mn Manganese *
****

SAMPLE: KMnO4 sat.H2O 5mm ¦ D2O 10mm
W1/2 4.2 Hz

CHEM SHIFT
KMnO4 sat.H2O == (X - 82.2126) 45.020278

RES. FREQ.
MHz 24.78929 24.7450 (KMnO4 sat. in D2O) (?) 24.67

(MHz) OBFRQ	(KHz) OBSET	(Hz) FREQU	(K) POINT	SCANS	IRMOD	(us) PW1	(deg) TILT	(s) WAIT
21.21	50.4	1000	8	1	0	5	18	1

****
* 59Co Cobalt *
****

SAMPLE: K3Co(CN)6 sat.H2O 5mm ¦ D2O 10mm
W1/2 4.0 Hz

CHEM SHIFT
K3Co(CN)6 sat.aq. == (X + Y 21260.4394) 47.035716

RES. FREQ.			
MHz	23.72710	23.7271 (sat. in D2O)	(23.614) (Co(CN)6-3 ?)
Y = 21100 to 21600 KHz			

(MHz) OBFRQ	(KHz) OBSET	(Hz) FREQU	(K) POINT	SCANS	IRMOD	(us) PW1	(deg) TILT	(s) WAIT
3.09	35.8	1000	16	200	4	130	90	8

****
* 73Ge Germanium *
****

SAMPLE: GeCl4 5mm ¦ D2O 10mm
W1/2 2.1 Hz

CHEM SHIFT
GeMe4 (X -35.7682) 319.92135 + 30.9

RES. FREQ.			
MHz	3.488315	3.4883 (90% in C6D6)	3.488315

(MHz)	(KHz)	(Hz)	(K)			(us)	(deg)	(s)
OBFRQ	OBSET	FREQU	POINT	SCANS	IRMOD	PW1	TILT	WAIT
17.05	61.2	5000	8	20	1	20	40	2

****
* 77Se Selenium *
****

SAMPLE: H2SeO3 sat.H2O 5mm ¦ D2O 10mm
W1/2 9. Hz

CHEM SHIFT
Me2Se == (X - 61.156) 58.441405 + 1282.

RES. FREQ.			
MHz	19.0720	19.0715 (98% in C6D6)	(19.091523) (?)

(MHz)	(KHz)	(Hz)	(K)			(us)	(deg)	(s)
OBFRQ	OBSET	FREQU	POINT	SCANS	IRMOD	PW1	TILT	WAIT
3.83	53.2	10000	4	4700	0	100	90	0.2

****
* 87Sr Strontium *
****

SAMPLE: Sr(NO3)2 near sat.aq. 10mm ¦ D2O 5mm
W1/2 280. Hz

CHEM SHIFT
Sr2+ inf. dil. == (X 53.2023) 257.51941 - 45.

RES. FREQ.			
MHz	4.3339	4.3338 (fr. SrCl2 .5M in D2O)	4.334

(MHz) OBFRQ	(KHz) OBSET	(Hz) FREQU	(K) POINT	SCANS	IRMOD	(us) PW1	(deg) TILT	(s) WAIT
5.79	49.4	500	16	200	0	60	80	16

****
* 95Mo Molybdenum *
****

SAMPLE: Na2Mo04 sat.H20 5mm ; D20 10mm
W1/2 2.3 Hz

CHEM SHIFT
Na2Mo04 sat.aq. == (X 49.4368) 171.24939

RES. FREQ.

MHz	6.516934	6.5169 (2M in D20)	(6.515) (Mo04-2)

(MHz) OBFRQ	(KHz) OBSET	(Hz) FREQU	(K) POINT	SCANS	IRMOD	(us) PW1	(deg) TILT	(s) WAIT
5.91	52.0	6000	8	1000	0	55	70	1

****
* 97Mo Molybdenum *
****

SAMPLE: Na2Mo04 sat.H20 5mm ; D20 10mm
W1/2 65.0 Hz

CHEM. SHIFT
Na2Mo04 sat.aq. == (X 51.9835) 167.72941

RES. FREQ.

MHz	6.65370	6.6536 (2M in D20)	(6.652) (Mo04-2)

(MHz)	(KHz)	(Hz)	(K)			(us)	(deg)	(s)
OBFRQ	OBSET	FREQU	POINT	SCANS	IRMOD	PW1	TILT	WAIT
31.87	58.0	1000	8	16	4	16	90	6

```
*******************
* 117Sn Tin       *
*******************
```

SAMPLE: SnEt4 5mm ; D20 10mm
W1/2 0.5 Hz

CHEM. SHIFT
SnMe4 == (X - 58.0344) 31.320437 + 1.4

RES. FREQ.

MHz	35.63231	35.6322 (98% in C6D6)	35.632295

(MHz)	(KHz)	(Hz)	(K)			(us)	(deg)	(s)
OBFRQ	OBSET	FREQU	POINT	SCANS	IRMOD	PW1	TILT	WAIT
33.35	64.0	1000	8	16	4	10	60	6

```
*******************
* 119Sn Tin       *
*******************
```

SAMPLE: SnEt4 5mm ; D20 10mm
W1/2 0.7 Hz

CHEM. SHIFT
SnMe4 == (X - 64.0042) 29.927571 + 1.4

RES. FREQ.

MHz	37.29068	37.2906 (98% in C6D6)	37.290662

(MHz) OBFRQ	(KHz) OBSET	(Hz) FREQU	(K) POINT	SCANS	IRMOD	(us) PW1	(deg) TILT	(s) WAIT
3.69	43.3	2000	4	7000	0	70	60	1

****
* 183W Tungsten *
****

SAMPLE: Na2WO4.2H2O sat.H2O 10mm ¦ D2O 5mm
W1/2 1.5 Hz

CHEM. SHIFT
WF6 == (X - 43.2628) 267.8622 + 1121.

RES. FREQ.

MHz	4.16173	4.1616 (fr. 1M Na2WO4 D2O)	4.161733

(MHz) OBFRQ	(KHz) OBSET	(Hz) FREQU	(K) POINT	SCANS	IRMOD	(us) PW1	(deg) TILT	(s) WAIT
19.21	52.2	1000	4	200	0	20	60	3

****
* 195Pt Platinum *
****

SAMPLE: Na2PtCl6 sat.H2O 5mm ¦ D2O 10mm
W1/2 15.0 Hz

CHEM. SHIFT
Na2PtCl6 sat.aq. == (X + Y 19262.1582) 51.915262

RES. FREQ.

MHz	21.49697	21.49689 (fr. Na2PtCl6 1.2M D2O)	21.496770 (PtCl6-2 in HCl)
Y = 19130 to 19390 KHz			

+¦

(MHz)	(KHz)	(Hz)	(K)			(us)	(deg)	(s)
OBFRQ	OBSET	FREQU	POINT	SCANS	IRMOD	PW1	TILT	WAIT
15.97	86.5	1000	4	650	4	10	30	4

```
********************
* 199Hg Mercury    *
********************
```

SAMPLE: Hg(SiMe3)2 C6H6 5mm ¦ D20 10mm
W1/2   1.5 Hz

CHEM SHIFT
HgMe2   ==   (X   86.4726) 62.280179 + 481.

RES. FREQ.
MHz   17.9107   17.9107   17.910841
(90% in C6D6)
(Artifact at 16.004MHz)

+¦

+¦

(MHz)	(KHz)	(Hz)	(K)			(us)	(deg)	(s)
OBFRQ	OBSET	FREQU	POINT	SCANS	IRMOD	PW1	TILT	WAIT
18.63	60.2	2000	4	100	0	10	30	1

```
********************
* 207Pb Lead       *
********************
```

SAMPLE: Pb(NO3)2 sat H2O 5mm ¦ D20 10mm
W1/2   3.5 Hz

CHEM. SHIFT
PbMe4   ==   (X + Y - 18690.2058) 53.50396 - 2961.2

RES. FREQ.
MHZ   20.92061   (20.9200)   20.920597
(fr. Pb(NO3)2 sat.in D20)
Y = 18570 to 18810 KHz

+¦

APPENDIX 2 CALCULATION OF PT PARAMETERS

Listings of computer programs used to calculate the PT parameters for the sequence INEPT (and UPT) are presented. Explanations of these programs are given in section 2.2.1.

FUNC

```
100   rem Programmed by P J.Watkinson 1982
200   print"FUNC calculates the theoretical output of the enhancement"
300   print"gained by a 5-pulse INEPT sequence,as a function of the"
400   print"timing parameter,A  "
500   print
2400  print"What is the nuclear spin,I =>";
2500  input A
2600  print"Timing,T,coupling const.,J, are related to the parameter ,A, by.."
2700  print"            A = 4*PI*J*T"
2800  print"                  "
2900  print"What is the smallest value for A ==>";
3000  input BD
3050  B=BD*3.141592654/180.0
3100  print"What is the largest value for A ==>";
3200  input BD10
3250  B10=BD10*3.141592654/180.0
3300  print"Now,what is the increment ==>";
3400  input BD2
3450  B2=BD2*3.141592654/180.0
3500  if B2>0 then 4300
3600  print"Put in some positive number     "
3700  go to 3300
4300  print"TIMING.  A      ENHANC.  OF SPIN =";A
4400  C=0
4500  C1=0
4600  A1=A
4700  A2=A1*B
4800  A3=A1*SIN(A2)
4900  C=A3+C
5100  A1=A1-1
5200  IF A1<0 THEN 5600
5300  GO TO 4700
5600  BA=B*180.0/3.141592654
5650  print  BA,
5700  B=B+B2
5800  if B>B10 then 6000
5900  go to 4400
6000  print"Do you want to try new input data (Y or N) =>";
6100  input Z$
6200  if Z$ = "Y" then 2400
6300  if Z$ = "N" then 8999
8999  end
```

PARITY

```
10    rem Programmed by P>J>Watkinson 1982
20    print"PARITY calculates the theoretical output of proton decoupled"
30    print"enhancement gained by a 7-pulse INEPT sequence,as a function"
40    print"of the timing parameter ,B . Assume time T is optimum."
50    print
60    print"See INTIME or TIM to see this sequence."
70    print
80    print"*************************************************************"
90    print
100   print"Decoupled enhancement,Ed, is a function of the number of attached"
110   print"protons,n, and the timing parameter, B  "
120   print
130   print"Timing ,D, and coupling constant,J, are related to B  by. . . . . "
140   print"                        B = D * 180 * J                (B in degrees)"
150   print"                    "
160   print" Ed(n,B) = k * n * sin(B) * cos(B) **(n-1)"
180   print
190   print"We set k=1 for a general nucleus, otherwise,for a specific nucleus"
200   print
210   print" k = <E(opt)> * g(H) /   g(I) * 2 ) "
220   print
230   print"Do you want output for a General or a Specific nucleus (G or S)=>";
240   input A$
250   IF A$ = "S" THEN 290
260   IF A$ = "G" THEN 270
270   AK=1
275   AI=0 \ AG=1
280   GO TO 462
290   print"What is the nuclear spin, I =>";
300   input AI
310   C=AI*2
315   E=2
320   IF C=1 THEN E=2
330   IF C=2 THEN E=1.
340   IF C=3 THEN E=.702728
350   IF C=4 THEN E=.547163
360   IF C=5 THEN E=.449614
370   IF C=6 THEN E=.382217
380   IF C=7 THEN E=.332680
390   IF C=8 THEN E=.294659
400   IF C=9 THEN E=.264520
410   IF C=10 THEN E=.240023
420   IF C=12 THEN E=.202595
430   IF C=14 THEN E=.175297
440   print"What is the magnet. ratio,g(I) of this nucleus(10-7radT-1s-1)=>";
450   input AG
460   AK=E*26.751/(2.*AG)
462   print"Finally,what is the value of n =>";
463   input AN
470   print"What is the smallest value for B =>";
480   input BD
485   B=BD*3.141592654/180.
490   print"What is the largest value of B =>";
500   input BD10
510   print"Now,what's the increment =>";
520   input BD2
530   IF BD2>0 THEN 560
540   print"You must input some positive number."
550   go to 510
560   print"VALUE OF    DECOUP   I=",AI;"     VALUE OF    D=1/"
570   print"   B        ENH     g(I)=";AG;"          c        /cJ"
580   IF AN=1 THEN 610
590   A=AK*AN*SIN(B)*(COS(B)**(AN-1))
600   GO TO 615
610   A=AK*AN*SIN(B)
615   IF BD=0 THEN 630
620   BJ=180./BD
630   print   BD,              A,                    BJ
640   BD=BD+BD2
650   IF BD>BD10 THEN 680
660   B=BD*3.141592654/180.
670   GO TO 580
680   print"Do you want new input data (Y or N)=>";
690   input Z$
700   if Z$ = "Y" then 230
710   if Z$ = "N" then 999
999   end
```

INTIME

```
100   rem Programmed by P. J. Watkinson, 1982
200   print"INTIME calculates the enhancement of a multiplet I, of nuclear spin I"
210   print"using a proton coupled or decoupled 5-pulse INEPT sequence."
212   print
300   print"Do you want to see the INEPT sequence referred to? (Y or N)=>";
310   input z$
320   if z$ = "Y" then go to 340
330   if z$ = "N" then go to 500
340   print \ print
350   print"(90xH)-T-(180xH)(180xI)-T-(90yH)(90xI)-D-ACQUIRE"
360   PRINT \ PRINT
370   print"ACQUISITION is with or without decoupling."
380   print"90 and 180 are tilt angles about a given axis"
390   print"for either a proton, H or an arbitrary nucleus, I."
400   print"T and D are timing parameters."
500   print
510   print"FURTHER NOMENCLATURE"
520   print"m(I)...nuclear spin q. no. for multiplet I"
530   print"M(H)...nuclear spin q. no. for proton "
540   print"J .....observable spin coupling constant "
550   print"g(I)...magnetogyric ratio for nucleus I "
560   print"n .....number of protons creating J "
570   print"E(opt).....Optimum enhancement , proton coupled INEPT"
580   print"Ed(opt).....Optimum enhance., proton decoupled INEPT"
590   print"<E(opt)>...E(opt) with M(H)=g(H)=g(I)=1"
600   print"<Ed(opt)>..Ed(opt) with g(H)=g(I)=1"
610   print
620   print"(A)"
630   print"<E(opt)> = SUM m(I)*sin[4*PI*m(I)*J*T(opt)] / SUM m(I)**2"
640   print"             m(I)                                m(I)"
650   print"(B)"
660   print"E(opt) = M(H)*g(H)/g(I)*<E(opt)>"
670   print
680   print"(C)"
690   print"Dd(opt) = arcsin[n**-.5] / PI*J"
700   print
710   print"(D)"
720   print"<Ed(opt)> = 0.5*(n)**0.5*(1-1/n)**[(n-1)/2]*<E(opt)>"
730   print
740   print"(E)"
750   print"Ed(opt) = g(H)/g(I)*<Ed(opt)>"
760   print
761   print"*************************************************"
762   print"****** TO EXIT...TYPE  F ************************"
765   print"To obtain a library of output for A, C, or D.....TYPE L"
770   print"To start one of the calculations...TYPE  A, B, C, D, or E";
780   input A$
790   if A$="A" then 1000
800   if A$="B" then 4000
810   if A$="C" then 5000
820   if A$="D" then 6000
830   if A$="E" then 7000
840   if A$="F" then 9999
850   if A$="L" then 8000
860   go to 610
1000  print \ print
1010  print"Calculation of <E(opt)> for any spin I,"
1020  print"by numerically finding T(opt)."
1030  print
1400  print"What is the nuclear spin , I ==>";
1500  input A
1600  print"Timing, T and coupling constant, J are related by...."
1700  print"           T = 1 /"
1800  print"                 / bJ"
1900  print"What is the smallest value for   b ==>";
2000  input B
2100  print"What is the largest value for   b ==>";
2200  input B10
2300  print"Now, what is the increment ==>";
2400  input B2
2500  if B2>0 then 2800
```

```
2600  print"You must put in some positive no.(Even if 1 b value is wanted)"
2700  go to 2300
2800  print"VALUE OF b        <E(opt)> FOR l=";A;"MULTIPLET"
2850  C=0
2870  C1=0
2900  A1=-A
3000  A2=3.1415926536*4.0*A1/B
3100  A3=A1*SIN(A2)
3200  C=A3+C
3250  C1=C1+A1*A1
3300  A1=A1+1
3400  if A1>A then 3550
3500  go to 3000
3550  C=C/C1
3600  print B,                C
3700  B=B+B2
3800  if B>B10 then 3910
3900  go to 2850
3910  print"Do you want to try new input data? (Y or N)==>";
3920  input z$
3930  if z$ = "Y" then 1400
3940  if z$ = "N" then 3950
3950  print"Do you want to input a J value(Y or N)=>";
3960  input A$
3970  if A$ = "Y" then 3990
3980  if A$ = "N" then 610
3990  print"What is b(opt) =>";
3991  input A5
3992  print"Now,what is J ,in Hz =>";
3993  input A6
3994  A7=1000.0/(A5*A6)
3995  print"For b(opt)=";A5;",  J=";A6;"Hz,  T(opt)=";A7;"ms"
3996  go to 3950
4000  print\print
4010  print"Calculation of the coupled enhancement of a specific nucleus"
4020  print"with a component M(H) , namely  E(opt)"
4025  print
4030  print"What is <E(opt)> =>";
4035  input E1
4040  print"What is g(I),in units 10-7 rad.s-1.T-1 =>";
4050  input G1
4060  print"Finally,what is M(H) =>";
4070  input G10
4080  E2=E1*G10/G1*26.7510
4085  print
4090  print"E(opt) = ";E2
4095  print
4100  print"Do you want more input data(Y or N)=>";
4110  input B$
4120  if B$= "Y" then 4030
4130  if B$= "N" then 610
5000  print\print
5005  print"Calculation of the optimum timing, D(opt) for a decoupled "
5010  print"spectrum of a compound with  n  protons creating J."
5015  print
5020  print"What is  n  =>";
5030  input D
5031  D1=1.0/(D**0.5)
5032  D2=1.0-D1*D1
5033  D3=(1.0-D2**0.5)/D1
5034  D4=2.0 * ATN(D3)
5050  DA=3.1415926536/D4
5060  print"The optimum timing,  D(opt) for";D;"attached protons is.."
5070  print"                        1 /  "
5080  print"                         /";DA;"J"
5090  print"Do you want to input a J value(Y or N)=>";
5100  input B$
5110  if B$= "Y" then 5130
5120  if B$= "N" then 5200
5130  print"J ,in Hz =>";
5140  input DC
5150  DD=1000.0/(DA*DC)
5160  print"For n=";D;",  J=";DC;"Hz,  D(opt) = ";DD;"ms"
5170  go to 5090
5200  print"Do you want more calcs.  of D(opt) (Y or N)=>";
5210  input B$
5220  if B$= "Y" then 5020
5230  if B$= "N" then 610
```

```
6000  print\print"Calculation of <Ed(opt)> for any spin 1,"
6010  print"given <E(opt)> and  n, the no. protons."
6020  print
6030  print"What is <E(opt)> =>";
6040  input E1
6050  print"What is n =>";
6060  input D
6070  E3=E1*0.5*(D**0.5)*((1.0-1.0/D)**((D-1.0)/2.0))
6075  print
6080  print"<Ed(opt)> = ";E3
6085  print
6090  print"Do you want more input data (Y or N)=>";
6100  input B$
6110  if B$= "Y" then 6030
6120  if B$= "N" then 610
7000  print\print
7010  print"Calculation of the decoupled enhancement of a specific nucleus"
7020  print"namely  Ed(opt) ."
7025  print
7030  print"What is <Ed(opt)  =>";
7040  input E3
7050  print"Finally,what is g(I),in units 10-7 rad.s-1.T-1 =>";
7060  input G1
7070  E4=E3/G1*26.7510
7075  print
7080  print"Ed(opt) = ";E4
7085  print
7090  print"Do you want more input data (Y or N) =>";
7100  input B$
7110  if B$ ="Y" then 7030
7120  if B$ ="N" then 610
8000  print
8005  print"Do you want coupled or decoupled data (CD or DD)=>";
8010  input C$
8020  if C$ ="CD" then 8040
8030  if C$ ="DD" then 8200
8040  print"1      ! T(opt)     <E(opt)>"
8041  print"-------!-------------------"
8050  print"0.5    ! 4          2"
8060  print"1      ! 8          1"
8070  print"1.5    ! 11.32      0.702728"
8080  print"2      ! 14.50      0.547163"
8090  print"2.5    ! 17.62      0.449614"
8100  print"3      ! 20.71      0.382217"
8110  print"3.5    ! 23.78      0.332680"
8120  print"4      ! 26.85      0.294659"
8130  print"4.5    ! 29.90      0.264520"
8140  print"5      ! 32.94      0.240023"
8141  print"6      ! 39.02      0.202585"
8142  print"7      ! 45.09      0.175297"
8145  print
8150  print"Do you want to see decoupled data (Y or N)=>";
8160  input C$
8170  if C$ = "Y" then 8200
8180  if C$ = "N" then 610
8200  print\print
8210  print"n      ! 1       2       3       4       5       6       9       12"
8211  print"-------!-----------------------------------------------------------"
8220  print"D(opt)! 2.0000 4.0000 5.1043 6.0000 6.7758 7.4705 9.2444 10.7279"
8230  print"       !"
8240  print"1      !                 <Ed(opt)>"
8242  print"-------!-----------------------------------------------------------"
8250  print"0.5    ! 1.000   1.000   1.15    1.30    1.43    1.55    1.87    2.15"
8260  print"1      ! 0.50    0.50    0.58    0.65    0.72    0.78    0.94    1.07"
8270  print"1.5    ! 0.35    0.35    0.40    0.45    0.50    0.54    0.66    0.75"
8280  print"2      ! 0.27    0.27    0.32    0.36    0.39    0.42    0.51    0.59"
8290  print"2.5    ! 0.22    0.22    0.26    0.29    0.32    0.35    0.42    0.48"
8300  print"3      ! 0.19    0.19    0.22    0.25    0.27    0.30    0.36    0.41"
8310  print"3.5    ! 0.17    0.17    0.19    0.22    0.24    0.26    0.31    0.36"
8340  print"4      ! 0.15    0.15    0.17    0.19    0.21    0.23    0.28    0.32"
8350  print"4.5    ! 0.13    0.13    0.15    0.17    0.19    0.21    0.25    0.28"
8360  print"5      ! 0.12    0.12    0.14    0.16    0.17    0.19    0.22    0.26"
8365  print
8370  print"Do you wish to see coupled data (Y or N)=>";
8380  input C$
8390  if B$ = "Y" then 8040
8400  if B$ = "N" then 610
8410  go to 610
9999  end
```

APPENDIX 3

INSTRUMENTAL PARAMTERS FOR GERMANIUM-73 NMR

Illustrations of the instrumental parameters used for germanium-73 NMR on the JEOL FX90Q are presented. Compounds with long (GeH_4) and short ($GeEt_3H$) relaxation times are used in these examples, with a single pulse reverse gated decoupled sequence (NNE) and decoupled INEPT. See TABLE A for the parameter symbols.

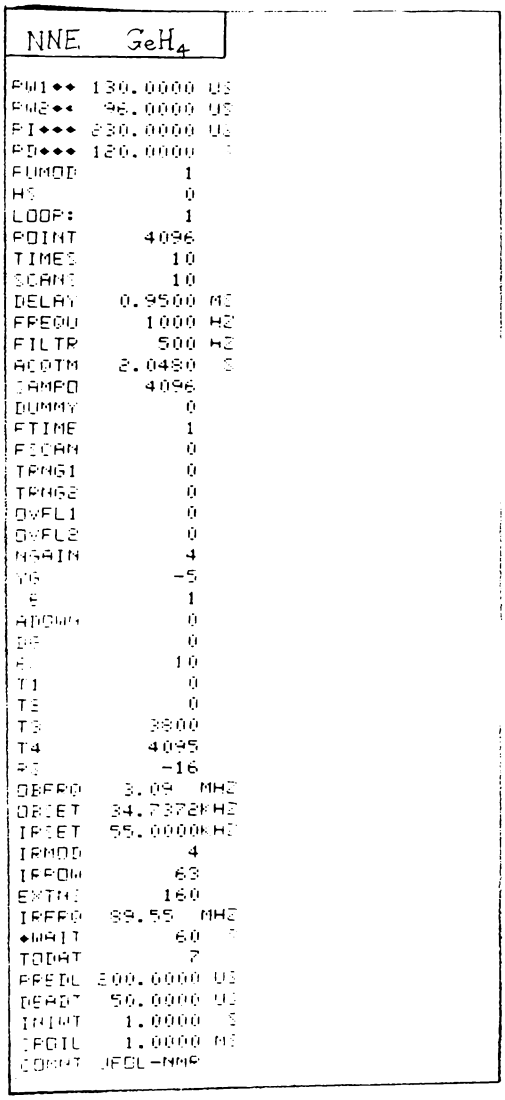

NNE GeH_4

PW1**	130.0000	US
PW2**	96.0000	US
PI***	230.0000	US
PD***	120.0000	S
PUMOD	1	
HS	0	
LOOP:	1	
POINT	4096	
TIMES	10	
SCANS	10	
DELAY	0.9500	MS
FREQU	1000	HZ
FILTR	500	HZ
ACQTM	2.0480	S
SAMPO	4096	
DUMMY	0	
FTIME	1	
FSCAN	0	
TRNG1	0	
TRNG2	0	
OVFL1	0	
OVFL2	0	
NGAIN	4	
YG	-5	
XE	1	
ADDWN	0	
DG	0	
EX	10	
T1	0	
T2	0	
T3	3800	
T4	4095	
RS	-16	
OBFRQ	3.09	MHZ
OBSET	34.7372	KHZ
IRSET	55.0000	KHZ
IRMOD	4	
IRPOW	63	
EXTNS	160	
IRFRQ	89.55	MHZ
*WAIT	60	S
TODAT	7	
PREDL	300.0000	US
DEADT	50.0000	US
INIWT	1.0000	S
SPOIL	1.0000	MS
COMNT	JEOL-NMR	

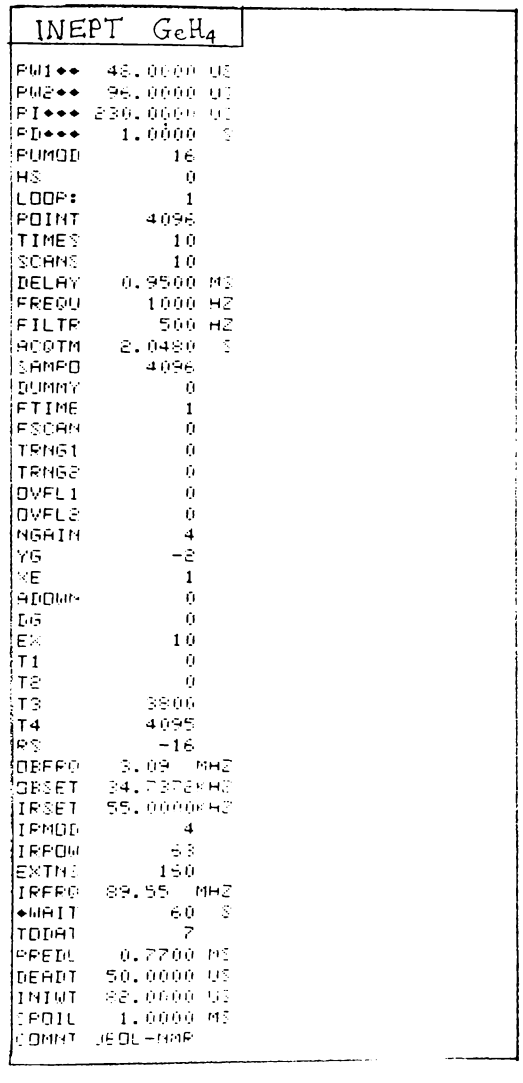

INEPT GeH_4

PW1**	48.0000	US
PW2**	96.0000	US
PI***	230.0000	US
PD***	1.0000	S
PUMOD	16	
HS	0	
LOOP:	1	
POINT	4096	
TIMES	10	
SCANS	10	
DELAY	0.9500	MS
FREQU	1000	HZ
FILTR	500	HZ
ACQTM	2.0480	S
SAMPO	4096	
DUMMY	0	
FTIME	1	
FSCAN	0	
TRNG1	0	
TRNG2	0	
OVFL1	0	
OVFL2	0	
NGAIN	4	
YG	-2	
XE	1	
ADDWN	0	
DG	0	
EX	10	
T1	0	
T2	0	
T3	3800	
T4	4095	
RS	-16	
OBFRQ	3.09	MHZ
OBSET	34.7372	KHZ
IRSET	55.0000	KHZ
IRMOD	4	
IRPOW	63	
EXTNS	160	
IRFRQ	89.55	MHZ
*WAIT	60	S
TODAT	7	
PREDL	0.7700	MS
DEADT	50.0000	US
INIWT	82.0000	US
SPOIL	1.0000	MS
COMNT	JEOL-NMR	

NNE $GeEt_3H$ ·

PW1◆◆	130.0000	US
PW2◆◆	48.0000	US
PI◆◆◆	265.0000	US
PD◆◆◆	59.6000	S
PUMOD	1	
HS	0	
LOOP:	1	
POINT	2048	
TIMES	50	
SCANS	50	
DELAY	400.0000	US
FREQU	3000	HZ
FILTR	1500	HZ
ACQTM	341.2000	MS
SAMPD	2048	
DUMMY	0	
FTIME	500	
FSCAN	0	
TRNS1	0	
TRNS2	0	
OVFL1	2100	
OVFL2	3400	
NGAIN	5	
YG	-4	
XE	1	
ADOWN	3	
DG	0	
EX	12	
T1	0	
T2	0	
T3	3800	
T4	4095	
PG	16	
OBFRQ	3.09	MHZ
OBSET	35.6200	KHZ
IRSET	54.2000	KHZ
IRMOD	4	
IRPOW	63	
EXTNC	160	
IRFRQ	89.55	MHZ
◆WAIT	50	S
TODAT	1	
PREDL	20.000	MS
DEADT	50.0000	US
INIMT	1.0000	S
IPOIL	1.0000	MS
COMNT	JEOL	

INEPT $GeEt_3H$

PW1◆◆	48.0000	US
PW2◆◆	96.0000	US
PI◆◆◆	265.0000	US
PD◆◆◆	59.6000	S
PUMOD	16	
HS	0	
LOOP:	1	
POINT	2048	
TIMES	50	
SCANS	50	
DELAY	400.0000	US
FREQU	3000	HZ
FILTR	1500	HZ
ACQTM	341.2000	MS
SAMPD	2048	
DUMMY	0	
FTIME	500	
FSCAN	0	
TRNS1	0	
TRNS2	0	
OVFL1	2100	
OVFL2	3400	
NGAIN	5	
YG	-3	
XE	1	
ADOWN	0	
DG	0	
EX	12	
T1	0	
T2	0	
T3	3800	
T4	4095	
PG	16	
OBFRQ	3.09	MHZ
OBSET	35.6200	KHZ
IRSET	54.2000	KHZ
IRMOD	4	
IRPOW	63	
EXTNC	160	
IRFRQ	89.55	MHZ
◆WAIT	50	S
TODAT	1	
PREDL	20.000	MS
DEADT	50.0000	US
INIMT	82.0000	US
IPOIL	1.0000	MS
COMNT	JEOL	

APPENDIX 4

POLARIZATION TRANSFER PULSE SEQUENCES

An introductory explanation of the PG200 pulse generator is followed by listings of some of the INEPT, DEPT, and UPT sequences for ^{73}Ge NMR, in machine language. (See PG200 manual for full explanations.)

The PG200 has 64 addresses, a 13 bit output register, 40 time parameters (TIM), 10 loop parameters (LO), (LOOP), 2 loop loading parameters (LD), 2 conditional jump commands (JC), unconditional jump commands (JMP) and up to 16 phase cycles. PUL is the sampling trigger and INT, the interval during acquisition.

Machine language printouts have parameter names and parameter addresses on the far right, output registers, and address numbers. Codes for TIM n include (n, brackets); PW1 (1), PW2 (2), PI (3), PD (4), DELAY (6), PREDL (7), DEADT (8), INIWT (9). Accumulation phases are (deg.): 0, 90, 270, 180, 180, 270, 90, 0. Output registers (* on, • off) (bit 1, far right) have the following contents for the PT sequences:

Bit Nos.	Contents
1	Observation gate
2	Observation phase: 0° (Off) or 180° (On)
3	Observation phase: 0° (Off) or 90° (On)
4	Phase reset
5	Receiver gate
6 (6)	[illegible]
7	AD trigger
8	Irradiation gate
A (9)	[illegible]
B (10)	[illegible]
C (11)	Ext. III
K (12)	[illegible]
13	Sampling trigger

INEPT

e

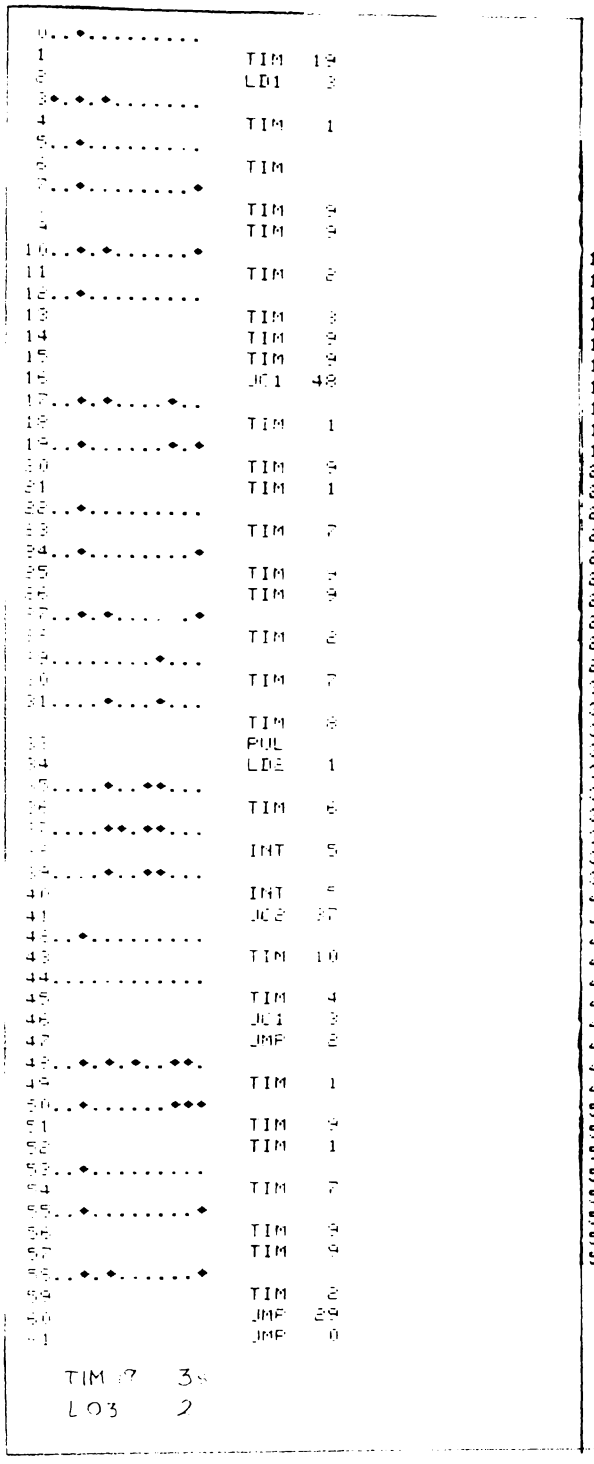

INEPT

b

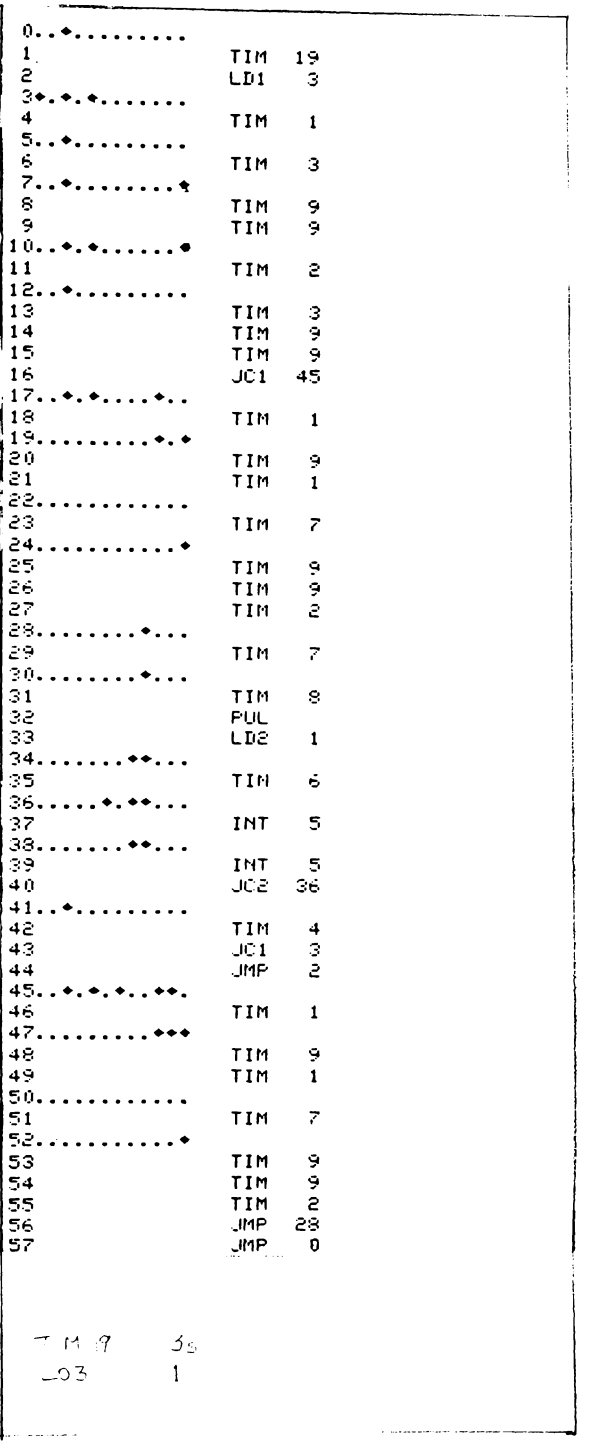

UPT

(b), FIG. 3-17

```
0..•.........
1                TIM  19
2                LD1   3
3..•.•.......
4                TIM   1
5..•.........
6                TIM   3
7                TIM   8
8                JC1  36
9..•.•.......
10               TIM   1
11               TIM   1
12..•.........•
13               TIM   7
14..•.........
15               TIM   3
16•.•.........•
17               TIM   9
18•.•.•.......•
19               TIM   2
20.........•...
21               TIM   3
22               TIM  11
23               PUL
24               LD2   1
25....•..••...
26               TIM   6
27....••.••...
28               INT   5
29....•..••...
30               INT   5
31               JC2  27
32............
33               TIM   4
34               JC1   3
35               JMP   2
36..•.•.•.....
37               TIM   1
38               TIM   1
39..•.........•
40               TIM   7
41..•.......•..
42               TIM   3
43•.•...•..•.•
44               TIM   9
45•.•.•.•..•.•
46               TIM   2
47               JMP  20
48............
49               JMP   0
```

TIM 11 = 9μs
TIM 19 = 3s
LO3 = 1

DEPT

(3). FIG. 3-17)

```
0..•.........
1                TIM  19
2                LD1   3
3•.•.•.......
4                TIM   1
5..•.........
6                TIM   3
7                TIM   8
8..•.........•
9                TIM   9
10..•.•......•
11               TIM   2
12..•.........
13               TIM   3
14               TIM   9
15               JC1  40
16..•.........•
17               TIM   8
18..•.•......•
19               TIM   7
20.........•...
21               TIM   3
22               TIM   9
23               TIM   8
24               TIM   1
25....•...•...
26               TIM  20
27               PUL
28               LD2   1
29....•..••...
30               TIM   6
31....••.••...
32               INT   5
33....•..••...
34               INT   5
35               JC2  31
36..•.........
                 TIM   4
                 JC1   3
34               JMP   2
40..•.......•.
41..•...•...••
42               TIM   8
43..•.•.•...••
44               TIM   7
45               JMP  20
46               JMP   0
```

TIM 19 = 3s
LO3 = 1

APPENDIX 5

MULTINUCLEAR NMR PARAMETERS OF TRANSITION METAL CARBONYLS

Multinuclear NMR parameters are presented for iron germanium carbonyls[132] (TABLES 1, 2), manganese-germanium carbonyls[203] (TABLE 3), and cobalt-germanium carbonyls[142] (TABLE 4). All chemical shifts are reported in ppm, using the conventions in appendix 1. Errors are typically ±0.2 ppm except for proton NMR, (H), ±0.01 ppm, δ values in brackets mean signals are low in S/N, and ? means an unassigned peak or tentative assignment. See section 4.3 for further conventions.

COMMENTS, TABLE 1

All the compounds in TABLE 1 exist as cis-isomers.[132] Proton NMR shows the expected chemical shifts and second order effects.[132]

Carbon-13 NMR is a sensitive structural assignment tool for these compounds. The cis and trans (to Ge ligand) CO assignments were made using reference,[132] and where there were two different Ge ligands these assignments were consistent with ^{13}C intensity ratios.

Oxygen-17 NMR gives a slightly larger spectral dispersion than ^{13}C NMR for these compounds (eg. sample (6) at RT: ^{17}O 2 signals, ^{13}C 1 signal) but requires a larger number of scans for a given N_d. The deviation of the ^{17}O δ value for sample (5) from the others may be due to a solvent effect.

As the ligands become more electronegative (H → Me) the ^{13}C δ (ppm) values increase as expected, but the reverse order is seen for ^{17}O, in line with metal backbonding to the carbonyls.[204]

COMMENTS, TABLE 2

Assignments for proton NMR are consistent with reference[132] and except for the presence of (D) in system (4) all the expected[132] major products were seen. In each system, ^{13}C and ^{73}Ge NMR are useful tools in signal identification.

For system (1), (A) is the major carbonyl product and for system (2), (C) is the major carbonyl product.

In system (3), most of the reaction occurred after 17 hours at RT, however, after 2 years at RT, both ^{13}C, ^{1}H and, ^{73}Ge NMR intensities show that the reaction had proceeded still further. After 2 years at RT there is no detectable $Fe(CO)_4(GeH_3)_2$, a reactant.

For system (4), the ^{1}H signal 0.96 (d, 3.5)* is probably due to (D) or (E); similarly for 0.95 (d, 3.5)*. An alternative assignment of these two signals to the two isomers of (E) is less likely, since both ^{13}C and ^{17}O CO signals are probably too well dispersed for isomers. Moreover, (E) is known to form (D) on weak illumination.[205]

COMMENTS, TABLE 3

Manganese-55 δ values of $Mn_2(CO)_{10}$ are close to literature values (-2325, in THF).[206] The higher (axial) symmetry of $Mn_2(CO)_{10}$ yields much smaller linewidths (30 Hz) than other, less symmetric carbonyls (3000 Hz), in line with the literature.[206]

Since the group electronegativity of $GeMe_3$ is greater than the electronegativity of H, to a first approximation one expects $\delta(^{55}Mn)$ $GeMe_3Mn(CO)_5$, (-2538) to be larger than for $HMn(CO)_5$, (-2630).[206] This expectation is obeyed.

The high receptivity and small T_1 of ^{55}Mn make it quicker to obtain a ^{55}Mn spectrum of a carbonyl than a ^{13}C carbonyl spectrum.

COMMENTS, TABLE 4

Although ^{59}Co has large linewidths for neutral carbonyls, the very large spectral dispersion allows $Me_2GeCo_2(CO)_7$, (called (B)), to be distinguished from $Me_2Ge[Co(CO)_4]_2$, (called (C)) having a 600 ppm difference in δ values. For mixtures of these two compounds, the broadest ^{59}Co signal always contained the largest peak area, and this was assigned to (B), which was the major product of the synthesis.[142] Furthermore, since (B) can exchange carbonyls and has a Co-Co bond, while (C) cannot exchange carbonyls, and lacks a Co-Co bond, one expects larger linewidths for (B).

The compounds (C) ($\delta(^{59}Co)$-3470) and $Ph_3GeCo(CO)_4$ (-3050)[207] have Co in a somewhat similar environment and δ values are relatively close for ^{59}Co NMR, as expected. On the other hand, replacement of a bridging CO in $Co_2(CO)_8$ ($\delta(^{59}Co)$ - 1860, $W_{\frac{1}{2}}$ 27100) by a bridging $GeMe_2$ to give (B) (-2860, 5590) gives a large shift to low frequency and a large reduction in linewidth. Further replacement of the bridging CO in (B) gives (A) (-3464, 2900) with a further shift to low frequency and a reduction in $W_{\frac{1}{2}}$.

Cobalt-59 NMR on carbonyls enjoys the same advantages over ^{13}C NMR as mentioned for ^{55}Mn NMR.

COMPOUND	SAMPLE	δ(C)	δ(O) ($W_{1/2}$)	OTHERS
$Fe(CO)_4(GeH_3)_2$	(1) neat	207.3 c	366.1 (15)	
	trace C_6H_{14}	205.9 t	360.9 (12)	
$Fe(CO)_4(GeH_3)(GeMeH_2)$		208.0 c		
		206.7 t		
	(2) neat	206.1 t		
	(1g sample)	-0.9		
	(3) neat	208.0 c	365.5 c (30)	H 4.15(q,3.4)
	(0.6g sample)	207.1 t	361.3 t (10)	3.81
		206.8 t	359.5 t (15)	1.02(t,3.4)
		-1.8		
$Fe(CO)_4(GeH_3)(GeMe_2H)$		208.2 c	365.7	H 4.57(h,3.4)
		207.2 t	363.5 (14)	3.97
	(4) neat	206.0 t	357.9 (12)	1.13(d,3.4)
		2.8		
$Fe(CO)_4(GeMeH_2)(GeMe_2H)$	(B)	208.5 c	466 (7)	H 4.8
	(A)	208.2 c	458 (5)	3.68(q,?)
	(5) C_6H_6 (B)	207.2 t		0.99(t,3.5)
	(A)	206.4 t		0.46(t,3.4)
		2.5		0.02(t,3.9)
		2.3		
$Fe(CO)_4(GeMe_3)_2$	(6) C_6H_{14}	208.2	355.9 (9)	
		7.5	355.5 (9)	
		and		
		208.9		
		208.0 (-20 °C)		
		7.5		
	(7) C_6H_6	208.2 (10 °C)		H 0.52
		7.5		

TABLE 1 NMR parameters for **iron-germanium carbonyls.** c=cis,t=trans,(to Ge ligand) (A)= $Fe(CO)_4(GeMeH_2)_2$ (B)= $Fe(CO)_4(GeMe_2H)_2$. Sample (5) may be a mixture of (A) and (B) .

STARTING MATERIALS	CONDITIONS	δ(C)	δ(H)	OTHERS
$Fe(CO)_4(GeH_3)(GeMeH_2)$ C_6H_6 SYSTEM (1)	2 years RT	5.7 (A) -11.6 $GeMeH_3$	3.70 3.34 0.90(d,2.9) (A) 3.34(q,4.2) -0.06(q,4.2) $GeMeH_3$ 3.23(d,1.8) 0.91(t,4.1) $(GeMeH_2)_2$?	Ge -206.9 $GeMeH_3$ Ge -296.8 GeH_4 Ge -214.8 $(GeMeH_2)_2$? H 2.94 GeH_4 H 3.14 (B)
$Fe(CO)_4(GeH_3)(GeMe_2H)$ SYSTEM (2)	several days RT	207.5 (C) ? 11.1 ? -6.2 $GeMe_2H_2$	4.16(h,3.9) 0.70(t,3.9) $GeMe_2H_2$ 3.97 $Fe(CO)_4(GeH_3)_2$ 3.85 (C)	Ge -125.3 $GeMe_2H_2$ H 3.50 0.74 ? H 3.79 (B)
$Fe(CO)_4(GeH_3)_2$ plus $Fe(CO)_4(GeMe_3)_2$ in C_6H_{14} SYSTEM (3)	1 hour RT	(starting materials only)		
	17 hours RT	209.1 204.6 (B)	4.18 0.48 $GeMe_3H$	
		6.2,4.7 4.0 ?	3.66 (B)	
		-3.1 $GeMe_3H$	3.43 GeH_4 ?	
	2 years RT	208.5 204.7 (B)	4.23(o,3.4) 0.50(d,2.9) $GeMe_3H$	Ge -57 $GeMe_3H$
		-2.8 ?	3.66 (B)	
		-3.2 $GeMe_3H$	2.60 ?	
$Fe(CO)_4(GeMe_3)(GeMeH_2)$ in C_6H_6 SYSTEM (4)	several days RT in light	209.3 (D) 205.0 5.7 (E) ? -3.3 $GeMe_3H$	4.56 0.96(d,3.5)* (D) 3.92(h,3.4) 0.04(d,3.4) $GeMe_3H$ 4.56 0.95(d,3.5)* (E)	O 361.3 (E) O 359.1 (D) H 1.13,0.27 ? H -3.1 Fe hydride Ge -56.5 $GeMe_3H$

TABLE 2 **Decomposition products of iron-germanium carbonyls.**

(A)=$[Fe(CO)_4(GeH_3)]_2GeMeH$ (B)=$[Fe(CO)_4(GeH_2)_2]_2$
(C)=$[Fe(CO)_4(GeH_3)]_2GeMe_2$ (D)=$Fe_2(CO)_7(GeMeH)_2$ (E)=$[Fe(CO)_4GeMeH]_2$

COMPOUND	SAMPLE	δ(Mn) ($W_{1/2}$)	δ(C)($W_{1/2}$)	OTHERS
$Mn_2(CO)_{10}$	in THF	-2370±2 (40±10)	-	
	in C_6H_6 with Mn carbonyls	-2190±2 (30±10)	-	
	with Mn carbonyls	-2310±2 (30 ±10)	-	
	with $[Mn(CO)_5GeH_2]_2$	-2274±2 (15±5)	-	
$Mn(CO)_5GeMe_3$	neat, some $Mn_2(CO)_{10}$	-2538±2 (2780±20)	5.9	H 0.99 (broad)
$[Mn(CO)_5GeH_2]_2$	in C_6H_6	-2430±2 (3500±50)	-	
$Mn(CO)_5GeH_3$	neat	*	213.8 (110) 219.5† (80)	

TABLE 3 NMR parameters for **manganese-germanium (and manganese) carbonyls** .

* Sample decomposed after ^{13}C accumulation. †shoulder.

COMPOUND	SAMPLE	δ(Co)($W_{1/2}$)	δ(C)($W_{1/2}$)	OTHER
$[Me_2GeCo(CO)_3]_2$ (A)	C_6H_{14}	-3464±100 (2900±100)	5.2 (low S/N)	H 1.35 (broad)
$Me_2GeCo_2(CO)_7$ (B)	85% in CH_2Cl_2 15% (C)	-2800±20 (7000±80)	206.2* (74) 11.0	H 1.69 (broad) O 375±10 (W1/2 50)
	C_6H_{14}, some (C)	-2860±20 (5590±80)	205.3 (50) 9.8	H 1.40 (broad)
	$SiCl_4$, some (C)	-2910±20 (6670±80)	-	-
$Me_2Ge[Co(CO)_4]_2$ (C)	15% in CH_2Cl_2 85% (B)	-3480±20 (6400±80)	206.2?* (74)? 11.0?	H 1.32 (broad) O 375±10?
	C_6H_{14}, mainly (B)	-3470±20 (4840±80)	205.3? (50)? 90?	H 1.01 (broad)
	$SiCl_4$, mainly (B)	-3480±20 (3170±80)	-	-

TABLE 4 NMR parameters for **cobalt-germanium carbonyls** .
* $^{13}C,^{17}O$ signal of these two compounds may overlap.

REFERENCES

1. M.L. Martin, J.J. Delpuech, G.J. Martin, *'Practical NMR Spectroscopy'*, Heyden, London (1980) (a) p8, (b) p222, (c) p438

2. E. Fukushima, S.B.W. Roeder, *'Experimental Pulse NMR: A Nuts and Bolts Approach'*, Addison-Wesley, London (1981)

3. J.A. Pople, W.G. Schneider, H.J. Bernstein, *'High Resolution NMR'*, McGraw-Hill, New York (1959)

4. A. Abragam, *'The Principles of Nuclear Magnetism'*, Clarendon Press, London (1961) (a) p88, (b) Ch 8

5. T.C. Farrar, E.D. Becker, *'Pulse and Fourier Transform NMR; Introduction to Theory and Methods'*, Academic Press, New York (1971) (a) p49

6. R.K. Harris, B.E. Mann (Eds.) *'NMR and the Periodic Table'*, Academic Press, New York (1978)
(a) p5, (b) p213, (c) p224, (d),(e) p7, (f) p11, (g) p93, (h) p91, (i) p341, (j) p215, (k) Ch 10, (l) Ch 9, (m) Ch 3, (n) p269, (p) p79

7. C. Brevard, P. Granger *'Handbook of High Resolution Multinuclear NMR'*, Wiley-Interscience, New York (1981)
(a) p10, (b) p16, (c) p134, (d) p47, (e) p48, (f) p14, (g) p61, (h) p73, (i) p18

8. J.B. Lambert, F.G. Riddell (Eds.) *'The Multinuclear Approach to NMR Spectroscopy'*, D. Reidel, Dordrecht (1983)
(a) Ch 19, (b) p4, (c) p15, (d) Ch 16

9. *Journal of Magnetic Resonance*, W.S. Brey (Ed.), Academic Press, New York

10. *Organic Magnetic Resonance*, P.M.E. Lewis (Ed.), Heyden, London

11. *Progress in NMR Spectroscopy*, J.W. Emsley, J. Feeney, L.H. Sutcliffe, (Eds.), Pergamon Press, Oxford

12. *Advances in Magnetic Resonance*, J.S. Waugh (Ed.), Academic Press, New York

13. *Annual Reports in NMR Spectroscopy*, E.F. Mooney (Ed.), Academic Press, New York

14. *NMR. Basic Principles and Progress*, P. Diehl, E. Fluck, R. Kosfield (Eds.), Springer-Verlag, Berlin.

15. *Nuclear Magnetic Resonance, Specialist Periodical Reports*, The Chemical Society, London

16. J.W. Emsley, J. Feeney, L.H. Sutcliffe (Eds.), *Progress in NMR Spectroscopy*, Pergamon, London, VOL. 1, (1966) to VOL. 9 (1973) (extending series.)

17. J.S. Waugh, (Ed.), *Advances in Magnetic Resonance*, VOL. 1. (1965) to VOL. 9, (1977) Academic, New York (extending series).

18. *Pure Appl. Chem*, *45*, 217 (1976)

19. *Org. Magn. Reson.*, *11*, 267 (1978)

20. S. Brownstein, J. Bornais, *J. Magn. Reson.*, *38*, 131 (1980)

21. R.J. Abraham, *"The Analysis of High Resolution NMR Spectra'*, Academic, New York, (1967)

22. D.E. Woessner, B.S. Snowden, G.H. Meyer, *J. Chem. Phys.*, *50*, 719 (1969)

23. G.C. Levy, J.D. Cargioli, F.A. Anet, *J. Am. Chem. Soc.*, *95*, 1527 (1973)

24. J.H. Noggle, R.E. Schirmer, *'The Nuclear Overhauser Effect, Chemical Applications'*, Academic, New York (1971)

25. T. Drakenberg, *Acta. Chem. Scandin. A*, *36*, 79 (1982)

26. W.B. Moniz, H.S. Gutowsky, *J. Chem. Phys.*, *38*, 1155 (1963)

27. T. Tsang, T.C. Farrar, *J. Chem. Phys.*, *50*, 3498 (1969)

28. R. Faure, E.J. Vincent, J.M. Ruiz, L. Lena, *Org. Magn. Reson.*, *15*, 401 (1980)

29. J.W. Akkitt, *Ann. Rep. NMR Spectry.*, *5A*, 465 (1972)

30. W.T. Huntress, Jr., *Advan. Magn. Reson.*, *4*, 1 (1970)

31. D.A. Gansow, K.M. Triplette, T.T. Peterson, R.E. Botto, J.D. Roberts, *Org. Magn. Reson.*, *13*, 77 (1980)

32. K. Bock, B. Meyer, M. Vignon, *J. Magn. Reson.*, *38*, 545 (1980)

33. E.L. Hahn, *Phys. Rev.*, *80*, 580 (1950)

34. P. Mansfield, *Phys. Rev.*, A, *137*, 961 (1965)

35. R.R. Ernst, W.A. Anderson, *Rev. Sci. Instrum.*, *37*, 93 (1966)

36. S.L. Patt, J.N. Schoolery, *J. Magn. Reson.*, *46*, 535 (1982)

37. S.L. Patt, *J. Magn. Reson.*, *49*, 161 (1982)

38. J.P. Jesson, P. Meakin, G. Kneissel, *J. Am. Chem. Soc.*, *95*, 918 (1973)

39. R.K. Harris, R.H. Newman, A. Okruszek, *Org. Magn. Reson.*, *9*, 58 (1977)

40. S.L. Patt, D.B. Sykes, *J. Chem. Phys.*, *56*, 3182 (1972)

41. D.W. Lowman, G.E. Maciel, *Anal. Chem.*, *51*, 85 (1979)

42. G. Bodenhausen, R. Freeman, G.A. Morris, *J. Magn. Reson.*, *23*, 171 (1976)

43. F.A.L. Anet, N. Jaffer, J. Strouse, *21st experimental NMR conference* (1980)

44. E.D. Becker, J.A. Ferretti, T.C. Farrar, *J. Am. Chem. Soc., 91,* 7784 (1969)

45. A. Allerhand, D.C. Cochran, *J. Am. Chem. Soc., 92,* 4482 (1970)

46. G.G. McDonald, J.S. Leigh, *J. Magn. Reson., 9,* 358 (1973)

47. M.H. Levitt, R. Freeman, *J. Magn. Reson., 33,* 473 (1979)

48. R. Freeman, S.P. Kempsell, M.H. Levitt, *J. Magn. Reson., 38,* 453 (1980)

49. S.J. Opella, D.J. Nelson, O. Jardetzky, *J. Chem. Phys., 64,* 2533 (1976)

50. R.K. Harris, R.H. Newman, *J. Magn. Reson., 24,* 449 (1976)

51. R.L. Vold, J.S. Waugh, M.P. Klein, D.E. Phelps, *J. Chem. Phys., 48,* 3831 (1968)

52. D.E. Demco, P. van Hecke, J.S. Waugh, *J. Magn. Reson., 16,* 467 (1974)

53. J. Kowalewski, G.C. Levy, L.F. Johnson, L. Palmer, *J. Magn. Reson., 26,* 533 (1977)

54. M. Sass, D. Ziessow, *J. Magn. Reson., 25,* 263 (1977)

55. H. Hanssum, W. Maurer, H. Rüterjans, *J. Magn. Reson., 31,* 231 (1978)

56. G.H. Weiss, R.K. Gupta, J.A. Ferretti, E.D. Becker, *J. Magn. Reson., 37,* 369 (1980)

57. E.D. Becker, J.A. Ferretti, R.K. Gupta, G.H. Weiss, *J. Magn. Reson., 37,* 381 (1980)

58. F.W. Wehrli, *Application Note Varian* N°. NMR 77-2 (1977)

59. E. Fukushima, S.B.W. Roeder, *J. Magn. Reson., 33,* 199 (1979)

60. J. Banck, A. Schwenk, *Z. Physik, 265,* 165 (1973)

61. D.M. Thomas, M.R. Bendall, D.T. Pegg, D.M. Doddrell, J. Field, *J. Magn. Reson., 42,* 298 (1981)

62. Y. Huang, S. Macura, R.R. Ernst, *J. Am. Chem. Soc., 103,* 5327 (1981)

63. A.J. Shaka, R. Freeman, *J. Magn. Reson., 50,* 502 (1982)

64. V. Rutar, T.C. Wong, *J. Magn. Reson., 53,* 495 (1983)

65. M.R. Bendall, D.T. Pegg, *J. Magn. Reson., 53,* 144 (1983)

66. V. Rutar, *J. Am. Chem. Soc., 105,* 4095 (1983)

67. J.R. Lyerla, D.M. Grant, *M.T.P. internat. Rev. Sci.*, Ch 5, (Phys. Chem. Series 1), Vol. 4 (C.A. McDowell, Ed.) Butterworths (1972)

68. S.R. Hartmann, E.L. Hahn, *Phys. Rev., 128,* 2042 (1962)

69. G.A. Morris, R. Freeman, *J. Am. Chem. Soc., 101,* 760 (1979)

70. G.A. Morris, *J. Am. Chem. Soc., 102,* 428 (1980)

71. H.J. Jackobsen, W.S. Brey, *J. Am. Chem. Soc., 101,* 774 (1979)

72. A. Pines, M.J. Gibby, J.S. Waugh, *J. Chem. Phys. 59,* 569 (1973)

73. R.D. Bertrand, W.G. Moniz, A.N. Garroway, G.C. Chingas, *J. Am. Chem. Soc., 100,* 5227 (1978)

74. P.D. Murphy, T. Taki, T. Sogabe, R. Metzler, T.G. Squires, B.C. Gerstein, *J. Am. Chem. Soc., 101,* 4055 (1979)

75. R.D. Bertrand, *Nineteenth Experimental NMR Conference,* Asilomar, Calif., (1979)

76. G.C. Chingas, A.N. Garroway, R.D. Bertrand, W.B. Moniz, *J. Chem. Phys. 74,* 127 (1981)

77. G.C. Chingas, A.N. Garroway, W.B. Moniz, R.D. Bertrand, *J. Am. Chem. Soc., 102,* 2526 (1980)

78. D.M. Doddrell, D.T. Pegg, *J. Am. Chem. Soc., 102,* 6388 (1980)

79. R.R. Ernst, *Eighteenth Experimental NMR Conference,* Asilomar, Calif., (1977), *Sixth Int. Symposium on Magn. Res.,* Banff, Canada (1977)

80. A.A. Maudsley, R.R. Ernst, *Chem. Phys. Lett., 50,* 368 (1977)

81. D.P. Burum, R.R. Ernst, *J. Magn. Reson., 39,* 163 (1980)

82. D.M. Doddrell, H. Bergen, D.M. Thomas, D.T. Pegg, M.R. Bendall, *J. Magn. Reson., 40,* 591 (1980)

83. K. Hikichi, M. Ohuchi, *'Jeol News', 18A,* 2 (1982)

84. D.M. Doddrell, D.T. Pegg, M. Bendall, W. Brooks, D. Thomas, *J. Magn. Reson., 41,* 492 (1980)

85. D.M. Doddrell, D.T. Pegg, W.M. Brooks, M.R. Bendall, *J. Am. Chem. Soc., 103,* 727 (1981)

86. D.T. Pegg, D.M. Doddrell, W.M. Brooks, M.R. Bendall, *J. Magn. Reson., 44,* 32 (1981)

87. J. Kowalewski, G.A. Morris, *J. Magn. Reson., 47,* 331 (1982)

88. M.R. Bendall, D.T. Pegg, D.M. Doddrell, *J. Magn. Reson., 45,* 8 (1981)

89. C. Brevard, G.C. van Stein, G. van Koten, *J. Am. Chem. Soc., 103,* 6746 (1981)

90. A.M.F.P. van der Ploeg, G. van Koten, C. Brevard, *Inorg. Chem.*, *21*, 2878 (1982)

91. G.C. van Stein, G. van Koten, C. Brevard, *J. Organom. Chem.*, *226*, C27 (1982)

92. B.J. Helmer, R. West, *Organometallics*, *1*, 877 (1982)

93. P.H. Bolton, *J. Magn. Reson.*, *41*, 287 (1980)

94. C. Brevard, R. Schimpf, *J. Magn. Reson.*, *47*, 528 (1982)

95. T. Jenny, W. Von Philispborn, J. Kronenbitter, A. Schwenk, *J. Organom. Chem.*, *205*, 211 (1981)

96. K.D. Grüninger, A. Schwenk, B.E. Mann, *J. Magn. Reson.*, *41*, 354 (1980)

97. P.L. Rinaldi, N.J. Baldwin, *J. Am. Chem. Soc.*, *104*, 5791 (1982)

98. G.A. Morris, *J. Magn. Reson.*, *41*, 185 (1980)

99. D. Marion, C. Garbay-Jaureguiberry, B.P. Roques, *J. Am. Chem. Soc.*, *104*, 5573 (1982)

100. O.W. Sørensen, R. Freeman, T. Frienkel, T.H. Mareci, R. Schuck, *J. Magn. Reson.*, *46*, 180 (1982)

101. A. Bax, R. Freeman, S.P. Kempsell, *J. Am. Chem. Soc.*, *102*, 4849 (1980)

102. V. Rutar, *J. Magn. Reson.*, *53*, 135 (1983)

103. H.J. Jackobsen, O.W. Sørensen, H. Bildsøe, *J. Magn. Reson.*, *51*, 157 (1983)

104. J. Brondeau, D. Canet, *J. Magn. Reson.*, *47*, 419 (1982)

105. G.A. Morris, R. Freeman, *J. Magn. Reson.*, *29*, 433 (1978)

106. D.M. Doddrell, D.T. Pegg, M.R. Bendall, *J. Magn. Reson.*, *48*, 323 (1982)

107. D.T. Pegg, D.M. Doddrell, M.R. Bendall, *J. Chem. Phys.*, *77*, 2745 (1982)

108. M.R. Bendall, D.T. Pegg, D.M. Doddrell, *J. Chem. Soc. Chem. Commun.*, 872 (1982)

109. M.R. Bendall, D.T. Pegg, D.M. Doddrell, D.H. Williams, *J. Org. Chem.*, *47*, 3021 (1981)

110. M.R. Bendall, D.T. Pegg, D.M. Doddrell, *J. Magn. Reson.*, *52*, 81 (1983)

111. M.R. Bendall, D.M. Doddrell, W.E. Hull, D.T. Pegg, *'Application Note on D.E.P.T.', Bruker, Analytische Messtechnik, Karlsruhe* (1982)

112. V. Rutar, *J. Magn. Reson.*, *53*, 49 (1983)

113. M.R. Bendall, D.T. Pegg, D.M. Doddrell, *J. Magn. Reson.*, *45*, 8 (1981)

114. R. Freeman, T.H. Mareci, G.A. Morris, *J. Magn. Reson.*, *42*, 341 (1981)

115. M.R. Bendall, D.T. Pegg, D.M. Doddrell, J. Field, *J. Magn. Reson.*, *51*, 520 (1983)

116. O.W. Sørensen, R.R. Ernst, *J. Magn. Reson.*, *51*, 477 (1983)

117. M.R. Bendall, D.T. Pegg, *J. Magn. Reson.*, *52*, 164 (1983)

118. D.T. Pegg, M.R. Bendall, *J. Magn. Reson.*, *55*, 51 (1983)

119. M.R. Bendall, D.T. Pegg, G. Max. Tyburn, C. Brevard, *J. Magn. Reson.*, *55*, 322 (1983)

120. Pei, Feng-kui, R. Freeman, *J. Magn. Reson.*, *48*, 318 (1982)

121. H.J. Jacköbsen, O.W. Sørensen, W.S. Brey, P. Kanyha, *J. Magn. Reson.*, *48*, 328 (1982)

122. G. Ayrey, D. Barnard, D.T. Woodbridge, *J. Chem. Soc.*, 2089 (1968)

123. M.L. Bird, F. Challenger, *J. Chem. Soc.*, 570 (1942)

124. J.D. Odom, W.H. Dawson, P.D. Ellis, *J. Am. Chem. Soc.*, *101*, 5815 (1979)

125. F. Glocking, *'The Chemistry of Germanium'*, *Academic Press*, (1969)

126. H. Dreeskamp, *Z. Naturforsch*, *19a*, 139 (1964)

127. J. Kaufmann, W. Sahm, A. Schwenk, *Z. Naturforsch*, *26a*, 1384 (1971)

128. J.D. Kennedy, W. McFarlane, *Unpublished results*, ^{1}H-{^{73}Ge} *double resonance*

129. J.W. Wehrli, *Ann. Rep. on NMR Spec.*, *'NMR of the less common quadrupolar nuclei'*, *9*, 176 (1979)

130. J.E. Griffiths, *J. Chem. Phys.*, *38*, 2879 (1963)

131. F. Cotton, G. Wilkinson, *'Advanced Inorganic Chemistry'*, *3rd ed*, p 115, *Interscience, New York* (1972)

132. J.A Christie, *'Germanium Hydride Derivatives of Transition Metal Carbonyls'*, *D. Phil. Thesis, Univ. of Waikato* (1981)

133. R.C. Weast, (Ed.) *'CRC Handbook of Chemistry and Physics'*, 58th ed., (1977) (a) F-49, (b) B-115

134. D.M. Doddrell et al, *Bruker Report*, *2*, 18-21 (1980)

135. E.H. Brooks, F. Glocking, *Inorg. Synth.*, *12*, 58 (1970) and references therein

136. Y.M. Choo, *'Studies on Germylsilanes', M. Sc. Thesis, Univ. of Waikato* (1979)

137. J.E. Drake, R.T. Hemmings, C. Riddle, *J. Chem. Soc.*, (A) 3359 (1970)

138. K.M. MacKay, K.J. Sutton, *J. Chem. Soc.*, (A) 2312 (1968)

139. F.S. Wong *'Studies on Digerman Derivatives', M. Sc. Thesis, Univ. of Waikato* (1976)

140. C.C. Ngo, *'Transition-Metal Carbonyl Derivatives of Silanes', M. Sc. Thesis, Univ. of Waikato* (1982)

141. Y.M. Choo, K.M. MacKay, *J. Chem. Res.*, (S) 76 (1981)

142. S.P. Foster, *'The Reactions of Group IV B Hydrides with Carbonyl Complexes of Cobalt and Manganese', D. Phil. Thesis, Univ. of Waikato* (1983)

143. H.C. Charles, C.A. Evans, *'Jeol Application Note'*, Jan. 81-1, New Jersey (1981)

144. C.A. Evans, H.C. Charles, *'Jeol Application Note'*, Jan. 81-3, New Jersey (1981)

145. D.M. Doddrell, private communication

146. R.G. Kidd, H.G. Spinney, *J. Am. Chem. Soc., 95,* 88 (1973)

147. V.A. Pestunovich, S.N. Tandura, B.Z. Shterenberg, N. Yu. Khromova, T.K. Gar, V.F. Mironov, M.G. Voronkov, *Izv. Akad. Nauk SSSR, Ser. Khim* 959 (1980)

148. H. Saji, *Phys. Lett., 45A,* 469 (1973)

149. H. Murakami, I. Kanazawa, T. Shimizu, K. Matsushita, *JEOL News, 18A,* 10 (1982)

150. D.K. Dalling, H.S. Gutowsky, *Govt. Rep. Announce. (U.S.)71,* 65 (1971); [Chem. Abs. *75,* 82238 (1971)]

151. P.T. Inglefield, L.W. Reeves, *J. Chem. Phys., 40,* 2425 (1964)

152. P.A. Dean, D.F. Evans, *J. Chem. Soc.*, (A) 698 (1967)

153. V.P. Tarasov, Yu. A. Buslaev, *J. Magn. Reson., 25,* 197 (1977)

154. P. Geerlings, C. Van Alsenoy, *J. Organomet. Chem., 117,* 13 (1976)

155. W. Sahm, A. Schwenk, *Z. Naturforsch, 29a,* 1763 (1974)

156. A. Schwenk, *Phys. Lett., 31A,* 513 (1970)

157. J. Banck, A. Schwenk, *Z. Physik, 265,* 165 (1973)

158. C.W. Burges, R. Koschneider, W. Sahm, A. Schwenk, *Z. Naturforsch, 28a,* 1753 (1973)

159. O. Lutz, A. Schwenk, G. Zimmermann, *Phys. Lett., 25A,* 653 (1967)

160. A.A. Cheremisin, P.V. Schastnev, *J. Magn. Reson., 40,* 459 (1980)

161. J. Scharml, J.M. Bellama, *'Determination of Organic Structures by Physical Methods'*, Vol 6, Ch 4 (F.C. Nachod, J.J. Zuckerman, E.W. Randall, Eds.,) (1976)

162. C. Schumann, H. Dreeskamp, *J. Magn. Reson., 3,* 204 (1970)

163. G.C. Levy, D.M. White, J.D. Cargioli, *J. Magn. Reson., 8,* 280 (1972)

164. W. McFarlane, *J. Chem. Soc.,* (A) 528 (1967)

165. A.L. Allred, *J. Inorg. Nucl. Chem., 17,* 215 (1961)

166. J. Schraml et al, *Collect. Czech. Chem. Commun., 44,* 854 (1979)

167. R.K. Harris, B.J. Kimber, *Adv. Mol. Relaxation Processes, 8,* 15 (1976)

168. P. Löwer, M. Vongehr, H.C. Marsmann, *Chem. Ztg., 99,* 33 (1975)

169. J.J. Burke, P.C. Lauterbur, *J. Am. Chem. Soc., 83,* 326 (1961)

170. B.R. McGarvey, M.J. Taylor, D.G. Tuck, *Inorg. Chem., 20,* 2010 (1981)

171. C.J. Jameson, H.S. Gutowsky, *J. Chem. Phys., 40,* 1714 (1964)

172. K.M. MacKay, *private communication*

173. L.P. Lindman, M.K. Wilson, *J. Chem. Phys., 22,* 1723 (1954)

174. V.W. Laurie, *J. Chem. Phys., 30,* 1210 (1959)

175. J. Vladimiroff, E.R. Malinowski, *J. Chem. Phys., 46,* 1830 (1967)

176. R. Colton, D. Dakternieks, *Aust. J. Chem., 33,* 2045 (1980)

177. G. Calingaert, H.A. Beatty, *J. Am. Chem. Soc., 61,* 2748 (1939)

178. L.S. Foster, A.F. Williston, *Inorg. Synth., 2,* 106 (1946)

179. H.Y. Carr, E.M. Purcell, *Phys. Rev., 94,* 630 (1954)

180. U. Dolega, *Ann. Phys., 16,* 153 (1955)

181. W. Sahm, *Diplomarbeit, Tübingen* (1970)

182. J. Reuben, Z. Luz, *J. Phys. Chem., 80,* 1357 (1976)

183. T.E. Bull, S. Forsen, D.L. Turner, *J. Chem. Phys., 70,* 3106 (1979)

184. T.J. Marks, L.A. Shimp, *J. Am. Chem. Soc., 94,* 1542 (1972)

185. E.J. Sparien, A.G. MacDiarmui, *Inorg. Chem., 2,* 215 (1963)

186. J.E. Griffiths, *Inorg. Chem.*, *2*, 375 (1963)

187. K.M. MacKay, R.D. George, P. Robinson, R. Watts, *J. Chem. Soc.*, (A) 1920 (1968)

188. K. Clusius, C. Faber, *Z. Phys. Chem.*, (B) *51*, 352 (1942)

189. N. Hao, B.G. Sayer, G. Dénès, D.G. Bickley, C. Detellier, M.J. McGlinchey, *J. Magn. Reson.*, *50*, 50 (1982)

190. I.R. Beattie, T. Gilson, K. Livingston, *J. Chem. Soc.* (A) 712 (1967)

191. J.J. Dechter, U. Henriksson, J. Kowalewski, Ann-Chatrin Nilsson, *J. Magn. Reson.*, *48*, 503 (1982)

192. K. Koga, Y. Kanazawa, *J. Phys. Chem.*, *87*, 5219 (1983)

193. Y.S. Li, J.R. Durig, *Inorg. Chem.*, *12*, 306 (1973)

194. E. Haid, D. Köhnlein, G. Kössler, O. Lutz, W. Schich, *J. Magn. Reson.*, *55*, 145 (1983)

195. R.J.C. Brown, J.P. Colpa, *J. Chem. Phys.*, *77*, 1501 (1982)

196. D.M. Doddrell, M.R. Bendall, P.C. Healy, G. Smith, C.H.L. Kennard, C.L. Raston, A.H. White, *Aust. J. Chem.*, *32*, 1219 (1979)

197. R.T. René, R.G. Kidd, *Ann. Rep. NMR Spec.*, *13*, 348 (1983)

198. M. Shporer, Z. Luz, *J. Am. Chem. Soc.*, *97*, 665 (1975)

199. T.P. Melia, R. Merrifield, *J. Chem. Soc.* (A) 1258 (1971)

200. 'JEOL Instructions, PG 200 Programmable Pulse Generator', Ch 6

201. R.J. Abraham, P. Loftus, *'Proton and Carbon-13 NMR Spectroscopy'*, p 130, Heyden, London (1978)

202. R. Crouch, S. Hurlbert, A. Ragouzeos, *J. Magn. Reson.*, *49*, 371 (1982)

203. F.S. Wong *'Studies on Polygermanyl-Transition Metal (Carbonyl) Derivatives' D.Phil. Thesis, Univ. of Waikato* (1978)

204. J.P. Hickey, J.R. Wilkinson, L.J. Todd, *J. Organomet. Chem.*, *179*, 159 (1979)

205. A. Bonny, K.M. MacKay, *J. Chem. Soc.*, (D) 506 (1978)

206. J. Calderazzo, E.A.C. Lucken, D.F. Williams, *J. Chem. Soc.*, (A) 154 (1967)

207. H.W. Speiss, R.K. Sheline, *J. Chem. Phys.*, *53*, 3036 (1970)

208. M.A. Cohen, D.R. Kidd, T.L. Brown, *J. Am. Chem. Soc.*, *97*, 4408 (1975)

LIST OF NMR SYMBOLS AND ABBREVIATIONS , TABLE A

A	line integral
ACQTM	FID acquisition time (for JEOL FX90Q spectrometer)
B_0	magnetic induction for spin-system orientation,called magnetic field in text
B_1	magnetic induction for resonance,called magnetic field in text
B_2	magnetic induction for double irradiation,called mag. field in text
B_{eff}	effective magnetic field
D	dimensionless pulse spacing , $(\Delta J)^{-1}$
Di	detectability of isotope i
DELAY	delay time between final pulse and acquisition (JEOL FX90Q)
E	magnetic energy , or S/N enhancement
Ea	activation energy (Arrhenius equation)
Ed	proton decoupled S/N enhancement
E%	% fraction of theoretical enhancement attained experimentally
ΔE	energy difference between two spin levels
f(t)	time function (fourier spectroscopy)
$f(\nu)$,$f(\omega)$	frequency function (fourier spectroscopy)
FREQU	observed frequency range (JEOL FX90Q)
I	observed NMR isotope
$I\tau$,$I\infty$	intensities of lines
J	coupling constant
K	reduced coupling constant
k	factor with Ξ yielding JEOL FX90Q resonant frequency
k_i	i=1,2,3,4 constants pertaining to PT enhancement
l^i	nuclear spin quantum number
L	linewidth factor
M_0	macroscopic magnetization
M_i	magnetization vector components (i= x,y,z)
m_H,M_H	proton spin, and total proton spin, respectively
m^i	discrete spin variable
m_i	orientational magnetic quantum number for isotope i
n^i	number of scalar coupled nuclei (protons) transferring PT or principal quantum number for valence orbital
N	natural abundance of an isotope (%)
N_d	number of resonating spins in the detector coil
OBFRQ	primary frequency parameter for (JEOL FX90Q) (MHz)
OBSET	carrier offset (JEOL FX90Q) (kHz)
-(opt)	optimum timing giving max. E(- = τ,Δ) or max. E (- = E,Ed)
P	nuclear angular momentum vector
PD	delay between acquisition and next pulse (JEOL FX90Q)
POINT	total number of computer memory locations (JEOL FX90Q)
PW1	pulse time (JEOL FX90Q) (μs)
q	electric field gradient (subscripts refer to tensor components)
Q	nuclear electric quadrupole moment
r	ratio of recycle time of INEPT,r_1 to that of single-pulse seq.,r_0
r_{IS}	distance between nucleus I and nucleus S (metres)
R_i	NMR receptivity of isotope i
R_i^k	NMR receptivity of isotope i relative to isotope k
R%	% contribution of a relaxation mechanism to total relaxation rate
RES	frequency resolution (JEOL FX90Q)
s	number of scans to reach a certain S/N
S	irradiated NMR isotope

T dimensionless pulse spacing $(\tau J)^{-1}$
T_1 spin-lattice (longitudinal) relaxation time
T_1° value of T_1 at infinitely high temperature
$T_{1\rho}$ T_1 in the rotating frame
T_{1x} T_1 from mechanism x,x=csa(chemical shift anisotropy),dd(dipole-dipole),(e)electron-nuclear,(q)quadrupolar,(sc)scalar,(sr)spin-rotation
T_2 spin-spin (transverse) relaxation time
T_2^* apparent spin-spin (transverse) relaxation time
T_{ex}, T_{th} experimental,theoretical pulse time delay, respectively
$T\%$ % deviation of experimental pulse sequence timing from theoretical
$t_{½}$ time for reactant signal to be reduced two fold
t_p duration of B_1 (s)
t_{90} pulse width of $\alpha=90°$ for isotope A
u dispersion component of $\underline{M}$
W waiting time between pulse sequences,including ACQTM
$W_{½}$ half height line width (Hz)
α tip angle of $\underline{M}$,or spin state,or a defined function of timing, τ
α_o optimal flip angle of $\underline{M}$
β spin state, or a defined function of timing, Δ
γ magnetogyric ratio
δ chemical shift
Δ the second inter-pulse spacing , or expresses a difference
η NOE enhancement factor
$\bar{\eta}$ macroscopic viscosity of a solution
η_a asymmetry parameter
$\theta i, \phi i$ r.f. pulse applied along i axis (default is x) with $\alpha=\theta°$,or $\phi°$
$90i, 180i$ r.f. pulse applied along i axis (default is x) with $\alpha=90°, 180°$
$\underline{\mu}$ magnetic moment vector
ν frequency (Hz)
σi screening constant for isotope i
τ the first inter-pulse spacing (defined for a given sequence)
τ_c correlation time for molecular reorientation
υ absorption component of $\underline{M}$
χ nuclear quadrupole coupling constant
χ' nuclear quadrupole coupling constant as a function of η_a
ω angular frequency $(rads^{-1})$
Ξ_I resonant frequency of isotope I in a field for which protons of TMS resonate at exactly 100.00 MHz

ADC analogue to digital converter
e.n.c. extreme narrowing condition
FID free induction decay
FIRFT fast inversion recovery FT
FT fourier transform
IRFT inversion recovery FT
LF low frequency
NQCC nuclear quadrupole coupling constant
NMR nuclear magnetic resonance
NOE nuclear Overhauser effect
o.d. outside diameter
PT polarization transfer
QPD quadrature phase detection
r.f. radio frequency
S/N signal to noise ratio
SRFT saturation recovery FT

TABLE 5.7B , AN AMMENDED VERSION OF TABLE 5.7

When isotope I is ^{13}C, inclusion of the factor n_H ,the number[1,196] of protons directly attached to carbon, to equation (1.17)[7,25] , yields the ammended equations;

$$\tau_C = (4.42)10^{-11}/(T_{1C}\, n_H) \qquad ---(5.3)$$

$$\chi'(^{73}Ge) = 2.135/(T_{1Ge}\, \tau_C)^{0.5} \qquad ---(5.4)$$

These equations are used to calculate the ammended values of τ_C and χ' contained in TABLE 5.7B , the new version of TABLE 5.7 .

COMPOUND	SAMPLE	T_{1C} (av) $(CH_3),(CH_2)$	τ_C (av)	χ' (^{73}Ge)
$GeMe_4$	75% v. n-Bu_2O	18.6, -	0.79	3.1
$GeEt_4$	25% v. n-Bu_2O	10.8,12.2	1.6	3.1
	75% v. n-Bu_2O	10.1,11.2	1.7	2.7
	neat	10.0,11.1	1.7	2.3
$Ge(n\text{-}Pr)_4$	neat	4.43,3.88	4.9	2.9
$Ge(n\text{-}Bu)_4$	neat	3.48,1.55	12	2.3
$Ge(n\text{-}Pn)_4$	neat	2.89,1.04	18	2.9
$Ge(n\text{-}Hx)_4$	neat	2.76,0.78	25	3.1
$GeMe_3H$	(a)	10.3, -	1.4	(3.1)
$GeMe_2H_2$	(a)	22.9, -	0.63	(4.9)
$GeMeH_3$	(a)	28.8, -	0.50	(3.9)
	0.7 atm. n-Bu_2O	25.0, -	0.60	(4.5)
GeH_3GeMeH_2	(a) , (GeH_3)	18.7, -	0.8	(4.7)
	(a) , ($GeMeH_2$)	18.7, -	0.8	(9.1)
$GeEt_3H$	neat	14.0,16.3	1.2	(17)

TABLE 5.7B Germanium-73 nuclear quadrupole coupling constants and correlation times for **Organogermanium compounds** . T_{1C},(s) and τ_C (ps) are averages in multiline spectra, χ' (MHz),values in brackets are rough estimates. Max. random errors: χ' (20%) , T_{1C} , τ_C (10%) , (a) Sample of $GeMe_2H_2$,Ge_2MeH_5 ,some $GeMeH_3$, $GeMe_3H$. n-Pn = n-C_5H_{11} , n-Hx = n-C_6H_{13} .

Corrections, D.Phil. Thesis — P.J. Watkinson, University of Waikato

Page	Line	
2	28	$\underline{\mu}.\underline{B}_o$ --> $\underline{\mu}\times\underline{B}_o$
3	4	$\omega_o = -\gamma B_o$ --> $\underline{\omega}_o = -\gamma\underline{B}_o$
3	8	take --> takes
8	1	proportioned --> proportional
8	17	$2mI_B + 1$ --> $2ml_B + 1$
8	19	multiplet --> multiplets
12	6	movement --> moment
12	15	assymmetry --> asymmetry
13	1	χ --> χ'
14	9	m^2 --> $10^{-28}m^2$
16	15	isotope l --> isotope I
17	6	$W_{\frac{1}{2}}^{1}$ --> $W_{\frac{1}{2}}'$
21	5	it --> its
28	3	braodening --> broadening
29	29	phase --> plane
38	3	(Caption) Correct line: position; being just outside the window,(b) acts as if it is
44	17	proton --> protio
50	20	relaxation --> reduction
52	6	n = 2,3,4 --> m = 2,3,4
53	19	Decouped --> Decoupled
57	7	magnetiziation --> magnetization
57	24	threre --> there
58	21	with --> such
59	2	Coten --> Koten

68 2 even, --> even,(INEPT)

71 27 trigomometric --> trigonometric

73 6 E(opt) --> < E(opt) >

79 8 techniques --> technique

106 27 73b --> 7d

116 3 3.4.8.2 --> 3.8.4.2

120 13 80., --> 80 ,

124 10 30% --> 70%

132 19 Loss --> loss

142 5 movement --> moment

149 4 (Caption) first pulse --> first and third pulse

157 24 I > Br > Cl --> I < Br < Cl

168 12 GeH_3GeMeH_2 --> GeH_3GeMe_2H

178 10 germane --> digermane

178 13 digermane --> trigermane

183 15 the --> than

185 2 grpup --> group

186 8 $(GeMeH)_2GeMeH$ --> $(GeMeH_2)_2GeMeH$

187 TABLE 4.21,far left,middle row. $(GeH_3)_2GeH_2$ --> $(GeH_3)_2\underline{Ge}H_2$

189 11 compound --> compounds

192 1 $)_n$ --> $)_m$

197 6 3,488,323 --> 3,488,423

197 23 Methylsilygermane --> Methylsilylgermane

204 9 $GeMeH_3$ --> $GeMe_3H$

204 20 398 --> 367

214 9 (ps) --> (s)

247 1 PARAMTERS --> PARAMETERS

254 14 27100) --> 27100)[208]